

MEMIS
4
2002

LIBRARY
Michigan State
University

PLACE IN RETURN BOX to remove this checkout from your record.
TO AVOID FINES return on or before date due.
MAY BE RECALLED with earlier due date if requested.

DATE DUE	DATE DUE	DATE DUE

ENVIRONMENTALLY BEGNIGN SYNTHESIS OF
AROMATIC COMPOUNDS FROM D-GLUCOSE

VOLUME I

By

Jessica L. Barker

A DISSERTATION

Submitted to
Michigan State University
in partial fulfillment of the requirements
for the degree of

DOCTOR OF PHILOSOPHY

Department of Chemistry

2001

ABSTRACT

ENVIRONMENTALLY BENIGN SYNTHESIS OF AROMATIC COMPOUNDS FROM D-GLUCOSE.

By Jessica L. Barker

As the 21st century dawns, alternative methods are being sought for the synthesis of aromatic compounds. Today, 98% of aromatic compounds are currently derived from petroleum. As petroleum supplies continue to be depleted, there will be a need to find alternative routes to these commercially important chemicals that are derived from renewable feedstocks, such as cellulose, hemi-cellulose, and starch. In this dissertation, alternative routes to *p*-hydroxybenzoic acid, hydroquinone, *p*-cresol, and phenol will be elaborated that not only originate with D-glucose, but also utilize environmentally benign processes.

p-Hydroxybenzoic acid is the starting material for a class of antimicrobial compounds known as parabens and is a common monomer in liquid crystalline polymers. Industrially *p*-hydroxybenzoic acid is synthesized using the Kolbe-Schmidt reaction in which phenol is carboxylated to *p*-hydroxybenzoic acid under harsh conditions. A series of recombinant *Escherichia coli* strains have now been constructed and evaluated for their ability to synthesize *p*-hydroxybenzoic acid. Constructs differed in the strategy used for the overexpression of chorismate lyase and also differed as to whether mutations were present in the host *E. coli* to inactivate other chorismate-utilizing enzymes. The maximum concentration of *p*-hydroxybenzoic acid synthesized was 12 g/L in a 13% (mol/mol) yield from glucose when *E. coli* JB161/pJB2.274 was cultured under fed-batch fermentor conditions. The toxicity of *p*-hydroxybenzoic acid towards *E. coli* metabolism and growth was also evaluated.

Hydroquinone is a fine chemical used in photo development and as an antioxidant. *p*-Cresol is used in the manufacture of phenolic resins and as the starting material for the antioxidant butylated hydroxy toluene. Environmentally benign syntheses of these molecules are elaborated in which microbe-synthesized *p*-hydroxybenzoic acid is converted to hydroquinone by either the fungus *Phanerochaete chrysosporium* or the yeast *Candida parapsilosis*. Using *C. parapsilosis* as a whole-cell biocatalyst, *p*-hydroxybenzoic acid could be converted to hydroquinone in a 48% isolated yield. Under different culturing conditions, *P. chrysosporium* can be used to reduce *p*-hydroxybenzoic acid to *p*-hydroxybenzyl alcohol. Hydrogenation of the resulting alcohol affords *p*-cresol in a 46% yield from *p*-hydroxybenzoic acid.

An environmentally benign synthesis of phenol, derived from glucose via shikimic acid intermediacy, has also been established. Phenol, the second largest volume chemical currently derived from benzene, is used in the manufacture of phenolic resins, bisphenol A, and a variety of other commercially important chemicals. The current microbial synthesis of shikimic acid is plagued by contaminating quinic acid formation. Quinic acid formation has now virtually been eliminated by replacement of the native *E.coli* DHQ dehydratase and shikimate dehydrogenase activities by the *Nicotiana tobacum* bifunctional AroD·AroE enzyme. Shikimic acid can now be synthesized in 34 g/L in a molar ratio to quinic acid of 30:1. Purified shikimic acid can then be converted to phenol in a 45% yield by heating an aqueous solution of the acid to the subcritical temperature of 350 °C. The byproduct *m*-hydroxybenzoic acid can be decarboxylated to phenol in subcritical water in the presence of copper to yield an additional 6% yield of phenol. Overall, shikimic acid can be converted to phenol in a 51% isolated yield.

Copyright by
Jessica L. Barker
2001

**To Tim and my family
For their unfailing love and support**

ACKNOWLEDGMENTS

I would first like to thank Professor John W. Frost for his patience, understanding, and guidance through the course of my Ph.D. studies. John's dedication and demand for high quality research will be a standard I will try to maintain throughout my career. Through five and a half years of hard work, he has shown me that I am capable of more than I ever conceived of as a first year student. I am grateful for this lesson and have always tried to do my best in return. In addition, I would like to thank the members of my graduate committee Professor Greg Baker, Professor Gary J. Blanchard, and Professor John Allison for their input during the preparation of this thesis. A special thanks to Professor Baker who was always available for advice.

I am grateful to Dr. Karen M. Draths for both her friendship and wealth of knowledge that she freely shared with me. I am also indebted to Dr. Kai Li for his friendship while patiently teaching me techniques and answering my endless onslaught of questions. A special thanks is also due to Sunil Chandran, Chad Hansen, Dave Knop, and Padmesh Venkitasubramanian for their friendship and the countless timepoints and favors they have given me. I am in your debt. Kudos also to all present and past members of the Frost group that I have been lucky to work with: Prof. Jean-Luc Montchamp, Dr. John Arthur, Dr. Mason Harrup, Dr. Amy Dean, Dr. Feng Tian, Dr. Spiros Kambourakis, Mark Mikola, Jian Yi, Wei Nu, Jianto Guo, Ningqing Ran, and Satyamaheshwar Peddibhotla. I would also like to thank Prof. Mike Gibson, Josh Thomas, and Phillip Thomas for their contribution on the phenol project.

The unconditional love and support I have received from my parents, my brother Sam, my family, and my friends Tina and Ben Weihl, and Micah Stowe have been the foundation of my success. I simply would not be where I am today without them. I am eternally grateful. I also thank my father, Michael Barker, for his help in preparing this manuscript. Finally, I especially need to thank my fiancée Tim Tischler. I could not have

made it through my graduate career without him. He my source of laughter, joy, encouragement, and love.

TABLE OF CONTENTS	viii
LIST OF TABLES	xii
LIST OF FIGURES	xiv
LIST OF ABBREVIATIONS	xxi
CHAPTER ONE	
ALTERNATIVE CHEMICAL SYNTHESIS: BIOCATALYSIS AND THE SHIKIMATE PATHWAY	1
Introduction	1
I. Biocatalysis	2
II. The Common Pathway of Aromatic Amino Acid Biosynthesis.	7
A. The Shikimate Pathway of <i>Escherichia coli</i> .	7
B. Microbial Synthesis of Chemicals Derived from the Shikimate Pathway	14
C. Metabolic Engineering to Increase Yields and Titrers in the Shikimate Pathway of <i>E. coli</i> .	24
References	33
CHAPTER TWO	
MICROBIAL SYNTHESIS OF <i>p</i>-HYDROXYBENZOIC ACID FROM GLUCOSE	39
Introduction	39
I. Design and Assembly of the Microbial Catalyst.	44
A. Construction of <i>E. coli</i> Host Strains.	44
B. Plasmid Constructions.	59
II. Microbial Synthesis of PHB from Glucose.	71
A. Fed-Batch Fermentator Conditions for PHB-Producing Microbes.	71
B. Fermentation Results	75
C. Chorismate Lyase and DAHP Synthase Activities.	84
III. Microbial Toxicity of PHB.	88
A. Toxicity of PHB on <i>E. coli</i> KL3/pKL4.130B.	88
B. Increasing Tolerance to PHB.	91
IV. PHB <i>O</i> - β -D-Glucoside.	96
A. PHB <i>O</i> - β -D-Glucoside Toxcity Towards <i>E. coli</i> .	96
B. Heterologous Expression of a Tobacco Glucosyltransferase in <i>E. coli</i> .	100
V. Discussion	105
References	123
CHAPTER THREE	
BIOTRANSFROMATION OF PHB INTO HYDROQUINONE AND <i>p</i>-CRESOL.	126

Introduction	126
I. Hydroquinone	129
A. Chemical Background	129
B. Synthesis of Hydroquinone using <i>Phanerochaete chrysosporium</i>	134
i) Background	134
ii) Conditions for the Biotransformation of PHB using <i>P. Chrysosporium</i>	138
C. Synthesis of Hydroquinone using <i>Candida parapsilosis</i>	145
i) Background	145
ii) Conditions for the Biotransformation of PHB using <i>C. parapsilosis</i>	148
D. Purification of Hydroquinone	153
II. <i>p</i> -CRESOL	155
A. Background	155
B. Synthesis of <i>p</i> -Cresol from PHB.	159
III. Discussion	166
References	177
CHAPTER FOUR	
SYNTHESIS OF SHIKIMIC ACID AND PHENOL	182
Introduction	182
I. Shikimic Acid	184
A. Background	184
B. Biocatalytic Synthesis of Shikimic Acid.	185
C. <i>N. tabacum</i> DHQ dehydratase/Shikimate Dehydrogenase.	191
D. Preparation of <i>E. coli</i> JB4/pJB5.291.	191
E. Fed-Batch Fermentation of JB4/pJB5.291.	199
F. Can the Tobacco DHQ Dehydratase/Shikimate Dehydrogenase Catalyze Quinic Acid Formation?	204
G. Feedback Inhibition of the Tobacco DHQ dehydratase/Shikimate Dehydrogenase.	205
II. Conversion of Shikimic Acid to Phenol.	209
Introduction	209
A. Dehydration of Shikimic Acid.	211
B. Subcritical Water.	214
C. Reaction of Shikimic Acid in Subcritical Water.	216
D. Copper Assisted Decarboxylation of MHB	221
E. Two-Step Conversion of Shikimic Acid to Phenol.	222
F. Conversion of Fermentation Broth to Phenol.	224
G. Extraction of Shikimic Acid from Fermentation Broth.	230
III. Discussion	231
References	239
Appendix	242

CHAPTER FIVE	
EXPERIMENTAL	252
I. General Methods	252
A. Chromatography	252
B. Spectroscopic Measurements.	253
C. Bacterial Strains and Plasmids.	254
D. Storage of Bacterial Strains and Plasmids.	254
E. Culture Medium	254
F. General Fed-Batch Fermentation Conditions.	256
G. Analysis of Culture Supernatant.	258
II. Genetic Manipulations.	259
A. General Procedures	259
B. Large Scale Purification of Plasmid DNA.	260
C. Small Scale Purification of Plasmid DNA.	262
D. Restriction Enzyme Digestion of DNA.	263
E. Agarose Gel Electrophoresis.	264
F. Isolation of DNA from Agarose	264
G. Treatment of Vector DNA with Calf Intestinal Alkaline Phosphatase.	264
H. Treatment of DNA with Klenow fragment.	265
I. Ligation of DNA.	265
J. Preparation and Transformation of Competent Cells.	266
K. Purification of Genomic DNA.	267
L. Generation of P1 lysate.	268
M. P1 Transduction	269
N. λ DE3 lysogeny.	270
III. Enzyme Assays.	270
A. General.	270
B. DAHP Synthase.	271
C. Chorismate Lyase.	272
D. <i>p</i> -Hydroxybenzoate Hydroxylase.	273
E. <i>N. tabacum</i> DHQ Dehydratase/Shikimate Dehydrogenase	273
F. Aryl Aldehyde Dehydrogenase.	274
IV. Chapter Two.	274
A. Purification of PHB from Fermentation Broth	274
B. Preparation of JB161 and JB161(DE3)	275
C. Preparation of RB38 and RB38(DE3)	277
D. Southern Hybridization to Confirm Phenotype of JB161.	277
E. Preparation of Plasmids	281
F. Purification of <i>p</i> -Hydroxybenzoate Hydroxylase.	284
G. Isolation of Chorismic Acid.	285
H. Feedback inhibition of Chorismate Lyase.	287
I. Feedback inhibition of DHQ synthase.	288
J. Isolation of <i>E. coli</i> 98042-42.	289
K. Synthesis of PHB <i>O</i> - β -D-Glucoside.	289
L. Disk Diffusion Experiment with <i>p</i> -Hydroxybenzoate	

<i>O</i> - β -D-Glucopyranoside	291
M. Cloning of <i>N. tabacum</i> <i>TOGT1</i> .	291
N. Microbial Synthesis of PHB <i>O</i> - β -D-Glucoside.	294
V. Chapter Three.	295
A. Maintenance and Storage of Fungal Strains.	295
B. Culture Media for Fungal Strains.	296
C. Conditions for Shake-Flask Cultivation of <i>P. chrysosporium</i> .	297
i) Conversion of PHB to Hydroquinone	297
ii) Conversion of PHB to <i>p</i> -Hydroxybenzyl Alcohol	300
D. Conditions for Shake-Flask Cultivation of <i>C. Parapsilosis</i> .	302
E. Purification of Hydroquinone from <i>P. chrysosporium</i> Culture Supernatant.	304
F. Purification of Hydroquinone from the Culture Supernatant of <i>C. parapsilosis</i> .	305
G. Purification of <i>p</i> -Hydroxybenzyl Alcohol from the Culture Supernatant of <i>P. chrysosporium</i> .	305
H. Hydrogenation of <i>p</i> -Hydroxybenzyl Alcohol.	306
VI. Chapter Four.	306
A. Construction of Strains.	306
B. Preparation of Plasmids	308
C. In Vitro Quinic Acid Accumulation.	309
D. Enzyme Kinetics of the <i>N. tabacum</i> DHQ Dehydratase /Shikimate Dehydrogenase.	309
E. Conversion of Shikimic Acid to <i>p</i> -Hydroxybenzoic Acid.	311
F. Purification of Shikimic Acid from Fermentation Broth.	312
G. Conversion of Shimikic Acid to Phenol.	313
H. Conversion of Shikimic Acid to Phenol at Various Temperatures.	314
I. Decarboxylation of <i>m</i> -Hydroxybenzoic Acid.	315
J. Conversion of Fermentation Broth	315
K. Sample A Reacted at Various Temperatures.	318
L. Reduction of DHS to Shikimate and 3- <i>epi</i> -Shikimate.	318
VII. Appendix.	319
A. Cultivation of <i>N. crassa</i> .	319
B. Purification of Aryl Aldehyde Dehydrogenase.	319
C. Colorimetic Detection of Aryl Aldehyde Dehydrogenase Activity.	326
References	328

LIST OF TABLES

Table 1. Comparison of Bulk Petrochemicals and Fermentation-Derived Chemicals.	6
Table 2. Plate Selection for Characterization of Genomic Insertion.	55
Table 3. Titters and Yields of PHB and Titters of Accumulated Metabolites.	75
Table 4. Chorismate Lyase Specific Activities.	85
Table 5. DAHP Synthase Specific Activities.	87
Table 6. Impact of PHB on DAHP Synthase Specific Activities.	91
Table 7. Plate Selection for 98042-42.	92
Table 8. Titters and Yields of PHB and Titters of Accumulated Metabolites for 98042-42.	94
Table 9. DAHP Synthase and Chorismate Lyase Specific Activities for 98042-42.	94
Table 10. Metabolite Comparison of PHB-Producers with and without Glucosyltrasferase Expression.	105
Table 11. Titters and Yields from reaction A.	140
Table 12. Titters and Yields from Reactions B and C.	142
Table 13. Results of Reactions A, B, and C.	149
Table 14. Results of Reactions D and E.	151
Table 15. Results of Reactions F, G, H, and I.	153
Table 16. Reduction of PHB to PHBA using <i>P. chrysosporium</i> : reactions A, B, C, and D.	163
Table 17. Titters and Yields of Shikimic acid and Titters of Accumulated Metabolites.	189
Table 18. Enzyme Activities for Shikimic Acid Producing Constructs.	203
Table 19. Comparison of Water's Properties at Different Temperatures.	214

Table 20. Conversion of Shikimic Acid to Phenol at Various Temperatures.	217
Table 21. Decarboxylation of <i>m</i> -Hydroxybenzoic Acid in the Presence of Copper Catalysts.	222
Table 22. Conversion of Fermentation Broth at Different Levels of Purity (Samples A-F) to Phenol	229
Table 23. Conversion of Sample A at Various Temperatures.	229
Table 24. Aryl Aldehyde Dehydrogenase Purification A.	322
Table 25. Aryl Aldehyde Dehydrogenase Purification B	323
Table 26. Aryl Aldehyde Dehydrogenase Purification C	325
Table 27. Aryl Aldehyde Dehydrogenase Purification D.	326

LIST OF FIGURES

Figure 1. Reichstein Synthesis of Ascorbic Acid.	3
Figure 2. Examples of Molecules Derived by Commercial Fermentation.	5
Figure 3. Common Pathway of Aromatic Amino Acid Biosynthesis	8
Figure 4. Biosynthesis of Tyrosine, Phenylalanine and Tryptophan from Chorismic Acid.	12
Figure 5. Biosynthesis of Aromatic Metabolites.	13
Figure 6. Biocatalytic Routes to Aspartame and Indigo.	15
Figure 7. Products Derived from DHS.	16
Figure 8. Comparison of Synthetic and Biocatalytic Routes to Vanillin.	17
Figure 9. Comparison of the Commercial and Biocatalytic Routes to Catechol.	20
Figure 10. Comparison of the Commercial and Biocatalytic Routes to Adipic Acid.	21
Figure 11. Comparison of the Commercial and Biosynthetic Routes to Gallic Acid.	23
Figure 12. Intracellular Uses of PEP: PTS Uptake System and Synthesis of DAHP.	27
Figure 13. Biosynthesis of E4P.	29
Figure 14. Rate-Limiting Enzymes in the Common Pathway.	32
Figure 15. Structures of Shikonin and Ubiquinone.	39
Figure 16. Biosynthesis of PHB in Microbes and Plants.	40
Figure 17. Structures of Xydar and Parabens.	41
Figure 18. Commercial Synthesis of PHB.	42
Figure 19. Serine Biosynthesis.	46
Figure 20. Preparation of Plasmid pJB2.8	50

Figure 21. Preparation of Plasmid pJB2.100.	51
Figure 22. Preparation of Plasmid pJB1.37	52
Figure 23. Preparation of Plasmid pJB2.102B.	53
Figure 24. Preparation of Plasmid pJB2.132	54
Figure 25. Restriction Map of Cassette	56
Figure 26. Southern Analysis of Strains D2704 and JB161 using a <i>serA</i> Probe.	57
Figure 27. Southern Analysis of pJB2.132), JB161, and KAD11D using an <i>aroL</i> Probe.	58
Figure 28. Preparation of Plasmid pJB1.137A.	63
Figure 29. Preparation of Plasmid pJB1.273A.	64
Figure 30. Preparation of Plasmid pJB2.125B.	65
Figure 31. Preparation of Plasmid pJB2.133.	66
Figure 32. Preparation of Plasmid pJB2.274.	67
Figure 33. Preparation of Plasmid pJB3.111A.	68
Figure 34. Preparation of Plasmid pJB3.127A	69
Figure 35. Preparation of Plasmid pJB3.144B.	70
Figure 36. B. Braun Fermentor.	72
Figure 37. Phenylalanine Synthesis in JB161.	76
Figure 38. JB161/pJB2.274	78
Figure 39. JB161(DE3)/pJB3.144B	79
Figure 40. RB38/pJB2.274	81
Figure 41. RB38(DE3)/pJB3.144B	82
Figure 42. Percent Inhibition of 3-Dehydroquinase Synthase by Tyrosine.	83

Figure 43. Specific Activities of Chorismate Lyase in the Presence of Various PHB Concentrations.	86
Figure 44. Construct KL3/pKL4.130B	89
Figure 45. KL3/pKL4.130B	89
Figure 46. 98042-42	95
Figure 47. Structures of PHB/Glucose Conjugates.	96
Figure 48. Synthesis of PHB <i>O</i> - β -D-Glucopyranoside.	97
Figure 49. Relative Toxicity of PHB and PHB <i>O</i> - β -D-Glucopyranoside	99
Figure 50. Preparation of Plasmid pJB5.203A	102
Figure 51. Preparation of Plasmid pJB5.205A	103
Figure 52. Control ¹ H NMR of PHB.	112
Figure 53. Control ¹ H NMR of Prephenic Acid.	113
Figure 54. Control ¹ H NMR of Phenylalanine.	114
Figure 55. Control ¹ H NMR of Tyrosine.	115
Figure 56. Control ¹ H NMR of DHS.	116
Figure 57. Control ¹ H NMR of DAH.	117
Figure 58. ¹ H NMR of a Typical JB161/pJB2.274 Fermentation Broth.	118
Figure 59. ¹ H NMR of a Typical RB38(DE3)/pJB3.144B Fermentation Broth.	119
Figure 60. ¹ H NMR of Synthesized PHB- <i>O</i> - β -D-Glucoside.	120
Figure 61. ¹ H NMR of JB161(DE34)/pJB2.274/pET-15b Culture Supernatant.	121
Figure 62. ¹ H NMR of JB161(DE34)/pJB2.274/pJB5.205A Culture Supernatant.	122
Figure 63. Structure of Hydroquinone and <i>p</i> -Cresol.	126

Figure 64. Yeast Catalyzed Reduction of Furfural to Furfuryl Alcohol.	127
Figure 65. Derivatives of Hydroquinone	130
Figure 66. Commercial Routes to Hydroquinone.	133
Figure 67. Environmentally Benign Synthesis of Hydroquinone from Glucose.	134
Figure 68. Schematic Structural Formula of Lignin, Adapted from Ander	136
Figure 69. Degradation Pathways for Vanillate in Microorganisms.	137
Figure 70. Reaction Stoichiometry for Vanillate Hydroxylase	138
Figure 71. Biotransformation of Fermentation-Derived PHB to Hydroquinone using <i>P. chrysosporium</i> .	144
Figure 72. Degradation of Hydroxylated Aromatics in <i>Pseudomonas</i> and <i>Candida</i> .	146
Figure 73. Reaction Stoichiometry for 4-Hydroxybenzoate 1-Hydroxylase.	147
Figure 74. Comparison of Hydroquinone Production in Reactions F, G, H, and I.	152
Figure 75. Structure of <i>o</i> -, <i>m</i> -, and <i>p</i> -Cresol.	155
Figure 76. Derivatives of <i>p</i> -Cresol.	156
Figure 77. Commercial Synthesis of <i>p</i> -Cresol via <i>p</i> -Toluenesulfonic acid.	157
Figure 78. Commercial Synthesis of <i>m</i> -, <i>p</i> -Cresol via Cymenes.	157
Figure 79. Benign Synthesis of <i>p</i> -Cresol	158
Figure 80. Relative Specific Activity of Aryl-Alcohol Dehydrogenase.	160
Figure 81. Reduction of <i>p</i> -Anisic Acid by White-Rot Fungi.	161
Figure 82. Reduction of Vanillate with <i>Pycnoporus cinnabarinus</i> .	161
Figure 83. Biotransformation of Fermentation-Derived PHB to PHBA using <i>P. chrysosporium</i>	164
Figure 84. Derivatives of <i>p</i> -Hydroxybenzaldehyde and PHBA.	170

Figure 85. Control ¹ H NMR of Hydroquinone.	171
Figure 86. Control ¹ H NMR of <i>p</i> -Hydroxybenzyl Alcohol.	172
Figure 87. Control ¹ H NMR of <i>p</i> -Cresol.	173
Figure 88. Typical ¹ H NMR of Hydroquinone Formation with <i>P. chrysosporium</i> .	174
Figure 89. Typical ¹ H NMR of Hydroquinone Formation with <i>Candida parapsilosis</i> .	175
Figure 90. Typical ¹ H NMR of <i>p</i> -Hydroxybenzyl Alcohol Formation with <i>P. chrysosporium</i> .	176
Figure 91. Environmentally Benign Synthesis of Phenol from Glucose	182
Figure 92. Environmentally Benign Synthesis of 1,2,3,4-Tetrahydroxybenzene from Glucose.	183
Figure 93. Structure of Tamiflu.	185
Figure 94. Bioynthesis of Shikimic Acid and Quinic Acid.	186
Figure 95. Shikimic Acid-Producing <i>E. coli</i> Construct SP1.1/pKD12.112.	188
Figure 96. Shikimic Acid-Producing <i>E. coli</i> Construct SP1.1/pKD12.138.	188
Figure 97. Preparation of JB4.	195
Figure 98. Preparation of Plasmid pJB5.272A.	196
Figure 99. Preparation of Plasmid pJB3.141.	197
Figure 100. Preparation of Plasmid pJB5.291	198
Figure 101. JB4/pJB5.291 at 33 °C.	200
Figure 102. JB4/pJB5.291 at 36 °C.	201
Figure 103. Percent Inhibition of Shikimate Dehydrogenase Specific Activity by Shikimic Acid.	206
Figure 104. Lineweaver-Burk Plot of SP3 Inhibition by Product Shikimate with DHS Substrate.	207

Figure 105. Dixon Plot of SP3 Inhibition by Product Shikimate with DHS Substrate.	207
Figure 106. Hanes-Woolf Plot of SP3 Inhibition by Product Shikimate with DHS	208
Figure 107. Determination of K_M and V_{MAX} for SP3 with DHQ as Substrate.	208
Figure 108. Structure of Phenol.	209
Figure 109. Hock Process for the Manufacture of Phenol.	210
Figure 110. Major Products Derived from Phenol.	211
Figure 111. Conversion of Shikimic Acid to PHB via Acid Catalyzed Dehydration.	213
Figure 112. Conversion of Shikimic Acid to Phenol at Various Temperatures.	218
Figure 113. Proposed Mechanism for the Conversion of Shikimic Acid to Phenol.	220
Figure 114. Overall Conversion of Glucose to Phenol.	223
Figure 115. Shikimic Acid Producing Construct SP1.1/pSC5.112.	224
Figure 116. Preparation of Samples A-F.	225
Figure 117. Concentration of Shikimic Acid Remaining in the Aqueous Layer over Time.	231
Figure 118. Control 1H NMR of Shikimic Acid.	234
Figure 119. Control 1H NMR of Quinic Acid.	235
Figure 120. Typical 1H NMR of JB4/pJB5.291 (36 °C) Fermentation Broth.	236
Figure 121. In vitro Accumulation of Quinic Acid with <i>KL3aroD</i> -/pJB5.272A lysate.	237
Figure 122. 1H NMR of Shikimic Acid and 3- <i>epi</i> -Shikimic Acid Generated by the Reduction of DHS.	238
Figure 123. Synthetic Route to Natural Vanillin.	243

Figure 124. SDS-PAGE gel of Proteins Submitted for Sequencing.	246
Figure 125. HPLC Trace of Eluted Protein from the Superdex Column	248
Figure 126. Structure of Pararosaniline.	249

LIST OF ABBREVIATIONS

ADC	4-amino-4-deoxychorismic acid
AMP	adenosine monophosphate
ATP	adenosine triphosphate
Ap	ampicillin
bp	base pair
BSTFA	N,N-bis(trimethylsilyl) trifluoroacetamide
CA	chorismic acid
cAMP	cyclic adenosine monophosphate
cDNA	complimentary DNA
FADH ₂	flavin adenine dinucleotide, reduced form
CIAP	calf intestinal alkaline phosphatase
Cm	chloramphenicol
COMT	catechol- <i>O</i> -methyltransferase
DAH	3-deoxy- <i>D-arabino</i> -heptulosonic acid
DAHP	3-deoxy- <i>D-arabino</i> -heptulosonic acid 7-phosphate
DCU	digital control unit
DEAE	diethylaminoethyl
2, 3-DHB	2,3-dihydroxybenzoic acid
DHQ	3-dehydroquinic acid
DHS	3-dehydroshikimic acid
L-DOPA	L-3,4-dihydroxyphenylalanine
DO	dissolved oxygen
DTT	dithiothreitol
E4P	D-erythrose 4-phosphate

EPSP	5-enolpyruvoylshikimate 3-phosphate
FBR	feedback resistant
FBS	feedback sensitive
GA	gallic acid
h	hour
HPLC	high pressure liquid chromatography
HQ	hydroquinone
IPTG	isopropyl β -D-thiogalactopyranoside
Kan	kanamycin
kb	kilobase
kg	kilogram
Ki	inhibition constant
Km	Michaelis constant
M	molar
MHB	<i>m</i> -hydroxybenzoic acid
min	minute
mL	milliliter
μ L	microliter
mM	millimolar
μ M	micromolar
MOPS	4-morpholinepropanesulfonic acid
mRNA	messenger RNA
MSG	monosodium glutamate
NADP	nicotinamide adenine dinucleotide phosphate, oxidized form
NADPH	nicotinamide adenine dinucleotide phosphate, reduced form

NMR	nuclear magnetic resonance spectroscopy
OD	optical density
ORF	open reading frame
PABA	<i>p</i> -aminobenzoic acid
PCA	protocatechuic acid
PEG	polyethylene glycol
PEP	phosphoenolpyruvic acid
pfu	plaque forming units
PHB	<i>p</i> -hydroxybenzoic acid
PHBA	<i>p</i> -hydroxybenzyl alcohol
PID	proportional-integral-derivative
Pck	PEP carboxykinase
PCR	polymerase chain reaction
Phe	L-phenylalanine
PMSF	phenylmethylsulfonyl fluoride
Ppc	PEP carboxylase
Pps	PEP synthase
psi	pounds per square inch
PTS	phosphotransferase system
QA	quinic acid
RBS	ribosome binding site
rpm	rotations per minute
SA	shikimic acid
SAM	<i>S</i> -adenosylmethionine
SDS	sodium dodecyl sulfate
S3P	shikimate 3-phosphate

Spec	spectinomycin
SP3	cDNA of tobacco AroD·AroE
TBA	thiobarbituric acid
Tc	tetracycline
Tc ^R	tetracycline resistant
Tc ^S	tetracycline sensitive
TCA	tricarboxylic acid
Trp	L-tryptophan
TSP	sodium 3-(trimethylsilyl)propionate-2,2,3,3- <i>d</i> ₄
Tyr	L-tyrosine
UDP	uridine diphosphate
UV	ultraviolet
V _{max}	maximal velocity
yr	year

Chapter One

ALTERNATIVE CHEMICAL SYNTHESIS:

BIOCATALYSIS AND THE SHIKIMATE PATHWAY

Introduction

During the past half-century, nonrenewable petroleum and natural gas have been not only an important source of energy, but also the primary feedstock for the manufacture of organic chemicals. In the 1950's, the increased availability of petroleum and natural gas led to their use as a raw material for chemical manufacture and an explosion of organic secondary products.¹ Today, approximately 95% of the petrochemical-based products are derived solely from oil and natural gas.² Of the chemicals obtained from fossil fuels, aromatic compounds are some of the most important, serving as starting materials for plastics, synthetic rubber and fibers, as well as pharmaceuticals. Currently, aromatics are obtained almost exclusively from fossil fuels and in 1990, 98% of aromatic compounds were derived from oil alone.³

As the worldwide demand for energy and manufactured goods continue to climb, the reserves of oil and natural gas dwindle. Current estimates predict that known crude oil reserves will be depleted by 2039 and natural gas reserves will be spent by 2050.⁴ While the utilities industry has focused attention on developing new sources of energy such as solar and nuclear power, less has been done by the chemical industry to curb its use of petroleum as a feedstock. While waste reduction and increased manufacturing

efficiency will help extend fossil fuel reserves, new technologies that are able to access the carbon locked in renewable feedstocks, such as lignin, cellulose, and starch, offer a permanent solution.

This dissertation explores the development of environmentally benign routes to commercially important aromatic compounds that originate with D-glucose and proceed through microbe-catalyzed, enzyme-catalyzed, or benign reaction conditions. Chapter one will present an overview of biocatalysis and a brief review of the use of the common pathway of aromatic amino acid biosynthesis in *Escherichia coli* to synthesize chemicals. In chapter two, the synthesis of *p*-hydroxybenzoic acid (PHB) from glucose using an *Escherichia coli* biocatalyst will be presented. Synthesized by manipulation of the common pathway, the outlined route to PHB provides a direct comparison of traditional chemical manufacture to biocatalysis. Chapter three of this dissertation will show how biocatalytically prepared PHB can be converted to hydroquinone and *p*-cresol using vanillate hydroxylase and vanillate reductases from the white-rot fungus *Phanerochaete chrysosporium* and 4-hydroxybenzoate hydroxylase from *Candida parapsilosis*. The combination of biocatalysis with benign, abiotic chemical synthesis is illustrated in chapter four with the conversion of biocatalytically derived shikimic acid to phenol under subcritical water reaction conditions.

I. Biocatalysis

The development of biocatalysis in conjunction with fermentation technology has been a major step towards the incorporation of renewable raw materials into mainstream chemical manufacture.⁵ Biocatalysis in its simplest form is the use of enzymes to

catalyze chemical reactions. Enzymes offer unparalleled chemoselectivity, regioselectivity, and enantioselectivity in a wide variety of reactions. Either as part of an intact microorganism or in purified form, enzymes such as lipases, hydrolases, and oxidoreductases have been successfully used in chemical synthesis.⁶ A commercial use of biocatalysis is the production of L-ascorbic acid (vitamin C) which has depended on the oxidation of sorbitol to sorbose by the bacterium *Acetobacter suboxydans* for more than 70 years (Figure 1).⁷ Today the Reichstein synthesis for ascorbic acid is responsible for 50,000 tons of this commodity chemical annually.⁸ Since it is estimated that 70% of pharmaceuticals will be required to be enantiomerically pure in the near future, compared to 25% today,⁹ industrial-scale biocatalysis will continue to be an important aspect of chemical manufacture.

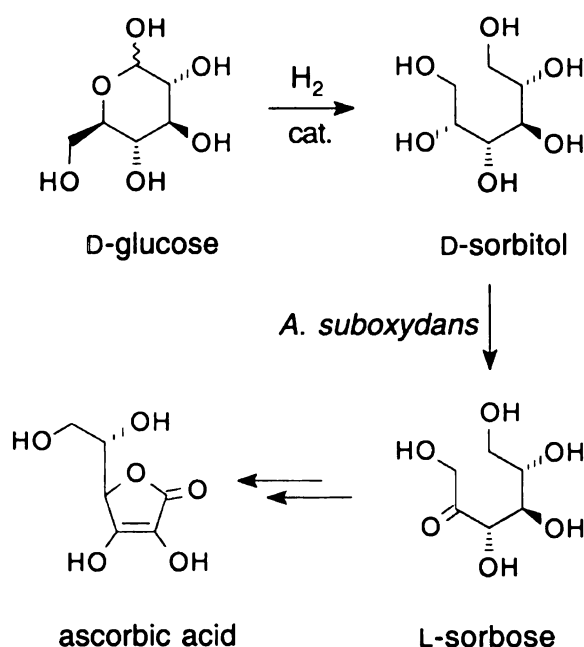


Figure 1. Reichstein Synthesis of Ascorbic Acid.

Besides the reaction specificity gained by enzymatic catalysis, two additional advantages set biocatalysis aside from traditional synthesis. Traditional chemical synthesis often employs harmful reagents, organic solvents, and extreme reaction conditions while generating hazardous waste streams. Alternatively, biocatalysis usually begins with non-toxic starting materials and proceeds through benign intermediates. These biotransformations are usually done under aqueous conditions at ambient temperatures and pressures. The other significant advantage biocatalysis offers over traditional chemical manufacture is the ability to utilize the carbon in renewable feedstocks.

Fermentation technology, the controlled growth of a microorganism, has been used for centuries. The conversion of carbohydrates to ethanol by *Saccharomyces cerevisiae* (yeast) in the manufacture of alcoholic beverages and the use of the fungus *Aspergillus niger* for the manufacture of soy sauce are just a few examples.¹⁰ Yields of fermentation products have increased in recent years due to improved reactor design, process control, and product recovery. Continued improvements in fermentor engineering and biocatalyst construction have allowed industrial biocatalysis to become an economically viable alternative to traditional chemical manufacture.

In 1997, more than 15 million tons of glucose were produced worldwide.¹¹ Isolated from a variety of sources, such as corn and molasses (cane and sugar beet), glucose is currently the starting material for such high volume chemicals as ethanol, L-lysine, and citric acid. In the United States alone, 94% of the fuel-grade ethanol is derived from *Saccharomyces cerevisiae* fermentations (Figure 2).¹² Most of the four million tons of ethanol produced annually in the U.S. (13 million tons worldwide) is used

as a gasoline additive.¹³ With other oxygen-rich additives such as methyl *t*-butyl ether coming under fire for groundwater contamination, the use of ethanol as a fuel oxidant could be expanded in the future.

Most of the cereal grains used for animal feed are deficient in the essential amino acid lysine (Figure 2). This creates a large demand for a chemical unattainable from petroleum feedstocks. While isolation from natural sources such as soybean meal represent a portion of the lysine market, fermentation-derived lysine accounts for the majority of the \$450 million a year market.¹⁴ Commercial fermentations of *Corynebacterium glutamicum* can reach titers of 170 g/L in a 54% yield from glucose (Figure 2).¹⁵

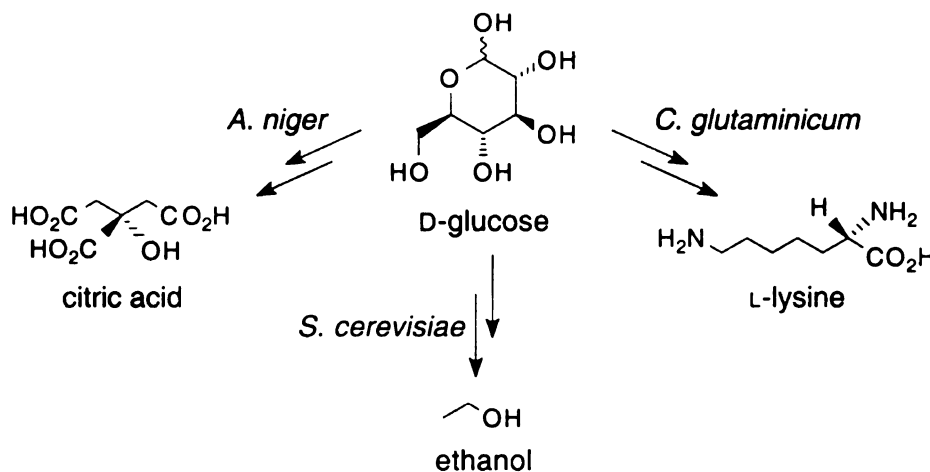


Figure 2. Examples of Molecules derived by Commercial Fermentation.

Worldwide production of citric acid, the major food acidulant, is approaching one million tons per year.¹⁶ Microbial production of citric acid was begun in 1923 by Pfizer, Inc. using certain strains of *Aspergillus niger* (Figure 2). Today, 90% of the citric acid market is still produced using *A. niger* in conjunction with improved culturing

techniques.¹⁷ The submerged process known as deep tank fermentation developed in the 1970's significantly improved the rate of citrate formation.¹⁸ Literature claims citric acid yields as high as 70% from the starting sugar.¹⁹ Interestingly, traditional chemical routes to citric acid have failed to become economically viable, leaving the remaining 10% of the citric acid market derived from lemon juice and pineapple wastes.²⁰ Together, the commercial routes to ethanol, lysine, and citric acid prove the feasibility of large-scale chemical manufacture from renewable feedstocks and biocatalysis, as they are at par with lower scale petrochemical bulk production (Table1).²¹

Table 1. Comparison of Bulk Petrochemicals and Fermentation-Derived Chemicals.

bulk petrochemicals	tons/year *	bulk biochemicals	tons/year *
benzene	2.3×10^7	glucose	1.5×10^6
phenol	5×10^6	ethanol	1.3×10^6
adipic acid	5×10^6	citric acid	8.0×10^5
isopropanol	2×10^6	L-lysine	3.5×10^5

* worldwide estimates for 1997

II. The Common Pathway of Aromatic Amino Acid Biosynthesis.

A. The Shikimate Pathway of *Escherichia coli*.

The three aromatic amino acids tyrosine, phenylalanine, and tryptophan are synthesized only by plants, bacteria, and fungi through the common pathway of aromatic amino acid biosynthesis.²² Also known as the shikimate pathway, after the first identified intermediate, it is unique not only as a way nature biosynthesizes aromatic compounds but also because of its absence in mammals. The biosyntheses of aromatic metabolites in microbes are derived from the aromatic amino acids or intermediates of the shikimate pathway.²³ The presence of the pathway in bacteria but not in humans also provides an opportunity for development of enzyme-targeted herbicides and antibiotics.

Interest in the shikimate pathway has led to the elucidation of all the genes, enzymes, and intermediates necessary for the production of tyrosine, phenylalanine, and tryptophan. Description of aromatic amino acid biosynthesis is best done in two parts; synthesis of the last common intermediate chorismic acid (Figure 3) and conversion of chorismic acid to the aromatic amino acids through three terminal pathways (Figure 4).

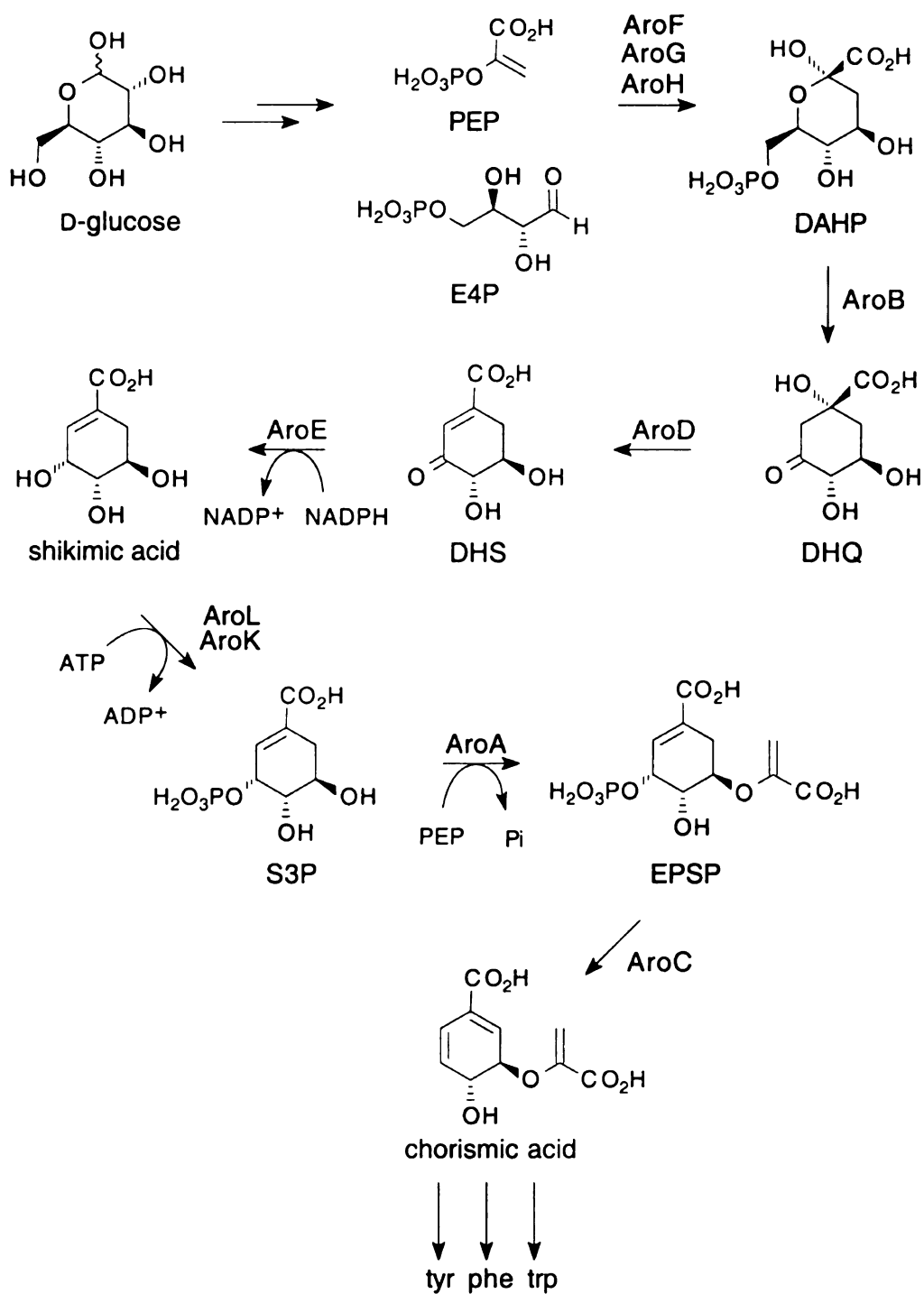


Figure 3. Common Pathway of Aromatic Amino Acid Biosynthesis. Enzymes are as follows: AroF, AroG, AroH: 3-deoxy-D-arabino-heptulosonate 7-phosphate (DAHP) synthase; AroB: 3-dehydroquinic acid (DHQ) synthase; AroD: DHQ dehydratase; AroE: shikimate dehydratase; AroL, AroK: shikimate kinase; AroA: 5-enolpyruvoylshikimate 3-phosphate (EPSP) synthase; AroC: chorismate synthase.

Chorismic acid is synthesized from phosphoenolpyruvate (PEP) and erythrose 4-phosphate (E4P) by seven enzymatic steps.²⁴ Carbon flow through the shikimate pathway is tightly controlled through transcriptional regulation and feedback inhibition of key enzymes. This level of control follows from the fact that the aromatic amino acids are the most energetically expensive of all the amino acids to biosynthesize as represented by the 78 moles of adenosine triphosphate (ATP) required to synthesize one mole of tryptophan.²⁵

Careful regulation of cellular resources is evidenced by the condensation of PEP and E4P to give 3-deoxy-D-*arabino*-heptulosonate 7-phosphate (DAHP).²⁶ This reaction, the first committed step of the shikimate pathway, is catalyzed by DAHP synthase whose activity is modulated by feedback inhibition, transcriptional control, and proteolytic degradation.²⁷ DAHP synthase is encoded by three isozymes which are subject to feedback inhibition by the three amino acid end products. The majority of DAHP synthase activity is contributed by the phenylalanine-sensitive isozyme, encoded by *aroG*, and the tyrosine-sensitive isozyme, encoded by *aroF*. The third, tryptophan-sensitive isozyme, encoded by *aroH*, constitutes only a trace amount of total DAHP synthase activity. Expression of *aroG* and *aroF* are also controlled by the TyrR protein.²⁸ Transcription of the two isozymes is prevented when the regulatory protein, encoded by *tyrR*. In the presence of tyrosine and/or tryptophan, TyrR binds to specific sequences upstream of the *aroG* and *aroF* known as *tyrR* boxes. It is also known that the tyrosine-sensitive DAHP synthase is subject to degradation by specific proteases when cells reach stationary growth phase or during starvation.

Once carbon is committed to the pathway as DAHP, it is converted to the six-membered carba-cyclic ring of 3-dehydroquinic acid (DHQ) by the enzyme DHQ synthase, encoded by *aroB*.²⁹ *Syn*-dehydration of the C-1 hydroxyl group of DHQ yields the α - β unsaturated ketone of the next intermediate 3-dehydroshikimic acid (DHS). Formation of DHS is catalyzed by DHQ dehydratase, which is encoded by *aroD*.³⁰ DHS is subsequently reduced to shikimic acid by the NADPH-dependant enzyme shikimate dehydrogenase. This reversible enzyme is encoded by *aroE*.³¹ Phosphorylation of the C-3 hydroxyl group of shikimic acid to yield shikimate 3-phosphate (S3P) is catalyzed by shikimate kinase at the expense of ATP. Shikimate kinase is encoded by two isozymes *aroL*³² and *aroK*³³, of which AroL is the major contributor of shikimate kinase activity due to its lower K_M relative to AroK (AroL: $K_M = 200 \mu\text{M}$, *aroK*: $K_M = 5 \text{ mM}$).³⁴ The *aroL* isozyme is also subject to transcriptional control by the TyrR protein.³⁵ A second mole of PEP is reacted with S3P to give 5-enol-pyruvoylshikimate 3-phosphate (EPSP) and inorganic phosphate. The formation of EPSP is catalyzed by EPSP synthase, which is encoded by *aroA*.³⁶ A *trans*-1,4-elimination of orthophosphate from EPSP introduces a second double bond into the ring to give chorismic acid. This elimination is catalyzed by chorismate synthase, which is encoded by *aroC*.³⁷

Chorismic acid is the last common intermediate en route to the aromatic amino acids as well as other aromatic metabolites. The two terminal pathways leading to tyrosine and phenylalanine first proceed through prephenic acid intermediacy (Figure 4). Two bifunctional enzymes are responsible for the Claisen rearrangement of chorismate to prephenate; chorismate mutase-prephenate dehydrogenase, encoded by *tyrA*,³⁸ and chorismate mutase-prephenate dehydratase, encoded by *pheA*.³⁹ The Claisen

rearrangement, a conversion rarely catalyzed by enzymes, has also been shown to proceed non-enzymatically although at a slower rate. To protect cellular levels of chorismic acid, the enzymatic conversion to prephenate is regulated by both feedback inhibition as well as transcriptional repression. Both reactions of TyrA and PheA are inhibited by their respective end-products tyrosine and phenylalanine. The *tyrA* locus is also part of the *tyr* regulon and transcription is prevented in the presence of the TryR and tyrosine. Expression of *pheA* is believed to be part of a monocistronic operon controlled by PheR and mediated through intracellular phenylalanine concentrations.

The second enzyme activities encoded by *tryA* and *pheA* catalyze a decarboxylation to yield *p*-hydroxyphenylpyruvic acid in the case of chorismate mutase-prephenate dehydrogenase and a sequential dehydration/decarboxylation to yield phenylpyruvic acid for chorismate mutase-prephenate dehydratase (Figure 4). The same enzyme, aromatic amino transferase, transaminates *p*-hydroxyphenylpyruvic acid and phenylpyruvic acid to give tyrosine and phenylalanine respectively while utilizing a molecule of glutamate as a nitrogen donor. The gene responsible for the transamination, *tyrB*,⁴⁰ is also under transcriptional control of TyrR.⁴¹

The terminal pathway from chorismic acid to tryptophan proceeds through five enzymatic steps (Figure 4). Anthranilate synthase and anthranilate phosphoribosyltransferase form a tetrameric enzyme complex that is responsible for the overall conversion of chorismate and glutamine to phosphoribosyl anthranilate. Activities of the polypeptides comprising the active complex, specified by *trpE* and *trpD*, are tightly controlled by tryptophan levels via feedback inhibition.⁴²

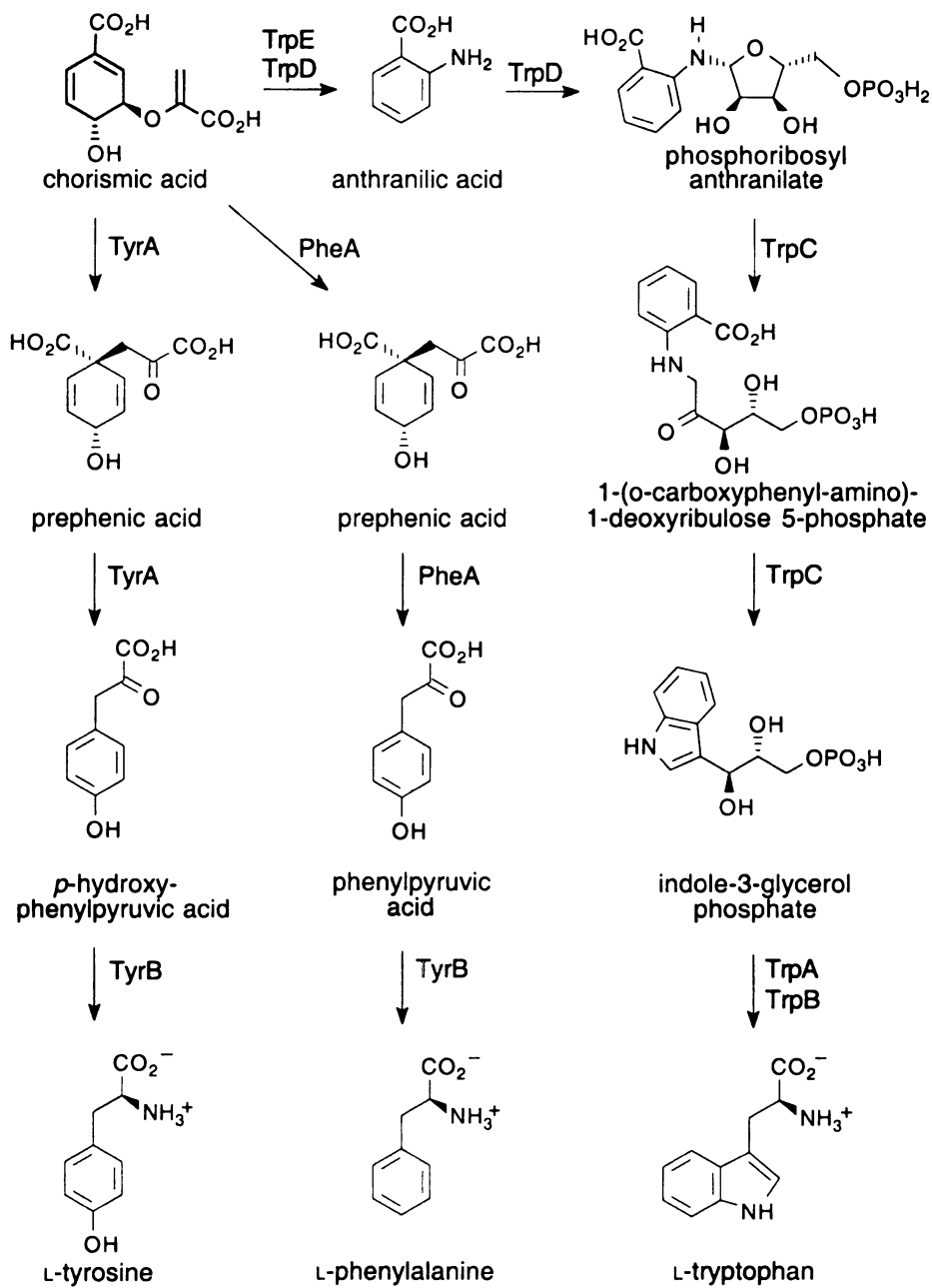


Figure 4. Biosynthesis of Tyrosine, Phenylalanine and Tryptophan from Chorismic Acid.

Chorismic acid also serves as the branch point for the biosynthesis of the aromatic metabolites folic acid, enterochelin, and ubiquinone (Figure 5). Folic acid is a substrate for coenzyme biosynthesis, enterochelin chelates iron for cellular uptake, and ubiquinone is involved in electron transport.⁴³ The amount of carbon leading to these terminal pathways represents a small drain on the chorismate pool when compared to the relative amount of tyrosine and phenylalanine biosynthesized.

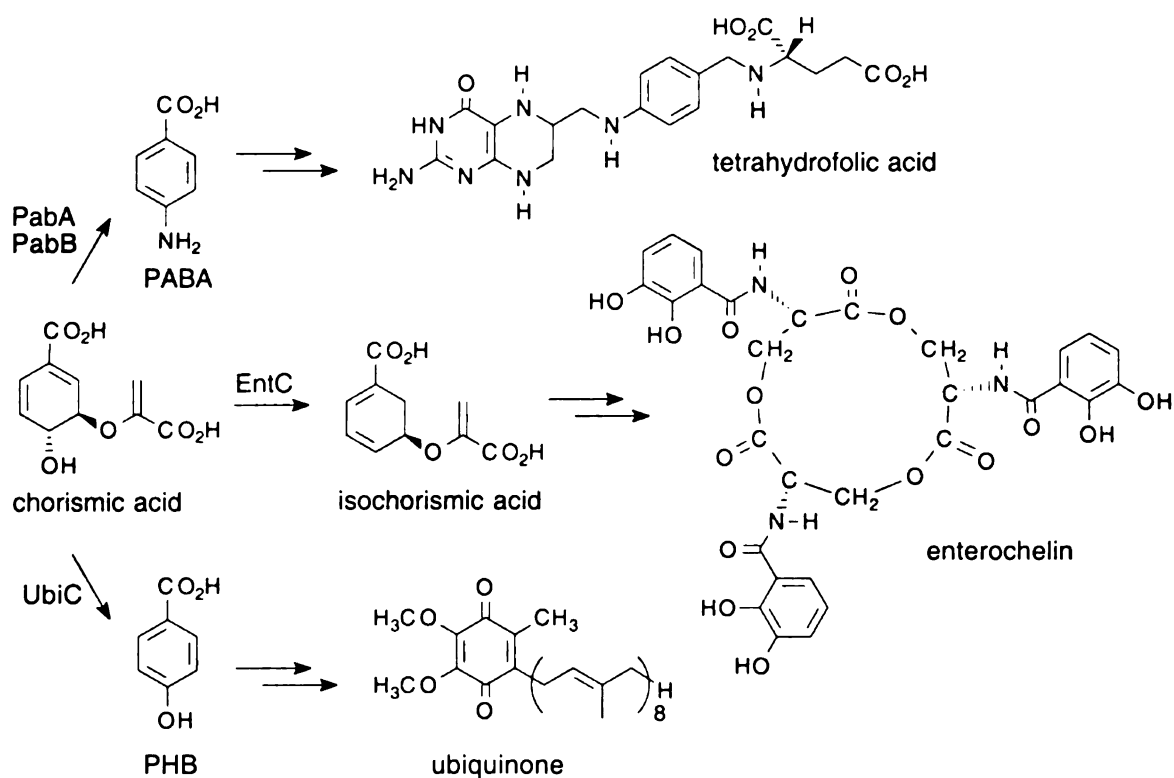


Figure 5. Biosynthesis of Aromatic Metabolites.

B. Microbial Synthesis of Chemicals Derived from the Shikimate Pathway

The shikimate pathway can be a valuable resource for the production of valuable chiral synthons and aromatic molecules. Microbial synthesis of common pathway intermediates offers routes to molecules that are synthetically challenging due to their multiple stereocenters or are difficult to purify from nature. Production of aromatics via modification of the shikimate pathway also offers environmentally appealing routes to compounds that are traditionally derived from petroleum and incorporate hazardous reagents and intermediates.

As aromatic amino acids are the major products of the shikimate pathway in microorganisms, it follows that the pathway can be utilized for their commercial manufacture. Phenylalanine and tryptophan are prominent examples of compounds synthesized microbially for use as both feed supplements and as starting materials for other commercially important compounds. Phenylalanine when coupled either chemically or enzymatically with L-aspartate yields the low-calorie sweetener aspartame (Figure 6).⁴⁴ Marketed under the tradename Nutrasweet, its sales represent the largest volume of all food additives. Indigo (Figure 6) can be produced in a tryptophan-synthesizing microbe by expressing naphthalene dioxygenase and tryptophanase in the same biocatalyst.⁴⁵ Indigo, the dye responsible for the color of blue jeans, is the largest volume dye produced worldwide.

Engineering biocatalysts to produce common pathway intermediates can provide a manufacturing platform for many other commercial chemicals. Microbial production of

3-dehydroshikimic acid (DHS) provides an excellent example. By making a strain of *E. coli* auxotrophic in shikimate dehydrogenase, DHS accumulates and is exported into the culture supernatant. Published reports show that DHS-producing biocatalysts can reach titers of 69 g/L when cultured under fed-batch fermentor conditions resulting in a 30% yield from glucose.⁴⁶ Current work by the Frost group has increased titers to 74 g/L in 38% yield.⁴⁷ DHS, besides having potent antioxidant activity, is the most advanced intermediate shared by both aromatic amino acid biosynthesis and routes to vanillin, catechol, *cis,cis*-muconic acid, and gallic acid (Figure 7).

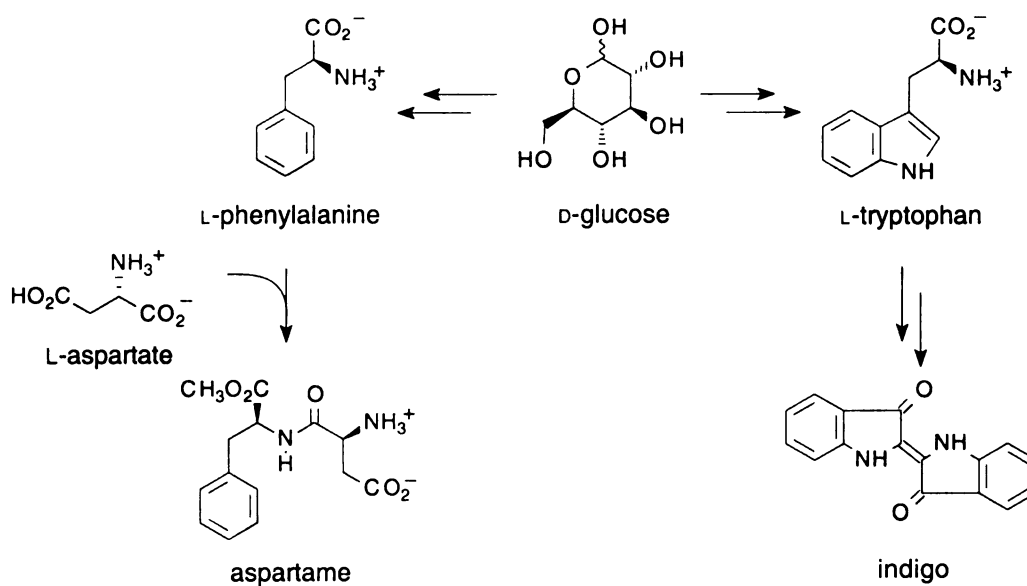


Figure 6. Biocatalytic Routes to Aspartame and Indigo.

Vanillin

Heterologous expression of the DHS dehydratase locus, *aroZ*,⁴⁸ in a DHS overproducing *E. coli* strain leads to the formation of protocatechuic acid (PCA) (Figure 8). Subsequent expression of rat-liver catechol-*O*-methyltransferase (COMT) cDNA in

the biocatalyst yields a strain that can synthesize 5.0 g/L of vanillic acid when cultured under fed-batch fermentor conditions. Isolated vanillic acid can then be enzymatically converted to vanillin in a 66% yield using aryl-aldehyde dehydrogenase partially purified from the fungus *Neurospora crassa*.⁴⁹

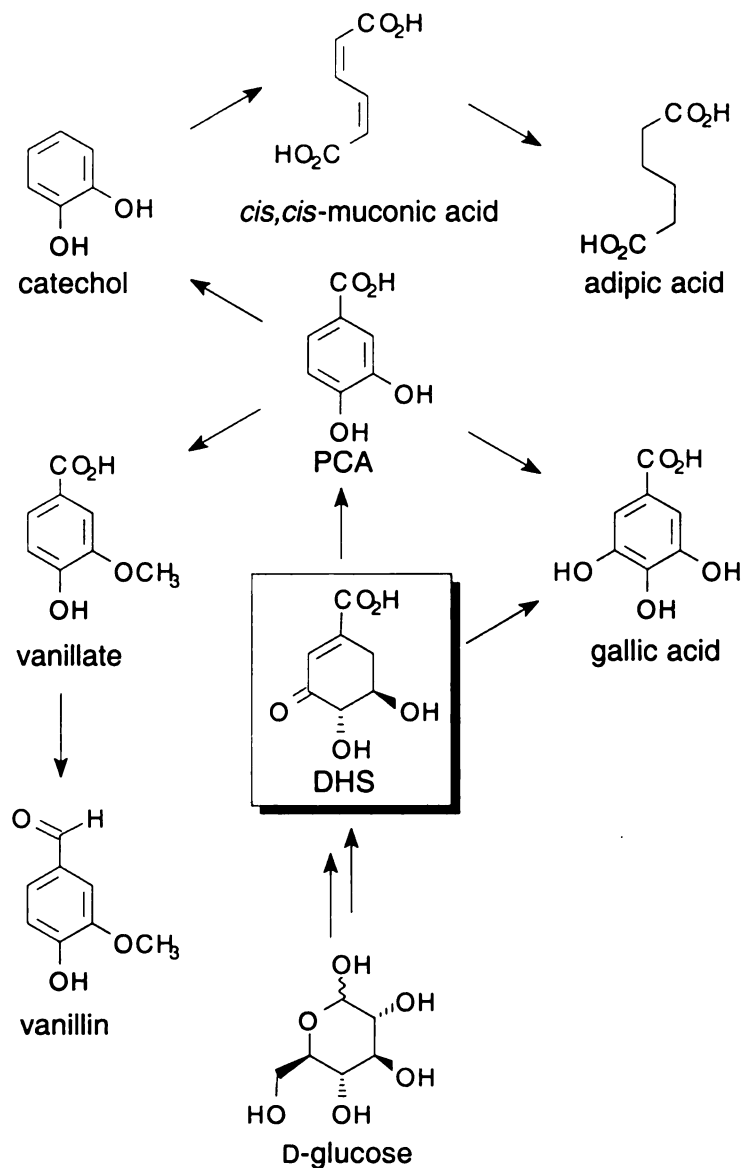


Figure 7. Products Derived from DHS.

The environmental aspects of this biosynthetic route to vanillin are superior when compared to the commercial route to synthetic vanillin (Figure 8). Originating with a catechol, a benzene-derived, nonrenewable starting material, the process proceeds with methylation via dimethyl sulfate to afford guaiacol. Condensation of guaiacol with glyoxylic acid produces 4-hydroxy-3-methoxymandelic acid. Air oxidation of the α -hydroxyl group to yield 4-hydroxy-3-methoxyphenyl glyoxylic acid followed by acid-promoted decarboxylation gives crude vanillin. Vacuum distillation and subsequent recrystallization produces commercial grades of vanillin. Besides being derived from carcinogenic benzene, catechol is toxic and corrosive while guaiacol is listed as a toxic irritant. The reagent dimethyl sulfate is also highly toxic and a cancer-suspect agent. Comparatively, the biocatalytic route to vanillin starts with renewable, nontoxic glucose and proceeds through benign intermediates.⁵⁰

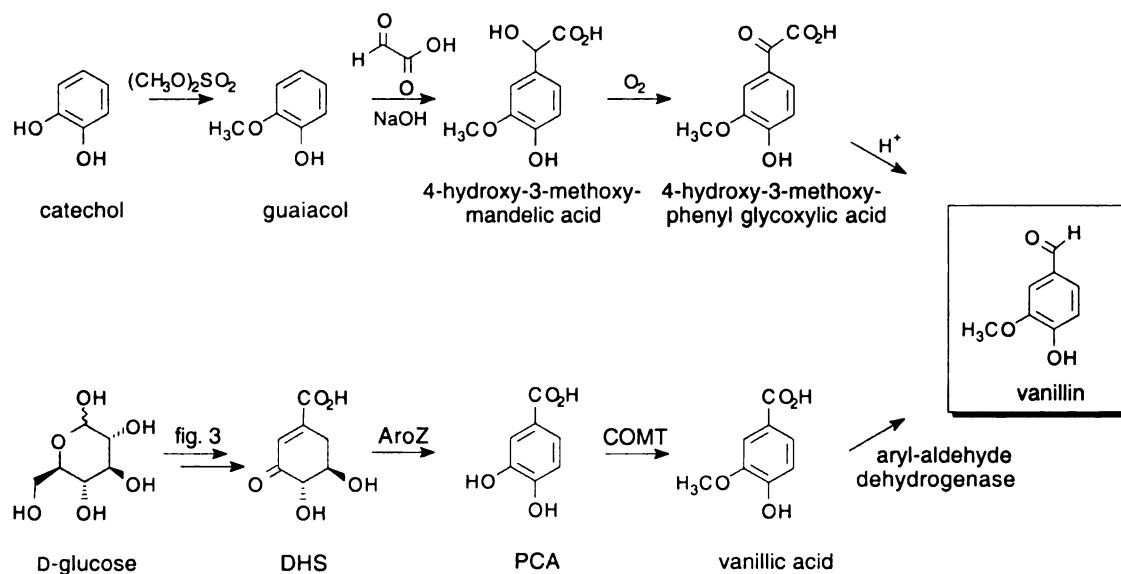


Figure 8. Comparison of Synthetic and Biocatalytic Routes to Vanillin.

The outlined synthesis of vanillin from glucose is important not only in its utilization of renewable feedstocks and benign reaction conditions but also because it can be sold as natural vanillin. As the major flavor component of vanilla, vanillin represents one of the most important compounds in the food and fragrance industry. With global production of 12×10^6 kg annually⁵¹, vanillin is second only to aspartame as a food additive, ahead of both citric acid and monosodium glutamate (MSG). Due to the difficulty of isolating vanilla directly from vanilla beans and the enhanced marketability that comes with the “natural” label, this combined microbial and enzymatic route to vanillin holds significant commercial value.

Catechol and Adipic Acid

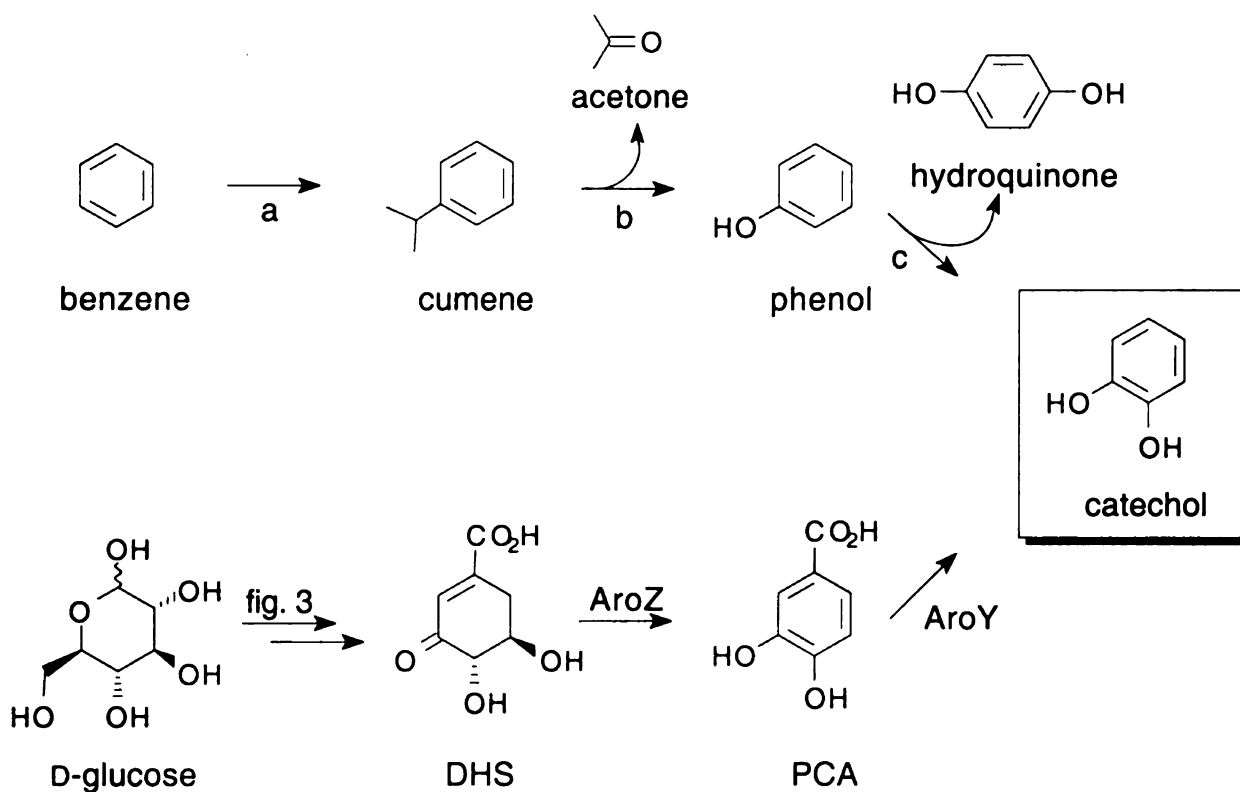
Other microbially produced chemicals proceeding through DHS intermediacy include catechol and *cis,cis*-muconic acid (Figure 7), which upon hydrogenation yields adipic acid. In addition to vanillin, catechol serves as a starting material for pharmaceuticals (L-Dopa, adrenaline, papaverine), flavors (eugenol, isoeugenol), agrochemicals (carbofuran, propoxur), and polymerization inhibitors and antioxidants (4-*tert*-butylcatechol, veratrol).⁵² Most of the 8.8×10^9 kg of adipic acid produced annually is funneled into the production of nylon-6,6.⁵³ A condensation polymer of adipic acid and hexamethylenediamine, nylon-6,6 is used for fabrics, tire reinforcements, and plastics.

The biosynthetic route to catechol also relies on the heterologous expression of DHS dehydratase in an *E. coli* host strain deficient in shikimate dehydrogenase (Figure 9).⁵⁴ As with vanillin, this phenotype allows for the accumulation of PCA. Cloning of

the *aroY* locus from *Klebsiella pneumoniae* into the biocatalyst allows for PCA decarboxylase mediated conversion of PCA to catechol. In shake flask experiments, catechol was established as the only product formed by ¹H NMR.

Biocatalytically produced catechol stands unopposed to the abiotic commercial route on environmental and safety issues. Catechol manufacture begins with a Friedel-Crafts alkylation of benzene to afford cumene (Figure 9).⁵⁵ Conversion to phenol is accomplished by the Hock process. Air oxidation of cumene to cumene hydroperoxide followed by subsequent proton-catalyzed cleavage affords acetone and phenol. Oxidation of phenol with 70% hydrogen peroxide in the presence of metal catalysts or with performic acid produces a mixture of catechol and hydroquinone. The mixture of 1,2- and 1,4-dihydroxybenzenes are then separated by distillation. Nonrenewable raw materials and harmful reagents and intermediates in the form of explosive peroxides and corrosive phenol will plague this route as chemical manufactures face ever tightening governmental and social policies.

A *cis,cis*-muconic acid producing biocatalyst is easily obtained from a catechol-producing microbe with the inclusion of the *catA* gene (Figure 10). Encoding for catechol 1,2-dioxygenase, this gene was isolated from *Acinetobacter calcoaceticus* as part of the benzoate branch of the β -ketoacid pathway.⁵⁶ Hydrogenation of the cell-free culture supernatant with 10% Pt on carbon at 50 psi and room temperature converts the *cis,cis*-muconic acid to adipic acid. Current work has enabled titers of *cis,cis*-muconic acid to reach 37 g/L in a fed-batch fermentation (Figure 10).⁵⁷



a = propylene, solid H_3PO_4 catalyst, 200-260 °C, 400-600 psi

b = i) O_2 , 80-130 °C, ii) SO_2 , 60-100 °C

c = 70% H_2O_2 , EDTA, Fe^{2+} or Cu^{2+} , 70-80 °C

Figure 9. Comparison of the Commercial and Biocatalytic Routes to Catechol.

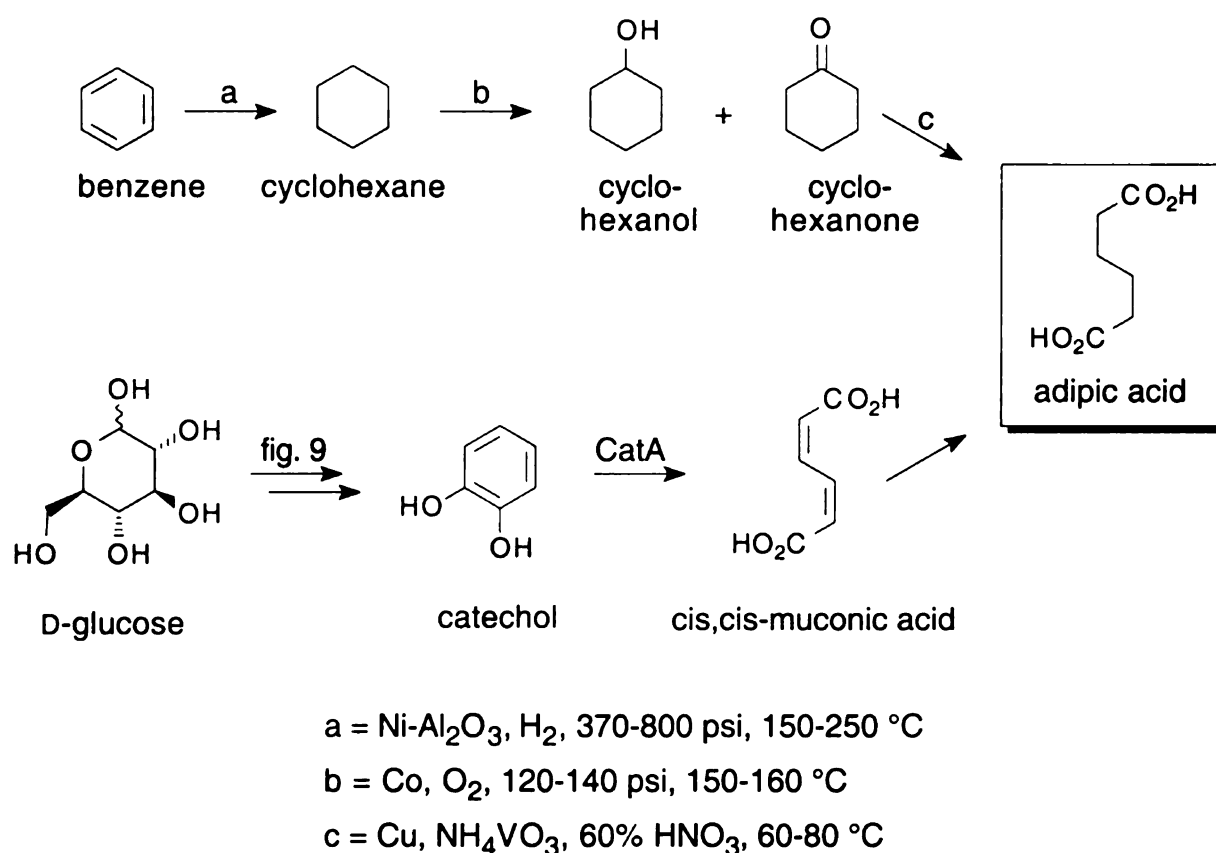


Figure 10. Comparison of the Commercial and Biocatalytic Routes to Adipic Acid.

The biocatalytic route from glucose to adipic acid via *cis,cis*-muconic acid is superior to the commercial process which is a benzene-derived route that proceeds through harsh reaction conditions. The current commercial manufacture of adipic acid also yields significant amounts of nitrous oxide, which is a known greenhouse gas and can lead to ozone depletion. The quantity of adipic acid produced is believed to contribute as much as 10% to the annual rise in atmospheric nitrous oxide levels.⁵⁸ The commercial route to adipic acid begins with the metal-catalyzed hydrogenation of benzene to cyclohexane (Figure 10).⁵⁹ Cobalt-mediated air oxidation of cyclohexane yields a mixture of cyclohexanol and cyclohexanone. Adipic acid manufacture is completed with nitric acid oxidation of this mixture.

Gallic Acid

3,4,5-Trihydroxybenzoic acid, known more commonly as gallic acid, is another molecule derived from DHS and PCA. Gallic acid is currently obtained by the hydrolysis of tannins isolated from gallnuts, Aleppo galls, and tara powder (Figure 11). Despite its exotic origins, about 1.7×10^5 kg of gallic acid are produced annually.⁶⁰ Gallic acid is used in inks, as a photographic developer, and in tanning and dye preparations. Esters of gallic acid, such as propyl gallate, are used as commercial antioxidants. Besides its own pharmacologic properties as an astringent and antihemorrhage agent, gallic acid is a useful starting material for pharmaceuticals such as trimethoprim, a broad-spectrum antibiotic, mescaline, a psychomimetic agent, and hexobendin, a coronary vasodilator.⁶¹

While isolation of gallic acid from plant sources is not environmentally challenged, the process is labor intensive and subject to uncontrollable factors such as weather and disease. A manufacturing process for gallic acid that can be easily scaled and is derived from a reliable, locally produced crop, such as corn, is therefore desirable. As mentioned earlier, DHS can be produced in high titers using an *E. coli* biocatalyst (Figure 7). Purified DHS can be chemically oxidized to gallic acid using catalytic amounts of Cu^{+2} or Zn^{+2} in the presence of O_2 (Figure 11).⁶² Gallic acid can also be directly biosynthesized by inclusion of the gene *pobA**, a mutant isozyme of *p*-hydroxybenzoate hydroxylase, in a biocatalyst engineered to produce PCA (Figure 11). Titrers of 20 g/L have been reached in fed-batch fermentations despite gallic acid toxicity towards the *E. coli* catalyst.⁶³

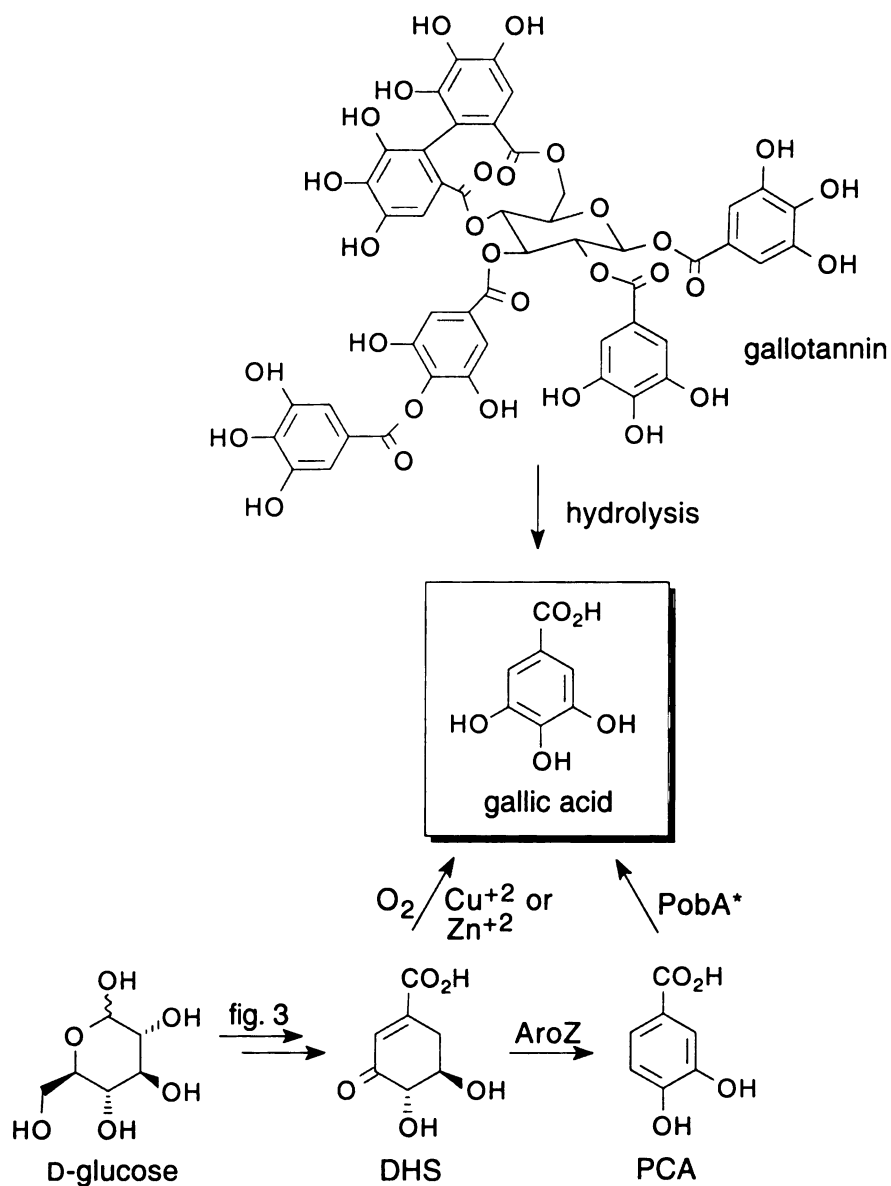


Figure 11. Comparison of the Commercial and Biosynthetic Routes to Gallic Acid.

The common pathway of aromatic amino acid biosynthesis has been shown to be a source for commercially important chemicals through the outlined routes to phenylalanine, tryptophan, vanillin, catechol, adipic acid, and gallic acid. Environmentally benign synthesis of vanillin and adipic acid was made possible by

combining an appropriately engineered biocatalyst with benign chemical synthetic methods. This dissertation will explore similar strategies for the synthesis of aromatic compounds. Genetic engineering of an *E. coli* strain for the production of *p*-hydroxybenzoic acid (PHB) relied on the experience gained from the synthesis of other molecules of the shikimate pathway. Conversion of fermentation-derived PHB to hydroquinone and *p*-cresol was accomplished by enzymes found in *Phanerochaete chrysosporium* and *Candida paraplois* in combination with catalytic hydrogenation.

C. Metabolic Engineering to Increase Yields and Titters in the Shikimate Pathway of *E. coli*.

While the biosynthetic routes outlined in the previous section would be favored over the current manufacturing processes from an environmental standpoint, their acceptance into the mainstream chemical industry comes down to their economic competitiveness with established technologies. A major factor in the profitability of fermentation-derived chemicals are yield (mol to mol from the starting carbohydrate) and titer (product concentration). A substantial amount of research has been conducted to increase and maintain the flow of carbon through the shikimate pathway. A summary of techniques will be presented here.

DAHP Synthase

One strategy to increase the flow of carbon into the common pathway revolves around overcoming the cellular regulations inherent with DAHP formation. DAHP synthase is subject to both transcriptional repression and feedback inhibition. Several

methods to alleviate the transcriptional control of DAHP synthase in order to increase enzyme activities have been explored. The two major isozymes responsible for DAHP synthase activity, AroF and AroG, are part of the *tyr* regulon. Specific sequences located in the promoter regions of the two loci, known as *tyrR* boxes, bind the *tyrR* gene product when activated by the correct effector molecules. Tyrosine or phenylalanine in high concentrations acts as effectors for *aroF* while phenylalanine and tryptophan act as the effector for *aroG*. One way to prevent repressor-mediated regulation is to introduce mutations in *tyrR*.⁶⁴ Without active repressor molecules, RNA polymerase is free to bind to the *aroF* and *aroG* promoter sequences regardless of the intracellular concentrations of the aromatic amino acids. The TyrR protein can also be titrated away by including an extra copy of *aroF* or just its promoter sequence on a multi-copy plasmid. This increases the number of *tyrR* boxes relative to a fixed amount of TyrR protein molecules. Transcriptional repression can be avoided altogether if one of the DAHP synthase isozymes, such as *aroF*, is expressed off of a different promoter such as P_{lac} , a strong *E. coli* promoter that is a combination of the *lac* and *trp* promoters.⁶⁵

Increased expression of DAHP synthase does not always translate to higher product formation because of feedback inhibition of the protein by the amino acid end products. Several feedback-resistant mutants of DAHP synthase have been reported that encompass all three isozymes.⁶⁶ The research presented in this work incorporates a feedback-resistant *aroF* locus obtained by UV mutagenesis. Sequencing of the mutant allele showed only a single amino acid change renders the gene product insensitive to tyrosine inhibition.⁶⁷ Development of the *aroF*^{FBR} locus in conjunction with transcriptional derepression allowed significant breakthroughs in the titer and yield of

DHS fermentations by increasing the catalytic activity of each molecule of DAHP synthase expressed.

PEP

With abundant DAHP synthase activity, availability of substrates becomes the next limitation to increased carbon flow through the shikimate pathway (Figure 3). Besides the two moles of phosphoenolpyruvate (PEP) used to synthesize chorismate, it plays a prominent role in *E. coli* metabolism. PEP also serves as substrates for the enzymes PEP carboxylase⁶⁸ (*ppc*) and pyruvate kinase⁶⁹ (*pykA*, *pykF*). Mutations in the *ppc* locus were developed as a way to increase phenylalanine titers but resulted in slower growing strains that were auxotrophic for a dicarboxylic acid and produced significant quantities of acetate.⁷⁰

The PEP-dependent carbohydrate phosphotransferase (PTS) system responsible for the uptake of glucose and other related sugars into the cell constitutes a significant drain on the pool of intracellular PEP (Figure 12). Several methods have been developed to circumvent this depletion of substrate PEP. One strategy utilizes pentoses as a carbon source. Xylose and arabinose have been used for the synthesis of DHS as they are transported by ATP-based permease system and therefore eliminates the mole of PEP lost for every mole of glucose transported under the PTS system.⁷¹ If glucose is maintained as the carbon source, the pyruvate formed as a byproduct of glucose phosphorylation can be recycled by plasmid-based overexpression of PEP synthase,⁷² encoded by *pps*. Phosphorylation of pyruvate back to PEP at the expense of ATP prevents the loss of carbon due to further pyruvate metabolism. Positive results have also been obtained by

expression of a glucose facilitator⁷³ (*glf*) from *Zymomonas mobilis*. This facilitated diffusion uptake system prevents the loss of PEP necessitated by the uptake of carbon. All of these methods have the added benefit of increasing the maximum theoretical yield of common pathway molecules. For example, the theoretical yield of DHS under the PTS system is 43%. When xylose is the sole carbon source, the theoretical yield jumps to 71% since less carbon is lost to undesired endproducts. With PEP recycling or diffusion-based uptake the theoretical yield is 80%.

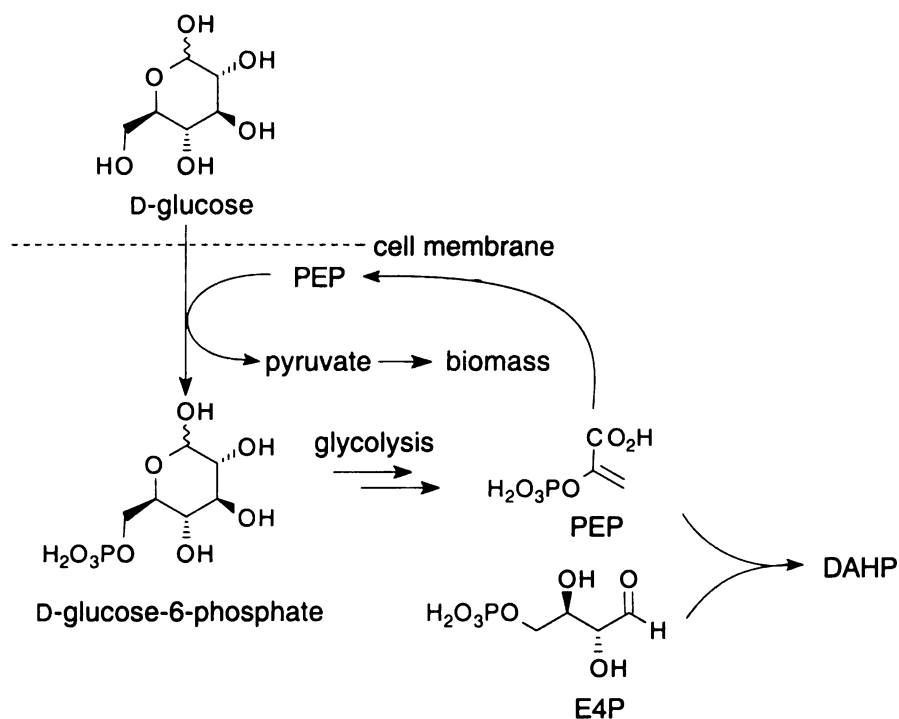


Figure 12. Intracellular Uses of PEP: PTS Uptake System and Synthesis of DAHP.

E4P

With ample quantities of DAHP synthase and PEP, the availability of D-erythrose 4-phosphate (E4P) becomes the next limitation in DAHP formation (Figure 3). Intracellular levels of E4P are normally maintained at low steady-state concentrations by

E. coli. It is believed that the rate of formation is matched closely to the rate of consumption due to the molecule's tendency to form dimers and trimers which degrade slowly back to free E4P.⁷⁴ One method of increasing E4P availability for direction into the common pathway has been to amplify expression of transketolase.⁷⁵ Encoded by *tktA*, transketolase (Figure 13) allows the conversion of two molecules of D-fructose 6-phosphate into three molecules of E4P as part of the nonoxidative pentose phosphate pathway. Two of the three reactions that generate E4P directly are catalyzed by transketolase. The second product of one of these reactions, D-sedoheptulose 7-phosphate, serves as substrate for the third E4P-generating reaction catalyzed by transaldolase. Plasmid-based overexpression of *tktA* have led to significant yield and titer improvements in DHS-producing biocatalysts cultured under fed-batch fermentor conditions.⁷⁶ Overexpression of transaldolase (Figure 13) should also improve endproduct formation but it has yet to be proven by fermentation results.⁷⁷

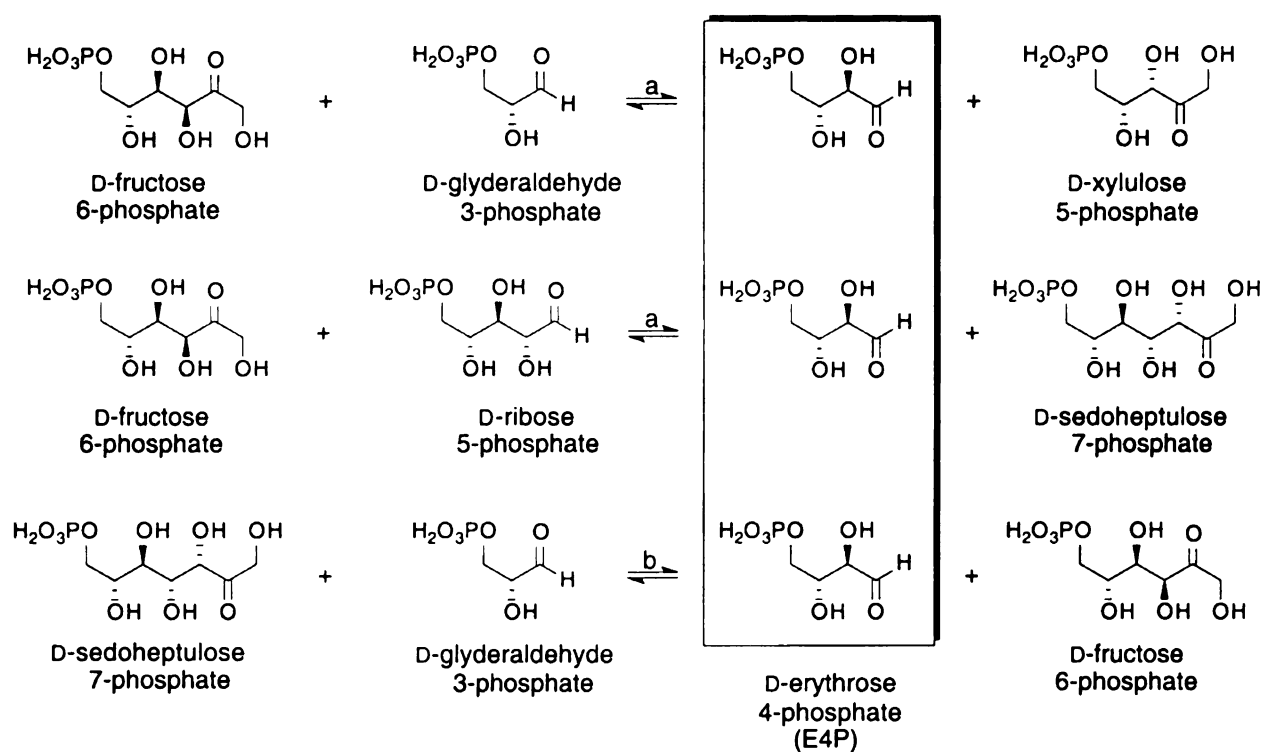


Figure 13. Biosynthesis of E4P. (a) transketolase, (b) transaldolase.

Rate-Limiting Enzymes

Once carbon flow is channeled into aromatic amino acid biosynthesis by commitment to DAHP, it must be maintained through to the desired molecule not only to prevent losses in titer but to control product purity. The first enzyme found to be rate-limiting under increased carbon flow was DHQ synthase (AroB)⁷⁸ (Figure 14). Without overexpression of *aroB*, it was found that D-*arabino*-heptulosonic acid (DAH), the dephosphorylated form of DAHP, accumulates in the culture supernatant. It was confirmed in both shake-flask and fermentation experiments that the addition of one extra copy of the *aroB* locus onto the host strain's genome is sufficient to alleviate DAH accumulation.⁷⁹

The next impediment to carbon flow through the shikimate pathway involves shikimate dehydrogenase (AroE) and shikimate kinase (AroL, AroK) (Figure 14). With

amplified levels of DAHP synthase and DHQ synthase, it was found that 3-dehydroshikimic acid (DHS) accumulates in culture supernatants. However, *aroE* overexpression failed to prevent DHS accumulation as was the case with *aroB* and DAH. Examination of the enzymology of shikimate dehydrogenase found it to be feedback inhibited ($K_i = 0.16\text{mM}$)⁸⁰ by shikimic acid, the subsequent intermediate in the pathway. Therefore, to prevent loss of carbon to DHS, the intracellular concentration of shikimic acid would have to be lowered. This requires an increase in shikimate kinase activity to rapidly convert shikimate to shikimate 3-phosphate (S3P), a molecule that does not inhibit shikimate dehydrogenase activity.

The conversion of shikimate to S3P, catalyzed by shikimate kinase, is subject to transcriptional regulation as *aroL* is part of the *tyr* regulon with *aroF* and *aroG*. It is unknown why this enzymatic step is subject to regulation as evidenced by *tyrR* boxes and dual isozymes but speculation has suggested a branch pathway leading from shikimate to an as yet unknown metabolite. Usually this type of regulation is seen at the beginning of a pathway, as with DAHP formation, to control cellular resources. As with AroF, one method to increase shikimate kinase activity is to remove transcriptional regulation by TyrR. This has been previously accomplished with mutations to the *tyrR* locus to prevent the synthesis of active TyrR protein.⁸¹ This resulted in the elimination of undesirable DHS and shikimate from culture supernatants.

With carbon flow channeled through to S3P, it was found that the last two enzymes of the common pathway become rate limiting (Figure 14).⁸² A second copy of the two loci, *aroA* (encoding EPSP synthase) and *aroC* (encoding chorismate synthase), introduced into the host's genome was sufficient to extend the flow of carbon to

chorismate and prevents the extracellular accumulation of the intermediates S3P and 5-enolpyruvylshikimate 3-phosphate (EPSP). The strategies to direct and maintain the flow of carbon through the shikimate pathway are invaluable to the biocatalytic production of *p*-hydroxybenzoic acid and shikimic acid presented in this work.

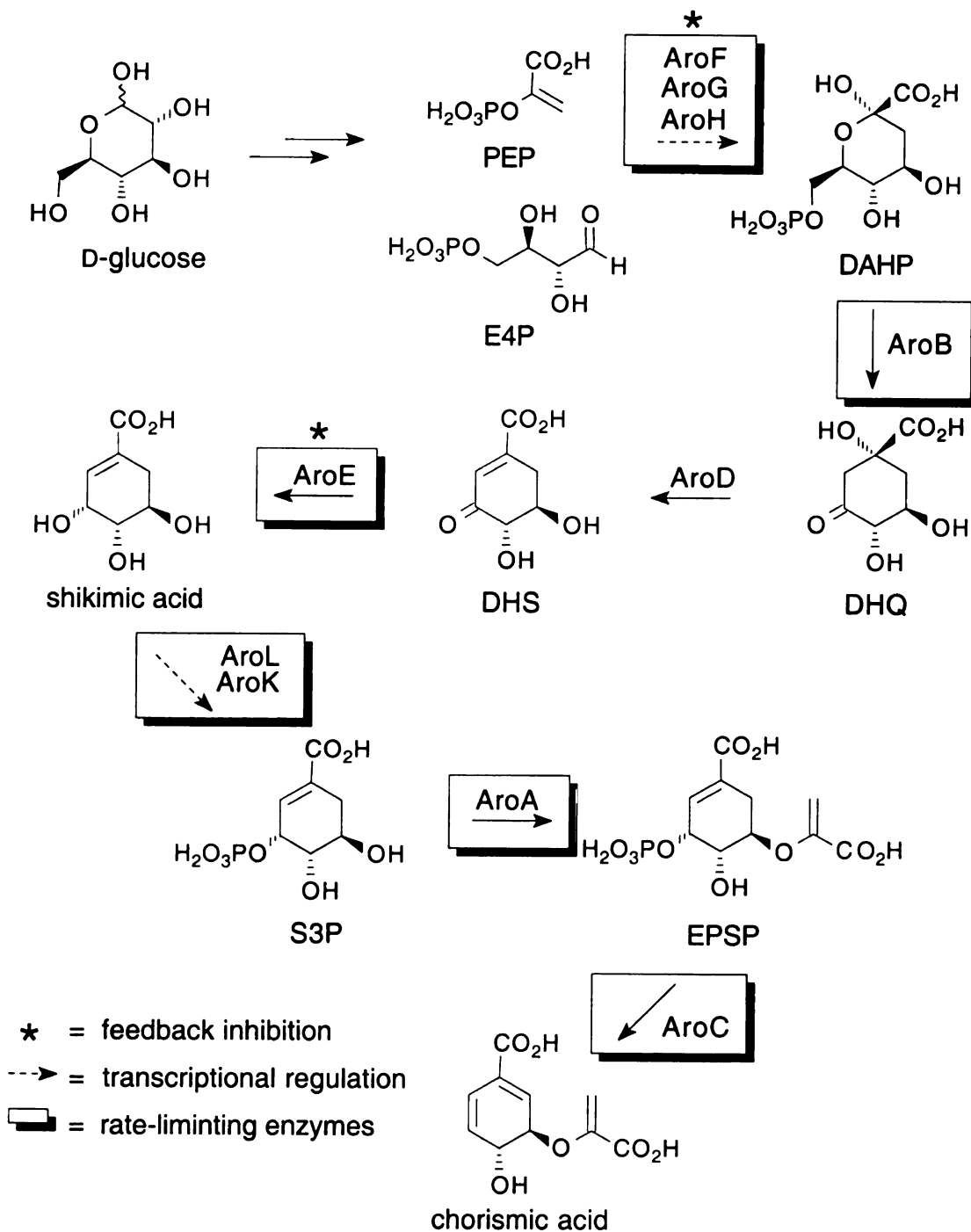


Figure 14. Rate-Limiting Enzymes in the Common Pathway.

References

-
- ¹ Weissermel, K.; Arpe, H.-J. *Industrial Organic Chemistry, 3rd ed.*; VCH: New York, 1997: p. 1-3.
 - ² Weissermel, K.; Arpe, H.-J. *Industrial Organic Chemistry, 3rd ed.*; VCH: New York, 1997: p. 8.
 - ³ Weissermel, K.; Arpe, H.-J. *Industrial Organic Chemistry, 3rd ed.*; VCH: New York, 1997: p. 316.
 - ⁴ Weissermel, K.; Arpe, H.-J. *Industrial Organic Chemistry, 3rd ed.*; VCH: New York, 1997: p. 3-4.
 - ⁵ Parekh, S.; Vinci, V.; Strobel, R. *Appl. Microb. Biotech.* **2000**, *54*, 287.
 - ⁶ (a) Schulze, B.; Wubbolts, M. *Curr. Opin. Biotech.* **1999**, *10*, 609. (b) Wandrey, C.; Liese, A.; Kihumbu, D. *Org. Proc. Res. Develop.* **2000**, *4*, 286.
 - ⁷ Lazarus, R.; Seymor, J.; Stafford, K.; Dennis, M.; Lazarus, M.; Marks, C.; Anderson, S. In *Biocatalysis*; Abramowicz, D. Ed.; Van Nostrand Reinhold: New York, 1990: p.135-155.
 - ⁸ Wilke, D. *Appl. Microb. Biotech.* **1999**, *52*, 135.
 - ⁹ Schulze, B.; Wubbolts, M. *Curr. Opin. Biotech.* **1999**, *10*, 609.
 - ¹⁰ Carlilie, M.; Watkinson, S. *The Fungi*; Academic Press: San Diego, 1994: p. 393-413.
 - ¹¹ Wilke, D. *Appl. Microb. Biotech.* **1999**, *52*, 135.
 - ¹² Roberts, S.; Turner, N.; Willetts, A.; Turner, M. *Introduction to Biocatalysis: Using Enzymes and Micro-organisms*; Cambridge University Press: New York, 1995: p 142.
 - ¹³ Wilke, D. *Appl. Microb. Biotech.* **1999**, *52*, 135.
 - ¹⁴ Demain, A. *Tibtech.* **2000**, *18*, 26.
 - ¹⁵ Eggeling, L.; Sahm, H. *Appl. Microb. Biotech.* **1999**, *52*, 146.
 - ¹⁶ Wilke, D. *Appl. Microb. Biotech.* **1999**, *52*, 135.
 - ¹⁷ Roberts, L. In *Encyclopedia of Chemical Processing and Design*; McKetta M. Ed.; Marcel Dekker: New York, 1990; Vol. 4, 324.

-
- ¹⁸ Blair, G.; Staal, P. In *Kirk-Othmer Encyclopedia of Chemical Technology*, 4th ed.; Kroschwitz, J.I., Howe-Grant, M., Ed.; Wiley: New York, 1997; Vol. 6, p. 362.
- ¹⁹ Roberts, L. In *Encyclopedia of Chemical Processing and Design*; McKetta M. Ed.; Marcel Dekker: New York, 1990; Vol. 4, 328.
- ²⁰ Roberts, L. In *Encyclopedia of Chemical Processing and Design*; McKetta M. Ed.; Marcel Dekker: New York, 1990; Vol. 4, 328.
- ²¹ Wilke, D. *Appl. Microb. Biotech.* **1999**, 52, 135.
- ²² (a) Haslam, E. *The Shikimate Pathway*; Wiley: New York, 1974. (b) Bently, R. *Crit Rev. Biochem. Mol. Biol.* **1990**, 25, 307. (c) Herrmann, K. M. In *Amino Acids: Biosynthesis and Genetic Regulation*; Herrmann, K. M., Somerville, R. L., Ed.; Addison-Wesley: Reading, 1983; p 301.
- ²³ Haslam, E. *The Shikimate Pathway*; Wiley: New York, 1974.
- ²⁴ (a) Haslam, E. *The Shikimate Pathway*; Wiley: New York, 1974. (b) Bently, R. *Crit Rev. Biochem. Mol. Biol.* **1990**, 25, 307. (c) Herrmann, K. M. In *Amino Acids: Biosynthesis and Genetic Regulation*; Herrmann, K. M., Somerville, R. L., Ed.; Addison-Wesley: Reading, 1983; p 301.
- ²⁵ Herrmann, K. M. In *Amino Acids: Biosynthesis and Genetic Regulation*; Herrmann, K. M., Somerville, R. L., Ed.; Addison-Wesley: Reading, 1983; p 301.
- ²⁶ Haslam, E. *The Shikimate Pathway*; Wiley: New York, 1974.
- ²⁷ Herrmann, K. M. In *Amino Acids: Biosynthesis and Genetic Regulation*; Herrmann, K. M., Somerville, R. L., Ed.; Addison-Wesley: Reading, 1983; p 301.
- ²⁸ (a) Muday, G. K.; Johnson, D. I.; Somerville, R. L.; Herrmann, K. M. *J. Bacteriol.* **1991**, 173, 3930. (b) Im, S. W. K.; Davidson, H.; Pittard, J. *J. Bacteriol.* **1971**, 108, 400. (c) Wallace, B. J.; Pittard, J. *J. Bacteriol.* **1969**, 97, 1234. (d) Im, S. K.; Pittard, J. *J. Bacteriol.* **1973**, 115, 1145.
- ²⁹ Carpenter, E. P.; Hawkins, A. R.; Frost, J. W.; Brown, K. A. *Nature* **1998**, 394, 299.
- ³⁰ (a) Haslem, E.; Smith, B. W.; Turner, M. J. *J. Chem Soc., Perkins Trans. 1* **1995**, 52. (b) Duncan, K.; Chaudhuri, S.; Campbell, M. S.; Coggins, J. R. *Biochem. J.* **1986**, 238, 475.
- ³¹ (a) Anton, I. A.; Coggins, J. R. *Biochem. J.* **1988**, 249, 319. (b) Chaudhuri, S.; Coggins, J. R. *Biochem. J.* **1985**, 226, 217.

-
- 32 (a) DeFeyter, R. C.; Pittard, J. *J. Bacteriol.* **1986**, *165*, 226. (b) DeFeyter, R. C.; Pittard, J. *J. Bacteriol.* **1986**, *165*, 231. (c) DeFeyter, R. C.; Pittard, J. *J. Bacteriol.* **1986**, *165*, 233.
- 33 Løbner-Olesen, A.; Marinus, M. G. *J. Bacteriol.* **1992**, *174*, 525.
- 34 Pittard, A. J. In *Escherichia coli and Salmonella typhimurium*; Neidhardt, F. C., Ed.; American Society for Microbiology: Washington D.C., 1987, Vol. 1, p. 368-394.
- 35 Ely, B.; Pittard, J. *J. Bacteriol.* **1987**, *169*, 2158.
- 36 Duncan, K.; Coggins, J. R. *Biochem. J.* **1986**, *234*, 49. (b) Duncan, K.; Lewendon, A.; Coggins, J. R. *FEBS Lett.* **1984**, *165*, 121.
- 37 White, P. J.; Millar, G.; Coggins, J. R. *Biochem. J.* **1988**, *251*, 313.
- 38 (a) Cotton, R. G.; Gibson, F. *Biochim. Biophys. Acta* **1967**, *147*, 222. (b) Dayan, J.; Sprinson, D. B. *J. Bacteriol.* **1971**, *108*, 1174. (c) Koch, G. L.; Shaw, D. C.; Gibson, F. *Biochim. Biophys. Acta* **1971**, *229*, 795.
- 39 (a) Edwards, J. M., Jackman, L. M. *Austral. J. Chem.* **1965**, *18*, 1227. (b) Andrews, P. R.; Cain, E. N.; Rizzardo, E.; Smith, G. D. *Biochemistry* **1977**, *16*, 4848. (c) Ife, R. J.; Ball, L. R.; Lowe, P.; Haslam, E. *J. Chem. Soc., Perkins Trans. 1* **1976**, 1776.
- 40 Gelfand, D. H.; Steinberg, R. *J. Bacteriol* **1977**, *130*, 429.
- 41 Wallace, B.; Pittard, J. *J. Bacteriol.* **1969**, *97*, 1234.
- 42 Pabst, M. J.; Kuhn, J. C.; Somerville, R. L. *J. Biol. Chem.* **1973**, *248*, 901.
- 43 (a) Haslam, E. *The Shikimate Pathway*; Wiley: New York, 1974. (b) Pittard, A. J. In *Escherichia coli and Salmonella typhimurium*; Neidhardt, F. C., Ed.; American Society for Microbiology: Washington D.C., 1987, Vol. 1, p. 512-520.
- 44 Wyama, K.; Irino, S.; Hagi, N. *Methods Enzymol.* **1987**, *136*, 503.
- 45 Thayer, A. M.; *Chem. Eng. News* **1991**, *69*, 9.
- 46 Li, K.; Mikola, M.; Draths, K. M.; Worden, R. M.; Frost, J. W. *Biotech. Bioeng.* **1999**, *64*, 61.
- 47 Yi, J.; Frost, J. W. Unpublished Results.
- 48 Draths, K. M.; Frost, J. W. *J. Am. Chem. Soc.* **1995**, *117*, 2395.

⁴⁹ Li, K.; Frost, J. W. *J. Am. Chem. Soc.* **1998**, *120*, 10545.

⁵⁰ (a) Lewis, Sr., R. J. *Hazardous Chemicals Desk Reference, Third Edition*; Van Nostrand Reinhold: New York, 1993. (b) Lenga, R. E.; Voutpal, K. L. *The Sigma-Aldrich Library of Regulatory and Safety Data*; Sigma-Aldrich: Milwaukee, WI, 1993.

⁵¹ Clark, G. S. *Perfum. Flavor.* **1990**, *15*, 45.

⁵² (a) Franck, H.-G.; Stadelhofer, J. W. *Industrial Aromatic Chemistry*; Springer Verlag: New York, 1988; p. 183-190. (b) Varagnat, J. In *Kirk-Othmer Encyclopedia of Chemical Technology, 3rd ed.*; Grayson, M., Ed.; Wiley: New York, 1981; vol. 13, p. 39-69. (c) Szmant, H. H. In *Organic Building Blocks of the Chemical Industry*; New York: Wiley, 1989, p. 512-519.

⁵³ Draths, K. M.; Frost, J. W. *J. Am. Chem. Soc.* **1994**, *116*, 399.

⁵⁴ (a) Draths, K. M.; Frost, J. W. *J. Am. Chem. Soc.* **1994**, *116*, 399. (b) Nu, W.; Frost, J. W. Unpublished results.

⁵⁵ (a) Franck, H.-G.; Stadelhofer, J. W. *Industrial Aromatic Chemistry*; Springer Verlag: New York, 1988; p. 183-190. (b) Varagnat, J. In *Kirk-Othmer Encyclopedia of Chemical Technology, 3rd ed.*; Grayson, M., Ed.; Wiley: New York, 1981; vol. 13, p. 39-69. (c) Szmant, H. H. In *Organic Building Blocks of the Chemical Industry*; New York: Wiley, 1989, p. 512-519.

⁵⁶ Draths, K. M.; Frost, J. W. *J. Am. Chem. Soc.* **1995**, *117*, 2395.

⁵⁷ Nu, W.; Frost, J. W. Unpublished results.

⁵⁸ Draths, K. M.; Frost, J. W. *J. Am. Chem. Soc.* **1994**, *116*, 399.

⁵⁹ Thiemens, M. H.; Trogler, W. C. *Science*, **1991**, *252*, 932.

⁶⁰ Kambourkis, S. PhD. Dissertation. Michigan State University, 2000.

⁶¹ (a) Miller, C.S. and Kuhremeyer, C. A, Ger. Pat. 1,086,719 Apr. 1, 1957. (b) Manchand, Pl. S.; Rosen, P.; Belica, P. S.; Perrotta, G. V.; Wang, H. S. *J. Org. Chem.* **1992**, *57*, 3531. (c) Tsao, M. U. *J. Am. Chem. Soc.* **1951**, *73*, 5495. (d) US Pat. 4, 701,460 1987. (a) Kashiwada, Y.; Novak, G.; Bastow, K. F. *J. Pharm. Sci.* **1993**, *82*, 487.

⁶² Kambourkis, S. PhD. Dissertation. Michigan State University, 2000.

⁶³ Kambourkis, S. PhD. Dissertation. Michigan State University, 2000.

-
- ⁶⁴ Pittard, A. J. In *Escherichia coli and Salmonella typhimurium*; Neidhardt, F. C., Ed.; American Society for Microbiology: Washington D.C., 1987, Vol. 1, p. 368-394.
- ⁶⁵ Li, K.; Mikola, M.; Draths, K. M.; Worden, R. M.; Frost, J. W. *Biotech. Bioeng.* **1999**, *64*, 61.
- ⁶⁶ (a) Weaver, L. M.; Herrmann, K. M. *J. Bacteriol.* **1990**, *172*, 6581. (b) Draths, K. M.; Pompliano, D.; Conley, D. L.; Frost, J. W.; Berry, A.; Disbrow, G. L.; Staversky, R. J.; Lievens, J. C. *J. Am. Chem. Soc.* **1992**, *114*, 3956. (c) Ray, J. M.; Yanofsky, C.; Bauerle, R. *J. Bacteriol.* **1988**, *170*, 5500.
- ⁶⁷ Li, K.; Mikola, M.; Draths, K. M.; Worden, R. M.; Frost, J. W. *Biotech. Bioeng.* **1999**, *64*, 61.
- ⁶⁸ (a) Miller, J. E.; Backman, K. C.; O'Conner, M. J.; Hatch, T. T. *J. Ind. Microbiol.* **1987**, *2*, 143. (b) Backman, K. C. U. S. Patent 5,169, 768 1992.
- ⁶⁹ Mori, M.; Yokota, A.; Sugitomo, S.; Kawamura, K. Patent JP 62, 205, 782, 1987.
- ⁷⁰ (a) Konstantinov, K. B.; Nishio, N.; Yoshida, T. *Ferment. Bioeng.* **1990**, *70*, 253. (b) Konstantinov, K. B.; Nishio, N.; Seki, T.; Yoshida, T. *Ferment. Bioeng.* **1991**, *71*, 350.
- ⁷¹ Li, K. Ph.D. Dissertation, Michigan State University, 1999.
- ⁷² Li, K.; Yi, J.; Frost, J. W. Unpublished results.
- ⁷³ Yi, J.; Frost, J. W. Unpublished results.
- ⁷⁴ Draths, K. M.; Pompliano, D.; Conley, D. L.; Frost, J. W.; Berry, A.; Disbrow, G. L.; Staversky, R. J.; Lievens, J. C. *J. Am. Chem. Soc.* **1992**, *114*, 3956.
- ⁷⁵ Draths, K. M.; Pompliano, D.; Conley, D. L.; Frost, J. W.; Berry, A.; Disbrow, G. L.; Staversky, R. J.; Lievens, J. C. *J. Am. Chem. Soc.* **1992**, *114*, 3956.
- ⁷⁶ Li, K.; Mikola, M.; Draths, K. M.; Worden, R. M.; Frost, J. W. *Biotech. Bioeng.* **1999**, *64*, 61.
- ⁷⁷ Farabaugh, M. A. M. S. Thesis, Michigan State University, 1996.
- ⁷⁸ Dell, K. A.; Frost, J. W. *J. Am. Chem. Soc.* **1993**, *115*, 11581.

⁷⁹ (a) Snell, K. A.; Draths, K. M.; Frost, J. W. *J. Am. Chem. Soc.* **1996**, *118*, 5605. (b) Li, K.; Mikola, M.; Draths, K. M.; Worden, R. M.; Frost, J. W. *Biotech. Bioeng.* **1999**, *64*, 61. (c) Li, K.; Frost, J. W. *J. Am. Chem. Soc.* **1998**, *120*, 10545.

⁸⁰ Dell, K. A.; Frost, J. W. *J. Am. Chem. Soc.* **1993**, *115*, 11581.

⁸¹ Snell, K. A.; Draths, K. M.; Frost, J. W. *J. Am. Chem. Soc.* 1996, *118*, 5605.

⁸² Dell, K. A.; Frost, J. W. *J. Am. Chem. Soc.* **1993**, *115*, 11581.

Chapter Two

MICROBIAL SYNTHESIS OF *p*-HYDROXYBENZOIC ACID FROM GLUCOSE

Introduction

p-Hydroxybenzoic acid (PHB) is a valuable intermediate in the biosynthesis of natural products and the chemical synthesis of commercial goods. Plants synthesize PHB as both a signaling molecule to defend against pathogens and as a precursor for other aromatic metabolites, such as the red pigment shikonin (Figure 15).¹ In plants and microbes, PHB provides the aromatic ring of ubiquinones (Figure 15). Also known as coenzyme Q, ubiquinones are membrane-soluble quinones involved in cell respiration.² PHB formation in plants results from tyrosine or phenylalanine degradation via the phenylpropanoid pathway (Figure 16).³ In microbes such as *Escherichia coli*, the last common intermediate in the shikimate pathway, chorismic acid, is aromatized to PHB in a single step catalyzed by *ubiC*-encoded chorismate lyase (Figure 16).⁴

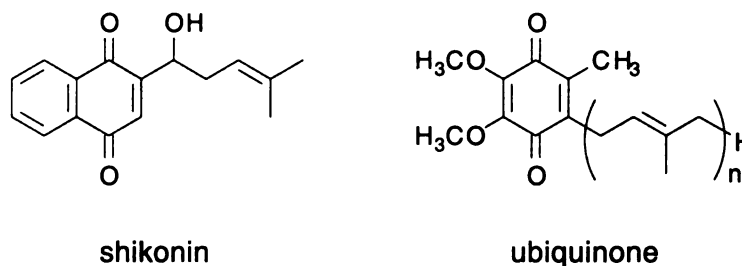


Figure 15. Structures of Shikonin and Ubiquinone.

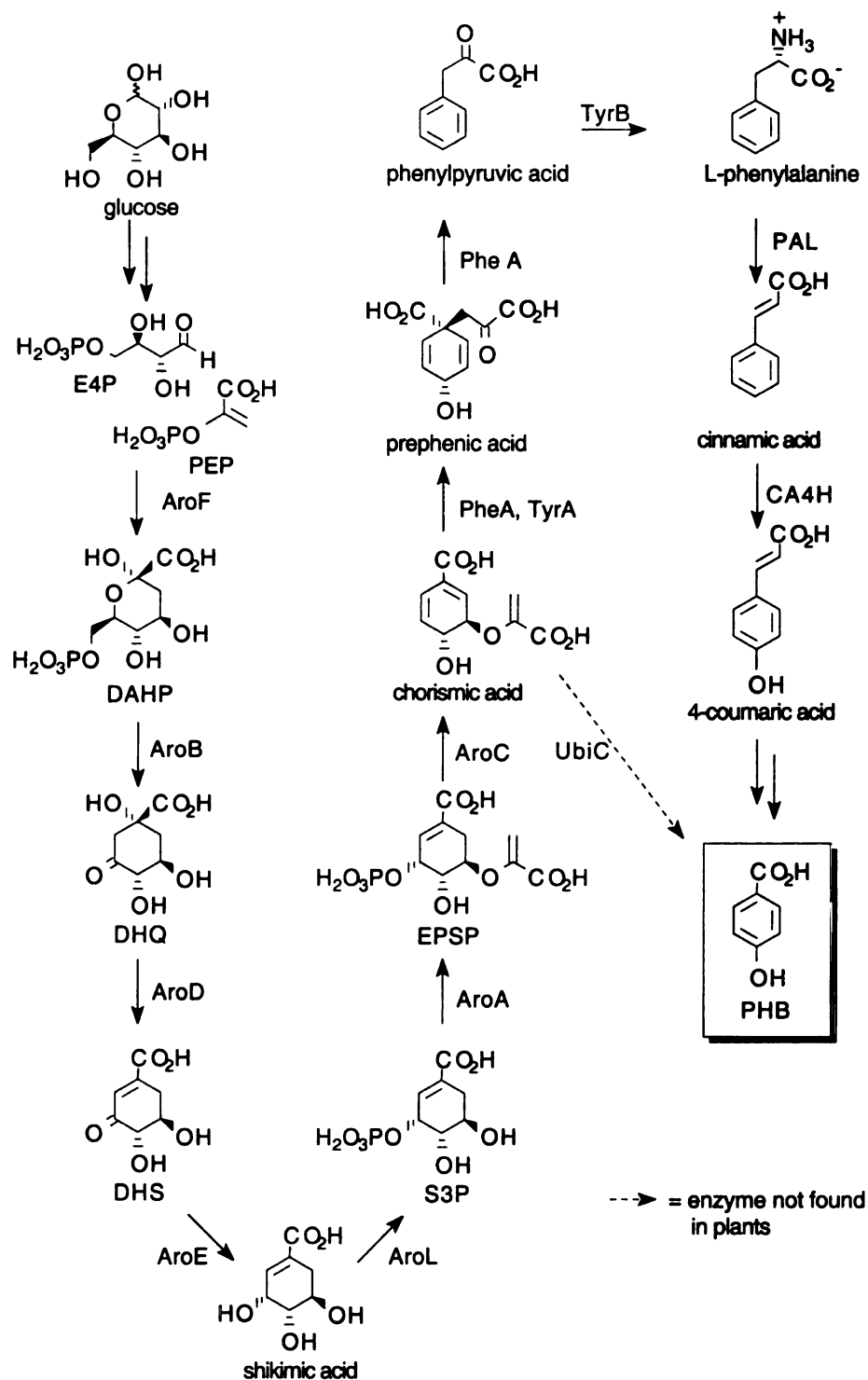
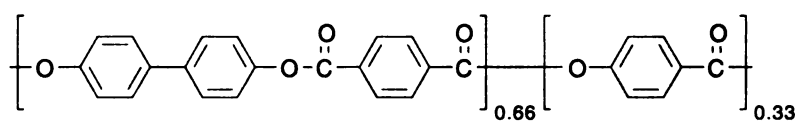


Figure 16. Biosynthesis of PHB in Microbes and Plants. Genetic loci are as follows: AroF, tyrosine-sensitive DAHP synthase; AroB, DHQ synthase; AroD, DHQ dehydratase; AroE, shikimate dehydrogenase; AroL, shikimate kinase; AroA, EPSP synthase; AroC, chorismate synthase; UbiC, chorismate lyase; PheA, chorismate mutase-prephenate dehydratase; TyrA, chorismate mutase-prephenate dehydrogenase; TyrB, aromatic aminotransferase; PAL, phenylalanine ammonia lyase; CA4H, cinnamic acid 4-hydroxylase.

PHB finds its niche in the chemical industry as the starting material for parabens and liquid crystalline polymers (LCP's).⁵ Esters of PHB, known as parabens (Figure 17), are widely used in the cosmetics, food, and pharmaceutical markets as antimicrobial agents. PHB also holds an important place in the expanding LCP industry. One of the first examples of an LCP was developed in the mid 1960's from PHB. The copolymer of PHB, terephthalic acid, and bisphenol led to a profitable family of melt processable copolyesters currently sold under the tradename Xydar (Figure 17).⁶ While the paraben market consumes 1.4×10^6 kg of PHB annually, further expansion of LCP technology could raise the yearly demand to over 50×10^6 kg.



Xydar

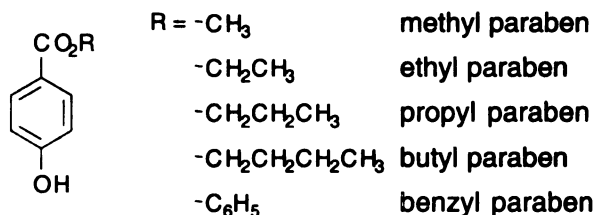


Figure 17. Structures of Xydar and Parabens.

Commercially, PHB is derived almost exclusively from phenol using a modification of the Kolbe-Schmitt reaction (Figure 18).⁷ Phenol is first converted to its potassium salt with KOH. The resulting potassium phenolate is carboxylated in the presence of dry CO₂ under elevated temperatures (180-250 °C) and pressures (20 atm).

Quantitative yields of the potassium salt of PHB are obtained. The free acid is formed by mineral acid treatment.

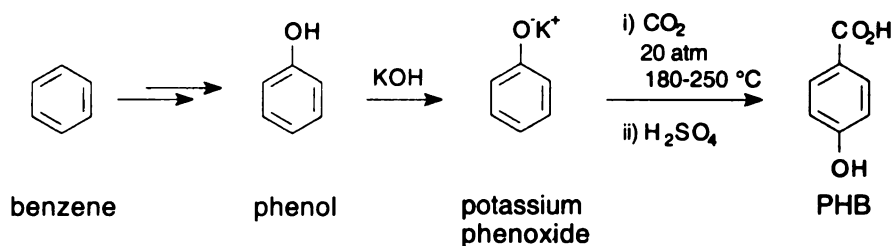


Figure 18. Commercial Synthesis of PHB.

Besides extreme reaction conditions, manufacturers of PHB must contend with highly toxic and corrosive phenol as a starting material. In an effort to employ milder reactions conditions, PHB has also been synthesized by enzyme-catalyzed carboxylation of phenol⁸ and microbial oxidation of toluene.⁹ However, these biocatalytic routes are similar to the chemical synthesis in their dependence on either toxic benzene or toluene, which are derived from the BTX fraction of nonrenewable petroleum. A different strategy is to take advantage of PHB's intermediacy in the biosynthesis of coenzyme Q in microbes and its formation in plants as a result of phenylpropanoid biodegradation. PHB can then be synthesized by recombinant microbes from immobilized CO₂ in the form of glucose, which is derived from renewable starch and cellulose, or synthesized directly from CO₂ by transgenic plants.

In *E. coli*, chorismic acid is directly aromatized into PHB by *ubiC*-encoded chorismate lyase (Figure 16). A more circuitous route for the biosynthesis of PHB is employed in plants where chorismic acid is converted into PHB by at least nine enzymatic reactions (Figure 16). These additional enzymatic steps required to form PHB in plants have been eliminated with the expression of the *E. coli ubiC* gene in *Nicotiana*

tabacum.¹⁰ The result is a large increase in the concentration of PHB that forms in plant tissue. Although microbial synthesis of small quantities of ¹³C-labeled PHB from ¹³C-labeled glucose had been reported using *Klebsiella pneumoniae*,¹¹ a suitable microbial synthesis has not been available for comparison with the engineered synthesis of PHB in plants. A basis for comparison became possible with the recent description of a PHB-producing *E. coli* strain resulting from two rounds of selection for spontaneous mutations and overexpression of *ubiC*-encoded chorismate lyase.¹²

In this chapter, a different approach to genetic manipulation of PHB biosynthesis in *E. coli* has been taken (Figure 16). Variables and design parameters were evaluated that are important to consider during any attempt to improve microbial synthesis of aromatics under fed-batch fermentor conditions. Quantified variables include: 3-deoxy-D-arabino-heptulosonic acid 7-phosphate (DAHP) synthase and chorismate lyase specific activities; and the concentrations of aromatic and nonaromatic metabolites that accumulated in culture supernatants. Design parameters that were considered include: the competition between chorismate lyase and other enzymes for chorismic acid; the expression of chorismate lyase; and the impact of PHB toxicity on *E. coli* metabolism.

I. Design and Assembly of the Microbial Catalyst.

A. Construction of *E. coli* Host Strains.

Overview

Two different microbial hosts were used for the direct conversion of glucose into PHB. *E. coli* D2704, a *pheA tyrA ΔtrpE-C* strain, lacked chorismate mutase-prephenate dehydratase, chorismate mutase-prephenate dehydrogenase and anthranilate synthase activities. Enzymatic competition with chorismate lyase for chorismic acid concentrations was thus reduced in constructs derived from *E. coli* D2704. Growth of all D2704-derived constructs required supplementation of culture medium with aromatic amino acids. *E. coli* RB791 was also used as a host strain. All of the chorismate-utilizing enzymes absent in *E. coli* D2704 were expressed in *E. coli* RB791. As a consequence, all constructs derived from *E. coli* RB791 were capable of growth in unsupplemented culture medium.

Chorismic acid, the last intermediate preceding PHB formation, is also the last metabolite in the common pathway of aromatic amino acid biosynthesis. This creates a challenge given previous observations that increased carbon flow into the common pathway of *E. coli* does not necessarily lead to increased chorismic acid formation.¹³ It was found that expression levels of individual common pathway enzymes need to be increased to ensure that substrate turnover is sufficiently rapid to avoid accumulation and export of substrates into the culture medium. Here, this was accomplished using a modification of the previously reported strategy by Snell.¹⁴ A

P_{tac}aroAaroLaroCaroBkan^R cassette was inserted into the genomes of *E. coli* D2704 and *E. coli* RB791 to generate *E. coli* JB161 and *E. coli* RB38. Resulting increases in the activities of 5-enolpyruvylshikimate 3-phosphate (AroA), shikimate kinase (AroL), chorismate synthase (AroC), and dehydroquinate synthase (AroB) allowed increased carbon flow directed into the common pathway to translate into increased synthesis of chorismic acid (Figure 16).

Preparation of the *P_{tac}aroAaroLaroCaroBkan^R* Cassette for Site-Specific Insertion.

Although plasmids are maintained in *E. coli* as extrachromosomal, circularized DNA, recombination events occasionally occur such that plasmid DNA is integrated into the chromosome of the host cell. Exploitation of this rare event provides a method for simple, site-specific insertion of a cassette by flanking the cassette with sequences homologous to the genomic region targeted for disruption. Identification of cells with integrated plasmid DNA is difficult since both freely replicating and integrated plasmids express resistance to drugs encoded by plasmid markers. By using a conditional non-replicative plasmid, selection of integrated plasmid DNA becomes possible since cells express drug resistance only if the plasmid resides in the genome.

Normal cloning and preparation of plasmids containing conditional origins of replication can be performed under permissive conditions whereas genomic insertions are accomplished under nonpermissive conditions where the replication machinery is inactive. Plasmids possessing a temperature-sensitive replicon are capable of being manipulated in this fashion. Plasmid pMAK705 contains a temperature-sensitive pSC101 replicon, a chloramphenicol resistance marker, and a convenient multiple

cloning site. The plasmid is able to replicate normally when the host cell is grown at 30 °C but is unstable to replicate when the host cell is cultured at 42 °C. Thus, genetic manipulations of the plasmid are carried out at 30 °C while the integration of the plasmid into the genome can be selected for at 42 °C.

The planned insertion of the $P_{tac}aroAaroLaroCaroBkan^R$ cassette into the genome of *E. coli* D2704 by homologous recombination necessitated construction of a pMAK705-derived plasmid containing the $P_{tac}aroAaroLaroCaroBkan^R$ cassette flanked by *serA* DNA. The *serA* locus was chosen for insertion of the cassette since *serA*-encoded phosphoglycerate dehydrogenase is an enzyme necessary for the biosynthesis of L-serine (Figure 19).¹⁵ Complementation of this auxothrophy provided the basis for plasmid maintenance for all PHB-producing constructs since growth in a medium lacking L-serine supplementation requires de novo biosynthesis of L-serine, which was possible only by expression of plasmid-localized *serA*. This strategy employing nutritional pressure for plasmid maintenance obviates any need for use of antibiotics and plasmid-localized antibiotic resistance markers.

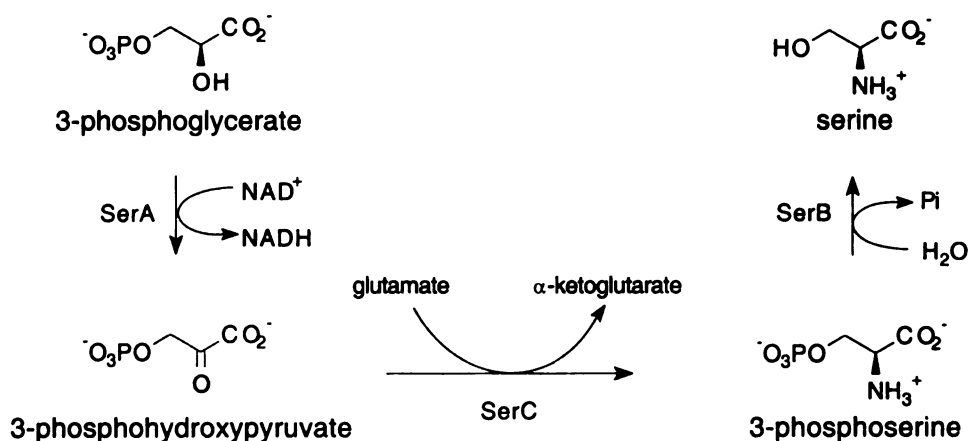


Figure 19. Serine Biosynthesis. Genetic loci are as follows: SerA, 3-phosphoglycerate dehydrogenase; SerC, 3-phosphoserine aminotransferase; SerB, 3-phosphoserine phosphatase.

Strain construction began with assembly of the genomic cassette. The previously synthesized *P_{tac}aroAaroCaroBkan^R* cassette, localized in plasmid pKAD77A, was prepared by Snell et al.¹⁶ This cassette was modified by ligating a *KpnI* terminated *aroL* locus to the *KpnI* site located between the *aroA* and *aroC* genes. The *aroL* locus was amplified from plasmid pJB2.8 (Figure 20) by PCR with primers containing terminal *KpnI* recognition sequences to yield a 0.8-kb fragment. Ligation of the resulting *aroL* PCR fragment to pKAD77A, which had previously been digested with *KpnI*, afforded the 10.6-kb plasmid pJB2.100. The *aroL* gene is transcribed in the same direction as *aroA*, *aroC*, *aroB*, and *kan^R* (Figure 21).

Plasmid pJB2.132 was constructed to prepare the *P_{tac}aroAaroLaroCaroBkan^R* cassette for site-specific recombination into the *serA* locus of D2704. Construction of pJB2.132 began with the vector pMAK705, which contains a temperature-sensitive pSC101 replicon. Plasmid pMAK705 contains two *EcoRI* restriction sites: one located within the *Cm^R* marker and one contained within the multiple cloning site. To facilitate future cloning, the *EcoRI* site within the multiple cloning site was destroyed. Partial digestion of pMAK705 with *EcoRI* followed by treatment with the Klenow fragment allowed for isolation of a 5.5-kb blunt end fragment from an agarose gel. Religation of the isolated DNA afforded plasmid pJB1.37 (Figure 22). Elimination of the *EcoRI* site within the multiple cloning site was confirmed by growth of DH5 α /pJB1.37 on LB medium containing Cm.

Localization of the *serA* gene in pJB1.37 followed by insertion of the *P_{tac}aroAaroLaroCaroBkan^R* cassette into an *EcoRI* site internal to the *serA* gene directed

recombination of the cassette into the *serA* locus of the D2704 genome. Digestion of pD2625 with *EcoRV* and *DraI* liberated a 1.9-kb *serA* fragment. Plasmid pJB1.37A was digested with *HincII* to produce blunt ends. Subsequent ligation of the *serA* fragment to pJB1.37A yielded the 7.4-kb plasmid pJB1.102B. The *serA* locus was oriented opposite the vector-localized *lacZ'* (Figure 23). The 6.3-kb *P_{lac}aroAaroLaroCaroBkan^R* cassette was liberated from pJB2.100 by digestion with *EcoRI*. Following *EcoRI* partial digestion of pJB1.102B, the DNA fragments were resolved on an agarose gel and the 7.4-kb fragment corresponding to the linearized plasmid was isolated. Ligation of linearized pJB1.102B to the 6.3-kb *EcoRI* fragment encoding the modified cassette afforded the 13.7-kb plasmid pJB2.132. The cassette is transcribed with all the genes in the same orientation as the *serA* promoter (Figure 24).

Genomic Insertion of the *P_{lac}aroAaroLaroCaroBkan^R* Cassette into D2704.

Conditions for homologous recombination were based on those previously described by Hamilton et al.¹⁷, Ohta et al.¹⁸, and Li et al.¹⁹ Competent D2704 cells were freshly prepared and transformed with pJB2.132. Following heat-shock treatment, cells were incubated in LB at 37 °C for 2 h and subsequently plated onto LB containing Cm and Kan. Plates were incubated at 42 °C for approximately 24 h. The resulting colonies were inoculated into 5 mL of LB containing no antibiotics, and the cells were grown at 30 °C for 12 h to allow excision of the plasmid from the genome. Cultures were diluted (1:20,000) in LB without antibiotics, and two more cycles of growth at 30 °C for 12 h were carried out to enrich cultures for more rapidly growing cells that had lost the temperature-sensitive replicon. Cultures were then diluted (1:20,000) in LB and grown at

44 °C for 12 h to promote plasmid loss from the cells. Serial dilutions of each culture were spread onto LB plates containing Kan and incubated at 30 °C overnight. The resulting colonies were screened on multiple plates to select for the correct phenotype. One candidate, *E. coli* JB161, was isolated based on the following growth characteristics: growth on M9 containing aromatic amino acids, aromatic vitamins, and serine, no growth on M9 containing aromatic amino acids and aromatic vitamins, growth on LB containing Kan, no growth on LB containing Cm, and growth on LB (Table 2). *E. coli* RB38 was prepared from *E. coli* RB791 using the same protocols described for preparation of JB161.

To confirm that all of the genes of the cassette were correctly inserted into the genome of JB161 at *serA*, a Southern hybridization²⁰ was performed. Genomic DNA was prepared from strains JB161 and D2704 and digests of the DNA samples were electrophoresed on an agarose gel. DNA from the gel was transferred to a Hybond-N⁺ membrane and probed with a ³²P-labeled probe of the 1.1 kb *PvuII/KpnI* fragment of *serA*. The resulting labeled fragments observed in the autoradiograph confirmed that site-specific genomic insertion of the *aroA*, *aroC*, *aroB*, and *kan^R* loci occurred at *serA* in JB161 (Figure 25, Figure 26).

The Southern hybridization described above failed to verify insertion of *aroL* into the *serA* locus of JB161 due to digestion of the JB161 genomic DNA samples with *KpnI*. Digestion with *KpnI* cleaved the *aroL* gene from the surrounding DNA fragments containing sequences homologous to the ³²P-labeled *serA* probe leaving any fragments encoding *aroL* undetectable (Figure 25). Verification of *aroL* insertion was performed with a ³²P-labeled probe of *aroL*. Genomic DNA was prepared from *E. coli* KAD11D for

use as a negative control while DNA of plasmid pJB2.132 was used as a positive control. Strain KAD11D, previously prepared in the group, contains a $P_{lac}aroAaroCaroBkan^R$ cassette inserted into the *serA* locus of its genome. Samples of pJB2.132 DNA and JB161 and KAD11D genomic DNA were digested, resolved on an agarose gel, and transferred to a Hybond-N⁺ membrane. After hybridization to a ³²P-labeled probe of *aroL*, autoradiography of the resulting membrane confirmed correct insertion of *aroL* between the *aroA* and *aroC* loci of the genomic cassette localized in *serA* (Figure 25, Figure 27).

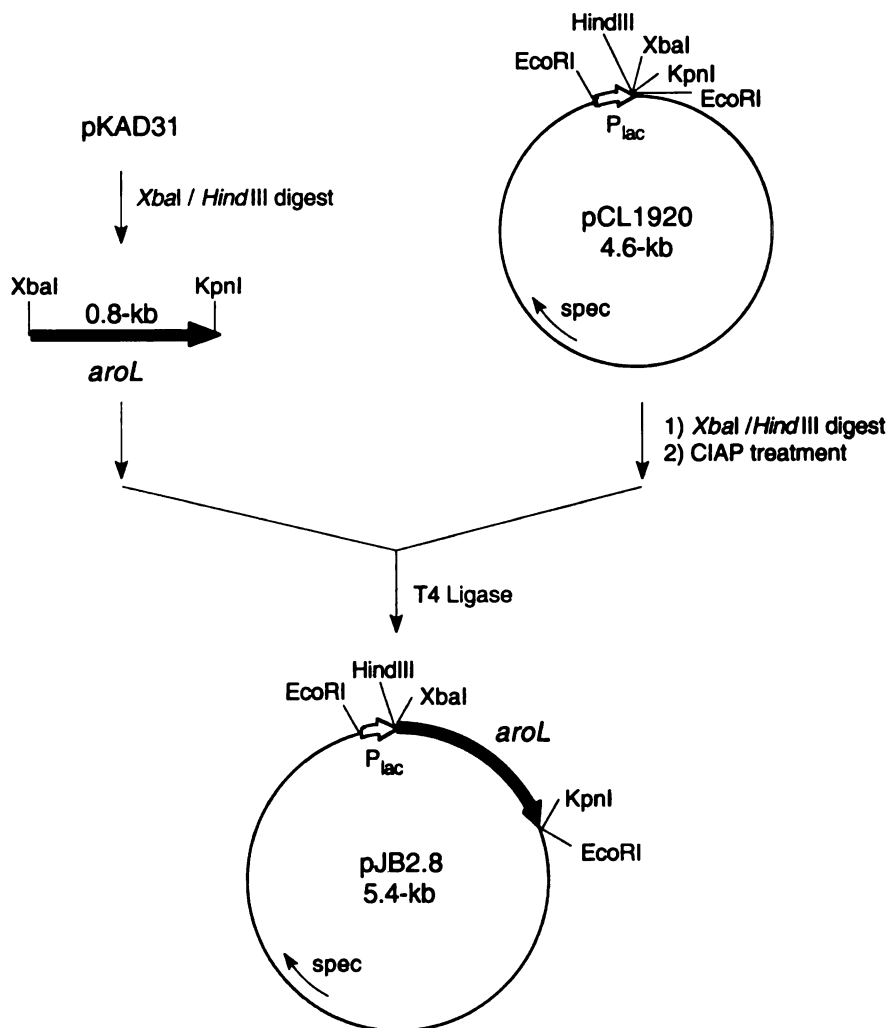


Figure 20. Preparation of Plasmid pJB2.8.

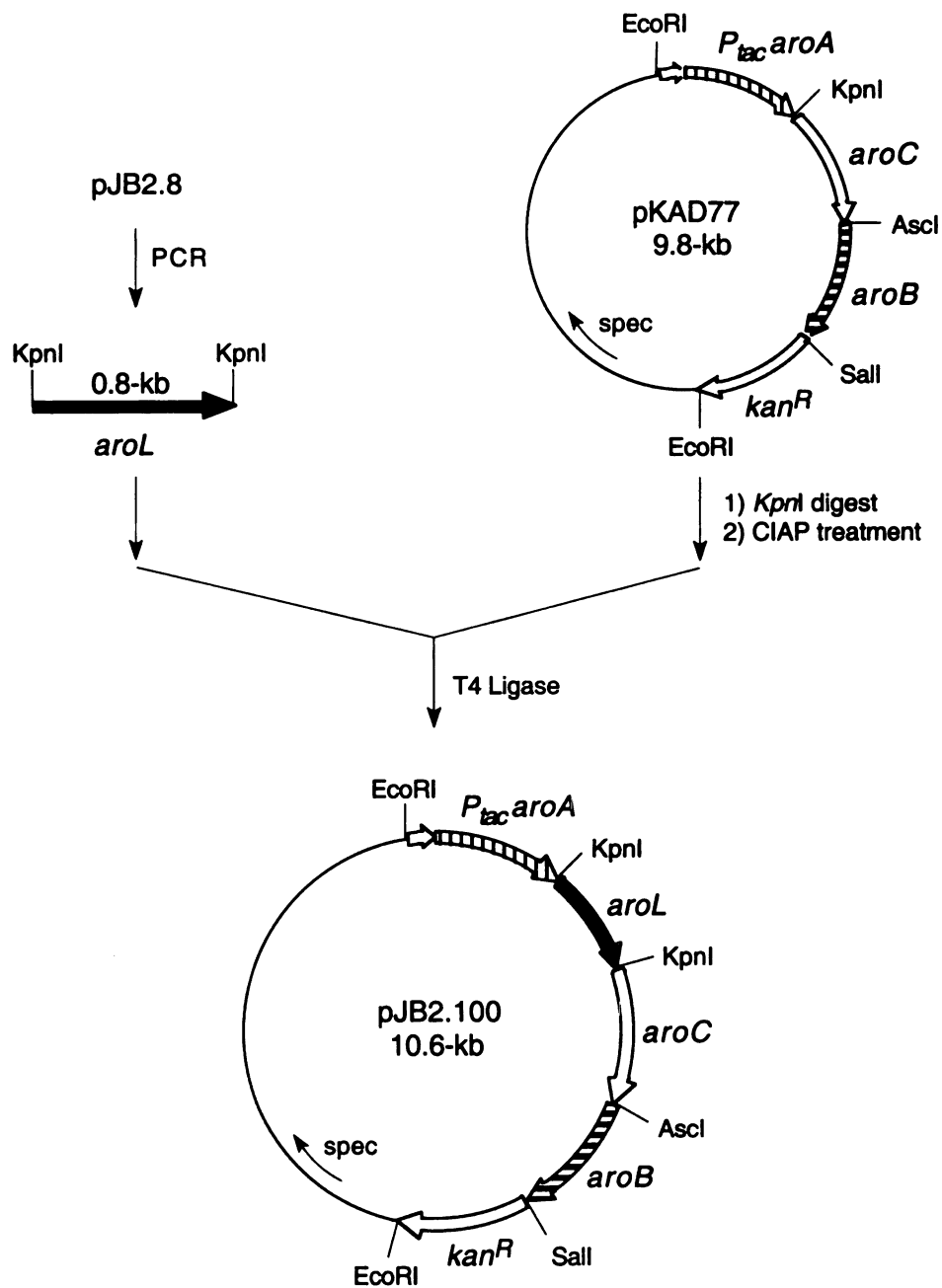


Figure 21. Preparation of Plasmid pJB2.100.

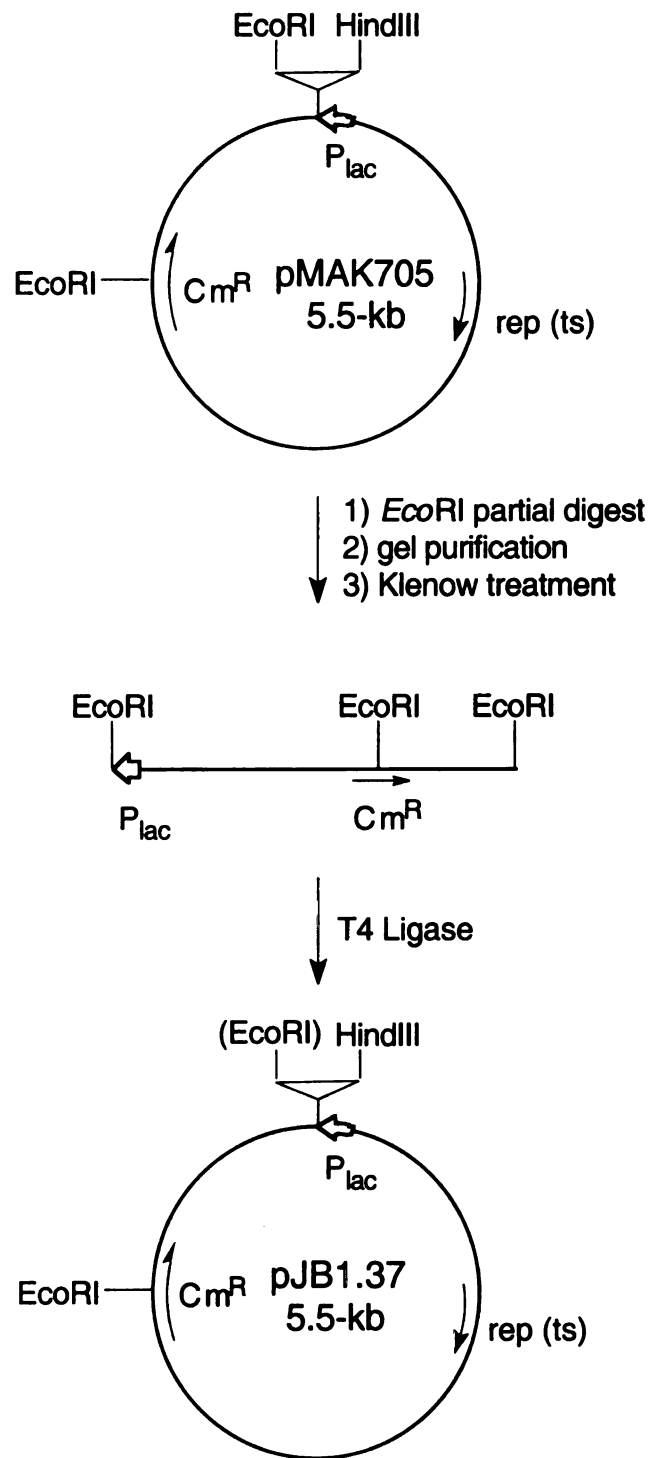


Figure 22. Preparation of Plasmid pJB1.37.

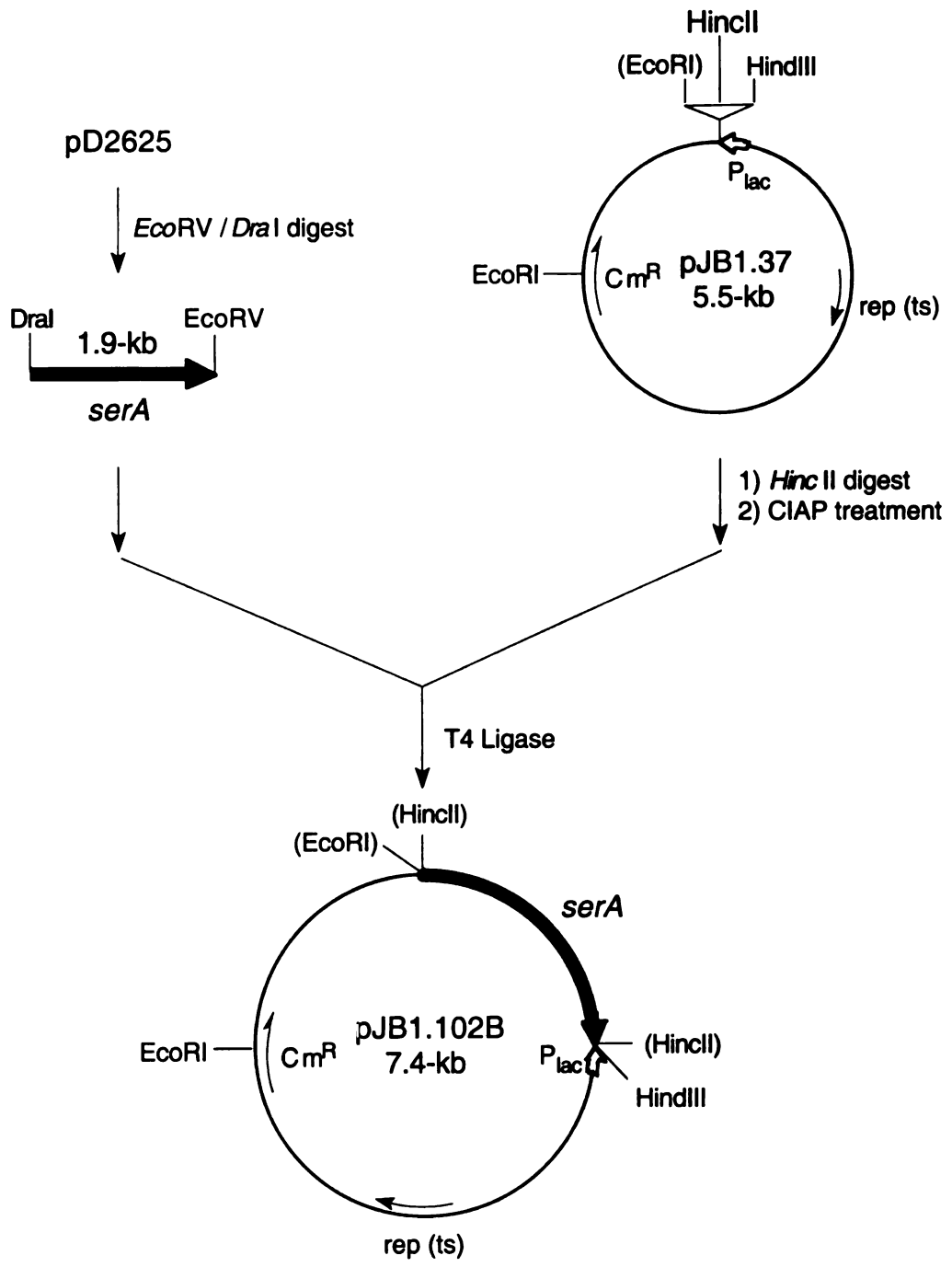


Figure 23. Preparation of Plasmid pJB2.102B.

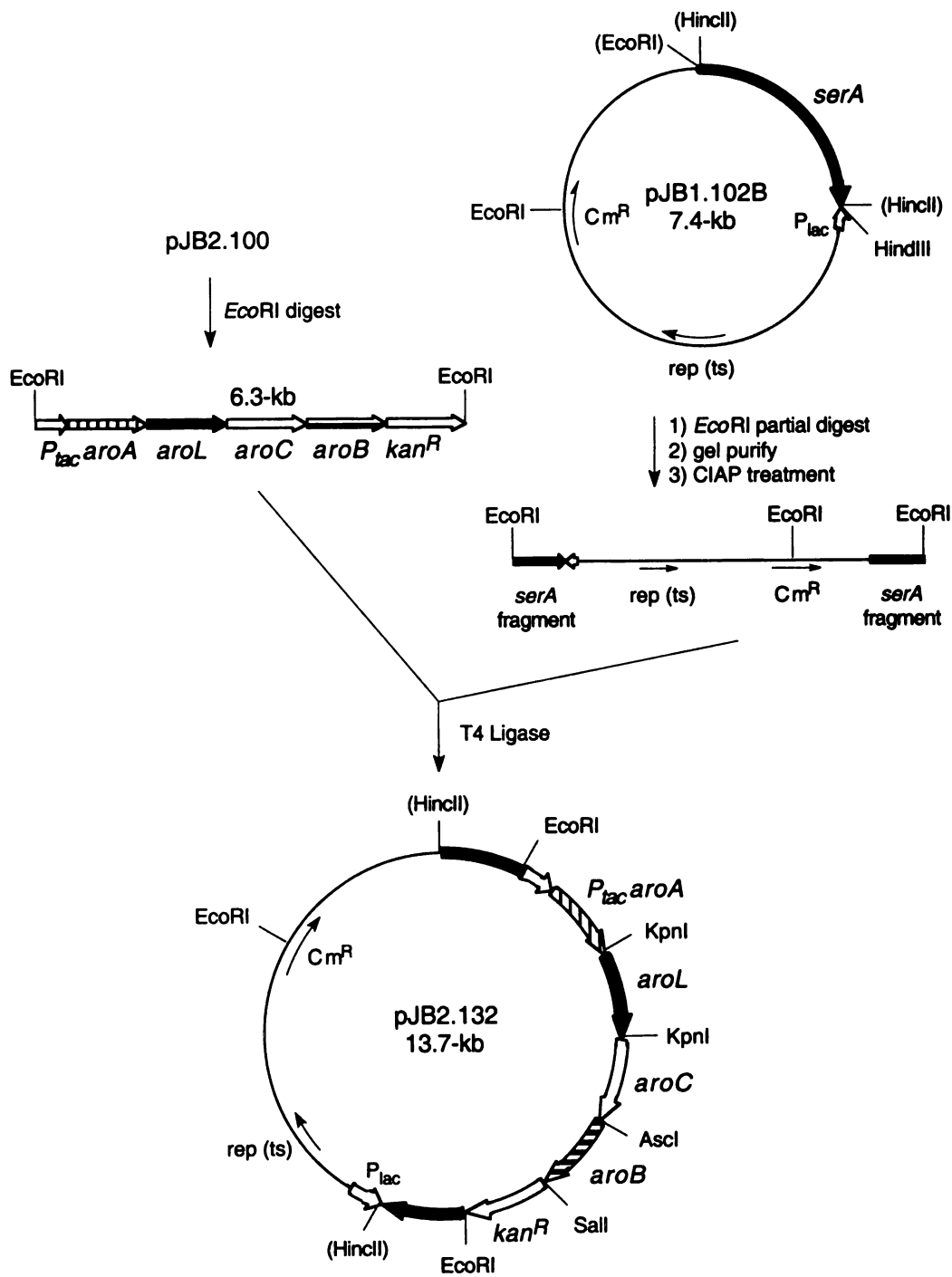
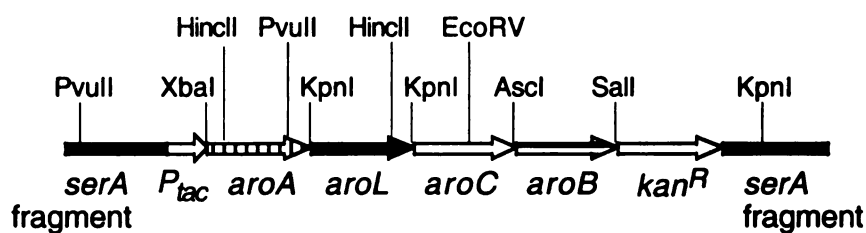


Figure 24. Preparation of Plasmid pJB2.132.

Table 2. Plate Selection for Characterization of Genomic Insertion.

strain	M9/glucose/Tyr Phe/Trp	M9/glucose/Tyr Phe/Trp/serine	LB/Cm	LB/Kan	LB
D2704	+	+	-	-	+
JB161	-	+	-	+	+

a



b

<i>serA</i> probe			
	<u>expected lengths of labeled bands (kb)</u>		
	D2704	JB161	
<i>PvuII</i> / <i>KpnI</i>	1.1	2.3, 4.3	
<i>PvuII</i> / <i>KpnI</i> / <i>XbaI</i>	1.1	1.1, 4.3	
<i>PvuII</i> / <i>KpnI</i> / <i>AscI</i>	1.1	2.3, 3.0	
<i>PvuII</i> / <i>KpnI</i> / <i>SalI</i>	1.1	2.3, 1.7	

<i>aroL</i> probe			
	<u>expected lengths of labeled bands (kb)</u>		
	pJB2.132	KAD11D	JB161
<i>KpnI</i>	0.8	—	0.8
<i>HincII</i>	1.4	—	1.4
<i>PvuII</i> / <i>EcoRV</i>	1.8	—	1.8

Figure 25. (a) Restriction enzyme sites within genomic cassette. (b) Expected lengths of radiolabeled DNA fragments using a *serA* probe and *aroL* probe.

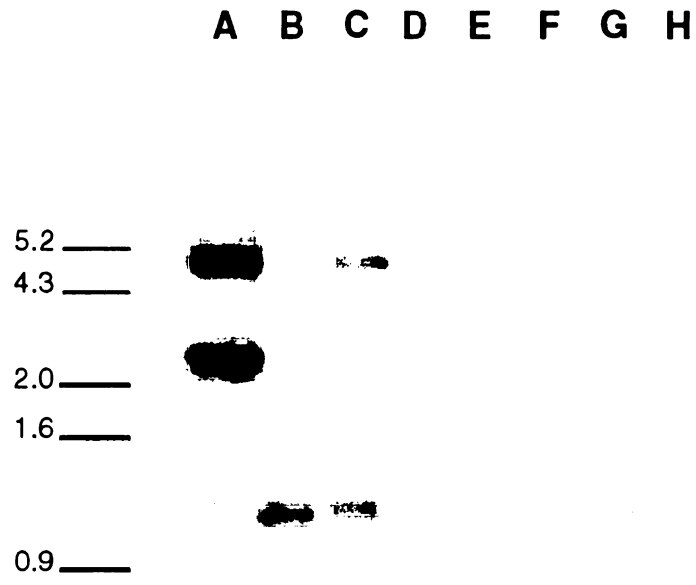


Figure 26. Southern analysis of strains D2704 (lanes B, D, F, and H) and JB161 (lanes A, C, E, and G) using a *serA* probe to confirm insertion of the cassette into the *EcoRI* site of *serA*. Genomic DNA samples were digested with *PvuII/KpnI* (lanes A and B), *PvuII/KpnI/XbaI* (lanes C and D), *PvuII/KpnI/AscI* (lanes E and F), and *PvuII/KpnI/SalI* (lanes G and H).

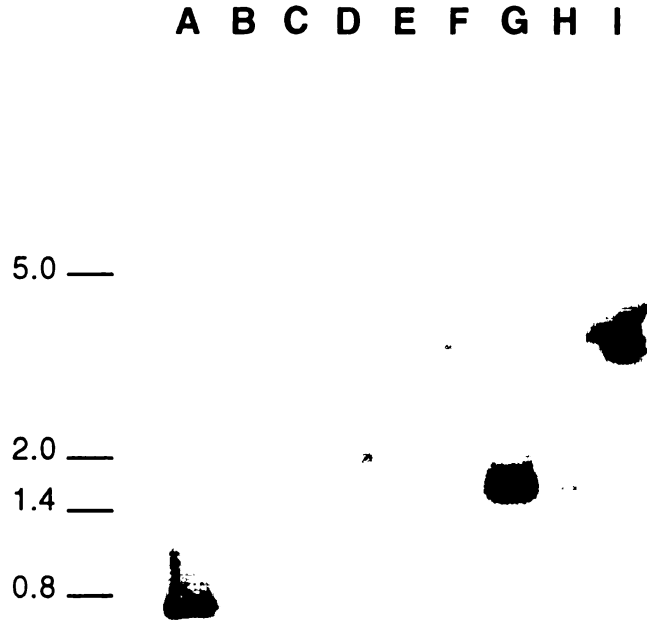


Figure 27. Southern analysis of pJB2.132 (lanes A, D, and G), JB161 (lanes B, E, and H), and KAD11D (lanes C, F, I) using an *aroL* probe to confirm insertion of *aroL* as part of the cassette inserted into the *EcoRI* site of *serA*. DNA samples were digested with *KpnI* (lanes A-C), *HincII* (lanes D-E), and *PvuII/EcoRI* (lanes G-I).

B. Plasmid Constructions.

Overview

Plasmid-localized genes were used to increase the in vivo activity of 3-deoxy-D-arabino-heptulosonic acid 7-phosphate (DAHP) synthase. As the first enzyme in aromatic amino acid biosynthesis, the amount of carbon flow directed into the common pathway is dictated by the in vivo activity of DAHP synthase (Figure 16). A feedback-insensitive isozyme of DAHP synthase²¹, encoded by *aroF^{FBR}* was employed in light of the importance²² of feedback inhibition in controlling this enzyme's in vivo activity. Along with *aroF^{FBR}*-encoded DAHP synthase, transketolase was overexpressed by plasmid localization of *tktA* to ensure that the availability of D-erythrose 4-phosphate did not limit the in vivo activity of overexpressed DAHP synthase (Figure 16).²³

To increase expression levels of chorismate lyase, the *ubiC* open reading frame was placed under the control of a *tac* promoter and plasmid-localized. This provided for efficient transcription and removed possible regulatory control associated with the *ubiCA* operon. In addition to insertion of *P_{tac}ubiC*, *aroF^{FBR}*, and *tktA* into vector pSU18, generating plasmid pJB2.274, a *serA* insert was included to complement loss of phosphoglycerate dehydrogenase resulting from the insertion of the *P_{tac}aroAaroLaroCaroBkan^R* cassette into the genomic *serA* locus. Vector pSU18 contains a *lac* promoter, a genetic marker encoding Cm resistance, and a *p15A* origin of replication with a copy number of approximately twelve per cell.

Another strategy for increasing chorismate lyase activity utilized a *T7* promoter for expression of the plasmid-localized *ubiC* open reading frame.²⁴ To provide the

needed *T7* RNA polymerase encoded by gene *l*, *E. coli* JB161(DE3) and *E. coli* RB38(DE3) were generated after *E. coli* JB161 and *E. coli* RB38, respectively, were lysogenized with λ DE3 phage to introduce a genomic copy of gene *l* under the control of a *lac* promoter. Plasmid localization of *lacI^Q* in pJB3.144B along with *P_{T7}ubiC* allowed chorismate lyase expression to be controlled by the amount of isopropyl β -D-thiogalactopyranoside (IPTG) added to the culture medium. In addition to *lacI^Q* and *P_{T7}ubiC*, plasmid pJB3.144B also carried *aroF^{FBR}*, *tktA*, and *serA* inserts.

Chorismate lyase activity can be controlled by IPTG concentrations because the *lac* operator sequence is included in the *T7* promoter region to regulate the transcription of *ubiC*. The Lac repressor protein, encoded by plasmid-localized *lacI^Q*, will repress the transcription of *ubiC*, but binding of lactose to the Lac repressor can cause a conformational change of the repressor so that the repressor no longer binds to the operator. Transcription of *ubiC*, under the control of the *T7* promoter, is thus derepressed. The advantage of this *PT7 / lacI^Q* system is the ability to modulate the concentration of the inducible gene products in the cell by varying the lactose inducer concentration. The frequently used inducer is the nonhydrolyzable analog of lactose IPTG.

Construction of pJB2.274 and pJB3.144B

The *E. coli ubiC* gene was amplified from *E. coli* RB791 genomic DNA using PCR primers containing *XbaI* terminal restriction sequences. Ligation of the resulting 0.8-kb *ubiC* fragment into the *XbaI* site of pSU18 afforded pKD10.049A in which *ubiC* is transcribed in the same orientation as *lacZ'*. The *ubiC* fragment was then excised from

pKD10.049A by *Xba*I digestion and ligated to the *Xba*I site of pKAD49 affording plasmid pJB1.137A (Figure 28). Expression of chorismate lyase from the *tac* promoter was optimized by construction of plasmid pJB1.237A. This 5.8-kb plasmid was constructed by ligating the open reading frame of *ubiC* into the *Eco*RI site of pJF118EH. Genes inserted in the multiple cloning site of vector pJF118EH, a pBR322-derived plasmid containing *lacI^q* and the *tac* promoter, are located at an optimum distance from the *tac* promoter achieving maximum expression. The *ubiC* fragment was amplified by PCR from pJB1.137A using primers containing *Eco*RI terminal recognition sequences. The amplified 0.50-kb PCR fragment was ligated into the *Eco*RI site of pJF118EH to create plasmid pJB1.273 in which the *ubiC* gene is transcribed in the same orientation as the external *tac* promoter (Figure 29).

The 4.1-kb plasmid pJB2.125B was constructed by inserting the *P_{tac}ubiC* sequence of pJB1.273A into the pSU18-derived plasmid pKL4.20B, which contains the *aroF^{FBR}* gene. The *P_{tac}ubiC* fragment was amplified from pJB1.273A using PCR primers containing *Kpn*I terminal recognition sequences. The 0.58-kb PCR product was ligated to the *Kpn*I site of pKL4.20B to create plasmid pJB2.125B. The *ubiC* gene is transcribed in the opposite orientation as *aroF^{FBR}* (Figure 30). The 6.0-kb plasmid pJB2.133 was created by ligation of a 1.9-kb fragment encoding *serA* into pJB2.125B. The *serA* locus was liberated from plasmid pJB1.102B by digestion with *Xba*I and *Hind*III and subsequently ligated to plasmid pJB2.125B that was previously digested with *Xba*I and *Hind*III. The *serA* gene is transcribed in the same orientation as *ubiC* (Figure 31). Plasmid pJB2.133 was subsequently digested with *Hind*III, and the overhanging ends were eliminated by treatment with Klenow fragment. The *tktA* locus was isolated from

pMF62A following *Bam*HI digestion and treatment with Klenow fragment to provide a fragment with blunt ends. Ligation of *tktA* to pJB2.133 afforded the 8.2-kb plasmid pJB2.274 in which *tktA* is transcribed in the same orientation as *ubiC* (Figure 32).

Construction of plasmid pJB3.144B began by placing *ubiC* under control of the *T7* promoter. The *ubiC* open reading frame was liberated from pJB1.273 using an *Eco*RI digest and subsequently treated with Klenow fragment. This 0.5-kb fragment was ligated to plasmid pET-15b that had been prepared by digestion with *Bam*HI and treated with Klenow fragment. The pBR322-derived vector pET-15b encodes *lacI*^Q and the strong *T7* promoter. Ligation of the two fragments created the 6.2-kb plasmid pJB3.111A. Restriction analysis of pJB3.111A verified that *ubiC* was correctly oriented behind the *T7* promoter (Figure 33).

The 8.3-kb plasmid pJB3.127A was created by inserting a single fragment encoding *P*_{*T7*}*ubiC* and *lacI*^Q into pKL4.33B, a pSU18-derived plasmid containing *serA* and *aroF*^{FBR} inserts. A 2.8-kb fragment encoding *P*_{*T7*}*ubiC* and *lacI*^Q was liberated from pJB3.111A by digestion with *Eco*RI and *Nru*I and treated with Klenow fragment. Plasmid pKL4.33B was digested with *Xba*I and treated with Klenow fragment. Subsequent ligation of the blunt fragments yielded plasmid pJB3.127A. The *lacI*^Q gene is transcribed in the same orientation as *aroF*^{FBR} and *serA* while *P*_{*T7*}*ubiC* is transcribed in the opposite orientation (Figure 34). Plasmid pJB2.144B was created by ligation of *tktA* into pJB3.127A. The 2.2-kb *tktA* gene was isolated from plasmid pMF62A by digestion with *Bam*HI and treated with Klenow fragment. Plasmid pJB3.127A was digested with *Sal*I and treated with Klenow fragment. Subsequent ligation of *tktA* to pJB3.127A

afforded the 10.5-kb plasmid pJB3.144B. The *tktA* gene is transcribed in the opposite orientation as $P_{T7}ubiC$ (Figure 35).

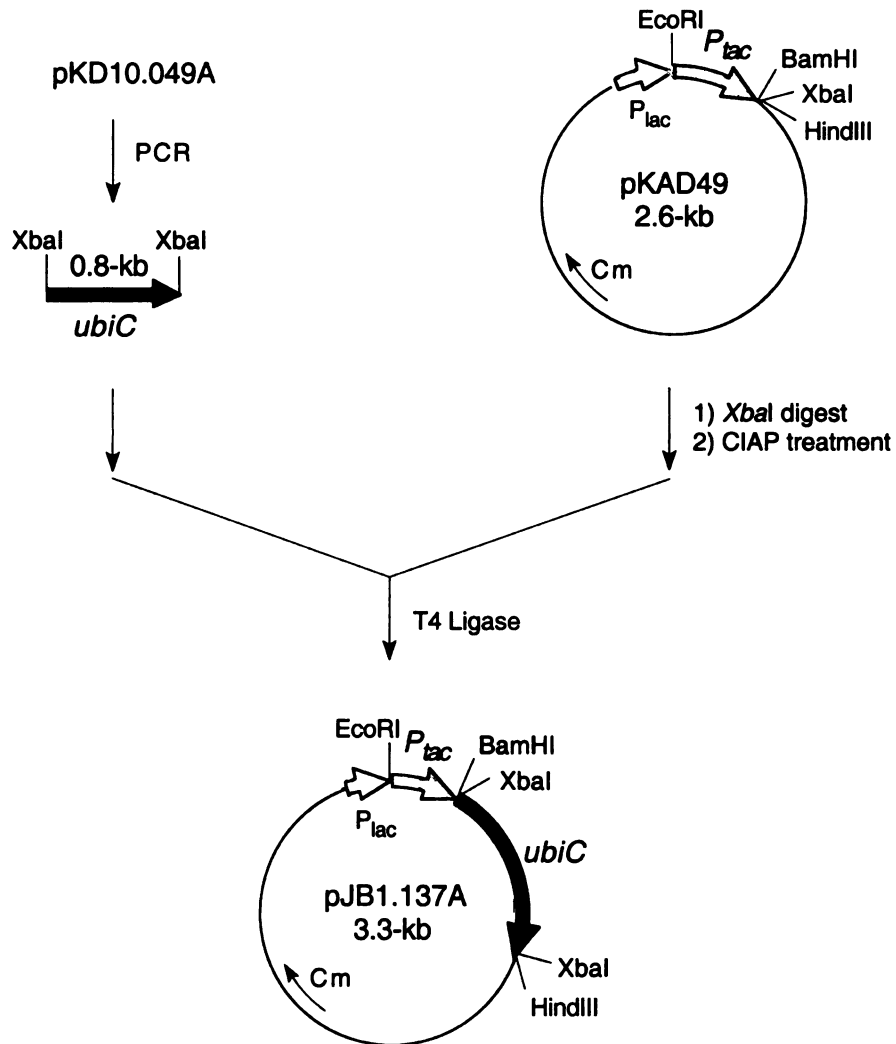


Figure 28. Preparation of Plasmid pJB1.137A.

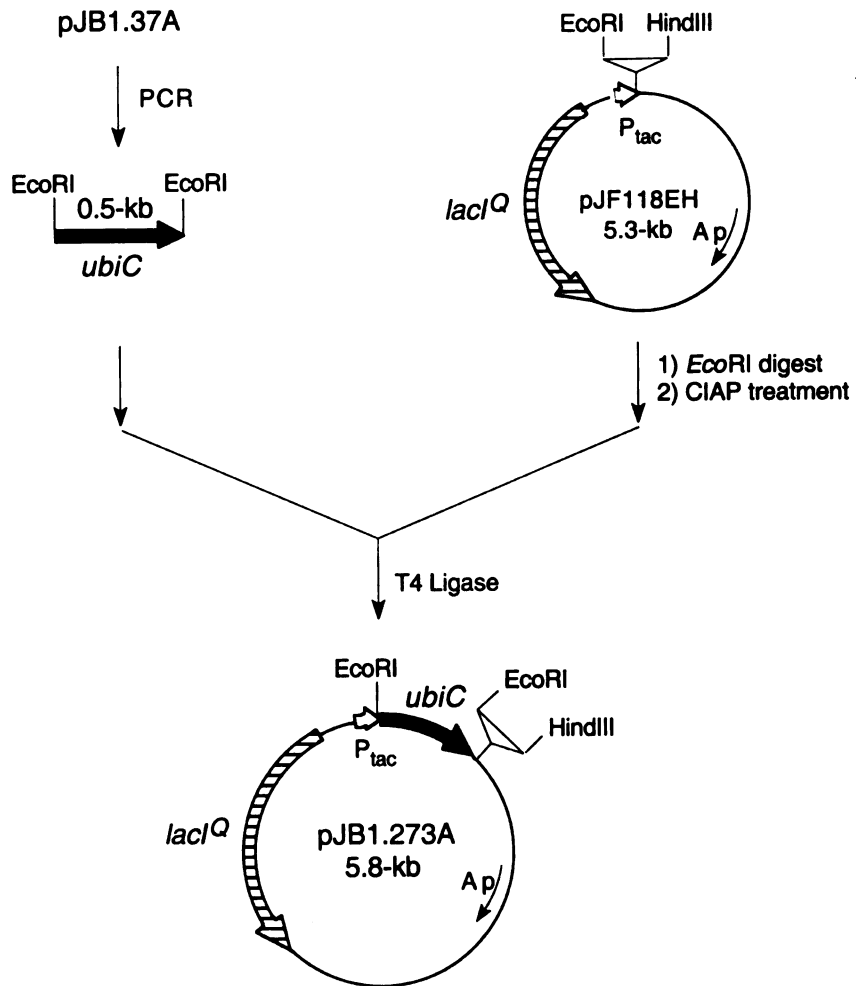


Figure 29. Preparation of Plasmid pJB1.273A.

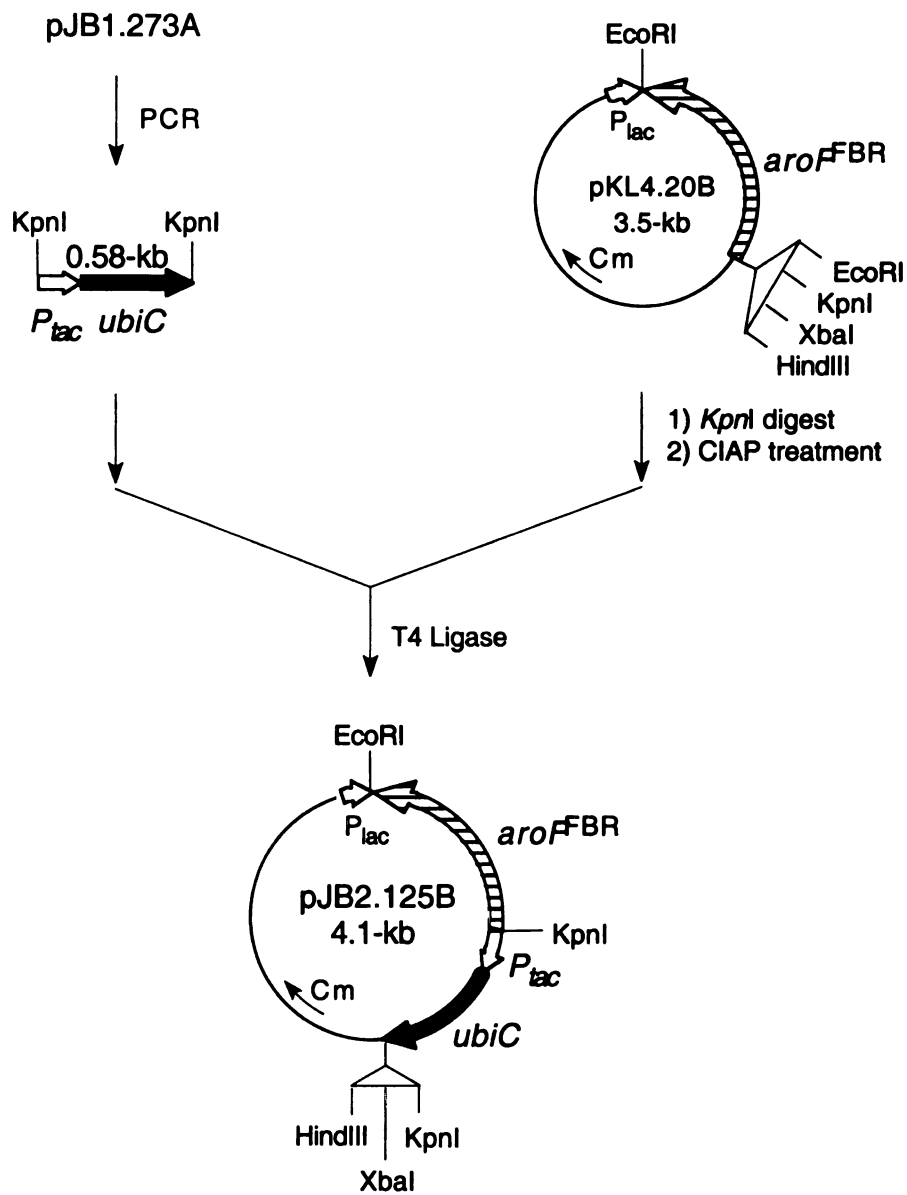


Figure 30. Preparation of Plasmid pJB2.125B.

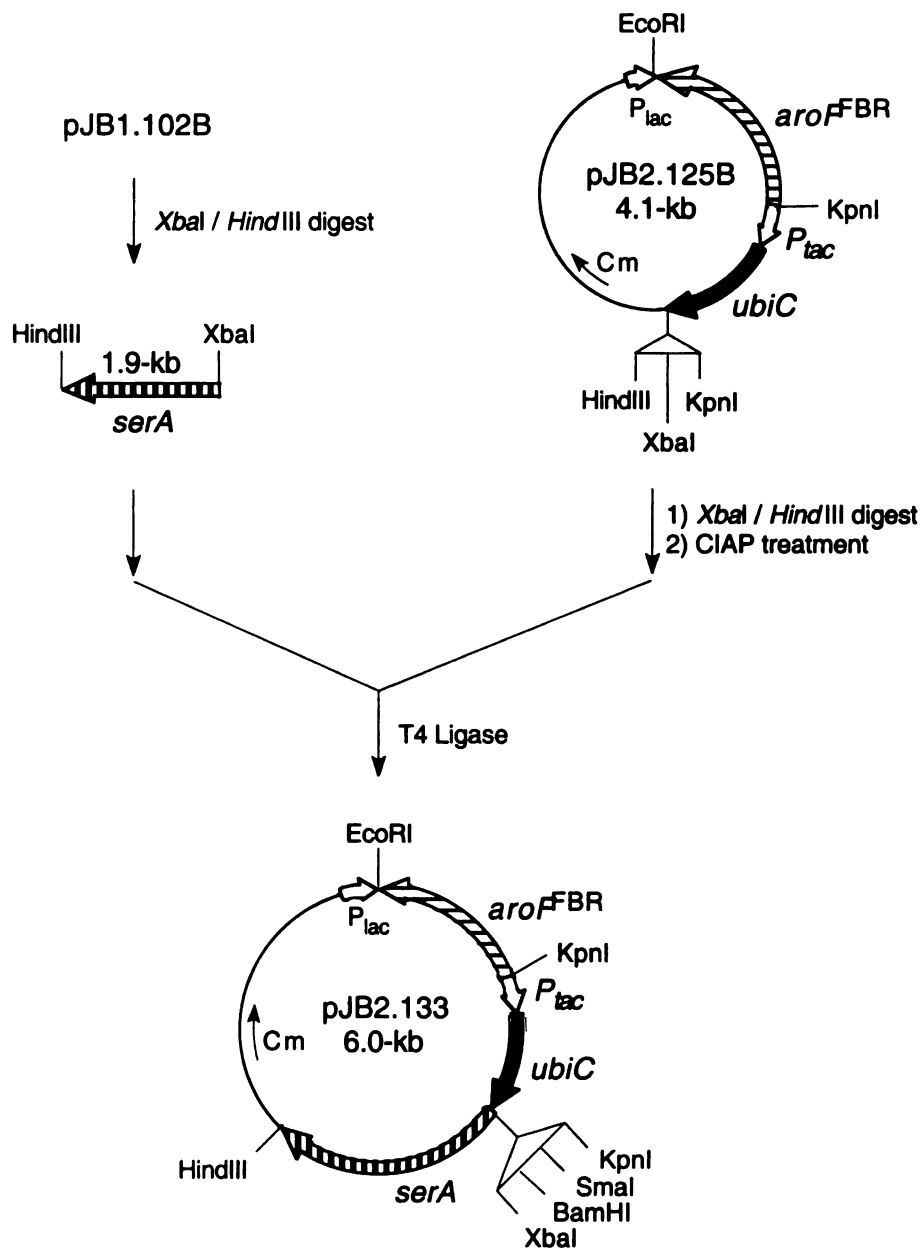


Figure 31. Preparation of Plasmid pJB2.133.

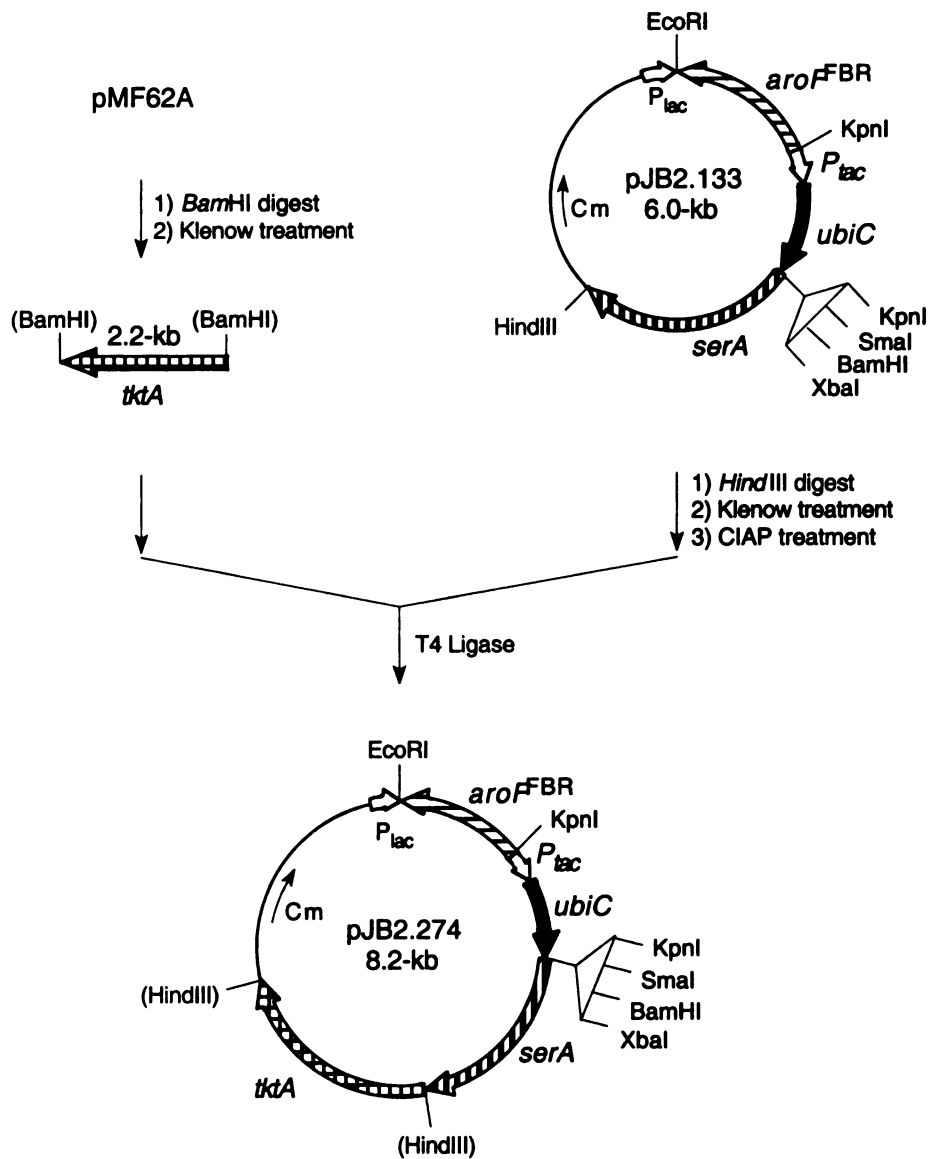


Figure 32. Preparation of Plasmid pJB2.274.

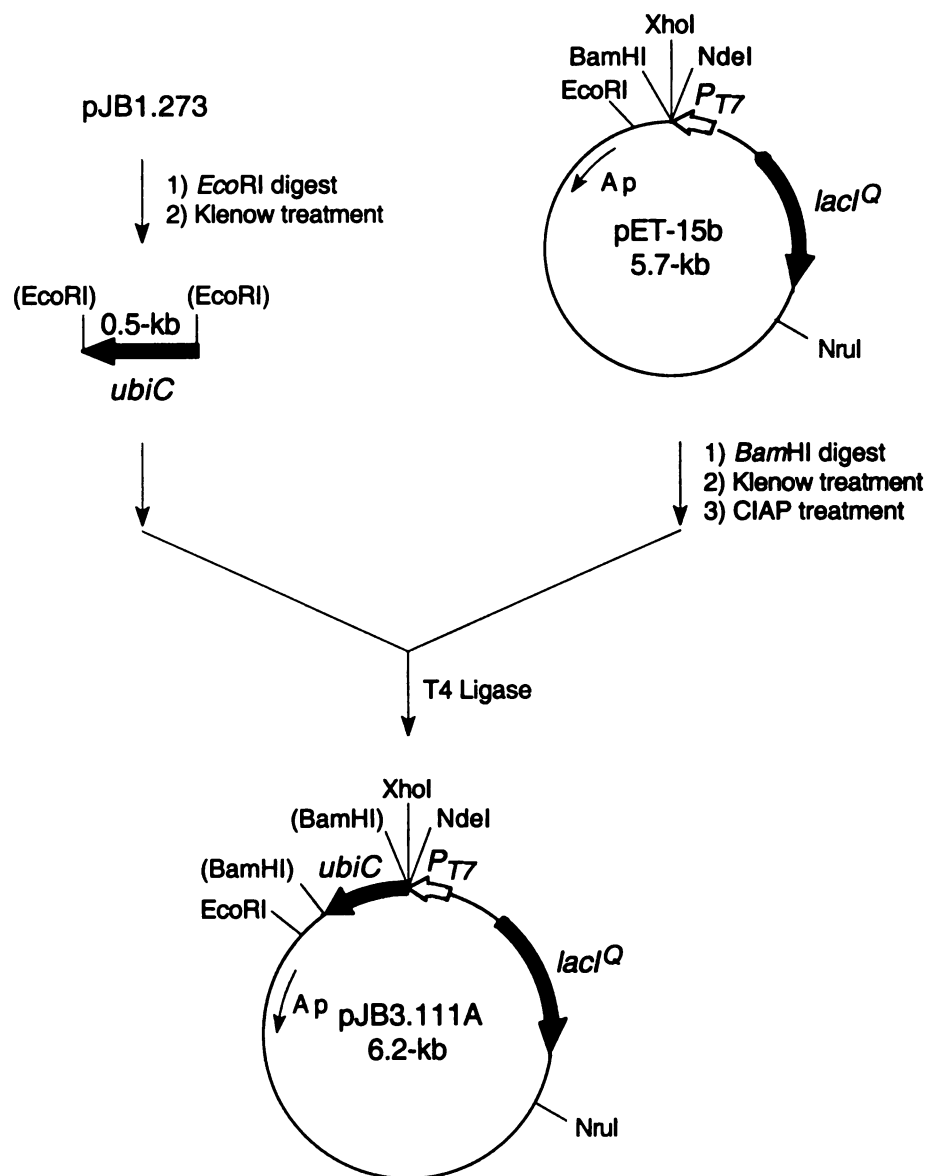


Figure 33. Preparation of Plasmid pJB3.111A.

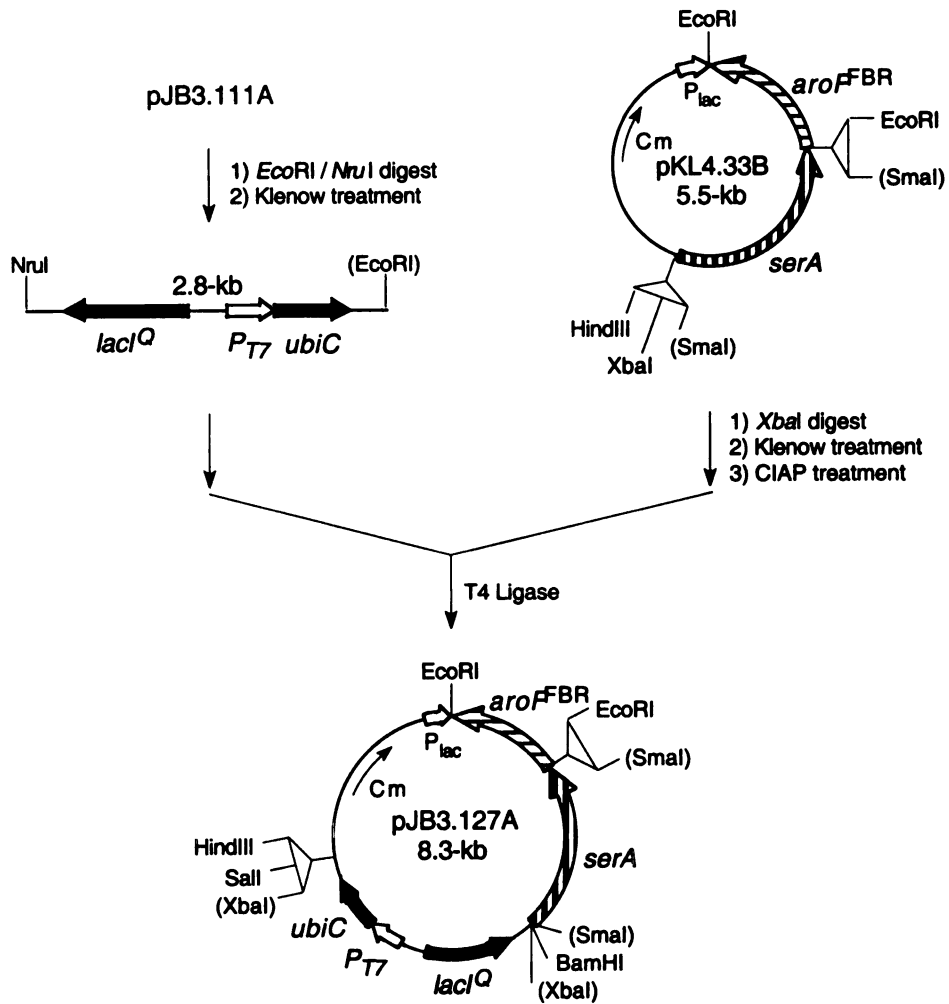


Figure 34. Preparation of Plasmid pJB3.127A.

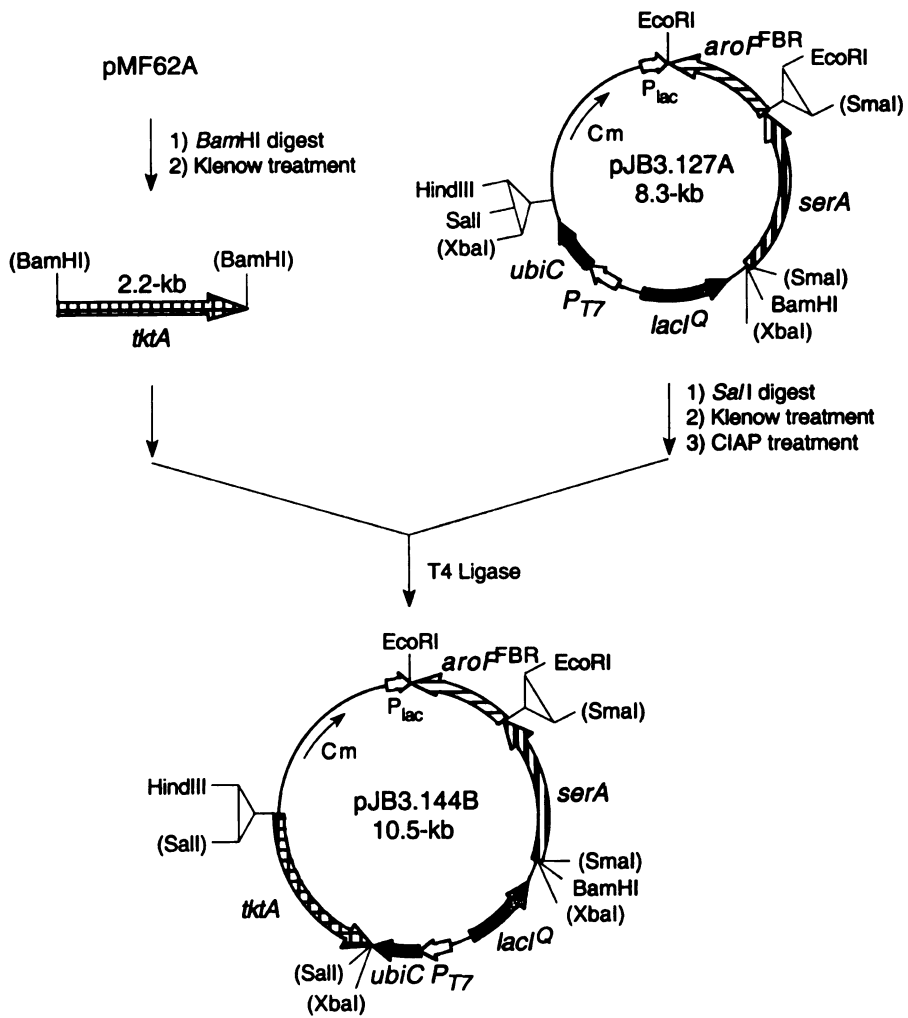


Figure 35. Preparation of Plasmid pJB3.144B.

II. Microbial Synthesis of PHB from Glucose.

A. Fed-Batch Fermentator Conditions for PHB-Producing Microbes.

Fed-batch fermentations were conducted in a B. Braun M2 culture vessel with a 2 L working capacity. The vessel was modified using a stainless steel baffle cage containing four 1/4" x 4" baffles. Environmental conditions were supplied by a B. Braun Biostat MD controlled by a DCU-1. Data was acquired on a Dell Optiplex Gs+ 5166M personal computer utilizing B. Braun MFCS/Win software. PID control loops were used to control temperature, pH, and glucose addition. The temperature was maintained at 33 °C, the pH was maintained at 7.0 by addition of NH₄OH or 2 N H₂SO₄, and glucose was added as a 40% (w/v). PID control parameters were set to 0.0 (off) for the derivative control (τ_D), and 999.9 s (minimum control action) for integral control (τ_I). X_p was set to 950.0% to achieve a K_C of 0.1. Dissolved oxygen (D.O.) was monitored using a Mettler-Toledo 12 mm sterilizable O₂ sensor fitted with and Ingold A-type O₂ permeable membrane. D.O. was maintained at 20% air saturation throughout the course of the fermentations. Antifoam (Sigma 204) was manually pumped into the vessel as needed.

Each inoculant was initiated by introduction of a single colony into 5 mL of M9 medium and grown at 37 °C with agitation for 12-24 h until the culture was turbid. After this time, the starter culture was transferred to 100 mL of M9 medium and grown for an additional 12 to 24 h at 37 °C and 250 rpm. After an appropriate OD₆₀₀ was reached (1.0-3.0), the inoculant was transferred to the fermentation vessel. The initial glucose

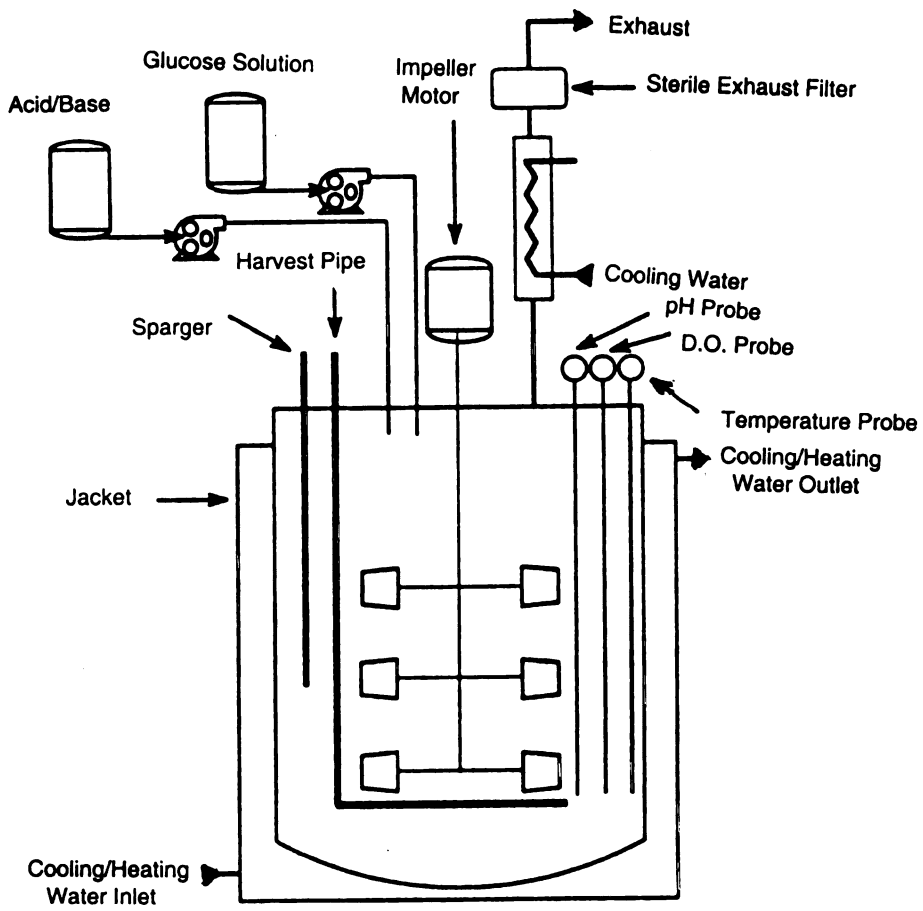


Figure 36. B. Braun Fermentor

concentration in the fermentation medium was 15 g/L for JB161/pJB2.274 and JB161(DE3)/pJB3.144B and 17 g/L for RB38/pJB2.274 and RB38(DE3)/pJB2.144B.

Three staged methods were used to maintain D.O. levels at 20% air saturation during the course of the run. With the airflow at an initial setting of 0.06 L/L/min, D.O. concentration was maintained by increasing the impeller speed from its initial set point of 50 rpm to its preset maximum of 500 rpm. With the impeller constant at 500 rpm, the mass flow controller then maintained D.O. levels by increasing the airflow rate from 0.06 L/L/min to a preset maximum of 1.0 L/L/min. At constant impeller speed and constant airflow rate, D.O. levels were finally maintained at 20% air saturation for the remainder of the fermentation by oxygen sensor-controlled glucose feeding. At the beginning of this stage, D.O. levels fell below 20% air saturation due to residual initial glucose in the medium. This lasted 0.5 to 1.5 h before glucose feeding (40% w/v) started. All strains were cultured in the fermentation vessel for a total of 72 h. Isopropyl β -D-thiogalactopyranoside (IPTG, 10 mg) was added every six hours beginning at the third phase of growth for fermentations using JB161(DE3)/pJB3.144B and RB38(DE3)/pJB3.144B. IPTG (10 mg/mL) was sterilized through 0.22- μ m membranes prior to addition.

Samples (5 mL) of fermentation broth were taken at indicated intervals. Cell densities were determined by dilution of fermentation broth with water (1:100) followed by measurement of absorption at 600 nm (OD_{600}). Dry cell weight (g/L) was obtained using a conversion coefficient of 0.43 g/L/ OD_{600} . The remaining fermentation broth was centrifuged using a Beckman microcentrifuge to obtain cell-free broth. Solute concentrations in the cell-free broth were determined by 1H NMR. For 1H NMR

quantitation of solute concentrations, solutions were concentrated to dryness under reduced pressure, concentrated to dryness an additional time from D₂O, and then redissolved in D₂O containing a known concentration of the sodium salt of 3-(trimethylsilyl)propionic-2,2,3,3-*d*₄ acid (TSP) purchased from Lancaster Synthesis Inc. Concentrations were determined by comparison of the integrals corresponding to each compound with the integral corresponding to TSP ($\delta=0.00$ ppm) in the ¹H NMR. Compounds were quantitated using the following resonances: *p*-hydroxybenzoic acid, doublet at 7.88 ppm (2 H); prephenic acid, multiplet at 6.00 ppm (4 H); L-phenylalanine, multiplet at 7.38 ppm (5 H); L-tyrosine, doublet at 7.20 ppm (2 H); 3-dehydroshikimic acid, doublet at 4.28 ppm (1 H); 3-deoxy-D-*arabino*-heptulosonic acid, triplet at 1.80 ppm (1 H); and acetate, singlet at 1.92 ppm (3 H). ¹H NMR spectra were recorded on a Varian VXR-300 FT-NMR Spectrometer (300 MHz).

In order to measure DAHP synthase and chorismate lyase activity, a portion (20 mL) of the fermentation broth was removed from the vessel at the indicated intervals and centrifuged at 3000g for 5 min at 4 °C. The harvested cells were resuspended in 5 mL of DAHP synthase lysate buffer (50 mM potassium phosphate, pH 6.5, 10 mM PEP, and 0.05 mM CoCl₂) and stored at -80 °C. Samples were analyzed for enzyme activities when the fermentor run was complete.

PHB-producing strains, when cultured under fed-batch fermentor conditions, typically entered logarithmic growth 6 to 24 h after inoculation. Approximately 24 to 36 h after inoculation, fermentor cultures moved from a logarithmic to a stationary growth phase. Microbial cell density normally reached a maximum of 25 to 30 g/L for JB161/pJB2.274 and RB38/pJB2.274 and a maximum of 15 to 20 g/L for

JB161(DE3)/pJB3.133B and RB38(DE3)/pJB3.144B. Over the course of the fermentations, the culture supernatant turned progressively darker resulting in a dark brown color at the end of the run. Significant PHB production typically began as cells entered a logarithmic growth phase and continued until 72 h. After 72 h, productivity in PHB synthesis began to level out and fermentations were not generally maintained beyond this time.

B. Fermentation Results

Table 3. Titrers and Yields of PHB and Titrers of Accumulated Metabolites.

	Construct			
	JB161/ pJB2.274	JB161(DE3)/ pJB3.144B	RB38/ pJB2.274	RB38(DE3)/ pJB3.144B
PHB ^{a,b}	12	6.3	0.59	4.4
% Yield ^c	13	7	0.4	4
PA ^{a,b}	6.3	3.0	1.1	3.2
Phe ^{a,b}	4.1	2.0	4.6	3.9
Tyr ^{a,b}	—	—	8.4	7.7
% PHB ^d	64	65	5	28
DAH ^{a,b}	—	—	5.5	5.5
DHS ^{a,b}	1.4	1.5	1.8	1.6
AcOH ^{a,b}	2.4	3.3	0.33	5.1

^aAbbreviations: PHB, *p*-hydroxybenzoic acid; PA, prephenic acid; Phe, L-phenylalanine; Tyr, L-tyrosine; DAH, 3-deoxy-D-*arabino*-heptulosonic acid; DHS, 3-dehydroshikimic acid; AcOH, acetic acid. ^bg/L. ^cmol PHB/mol glucose. ^dmol PHB/mol PA + mol Phe + mol Tyr + mol PHB.

JB161/pJB2.274 and JB161(DE3)/pJB3.144B

JB161/pJB2.274, which was constructed to reduce enzymatic competition for chorismic acid and expressed *ubiC* from a *tac* promoter, synthesized 12.0 g/L of PHB in 13% yield (mol/mol) from glucose (Figure 38, Table 3). Prephenic acid and L-phenylalanine were also synthesized. Formation of these post-chorismate products in a host strain lacking chorismate mutase and prephenate dehydratase activities can be explained by rapid nonenzymatic Claisen rearrangement of chorismic acid to prephenic acid and subsequent nonenzymatic decarboxylation of the prephenic acid to phenylpyruvic acid. Enzymatic transamination of phenylpyruvic acid then accounts for L-phenylalanine formation (Figure 37).²⁵

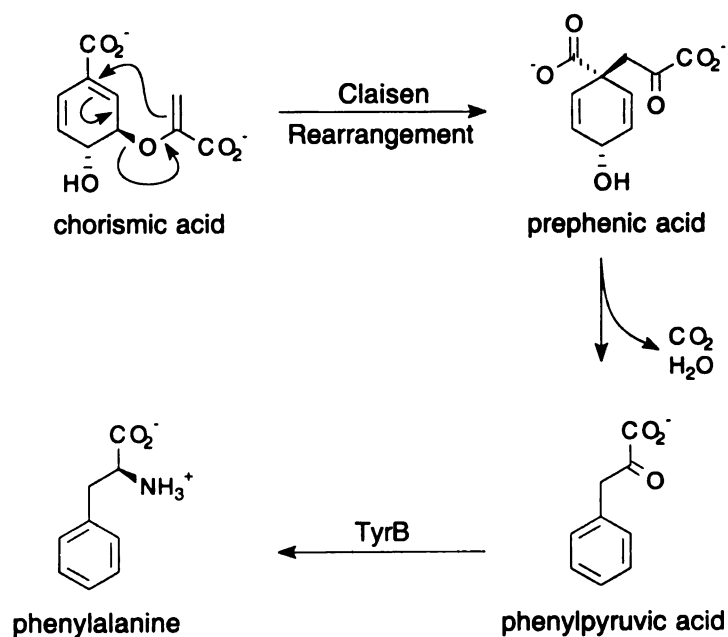


Figure 37. Phenylalanine Synthesis in JB161.
TyrB, aromatic aminotransferase

JB161(DE3)/pJB3.144B, which also had reduced enzymatic competition for chorismic acid but expressed *ubiC*-encoded chorismate lyase from a strong *T7* promoter, synthesized 6.3 g/L of PHB in 7% yield from glucose (Figure 39, Table 3). Relative to the concentrations of PHB, prephenic acid, and L-phenylalanine synthesized by JB161/pJB2.274, JB161(DE3)/pJB3.144B synthesized approximately one-half of the concentrations of these intermediates (Table 3). As a percentage (Table 3) of post-chorismate products, PHB synthesized by JB161(DE3)/pJB3.144B was essentially unchanged relative to JB161/pJB2.274. Similar concentrations of 3-dehydroshikimic acid and acetic acid accumulated in the culture supernatants of both JB161(DE3)/pJB3.144B and JB161/pJB2.274 (Table 3).

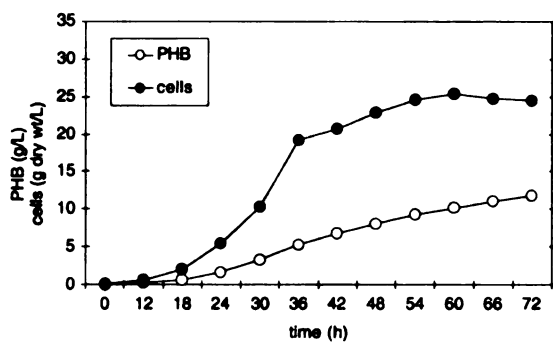
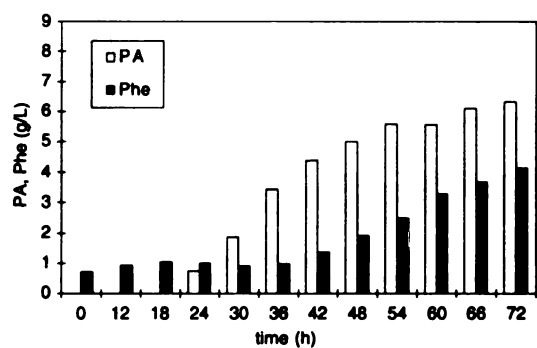
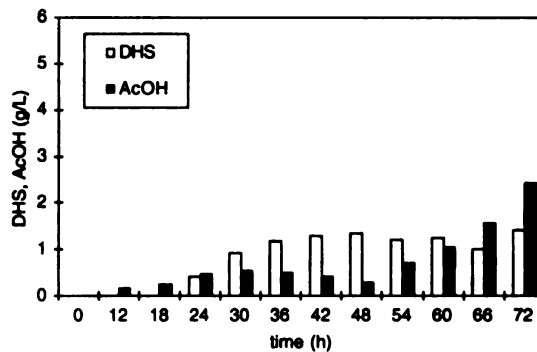
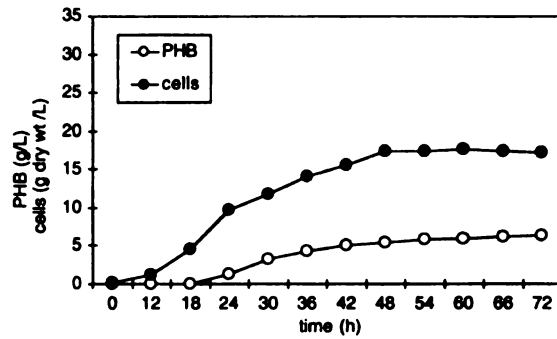
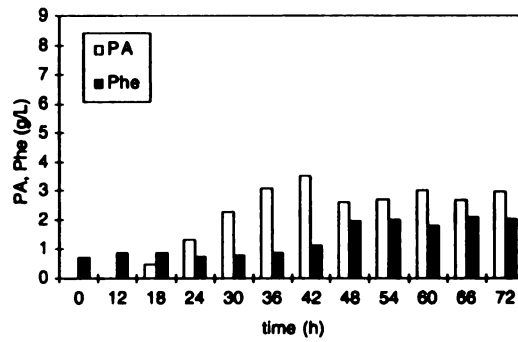
a**b****c**

Figure 38. JB161/pJB2.274 (a) cell growth, PHB. (b) aromatic byproducts: prephenic acid (PA), L-phenylalanine (Phe). (c) nonaromatic byproducts: 3-dehydroshikimic acid (DHS), acetic acid (AcOH).

a



b



c

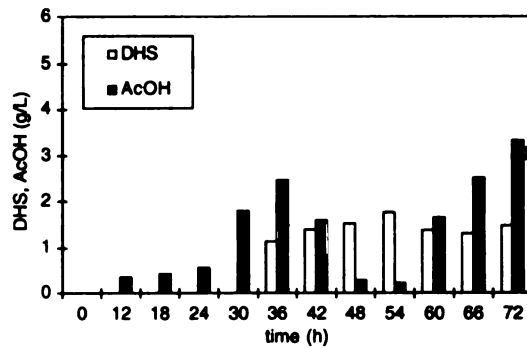


Figure 39. JB161(DE3)/pJB3.144B
(a) cell growth, PHB. (b) aromatic byproducts: prephenic acid (PA), L-phenylalanine (Phe). (c) nonaromatic byproducts: 3-dehydroshikimic acid (DHS), acetic acid (AcOH).

RB38/pJB2.274 and RB38(DE3)/pJB3.144B

RB38/pJB2.274 synthesized 0.59 g/L of PHB and 0.4% yield (mol/mol) from glucose (Figure 40, Table 3). This reflects the competition between chorismate lyase expressed from *P_{lac}ubiC* with other biosynthetic enzymes for in vivo concentrations of chorismic acid. Prephenic acid, L-phenylalanine, and L-tyrosine, 3-dehydroshikimic acid and 3-deoxy-D-*arabino*-heptulosonic acid (DAH) were also synthesized (Figure 40, Table 3) by RB38/pJB2.274. Chorismate lyase in RB38(DE3)/pJB3.144B which was expressed from *P_{T7}ubiC*, also had to compete with wild-type chorismate mutase and other chorismate-utilizing enzymes activities. RB38(DE3)/pJB3.144B synthesized 4.4 g/L of PHB in 4% yield (mol/mol) from glucose (Figure 41, Table 3) along with prephenic acid, L-phenylalanine, L-tyrosine, 3-dehydroshikimic acid, and DAH. PHB constituted 5.2% of the post chorismate products synthesized by RB38/pJB2.274 versus 28% of the post-chorismate products synthesized by RB38(DE3)/pJB3.144B (Table 3).

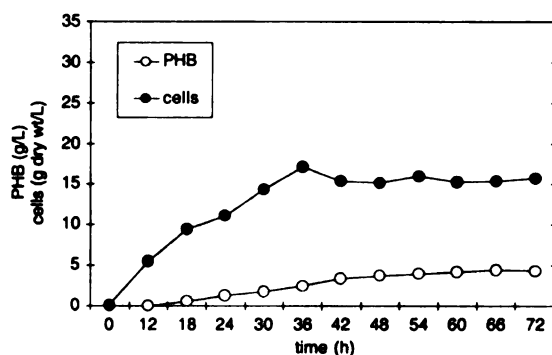
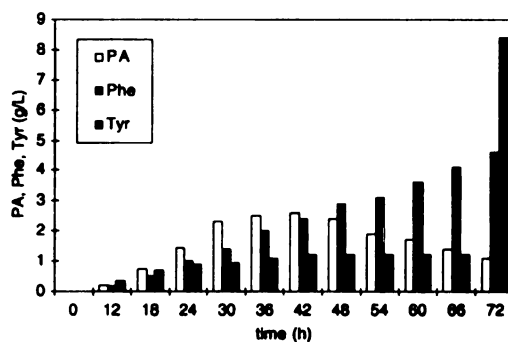
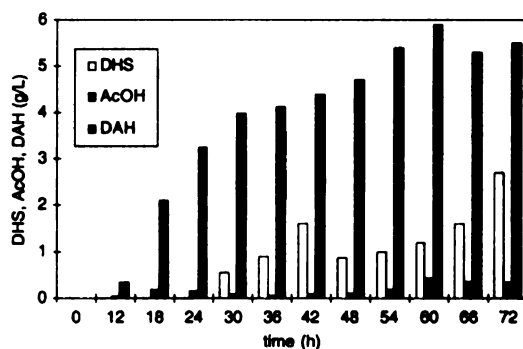
a**b****c**

Figure 40. RB38/pJB2.274 (a) cell growth, PHB. (b) aromatic byproducts: prephenic acid (PA), L-phenylalanine (Phe), L-tyrosine (Tyr). (c) nonaromatic byproducts: 3-dehydroshikimic acid (DHS), acetic acid (AcOH), 3-deoxy-D-arabino-heptulosonic acid (DAH).

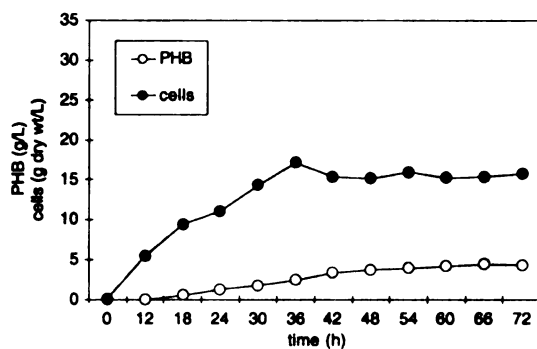
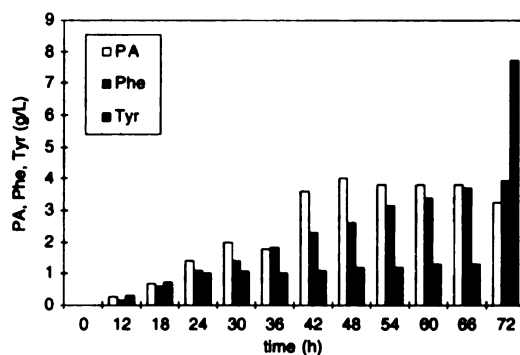
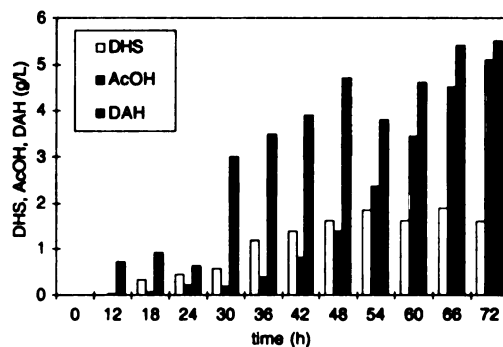
a**b****c**

Figure 41. RB38(DE3)/pJB3.144B (a) cell growth, PHB. (b) aromatic byproducts: prephenic acid (PA), L-phenylalanine (Phe), L-tyrosine (Tyr). (c) nonaromatic byproducts: 3-dehydroshikimic acid (DHS), acetic acid (AcOH), 3-deoxy-D-arabino-heptulosonic acid (DAH).

Inhibition of 3-Dehydroquinate Synthase Activity

L-Tyrosine was the dominant product synthesized by both RB38/pJB2.274 and RB38(DE3)/pJB3.144B. Surprisingly, RB38/pJB2.274 and RB38(DE3)/pJB3.144B both accumulated substantial concentrations of DAH (Figure 40, Figure 41, Table 3), the dephosphorylated substrate of *aroB*-encoded 3-dehydroquinate synthase. Accumulation of this common pathway intermediate has not previously been observed after insertion of a second *aroB* locus in the *E. coli* chromosome.²⁶

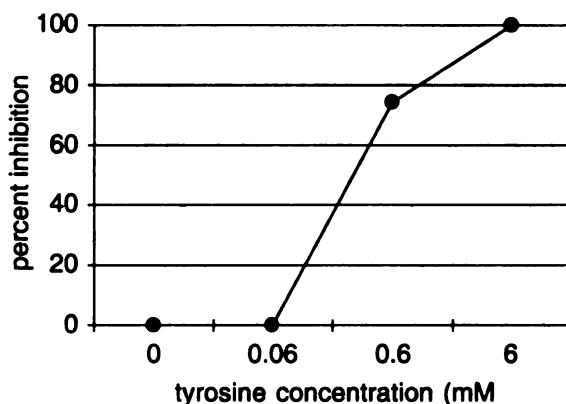
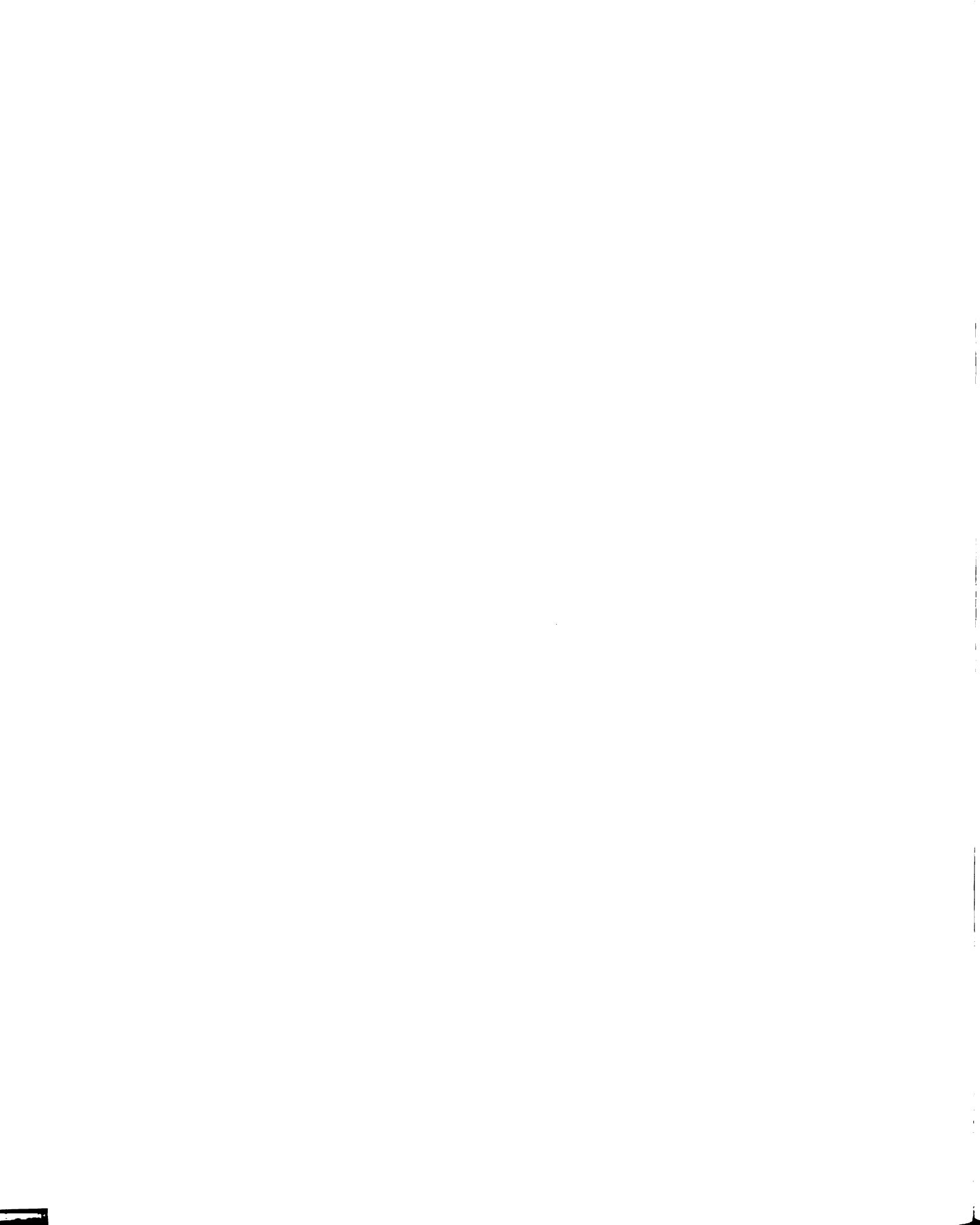


Figure 42. Percent Inhibition of 3-Dehydroquinate Synthase by Tyrosine.

To determine whether L-tyrosine and DAH accumulation were related, the impact of L-tyrosine concentrations on the activity of 3-dehydroquinate synthase was determined. No reduction in 3-dehydroquinate synthase activity was observed at 0.06 mM L-tyrosine concentrations (Figure 42). However, 3-dehydroquinate synthase activity was reduced by 74% and 100% at L-tyrosine concentrations of 0.6 mM and 6 mM, respectively (Figure 42). The 6 mM L-tyrosine approximates the concentrations of this aromatic amino acid that accumulates in the culture medium of RB38/pJB2.274 and



RB38(DE3)/pJB3.144B. Inhibition of 3-dehydroquinate synthase by L-tyrosine has not previously been reported.

C. Chorismate Lyase and DAHP Synthase Activities.

Chorismate Lyase

Amplified expression of *ubiC*-encoded chorismate lyase is particularly important because of this enzyme's low turnover number (49 min⁻¹).²⁷ Chorismate lyase specific activities were therefore quantified periodically over the course of the fermentations. Specific activities were assayed using a new method where *pobA*-encoded *p*-hydroxybenzoate hydroxylase from *Pseudomonas fluorescens* was used as a coupling enzyme.²⁸ *p*-Hydroxybenzoate hydroxylase catalyzes the conversion of PHB to protocatechuic acid. The consumption of NADPH during this hydroxylation and the associated decline in optical density at 340 nm provided the basis for a continuous assay of chorismate lyase-catalyzed formation of PHB from chorismic acid.

The specific activity of chorismate lyase expressed from plasmid-localized *ubiC* under the control of a *tac* promoter in JB161/pJB2.274 was 92-fold higher than wild-type chorismate lyase specific activities measured for JB161 (4.8×10^{-4} U/mg). Even higher chorismate lyase specific activities (Table 4) were achieved when *ubiC* was expressed from a *T7* promoter. For example, chorismate lyase specific activities were 6-fold to 8-fold higher (Table 4) over the course of the fermentor run for JB161(DE3)/pJB3.144B relative to JB161/pJB2.274. A more time-dependent increase in chorismate lyase activity was observed (Table 4) for RB38(DE3)/pJB3.144B. Specific activities for

RB38(DE3)/pJB3.144B increased 1.7-, 9.0-, 21-, and 52-fold relative to chorismate lyase specific activities for RB38/pJB2.274 at 18 h, 36 h, 54 h, and 72 h, respectively.

Table 4. Chorismate Lyase Specific Activities ($\mu\text{mol}/\text{min}/\text{mg}$).

time (h)	Construct			
	JB161/ pJB2.274	JB161(DE3)/ pJB3.144B	RB38/ pJB2.274	RB38(DE3)/ pJB3.144B
18	—	—	0.010	0.17
24	0.042	0.25	—	—
36	0.043	0.31	0.0078	0.07
54	0.047	0.31	0.0067	0.14
72	0.043	0.33	0.0052	0.27

PHB as a percentage of the post-chorismate products (65% versus 64%, Table 3) did not improve with increased chorismate lyase expression for JB161(DE3)/pJB3.144B relative to JB161/pJB2.274. Apparently, increasing chorismate lyase expression levels beyond the specific activities (Table 4) measured for JB161/pJB2.274 leads to little improvement in the synthesis of PHB. This suggests that a level of chorismate lyase activity may have been reached where further increases in chorismate lyase expression are countered by PHB's feedback inhibition of chorismate lyase. Relative to its specific activity in the absence of PHB using a starting concentration of 60 μM chorismic acid, a 38% and 87% reduction in specific activity of chorismate lyase was observed, respectively, in the presence of 15 μM and 120 μM concentrations of PHB (Figure 43).

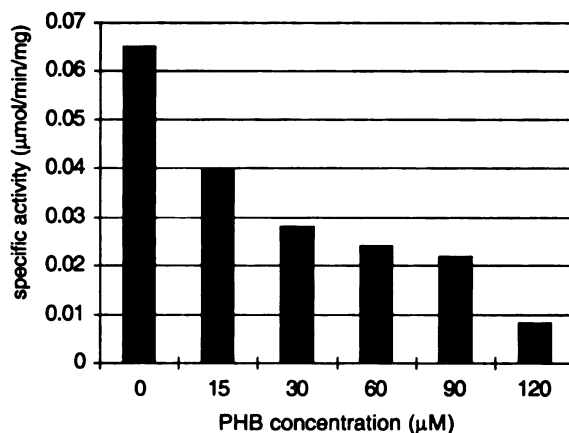


Figure 43. Specific Activities of Chorismate Lyase in the Presence of Various PHB Concentrations.

DAHP Synthase

DAHP synthase activities were also quantified over the course of the fermentations and the specific activities were determined using a standard literature technique.²⁹ It was found that improved chorismate lyase expression came at the expense of DAHP synthase expression. For example, the 6-fold to 8-fold increase in chorismate lyase specific activities (Table 5) for JB161(DE3)/pJB3.144B relative to JB161/pJB2.274 came with a 5-fold to 9-fold reduction in DAHP synthase specific activities (Table 5). A significantly less severe reduction in DAHP synthase specific activity associated with increased chorismate lyase activity was observed for RB38(DE3)/pJB3.144B relative to RB38/pJB3.144B. Less than a 3-fold reduction in DAHP synthase specific activity (Table 5) was observed for RB38(DE3)/pJB3.144B.

Table 5. DAHP Synthase Specific Activities ($\mu\text{mol}/\text{min}/\text{mg}$.)

time (h)	Construct			
	JB161/ pJB2.274	JB161(DE3)/ pJB3.144B	RB38/ pJB2.274	RB38(DE3)/ pJB3.144B
18	—	—	0.56	0.32
24	1.0	0.19	—	—
36	0.91	0.15	0.46	0.35
54	0.76	0.084	0.22	0.14
72	0.33	0.045	0.13	0.050

Increased chorismate lyase expression did substantially improve the concentration and yield of synthesized PHB (4% versus 0.4%, Table 3) and the amount of PHB synthesized as a percentage of all post-chorismate products (28% versus 5%, Table 3) for RB38(DE3)/pJB3.144B relative to RB38/pJB2.274. However, increasing chorismate lyase expression (Table 4) in JB161(DE3)/pJB3.144B relative to JB161/pJB2.274 resulted in a reduction in the concentrations and yields of synthesized PHB (7% versus 13%, Table 3). The decrease in DAHP synthase specific activities (Table 5) for JB161(DE3)/pJB3.144B relative to JB161/pJB2.274 certainly contributed to this reduction in synthesis of post chorismate products.

III. Microbial Toxicity of PHB.

A. Toxicity of PHB on *E. coli* KL3/pKL4.130B.

The most extensive examination of the toxicity of organic acids towards *E. coli* was the recent study by Zaldivar and Ingram.³⁰ PHB is one of the organic acids released from acid hydrolysis of the hemicellulose portion of woody plants due to the breakdown of lignin. The growth of *E. coli* LY01 was found to be inhibited by fifty percent (IC₅₀) by PHB concentrations of 0.8 g/L. Ethanol synthesis in this ethanogenic microbe was also found to be inhibited in the presence of PHB. The toxicity of organic acids is apparently due to diffusion of the protonated form of the acid into the cytoplasm where subsequent dissociation results in a collapse of transmembrane ΔpH , a component of the proton motive force, and an increase in the intracellular H⁺ and acetate concentrations.³¹ Along these lines, *E. coli* KL3/pKL4.130B (Figure 44), was employed to gauge the toxicity of PHB. This is a well-characterized³² construct that synthesizes nontoxic 3-dehydroshikimate acid. *E. coli* KL3/pKL4.130B was cultured in the presence and absence of 10 g/L of added PHB. This approximates the highest level of PHB synthesized from glucose that was observed for JB161/pJB2.274.

The fed-batch fermentor parameters employed to culture 3-dehydroshikimate-synthesizing KL3/pKL4.130B were based on the parameters used to culture the PHB-synthesizing constructs with the following exceptions. KL3/pKL4.130B was cultured in a nonbaffled culture vessel with an initial glucose concentration of 23 g/L in the fermentation medium. The maximum impeller speed that marks the end of the first

E. coli KL3 *aroE353 serA:aroB*

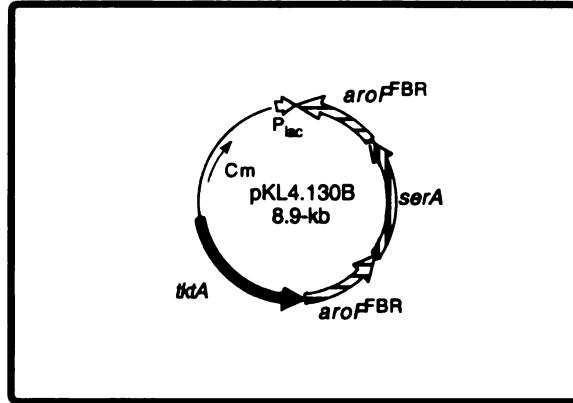
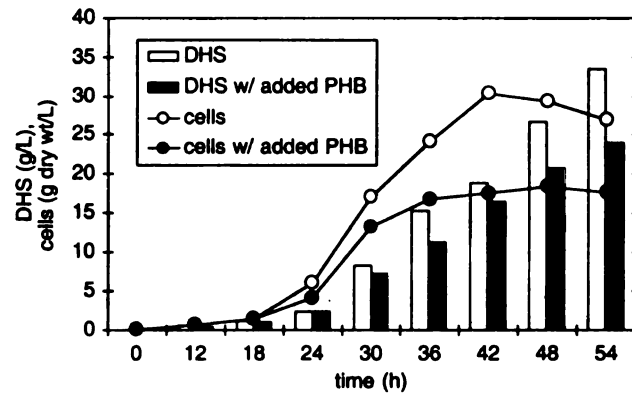


Figure 44. Construct KL3/pKL4.130B

a



b

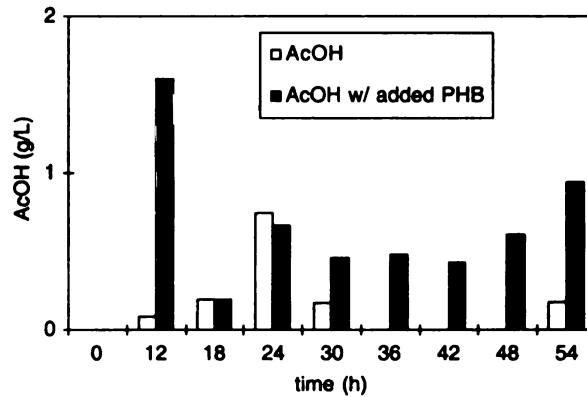


Figure 45. KL3/pKL4.130B (a) cell growth, 3-dehydroshikimic acid (DHS) synthesis and (b) acetic acid formation in the presence of added PHB (10 g/L)

growth phase was 940 rpm. A 60% (w/v) glucose solution was fed into the fermentation vessel during the third growth phase to maintain D.O. levels at 20% air saturation. Cells were cultured for a total of 54 h in the fermentation vessel. PHB was added to a fermentor run of KL3/pKL4.130B to a final concentration of 10 g/L. PHB was divided into two 5 g portions that were added at the beginning of the third stage of growth and 2 h following. PHB solutions was prepared by dissolving 5 g in 50 mL of H₂O, neutralizing to pH 7.0 with NaOH, and filtered through a sterile 0.22- μ m membrane.

In the presence of the added concentrations of PHB, KL3/pKL4.130B was still able to grow and synthesize 3-dehydroshikimic acid (Figure 45). However, added PHB resulted in a marked decrease in cell mass and a decrease in synthesized concentrations of 3-dehydroshikimic acid (Figure 45). Concentrations of acetic acid produced by KL3/pKL4.130B were also substantially higher (Figure 45) throughout the course of the fermentation to which PHB had been added. Only the specific activity of DAHP synthase remained essentially unchanged for KL3/pKL4.130B in the presence versus in the absence of PHB (Table 6). Increased acetic acid formation was also observed to correlate with increases in the concentrations of PHB that were synthesized *de novo* from glucose by RB38(DE3)/pJB3.144B relative to RB38/pJB2.274 (Figure 40, Figure 41, Table 3). The reduction in cell mass, reduced concentrations of synthesized 3-dehydroshikimic acid, and increased formation of acetic acid observed for KL3/pKL4.130B indicate that PHB at concentrations of 10 g/L is adversely affecting microbial growth and metabolism.

Table 6. Impact of PHB on DAHP Synthase Specific Activities ($\mu\text{mol}/\text{min}/\text{mg}$).

time (h)	KL3/pKL4.130B	
	w/out added PHB	^a with added PHB
18	1.9	1.6
30	0.98	0.88
42	0.71	0.85
54	0.40	0.70

^a10g/L

B. Increasing Tolerance to PHB.

Isolation of *E. coli* 98042-42

The decline in cell mass and DHS production concurrent with KL3/pKL4.130B cultured in the presence of PHB suggests that JB161/pJB2.274 is affected by the concentration of PHB it biosynthesizes. It would therefore be desirable to obtain a PHB-producing microbe with increased resistance to PHB. With the high cell densities and PHB concentrations achieved at the end of JB161/pJB2.274 fermentations, it is possible that cells are under sufficient selective pressure to induce an adaptive mutation.

Cells were removed from a fermentation of JB161/pJB2.274 at 42 h when the culture was in transition from logarithmic growth to stationary growth and streaked on M9 plates containing glucose and aromatic amino acids and M9 medium containing glucose, aromatic amino acids, and 50 mM PHB and grown for 48 h at 33 °C. Colonies were subsequently screened for improved growth at 33 °C on M9 plates containing

glucose, aromatic amino acids, and 0, 50, 80, 90, 95, and 100 mM PHB (Table 7). Cells obtained from the fermentation of JB161/pJB2.274 that were maintained on plates containing PHB not only grew faster but grew on significantly higher concentrations of PHB. After 48 h of incubation, fermentation-derived cells that were originally streaked on medium containing 50 mM PHB grew on all plates containing PHB while JB161/pJB2.274 and fermentation-derived cells that were originally streaked on medium without PHB only grew on plates containing 50 mM PHB. One of the colonies growing on 100 mM PHB was selected and named 98042-42. Comparison of the growth characteristics of fermentation-derived cells originally grown in the presence of 50 mM PHB versus fermentation-derived cells grown in the absence of PHB suggests that the adaptive mutation that allows growth on higher concentrations of PHB is easily lost when cells are grown without the selective pressure of PHB in the medium.

Table 7. Plate Selection for 98042-42.

strain	concentration of PHB (mM)					
	50	80	90	95	100	0
JB161/ pJB2.274	+	-	-	-	-	+++
42 h cells plated on 50 mM PHB	++	+	+	+	+ ^a	+++
42 h cells plated on 0 mM PHB	++	-	-	-	-	+++

^acolony selected from this plate and named 98042-42.

Fed-Batch Fermentation of 98042-42.

Fed-batch fermentor parameters employed to culture 98042-42 were based on the parameters used to culture JB161/pJB2.274. However, both the 5 mL starter culture and the 100 mL inoculum contained 50 mM PHB to maintain selective pressure on the mutated cells. 98042-42 synthesized 11 g/L of PHB in an 11% yield (mol/mol) from glucose (Figure 46, Table 8). Increased concentrations of prephenic acid and L-phenylalanine were synthesized by 98042-42 relative to JB161/pJB2.274 (Table 8, Table 3). As a percentage (Table 8) of post-chorismate products, the PHB synthesized by 98042-42 is lower relative to JB161/pJB2.274 (Table 3). The concentration of 3-dehydroshikimic acid and chorismate lyase specific activities remained essentially unchanged for 98042-42 (Table 8, Table 9) versus JB161/pJB2.274 (Table 3, Table 4). Relative to JB161/pJB2.274 (Table 3), 98042-42 (Table 9) synthesized 4-fold less acetic acid suggesting that PHB is less toxic to the metabolism of 98042-42. Comparison of DAHP synthase activities, show a 1.5-fold to 1.9-fold decline in specific activities in 98042-42 (Table 9) relative to JB161/pJB2.274 (Table 5). However, the molar quantity of post-chorismate products synthesized by 98042-42 (0.15 M, Table 8) is slightly higher than that synthesized by JB161/pJB2.274 (0.13M, Table 3). Although spontaneous mutations in 98042-42 resulted in improved growth characteristics on plates and in the fermentor, these adaptations did not translate to improved biosynthesis of PHB.

Table 8. Titrers and Yields of PHB and Titrers of Accumulated Metabolites for 98042-42.

PHB ^{a,b}	%yield ^c	PA ^{a,b}	Phe ^{a,b}	%PHB ^d	DHS ^{a,b}	AcOH ^{a,b}
11	11%	7.3	5.3	56%	1.8	0.6

^aAbbreviations: *p*-hydroxybenzoic acid (PHB), prephenic acid (PA), L-phenylalanine (phe), 3-dehydroshikimate (DHS), acetic acid (AcOH). ^bg/L. ^cmol PHB/mol glucose. ^dmolPHB/mol PHB + mol PA + mol Phe.

Table 9. DAHP synthase and Chorismate Lyase Specific Activities for 98042-42.

enzyme	time (h)			
	18	36	54	72
DAHP synthase	0.62	0.60	0.41	0.22
chorismate lyase	0.045	0.047	0.046	0.045

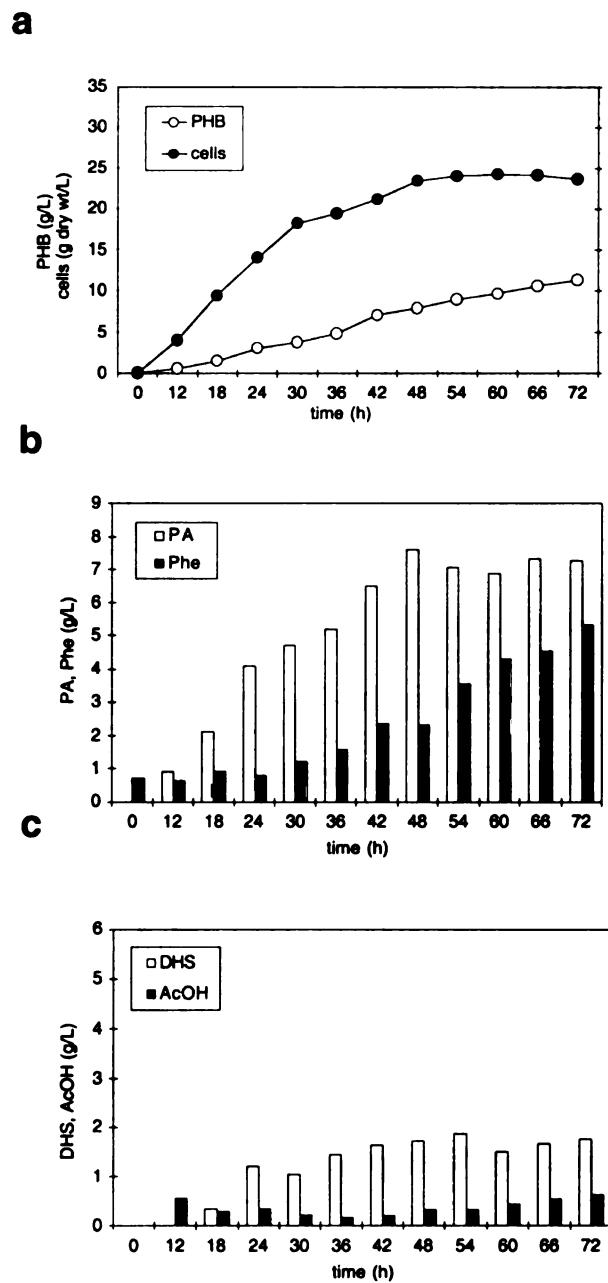


Figure 46. 98042-42 (a) cell growth, PHB. (b) aromatic byproducts: prephenic acid (PA), L-phenylalanine (Phe). (c) nonaromatic byproducts: 3-dehydroshikimic acid (DHS), acetic acid (AcOH).

IV. PHB *O*- β -D-Glucoside.

A. PHB *O*- β -D-Glucoside Toxicity Towards *E. coli*.

Glucosyltransferases, enzymes catalyzing the conjugation of UDP-glucose with phenolic compounds, have been found in a wide variety of plants. This family of enzymes is responsible for converting phenolic compounds such as PHB, salicylic acid, and vanillic acid into their corresponding β -D-glucoside or β -D-glucosyl ester (Figure 47).³³ Glucoside formation is believed to precede the incorporation of these lignin monomers into the cell wall.³⁴ Glycosylation of signaling molecules, such as PHB and salicylic acid, may also play a role in regulating plant hormone levels. Conjugation of phenolics may also serve as a detoxification mechanism. Therefore, this same mechanism could be applied to PHB-synthesizing *E. coli* strains to alleviate product toxicity and potential feedback inhibition of chorismate lyase. Heterologous expression of a plant glucosyltransferase in PHB-producing *E. coli* strain would lead to the accumulation of PHB *O*- β -D-glucoside in the culture supernatant. Unconjugated PHB and glucose could be obtained via acid hydrolysis of the clarified culture supernatant followed by organic extraction of PHB.

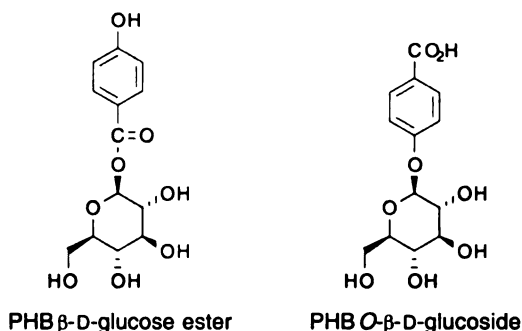


Figure 47. Structures of PHB/Glucose Conjugates.

Synthesis of *p*-Hydroxybenzoate *O*- β -D-Glucopyranoside.

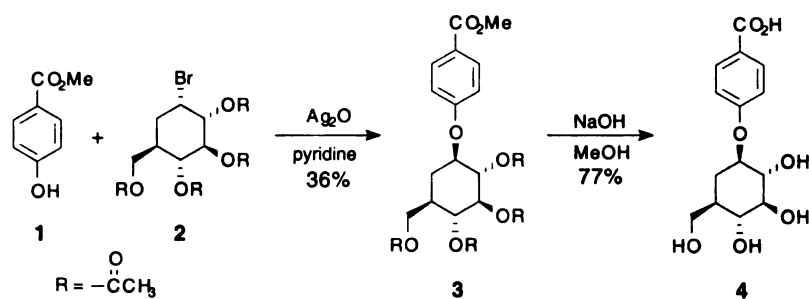


Figure 48. Synthesis of PHB *O*- β -D-Glucopyranoside.

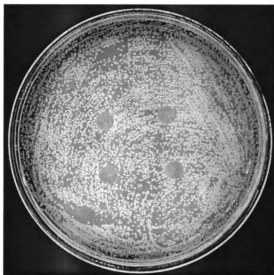
To verify that glycosylation of PHB would alleviate the toxicity imparted to *E. coli* growth and metabolism by PHB, the *O*- β -D-glucoside of PHB was synthesized³⁵ and its antimicrobial activity measured. The synthesis (Figure 48) of *p*-hydroxybenzoate *O*- β -D-glucopyranoside (PHB *O*- β -D-glucoside) was based on the method Grykiewicz et al. described for the synthesis of salicylic acid *O*- β -D-glucopyranoside. Starting material *p*-hydroxybenzoate methyl ester (1) was combined with molar equivalents of tetra-*O*-acetyl- α -D-glucopyranosyl bromide (2) and silver (II) oxide. Pyridine was added and the mixture was allowed to stir vigorously at room temperature until the reaction was complete. The coupled product, following CHCl_3 extraction and recrystallization from boiling MeOH, was isolated as white crystals in 36% yield. 4-Carbomethoxyphenyl 2,3,4,6-tetra-*O*-acetyl- β -D-glucopyranoside (3) was dissolved in methanol and deprotected at room temperature by the addition of NaOH. After the reaction was complete, the base was neutralized by the addition of Dowex-50 (H^+) and the mixture filtered. The reaction mixture was evaporated to dryness and the resulting solid

recrystallized from boiling MeOH. *p*-Hydroxybenzoate *O*- β -D-glucopyranoside (4) was obtained as white crystals in a 77% yield.

Toxicity of PHB *O*- β -D-glucoside versus PHB

The relative toxicity of PHB and its glucoside was gauged by inhibition zones using the paper disc diffusion method.³⁶ In this assay, cells from a growing culture of *E. coli* RB791 were diluted and spread evenly onto an M9 plate. A known amount of compound was absorbed into a paper disk and the disk was placed onto the M9 plate. After incubating at 37 °C for 24 h, the diameter of the zone (inhibition zone) surrounding each disk that did not support growth due to leaching of the applied compound into the surrounding medium was measured. To measure the inhibition zones corresponding PHB and PHB *O*- β -D-glucoside, a 1 M solution of each compound was made and the pH adjusted to 7.0 with NaOH. Disks were submerged in the respective solutions (2.5×10^5 moles of compound absorbed per disk), blotted on filter paper and pressed lightly onto the prepared M9 plate. After 24 h of incubation, PHB produced an inhibition zone of 1.6 cm while PHB *O*- β -D-glucoside showed no toxicity towards *E. coli* as an inhibition zone was not formed (Figure 49).

a



b

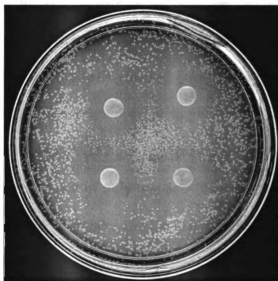


Figure 49. Relative Toxicity of PHB and PHB *O*- β -D-Glucopyranoside. (a) Zones of inhibition due to PHB *O*- β -D-Glucopyranoside. (b) Zones of inhibition due to PHB.

B. Heterologous Expression of a Tobacco Glucosyltransferase in *E. coli*.

Cloning of *TOGT1*

Two homologous 1.4-kb cDNA sequences, *IS5a* and *IS10a*, were isolated by Horvath and Chua³⁷ from cycloheximide-pretreated salicylic acid-induced *Nicotiana tabacum* BY-2 cells. Comparison of the predicted amino acid sequences showed homology to known glucosyltransferases. Using primers designed from the cDNA sequences of *IS5a* and *IS10a*, Fraissinet-Tachet et al.³⁸ amplified two 1.4-kb genes, *TOGT1* and *TOGT2*, from genomic DNA isolated from *N. tabacum* cv. *Samsun NN*. Studies on the recombinant TOGT1 protein revealed the ability to transfer the glucosyl moiety from UDP-glucose to both the hydroxyl and carboxyl group of PHB synthesizing the PHB *O*- β -D-glucoside and the PHB glucosyl ester. Analysis of *TOGT1* and *TOGT2* revealed almost identical gene sequences distinguished by a *SaII* site in *TOGT2*. Comparison of the *TOGT1* and *TOGT2* genomic sequences to the *IS5a* and *IS10a* cDNA sequences revealed the difference of only one and three nucleotides respectively. The homology between the cDNA sequences and the genomic sequences implies that introns, untranslated segments of DNA found in many eucaryotic genes, are not present in *TOGT1* and *TOGT2*. Therefore, these glucosyltransferases can be amplified from genomic DNA and directly expressed in *E. coli*.

The *TOTG1* gene was amplified from genomic DNA isolated from the leaves of wild-type *N. tabacum* *SR 1* seedlings. *N. tabacum* was cultured under sterile conditions on Murashige and Skoog medium for 13 days with a 24 h photo period. Genomic DNA

(32 μ g) was isolated from 153 mg of frozen leaf tissue based on the method of Verwoerd et al. Primers, containing terminal *Bam*HI recognition sequences, were designed to amplify the open reading frame of *TOGT1* or *TOGT2*. Either gene could be amplified with the same primers due to their high sequence homology. The resulting 1.4-kb PCR fragment was shown to be *TOGT1* after *Sal*I digestion. Plasmid pSU18 was digested with *Bam*HI and ligated to the *TOGT1* PCR fragment affording the 3.7-kb plasmid pJB5.203A with *TOGT1* transcribed in the same orientation as *lacZ'* (Figure 50). Plasmid pJB5.205A was created to express *TOGT1* from the *T7* promoter. The *TOGT1* open reading frame was liberated from pJB2.203A using a *Bam*HI digest. This 1.4-kb fragment was ligated to plasmid pET-15b that had been prepared by digestion with *Bam*HI. Ligation of the two fragments created the 7.1-kb plasmid pJB5.205A. Restriction analysis of pJB5.205A verified that *TOGT1* was correctly oriented behind the *T7* promoter (Figure 51).

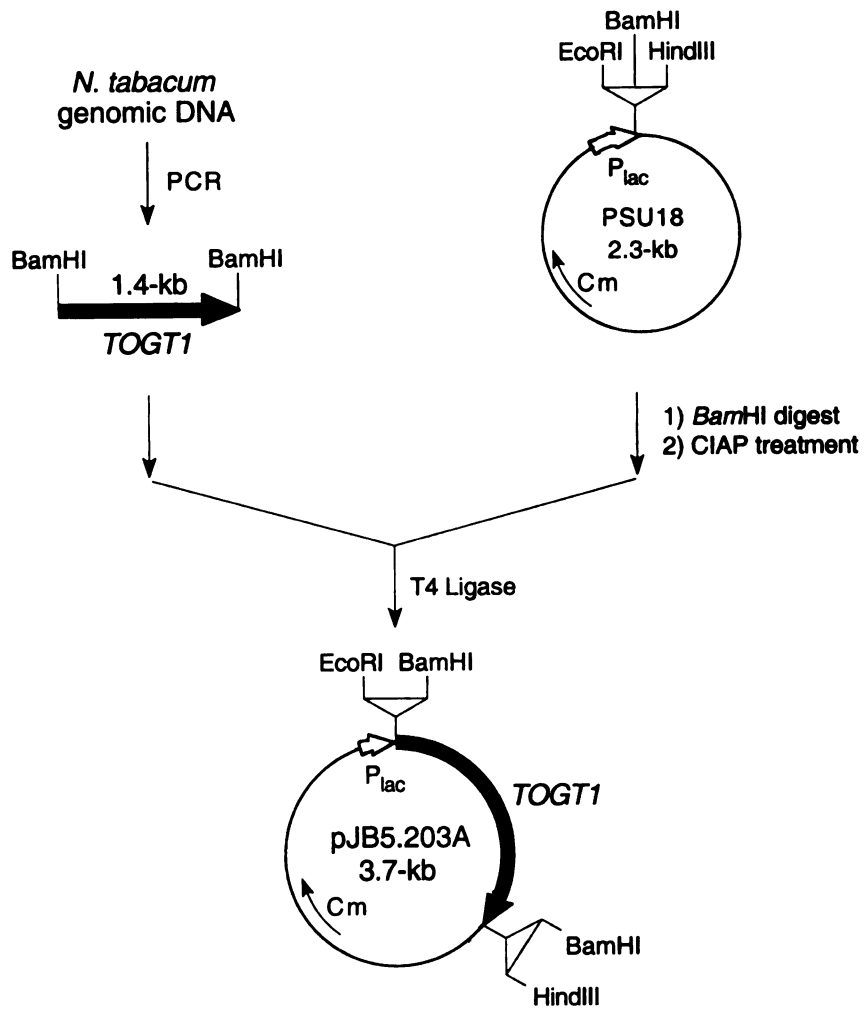


Figure 50. Preparation of Plasmid pJB5.203A

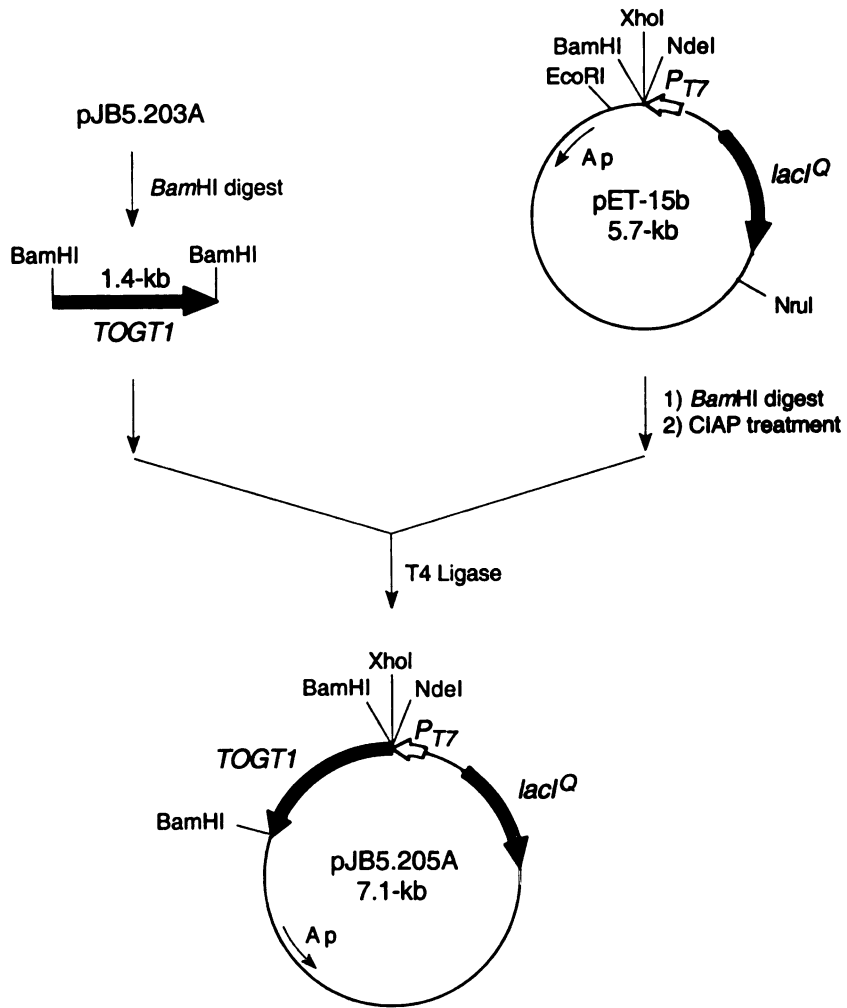


Figure 51. Preparation of Plasmid pJB5.205A.

Microbial Synthesis of PHB *O*- β -D-Glucoside.

JB161(DE3)/pJB2.274/pJB5.205A was cultured in shake flasks to test for the *in vivo* accumulation of PHB *O*- β -D-glucoside. This PHB-producing strain should export PHB as the *O*- β -D-glucoside to its culture supernatant due to the localization of *P*₇₇*TOGT1* on plasmid pJB5.205A. JB161(DE3)/pJB2.274/pET-15b was cultured in parallel as a control strain absent in glucosyltransferase activity. Each strain was inoculated into a 2 L Erlenmeyer flask containing 500 mL of LB, Amp (2 x), Cm, Kan, and IPTG (0.2 mM) and grown for 12 h with agitation at 250 rpm and 37 °C. Cells were harvested by centrifugation (4000g, 5 min. 4 °C) and resuspended in 500 mL of M9 medium containing glucose (5 g/L), Amp (2 x), Cm, Kan, Phe, Tyr, Trp, and IPTG (0.2 mM) and the cells were grown for 48 h. The pH was adjusted to 7.0 with NaOH after 2, 6, and 7.5 h. After 24 h, ¹H NMR analysis of the culture supernatant showed glucose to be depleted from both cultures and an additional 10 g of glucose was added to each.

After 48 h, JB161(DE3)/pJB2.274/pJB5.205A and JB161(DE3)/pJB2.274/pET-15b produced 7.5 mM and 7.9 mM of PHB (Table 10), respectively. L-Phenylalanine and acetate were also produced (Table 10) by both strains while prephenic acid, which was present in both cultures at 24 h, was only present in the culture supernatant of JB161(DE3)/pJB2.274/pET-15b at 48 h (Table 10). As a percentage of post-chorismate products, JB161(DE3)/pJB2.274/pJB5.205A produced 84% PHB and JB161(DE3)/pJB2.274/pET-15b produced 74% PHB (Table 10).

By 72 h however, the difference in product ratios narrowed as PHB constituted 83% of the post-chorismate products synthesized by JB161(DE3)/pJB2.274/pJB5.205A versus 80% of the post-chorismate products synthesized by JB161(DE3)/pJB2.274/pET-

15b (Table 10). The strain absent in glucosyltransferase activity produced slightly more PHB than the strain expressing *TOTG1*. JB161(DE3)/pJB2.274/pET-15b synthesized 12 mM PHB compared to the 10 mM synthesized by JB161(DE3)/pJB2.274/pJB5.205A.

Table 10. Metabolite Comparison of PHB-Producers with and without Glucosyltransferase Expression.

	JB161(DE3)/ pJB2.274/pET-15b			JB161(DE3)/ pJB2.274/pJB5.205A		
	24h	48h	72h	24h	48h	72h
PHB ^{a,b}	3.7	7.9	12	4.1	7.5	10.2
PA ^{a,b}	1.1	1.6	—	0.92	—	—
Phe ^{a,b}	0.56	1.2	3.0	0.51	1.5	2.1
%PHB ^c	69%	74%	80%	74%	84%	83%
glucose ^b	—	38	—	—	40	40
AcOH ^{a,b}	—	15	16	—	16	18

^aAbbreviations: *p*-hydroxybenzoic acid (PHB), prephenic acid (PA), L-phenylalanine (Phe), acetic acid (AcOH). ^bmM. ^cmol PHB/mol PHB + mol PA + mol Phe.

While it appeared that feedback inhibition of chorismate lyase may have been partially ameliorated, as represented by the increased ratio of PHB to other post-chorismate products in JB161(DE3)/pJB2.274/pJB5.205A relative to JB161(DE3)/pJB2.274/pET-15b (Table 10), ¹H NMR analysis of the culture supernatant did not reveal the presence of PHB *O*-β-D-glucoside. Comparison of key resonances for PHB and glucose reveal the same chemical shifts in the ¹H NMR spectra of the two strains (Figure 62, Figure 63). A second line of evidence can be drawn by comparing the ratio of the integrals of the α and β signals corresponding to the anomeric proton of

carbon. Assuming that both α and β forms of glucose are non-preferentially taken into the cell, the ratio of the α to β ^1H NMR signals should stay constant unless PHB accumulates in the culture supernatant as its β glucoside, increasing the ratio in favor of the β peak. Analysis of the culture supernatants of both JB161(DE3)/pJB2.274/pJB5.205A (Figure 62) and JB161(DE3)/pJB2.274/pET-15b (Figure 61) show the same ratio of the integrals corresponding to the α and β signals of the anomeric proton of glucose. Failure of JB161(DE3)/pJB2.274/pJB5.205A to accumulate PHB as its glucoside could have been due to low availability of UDP-glucose, a co-substrate necessary for glucosyltransferase activity. In *E. coli*, UDP-glucose is essential for the biosynthesis of cell wall components.

V. Discussion

Modest yields and titers of PHB have been synthesized from glucose using *E. coli* by overexpressing feedback-insensitive DAHP synthase, increasing expression of common pathway enzymes, and using overexpressed chorismate lyase to aromatize chorismic acid. Increasing expression levels of chorismate lyase above wild-type levels initially leads to increases in the concentrations and yields of synthesized PHB. However, expression levels are realized above which further increases in chorismate lyase fails to improve synthesis of PHB even in the absence of enzymes that normally compete with chorismic acid. Part of the problem can be explained by the substantial decreases in DAPH synthase expression that is observed when expression of chorismate lyase is increased. Feedback inhibition of chorismate lyase by PHB is also a likely factor

that prevents increased expression of this enzyme from translating into improved product synthesis. An unexpected discovery was the observation that inhibition of 3-dehydroquinate synthase by tyrosine is a major impediment to the flow of carbon through the common pathway.

Comparison of Microbial Syntheses of PHB from Glucose.

The previous report³⁹ of microbial synthesis of PHB from glucose employed amplified expression of *ubiC*-encoded chorismate lyase in a host *E. coli* strain that synthesized increased concentrations of PHB after two rounds of selection for spontaneous mutations. Selection based on resistance to either fluorophenylalanine or β -2-thienylalanine was used in the first round of mutagenesis. Although no enzymological characterization of DAHP synthase in strains resistant to these antimetabolites of L-phenylalanine was provided, isozymes of DAHP synthase (Figure 3) that were insensitive to feedback inhibition by aromatic amino acids were likely selected. Expression levels of the putative feedback-insensitive DAHP synthase were not analyzed and were likely limited by the chromosomal localization of the encoding locus. In this report, a significantly different approach was taken. A well-characterized isozyme of DAHP synthase insensitive to feedback inhibition and encoded by *aroF*^{FBR} was plasmid-localized and overexpressed in the PHB-synthesizing *E. coli* strains.

Selection of strains resistant to *p*-aminobenzoic acid was used for the second round of mutagenesis. *p*-Aminobenzoic acid is an alternative substrate of *ubiA*-encoded *p*-hydroxybenzoate octaprenyltransferase. Inhibition of *p*-hydroxybenzoate octaprenyltransferase by *p*-aminobenzoic acid prevents the prenylation of PHB disrupting

the biosynthesis of ubiquinone. Resistance to *p*-aminobenzoic acid is known to result from increased biosynthesis of PHB.⁴⁰ In the previous report, the molecular basis for this increased biosynthesis of PHB was not delineated. For example, impediments to the flow of carbon through the common pathway of amino acid biosynthesis can be removed by mutations that increase expression of common pathway enzymes. Increased expression of enzymes in the common pathway has been previously demonstrated to have a significant impact on the concentration and yield of aromatics synthesized by *E. coli*. Increased biosynthesis of PHB might alternatively result from mutations that reduce expression levels of the chorismate mutases, which compete with chorismate lyase for chorismic acid. Notably, the highest concentration and yield of PHB obtained in this study was synthesized by JB161/pJB2.274, which lacks chorismate mutase activity. Finally, mutations that lead to isozymes of chorismate lyase that are insensitive to feedback inhibition could increase the ability of this enzyme to compete for in vivo concentrations of chorismic acid. In contrast to DAHP synthase, feedback-insensitive isozymes of chorismate lyase have not been reported.

Both this and the earlier report⁴¹ of the improved biosynthesis of PHB relied on plasmid localization of *ubiC* to achieve significant overexpression of chorismate lyase. The use of anion exchange resin to remove products during fermentation runs had a particularly pronounced impact in the earlier report on the microbial production of PHB. In the absence of product removal using anion exchange resin during the course of a fermentation run, 6.2 g/L of PHB was synthesized by the construct resulting from two rounds of mutagenesis and overexpression of plasmid-localized *ubiC*. This product concentration is similar to the 4.4 g/L of chorismic acid synthesized by RB38/pJB2.274.

However, a total of 22.9 g/L of PHB was synthesized by a closely related *E. coli* construct when anion exchange resin was used to remove product during the course of the fermentation. Although a portion (8.7 g/L) of the PHB accumulated in the culture medium, the remainder of the synthesized PHB (the equivalent of 14.2 g/L) bound to the anion exchange resin. By repeatedly passing culture medium through the anion exchange resin during the fermentation, the concentration of PHB in the culture medium was likely kept at a level that reduced its toxicity towards the producing microbe. This is not to suggest that PHB toxicity was completely avoided. We observed a substantial reduction in cell biomass and product concentration at PHB concentrations of 10 g/L. Attempts to alleviate PHB toxicity in this report included random mutagenesis and PHB glycosylation. Neither method resulted in increased PHB biosynthesis. One point that must be kept in mind while addressing PHB's toxicity towards *E. coli* is that if the cell metabolism was unhampered by reduced product toxicity, the increased flow of carbon through the common pathway will not translate to higher PHB concentrations relative to other post-chorismate products due to feedback inhibition of chorismate lyase. It is therefore most desirable to develop a method that completely removes free PHB from the culture supernatant to alleviate both toxicity and feedback inhibition. The concept of exporting PHB as its *O*- β -D-glucoside is therefore a novel approach that addresses both of these limitations. Modification of a strain that expresses a glucosyltransferase to over-produce UDP-glucose could be a general method that could be employed whenever a toxic phenolic product, such as gallic acid, catechol, and vanillin, is synthesized by *E. coli*.

Microbe-Based Versus Plant-Based Synthesis of PHB.

N. tabacum expressing *ubiC* synthesized 0.24 grams of PHB per gram of dried plant tissue.⁴² This level of PHB synthesized by transgenic *N. tabacum* is 1000-fold higher than the levels of PHB synthesized by wild-type *N. tabacum*. For comparison, *E. coli* RB38(DE3)/pJB3.144B synthesized approximately 0.43 grams of PHB per gram of cells (dry cell weight) in its culture supernatant. The absence of any need to supplement cultures of *E. coli* RB38(DE3)/pJB3.144B with aromatic amino acids makes this microbe and its synthesis of PHB the most suitable for comparison with plant-based synthesis.

Of the PHB synthesized by transgenic *N. tabacum*, 99% is conjugated as phenolic and ester β -D-glucosides. This glucosylation is both an asset and a problem in plant-based synthesis. The toxicity of PHB is likely significantly attenuated towards the plant upon glucosylation. The *in vivo* catalytic activity of chorismate lyase may be maintained by the removal of PHB's feedback inhibition upon glycosylation. However, glucosylation is also involved in the incorporation of aromatics during cell wall biosynthesis. The actual amount of PHB synthesized by transgenic *N. tabacum* may be twofold higher than what has been detected but could not be extracted due to its incorporation into plant cell walls. In contrast to plants, all of the PHB synthesized in *E. coli* is unconjugated and conveniently accumulates extracellularly in the fermentation broth.

Perhaps the most intriguing aspect of plant-based synthesis of PHB is the appeal of directly synthesizing a chemical from CO₂. Besides being nontoxic, CO₂ is the most abundant and inexpensive source of carbon. The nontoxic glucose used as the starting

material for microbial synthesis can be obtained from plant-derived starch and cellulose, which are ultimately biosynthesized from CO₂. Plant-based synthesis thus bypasses the multistep processing that is necessary to grow, harvest, refine and depolymerize starch and cellulose to glucose that is sufficiently pure for use in microbial synthesis.

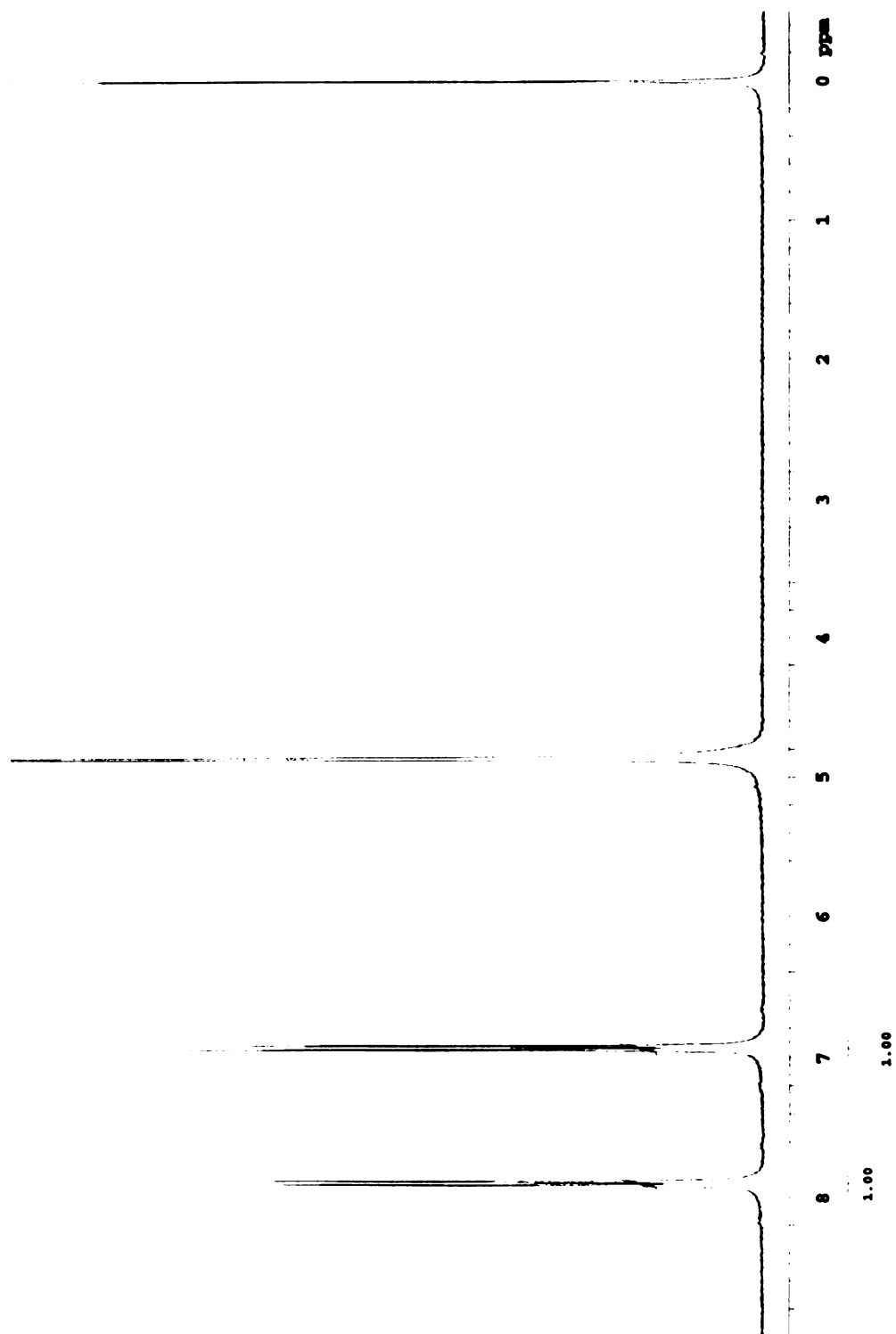


Figure 52. Control ¹H NMR of PHB. Resonances: δ 7.89 (d, 2 H), 6.93(d, 2 H).

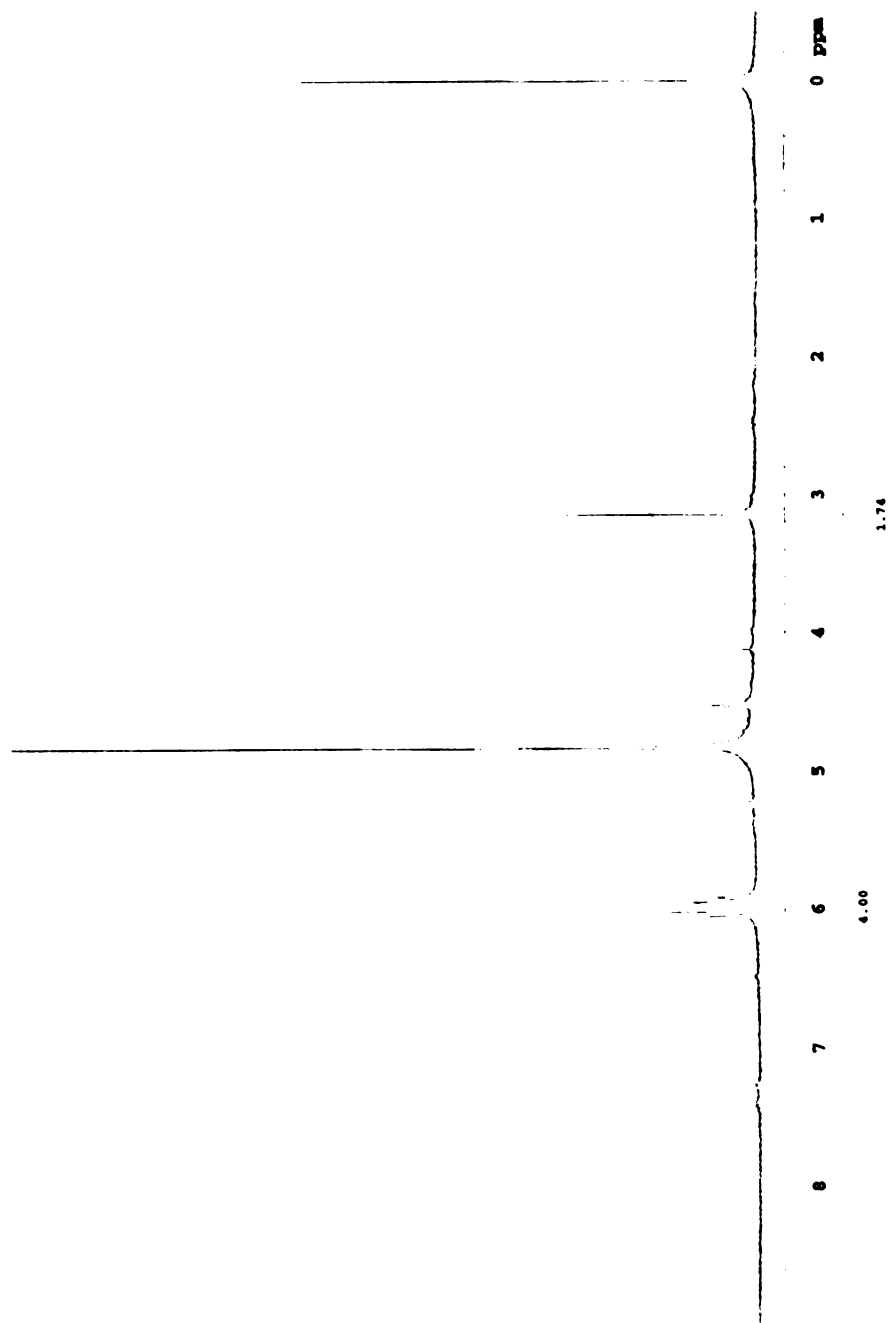


Figure 53. Control ¹H NMR of Prephenic Acid. Resonances: δ 6.00 (dd, 4 H), 4.57 (s, 1 H), 3.15 (s, 2 H).

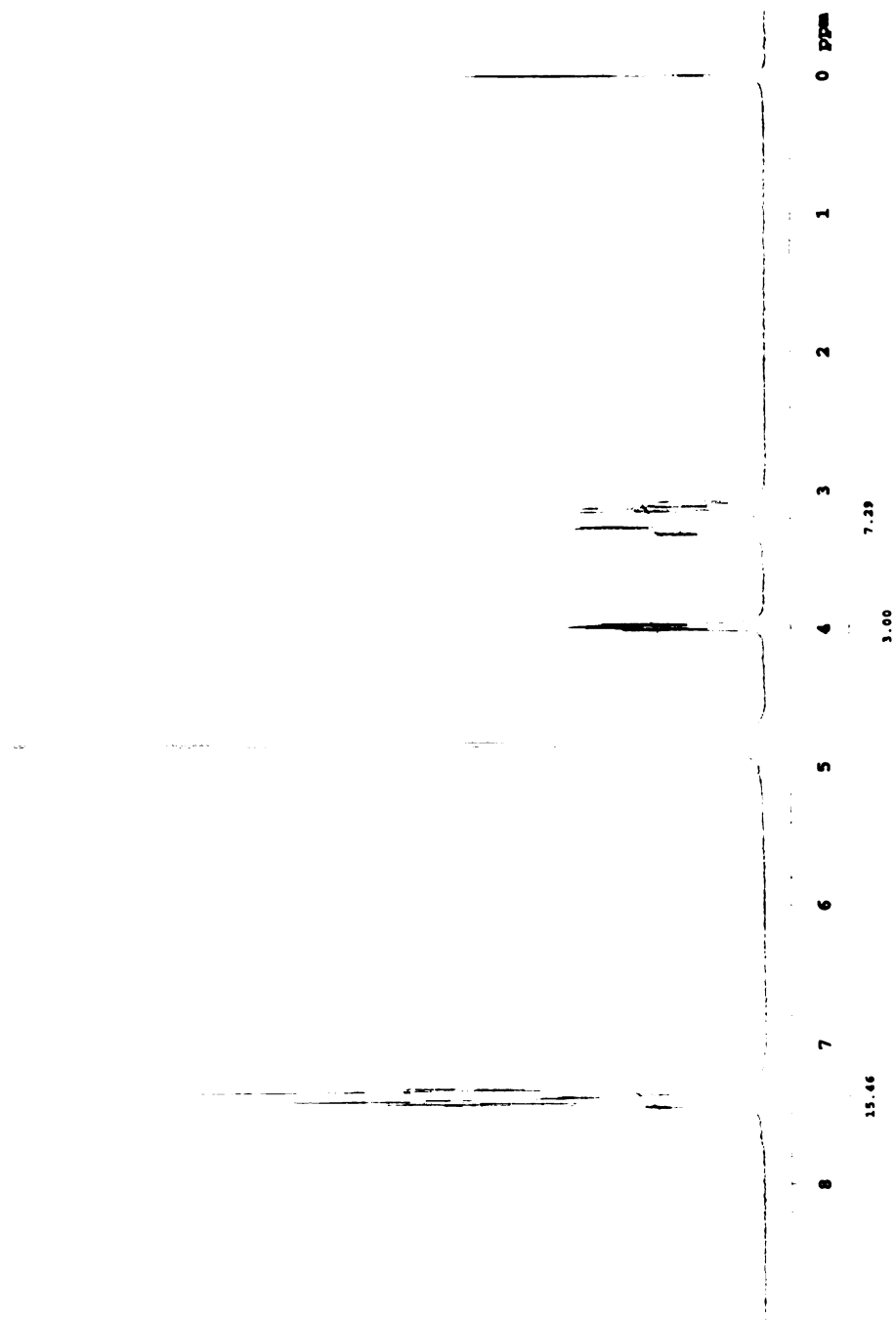


Figure 54. Control ¹H NMR of Phenylalanine. Resonances: δ 7.38 (m, 5 H), 4.40 (m, 1 H), 3.20 (ddd, 2 H).

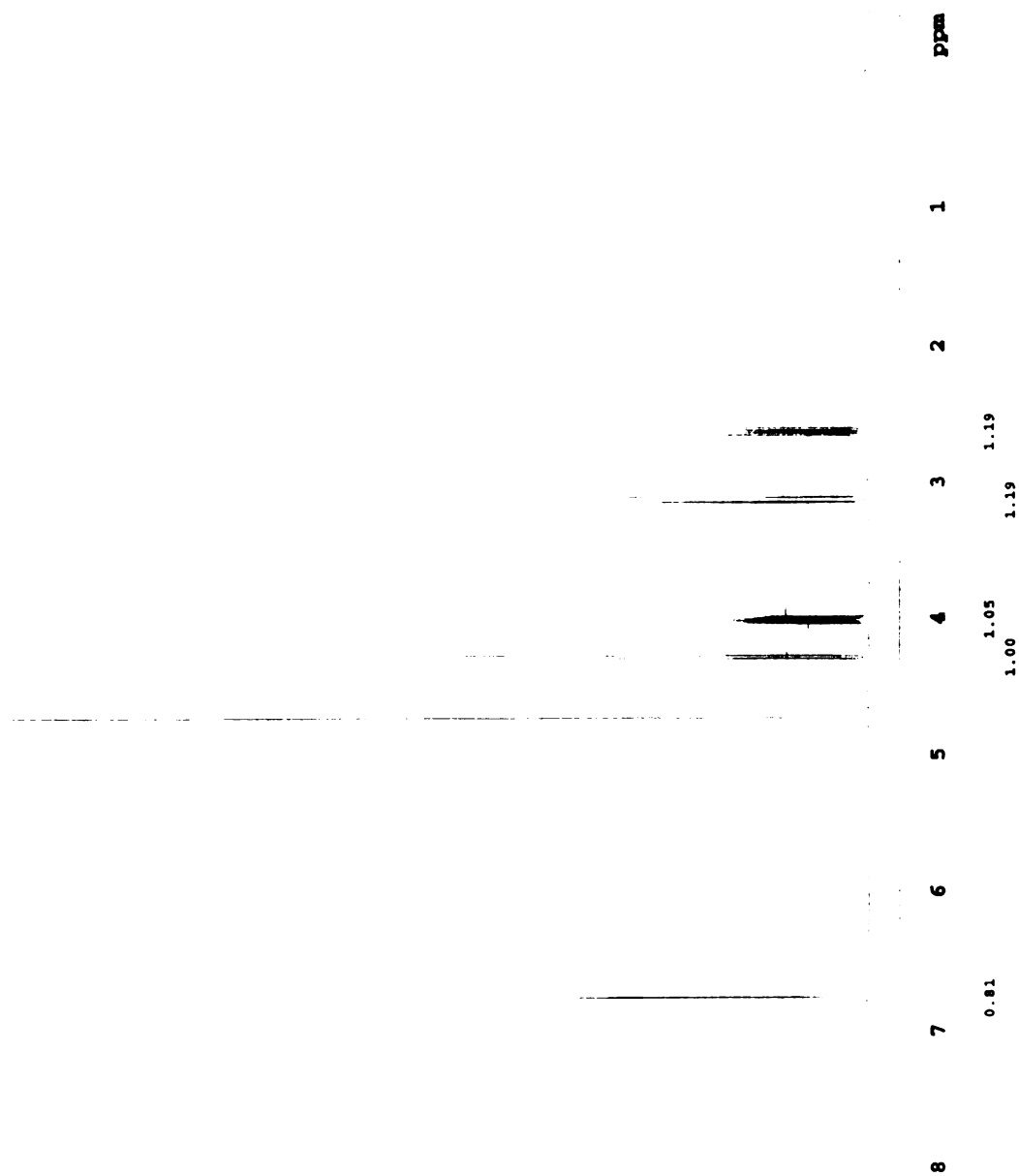


Figure 55. Control ¹H NMR of Tyrosine. Resonances: δ 7.00 (d, 2 H), 6.6 (d, 2 H), 3.42 (t, 1 H), 2.77 (ddd, 2H).

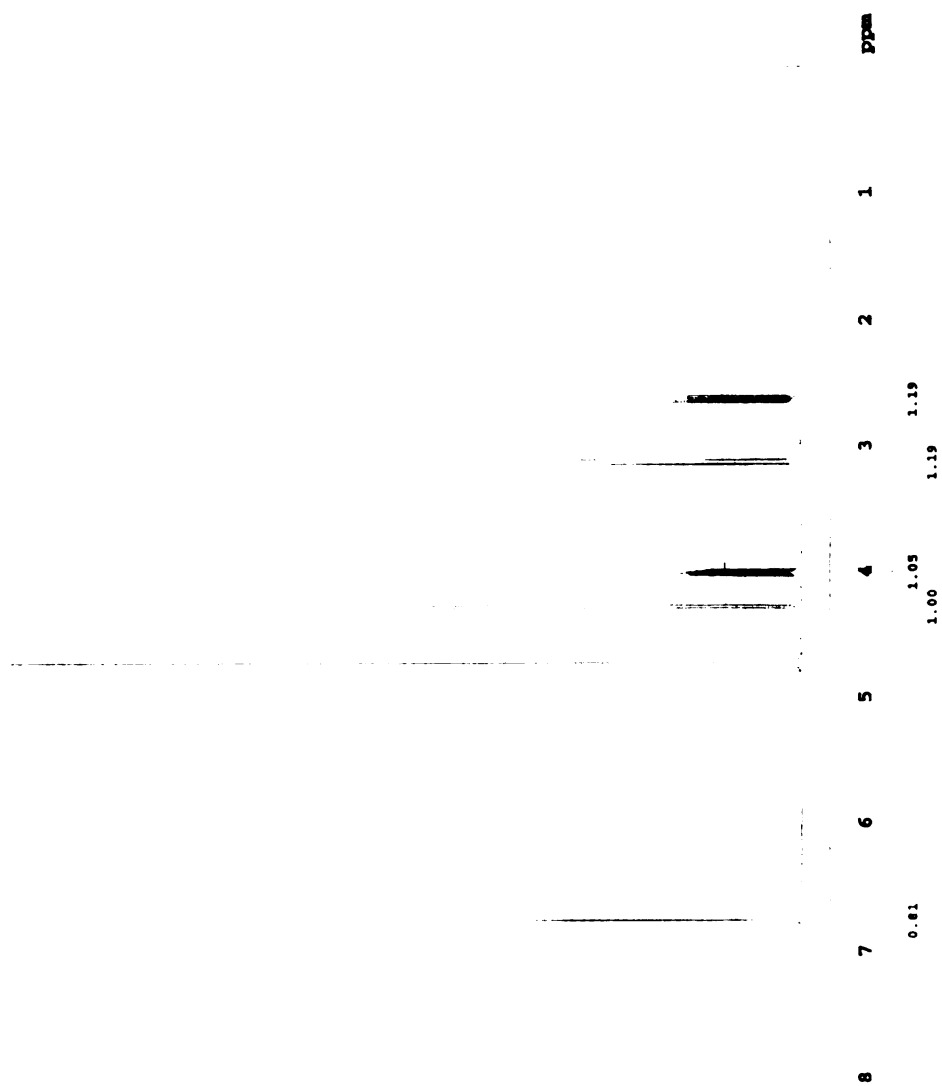


Figure 56. Control ¹H NMR of DHS. Resonances: δ 6.42 (d, 1 H), 4.28 (d, 1 H), 4.00 (ddd, 1 H), 3.07 (dd, 1 H), 2.66 (ddd, 1 H).

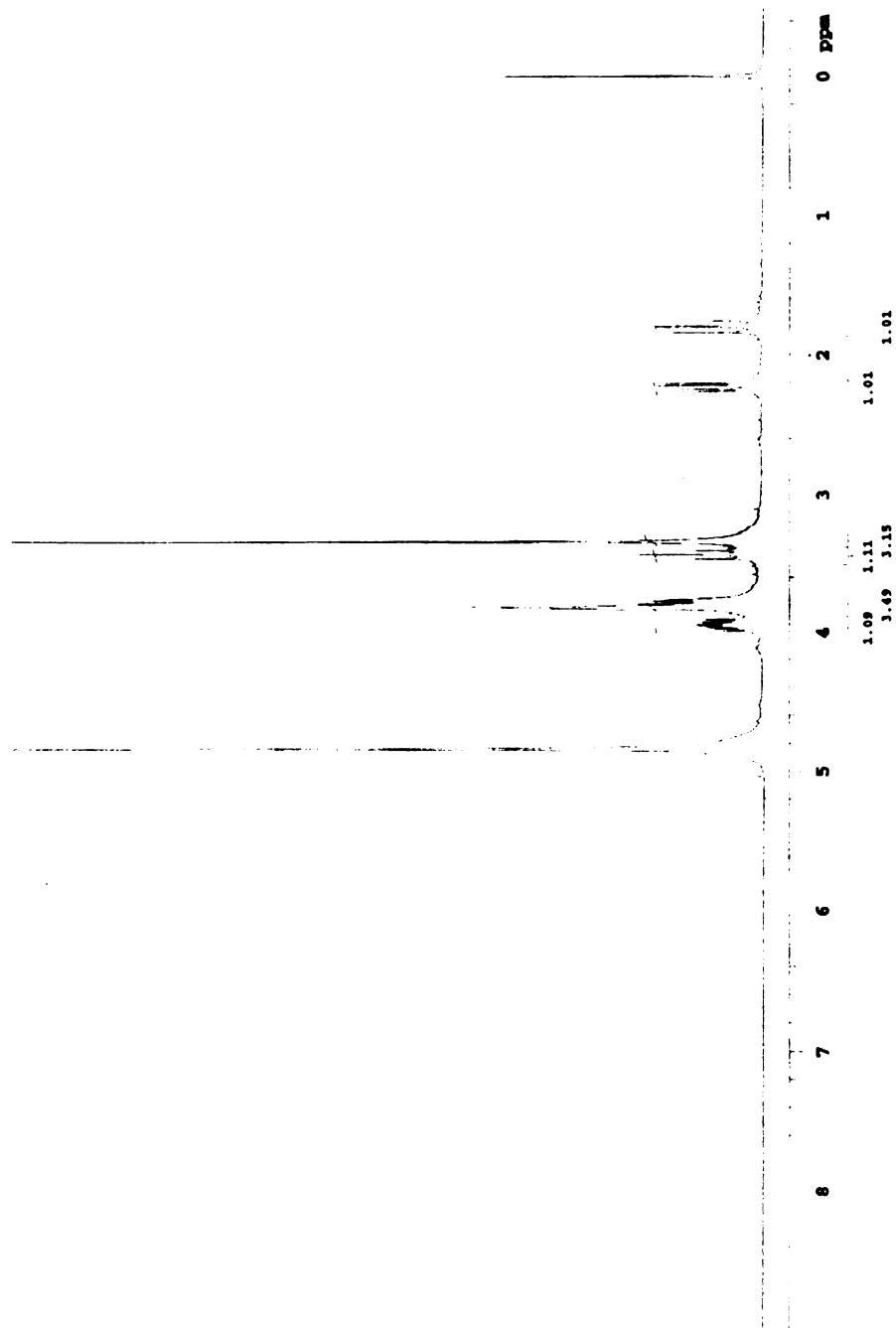


Figure 57. Control ¹H NMR of DAH. Resonances: δ 3.92 (m, 1 H), 3.81 (m, 3 H), 3.43 (t, 1 H), 2.23 (dd, 1 H), 1.80 (t, 1 H).

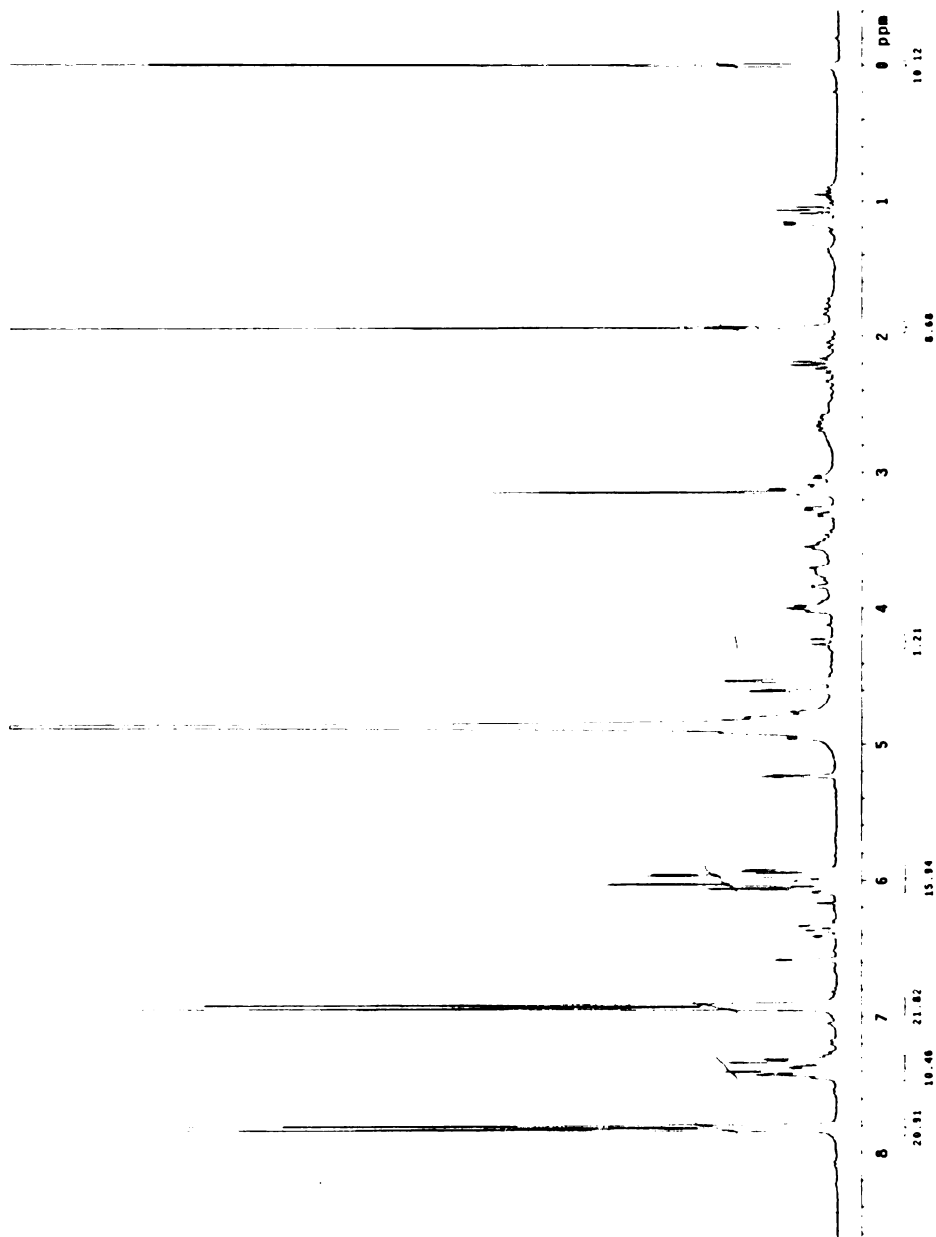


Figure 58. ^1H NMR of a Typical JB161/pJB2.274 Fermentation Broth. PHB resonances: δ 7.89 (d, 2 H), 6.93 (d, 2 H).

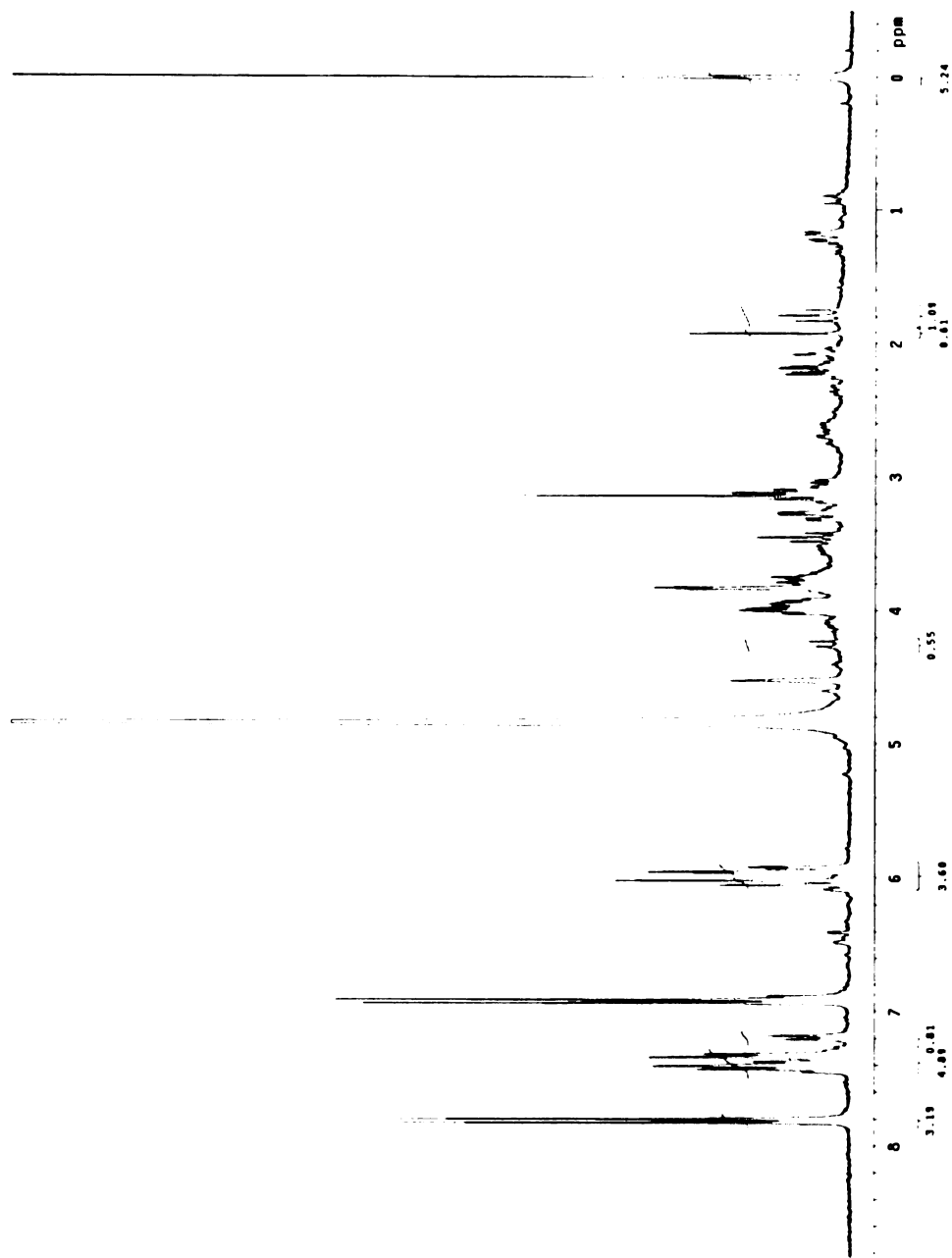


Figure 59. ^1H NMR of a Typical RB38(DE3)/pJB3.144B Fermentation Broth. PHB resonances: δ 7.89 (d, 2 H), 6.93 (d, 2 H).

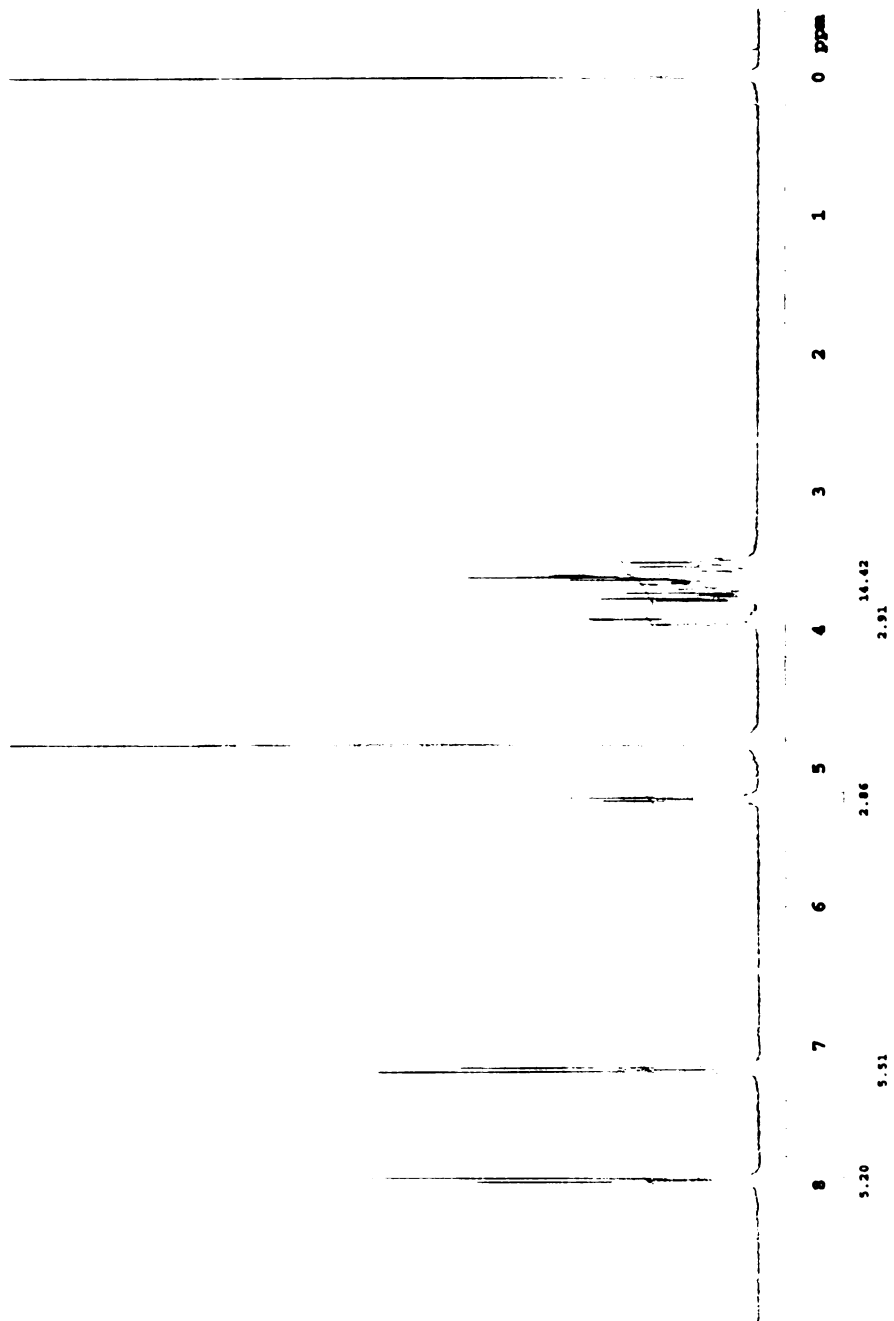


Figure 60. ¹H NMR of Synthesized PHB-*O*-β-D-Glucoside. Resonances: δ 7.97 (d, 2 H), 7.18 (d, 2 H), 5.25 (d, 1 H), 3.94 (d, 1 H), 3.65 (m, 5 H).

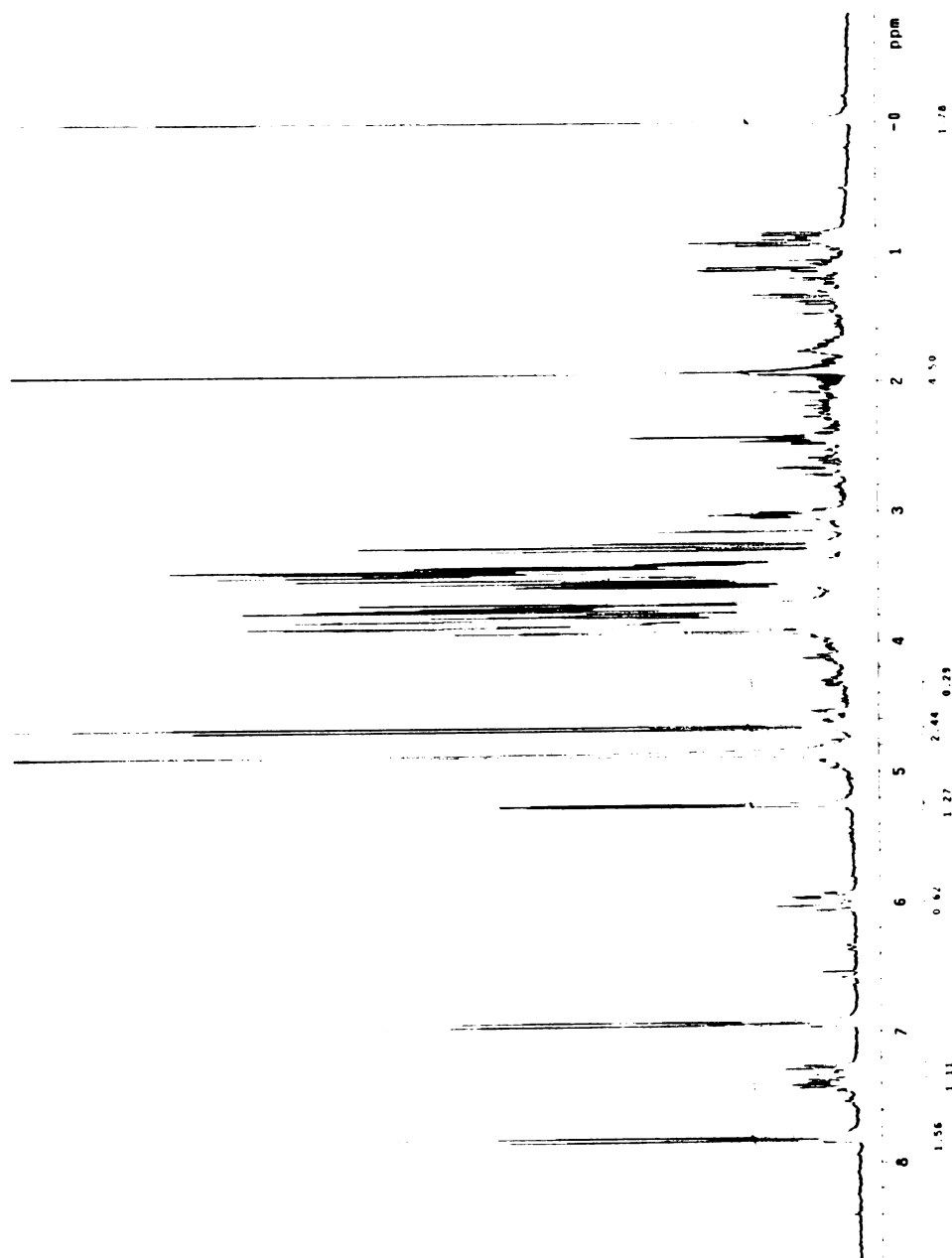


Figure 61. ¹H NMR of JB161(DE3)/pJB2.274/pET-15b Culture Supernatant. Ratio of α (δ 4.65) to β (δ 5.25) peak is 1:1.9.

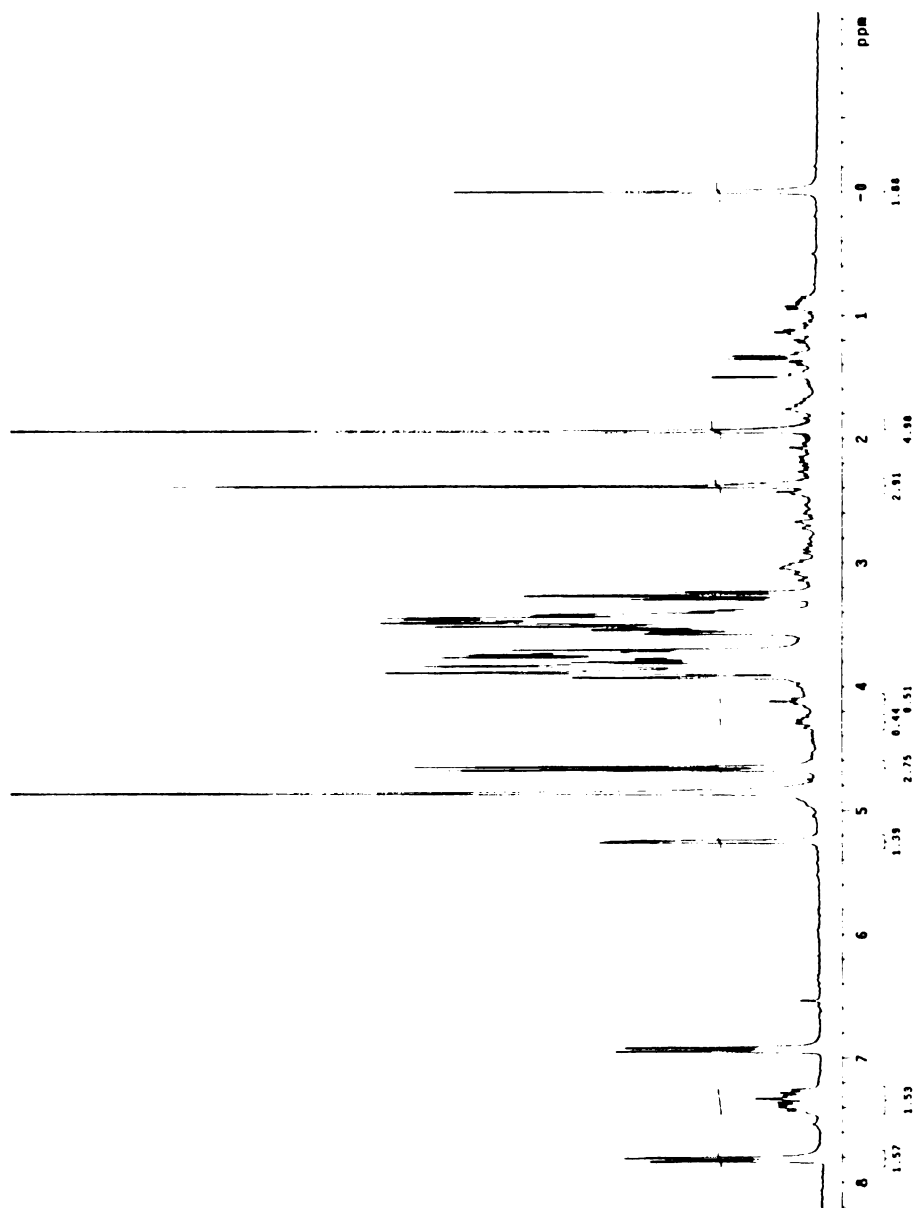


Figure 62. ¹H NMR of JB161(DE3)/pJB2.274/pJB5.205A Culture Supernatant. Ratio of α (δ 4.65) to β (δ 5.25) peak is 1:2.

References

- ¹ Loscher, R.; Heide, L. *Plant Physiol.* **1994**, *106*, 271.
- ² Dewick, P. M. *Nat. Prod. Rep.* **1993**, *10*, 233.
- ³ Heide, L.; Floss, H. G.; Tabata, M. *Phytochemistry* **1989**, *28*, 2643.
- ⁴ Dewick, P. M. *Nat. Prod. Rep.* **1993**, *10*, 233.
- ⁵ (a) Kirsch, M. A.; Williams, D. J. *Chemtech* **1994**, *24* (4), 40. (b) Russell, A. D.; J. *Appl. Bacteriol.* **1991**, *71*, 191.
- ⁶ Economy, J. *Angew. Chem. Int. Ed. Engl.* **1990**, *29*, 1256.
- ⁷ Frank, H. G.; Stadelhofer, J. W. *Industrial Aromatic Chemistry*; Springer-Verlag: New York, 1988; p. 146-150. (b) Erickson, S. H. In *Kirk-Othmer Encyclopedia of Chemical Technology*, 3rd ed.; Wiley: New York, 1982, Vol. 20, p. 517-519.
- ⁸ Arestra, M.; Quaranta, E.; Dileo, C.; Tommasi, I. *Tetrahedron* **1998**, *54*, 8841.
- ⁹ Grelak, R. L.; Chen, K. K. *Int. Pat. Appl.* WO 9856920, 1998.
- ¹⁰ Siebert, M.; Sommer, S.; Li, S.; Wang, Z.; Severin, K.; Heide, L. *Plant Physiol.* **1996**, *112*, 811.
- ¹¹ Müller, R.; Wagener, A.; Schmidt, K.; Leistner, E. *Appl. Microbio. Biotechnol.* **1995**, *43*, 985.
- ¹² Amaratunga, M.; Lobos, J. H.; Johnson, B. F.; Williams, D. US Pat. 6030819, 2000.
- ¹³ (a) Dell, K. A.; Frost, J. W. *J. Am. Chem. Soc.* **1993**, *115*, 11581. (b) Snell, K. A.; Draths, K. M.; Frost, J. W. *J. Am. Chem. Soc.* **1996**, *118*, 5605.
- ¹⁴ Snell, K. A.; Draths, K. M.; Frost, J. W. *J. Am. Chem. Soc.* **1996**, *118*, 5605.
- ¹⁵ Stauffer, G. V. In *Escherichia coli and Salmonella Typhimurium*; Neidhardt, F. C., Ed.; American Society for Microbiology: Washington D. C., 1987; Vol. 1, p. 412-418.
- ¹⁶ Snell, K. A.; Draths, K. M.; Frost, J. W. *J. Am. Chem. Soc.* **1996**, *118*, 5605.
- ¹⁷ Hamilton, C. M.; Aldea, M.; Washburn, B. K.; Babitzke, P.; Kushner, S. P. *J. Bacteriol.* **1989**, *171*, 4617.

-
- ¹⁸ Ohta, K.; Beall, D. S.; Mejua, J. P.; Shanmugam, K. T.; Ingram, L. O. *Appl. Environ. Microbiol.* **1991**, *57*, 893.
- ¹⁹ Li, K.; Mikola, M. R.; Draths, K. M.; Worden, R. M.; Frost, J. W. *Biotech. Bioeng.* **1999**, *64*, 61.
- ²⁰ Southern, E. M. *J. Mol. Biol.* **1975**, *98*, 503.
- ²¹ Weaver, L. M.; Herrmann, K. M. *J. Bacteriol.* **1990**, *172*, 6581.
- ²² Ogino, T.; Garner, C.; Markley, Herrmann, K. M. *Proc. Natl. Acad. Sci.* **1982**, *79*, 5828.
- ²³ (a) Draths, K. M.; Frost, J. W. *J. Am. Chem. Soc.* **1990**, *112*, 1657. (b) Draths, K. M.; Pompliano, D. L.; Conley, D. L.; Frost, J. W.; Berry, A.; Disbrow, G. L.; Stavesky, R. J.; Lievense, J. C. *J. Am. Chem. Soc.* **1992**, *114*, 3956. (c) Patnaik, R.; Liao, J. C. *Appl. Environ. Microbiol.* **1994**, *60*, 3903.
- ²⁴ (a) Siebert, M.; Bechthold, A.; Melzer, M.; May, U.; Berger, U.; Schroder, G.; Schroder, J.; Severin, K.; Heide, L. *FEBS Lett.* **1992**, *307*, 347. (b) Siebert, M.; Severin, K.; Heide, L. *Microbiol.* **1994**, *140*, 897. (c) Nichols, B. P.; Green, J. M. *J. Bacteriol.* **1992**, *174*, 5309.
- ²⁵ (a) Dell, K. A.; Frost, J. W. *J. Am. Chem. Soc.* **1993**, *115*, 11581. (b) Snell, K. A.; Draths, K. M.; Frost, J. W. *J. Am. Chem. Soc.* **1996**, *118*, 5605.
- ²⁶ Snell, K. A.; Draths, K. M.; Frost, J. W. *J. Am. Chem. Soc.* **1996**, *118*, 5605.
- ²⁷ Nichols, B. P.; Green, J. M. *J. Bacteriol.* **1992**, *174*, 5309.
- ²⁸ Seibold, B.; Matthes, M.; Eppink, M. H.; Lingens, F.; Van Berkel, W. J. H.; Muller, R. *Eur. J. Biochem.* **1996**, *239*, 469.
- ²⁹ Schoner, R.; Herrmann, K. M. *J. Biol. Chem.* **1976**, *251*, 5440.
- ³⁰ Zaldivar, J.; Ingram, L. O. *Biotechnol. Bioeng.* **1999**, *66*, 203.
- ³¹ Lambert, L. A.; Abshire, K.; Blankenhorn, D.; Slonczewski, J. L. *J. Bacteriol.* **1997**, *179*, 7595.
- ³² Li, K.; Mikola, M. R.; Draths, K. M.; Worden, R. M.; Frost, J. W. *Biotechnol. Bioeng.* **1999**, *64*, 61.

-
- ³³ (a) Smith-Becker, J.; Marois, E.; Huguet, E. J.; Midland, S. L.; Sims, J. J.; Keen, N. T. *Plant. Physiol.* **1998**, *116*, 231. (b) Conrath, U.; Kleesig, D. F.; Bachmair, A. *Plant Cell Reports* **1998**, *17*, 876. (c) Shah, J.; Tsui, F.; Klessig, D. F. *Mol. Plant-Microbe Interact.* **1997**, *10*, 69.
- ³⁴ Siebert, M.; Sommer, S.; Li, S.; Wang, Z.; Severin, K.; Heide, L. *Plant Physiol.* **1996**, *112*, 811.
- ³⁵ Grynkiewicz, G.; Achmatowicz, J.; Hennig, J.; Indulski, J.; Klessig, D. F. *Polish J. Chem.* **1993**, *67*, 1251.
- ³⁶ Stokes, E.J.; Ridgway, G. L.; Wren, M. W. D. *Clinical Microbiology*; Edward Arnold: London, 1993, 234.
- ³⁷ Horvath, D. M.; Chua, N.-H. *Plant Molecular Biology* **1996**, *31*, 1061.
- ³⁸ Fraissinet-Tachet, L.; Baltz, R.; Chong, J.; Kauffmann, S.; Fritig, B.; Saindrenan, P. *FEBS Lett.* **1998**, *437*, 319.
- ³⁹ Amaratunga, M.; Lobos, J. H.; Johnson, B. F.; Williams, D. US Pat. 6030819, 2000.
- ⁴⁰ (a) Hamilton, J.A.; Cox, G. B. *Biochem. J.* **1971**, *123*, 435. (b) Davis, B. D. *J. Exp. Med.* **1951**, *94*, 243. (c) Lawrence, J.; Cox, G. B.; Gibson, F. *J. Bacteriol.* **1974**, *118*, 41.
- ⁴¹ (a) Amaratunga, M.; Lobos, J. H.; Johnson, B. F.; Williams, D. US Pat. 6030819, 2000. (b) Johnson, B. F.; Amaratunga, M.; Lobos, J. H. US Pat 6114157, 2000.
- ⁴² Siebert, M.; Sommer, S.; Li, S.; Wang, Z.; Severin, K.; Heide, L. *Plant Physiol.* **1996**, *112*, 811.

Bl

cher

enzy

val

bio

in

hy

Pl

fi

c

c

c

CHAPTER THREE

BIOTRANSFORMATION OF PHB INTO HYDROQUINONE AND *p*-CRESOL.

Introduction

Biocatalysis, as referred to in chapter one, was the use of enzymes to catalyze chemical reactions. Chapter two outlined one area of biocatalysis that utilized multiple enzymatic pathways in an intact organism to convert a renewable carbohydrate into a value-added chemical. In this chapter, biocatalysis in the form of whole-cell biotransformations will be explored. In this approach, individual enzymes are exploited *in vivo* to perform a specific reaction. The oxidative decarboxylation of PHB to hydroquinone (Figure 63), catalyzed by whole-cell biotransformations using the fungus *Phanerochaete chrysosporium* and the yeast *Candida parapsilosis*, will be examined first. The biotransformation of PHB to *p*-hydroxybenzyl alcohol, also catalyzed by *P. chrysosporium*, will be explored as a route to *p*-cresol (Figure 63). The enzymatic conversion of fermentation-derived PHB to hydroquinone and *p*-cresol presented here offer environmentally friendly routes to aromatic compounds that are traditionally derived from petroleum.

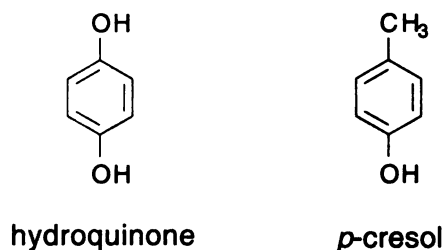


Figure 63. Structure of Hydroquinone and *p*-Cresol.

Precedent for industrial and bench-top whole-cell biotransformations has already been set by numerous organisms. Among the most common examples are the use of yeast, classified as *Saccharomyces cerevisiae*, to catalyze reductions. For at least 8000 years, mankind has been using yeast for the brewing of beer and since ~4000 B.C. to make leavened bread.¹ Although brewers and bakers knew yeast to be a necessary ingredient, it wasn't until the mid 1800's that Pasteur proposed the radical idea that sugars were taken up by the yeast cells and underwent "catalytic reactions" to produce ethanol.² The proposition that a chemical transformation could be conducted by a living organism was first met with opposition as the existing theory, promoted by Justis Leibig, held that ethanol formation was the result of "inanimate interaction between the motions of the bodies of the yeast and the organic reagents".³ By the 1870's Pasteur's ideas became accepted and in 1898, the use of yeast as a chemical reagent was published with the reduction of furfural to furfuryl alcohol (Figure 64).⁴

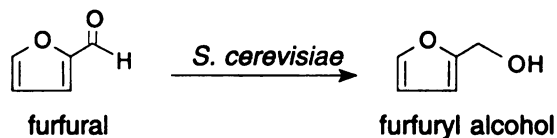


Figure 64. Yeast Catalyzed Reduction of Furfural to Furfuryl Alcohol.

Today, the use of yeast to promote chemical reactions has become widespread and has been much reviewed in the chemical literature. Utilization of the enzymes in yeast, namely alcohol dehydrogenase and β -ketoester reductases, have become a popular alternative to traditional chemical reducing reagents because of their ability to carry out a wide range of reactions and their regiochemical and stereochemical selectivity.⁵ Often, enantiomeric excesses greater than 90% can be achieved. While yeast-catalyzed carbonyl

reductions represent the largest class of reactions studied by chemists, yeast has also been used to reduce carbon-carbon double bonds, hydrolyze esters, and promote carbon-carbon bond formation.⁶ In fact, the condensation of benzaldehyde and acetaldehyde by yeast was the first microbial transformation industrialized.⁷

Whole-cell biotransformations offer many advantages over traditional chemical synthesis and reactions with purified enzymes. Organisms are usually inexpensive relative to purified enzymes and unlike some chemical reagents are stable to air and water. Compared to traditional synthesis, whole-cell biotransformations do not employ organic solvents nor generate toxic waste streams. Although reactions with purified enzymes are also environmentally benign, the need for added co-factors, such as ATP and NADPH, requires a costly surplus of these molecules or development of a co-factor recycling system. In a living cell, these co-factors are synthesized and recycled *in vivo*, thus bypassing the need for expensive additives. It should be mentioned that the major disadvantage of whole-cell biotransformations are undesirable side reactions. The added starting material can serve as a substrate for several enzymes besides the desired reaction leading to byproduct formation. Another concern is overmetabolism. If the starting material is a natural substrate for the organism, the desired product can be further metabolized resulting in poor yields. However, neither of these disadvantages have prevented whole-cell biotransformations from becoming a valuable tool in chemical synthesis.

I. Hydroquinone

A. Chemical Background

Commonly known as hydroquinone (Figure 63), 1,4-dihydroxybenzene is a fine chemical with an annual production of 47,500 tons.⁸ The compound was first isolated in 1820, as a derivative of quinic acid, hence the similar "quin" root word. In nature, hydroquinone is commonly found as the monoglucoside arbutin.⁹ Isolated from plants or synthesized from hydroquinone, arbutin has found use as an urethral disinfectant and as a cosmetic bleaching agent, since it was found to be suppressor of melanin synthesis in human skin.¹⁰

The major use of hydroquinone is as a developer in black-and-white photography and related graphic arts.¹¹ Stabilized by sodium sulfite, buffered solutions of hydroquinone reduce the exposed silver halide grains in a photographic emulsion at a faster rate than that of unexposed grains allowing very fine grain and high contrast images. Hydroquinone is also used as a developer for lithography, photoengraving, and X-ray films.

The second largest market for hydroquinone is as a preservative.¹² It has found applications as an antioxidant for both rubber and food products. As an example, hydroquinone and its derivative butylated hydroxyanisole (BHA, Figure 65) are used to stabilize vitamin A in fish oil as well as vitamins and antibiotics in animal feeds. Another use of hydroquinone is as a radical inhibitor in monomer processing, shipping,

and sto

for ac

alkyla

wides

meth

liqui

of th

thes

eth

Sci

kn

ar

(I

and storage. At concentrations of 5 to 300 ppm, hydroquinone is the preferred inhibitor for acrylic and methacrylic esters, acrylonitrile, and vinyl acetate.

Hydroquinone shows similar reactivity with benzene and phenol in regards to alkylation, substitution, and oxidation reactions. As a result, hydroquinone has found widespread use as an intermediate in the manufacture of industrial chemicals.¹³ Chloro-, methyl-, and phenyl- substituted hydroquinones (Figure 65) have been used to make liquid crystalline polymers. The introduction of substituents allows for internal rotation of the rigid units to occur thereby decreasing the melting point of polyesters containing these units. Chloroneb (Figure 65), the chlorinated derivative of hydroquinone dimethyl ether, is a systemic fungicide used in the treatment of turf and some plant seeds. Kolbe-Schmitt carboxylation of hydroquinone produces 2,5-dihydroxybenzoic acid. Commonly known as gentisic acid (Figure 65), it is used medicinally as an analgesic and antirheumatic. Hydroquinone is also used in dye manufacture, such as disazo dyes (Figure 65) used in ink jet printing.

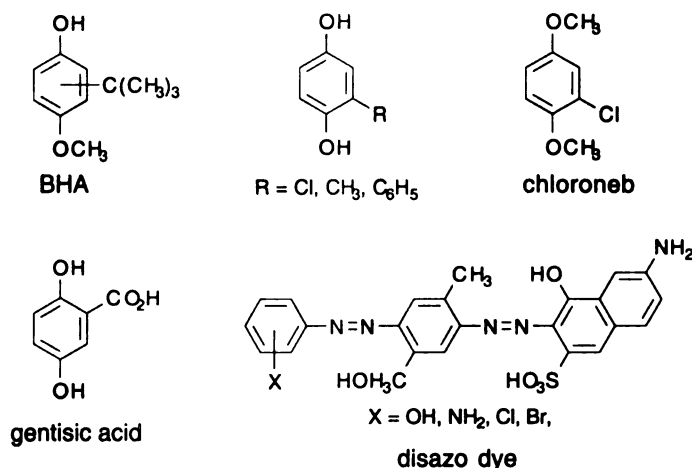


Figure 65. Derivatives of hydroquinone

There are three major processes for the industrial manufacture of hydroquinone, all of which are derived from benzene. The oldest route (Figure 66) utilizes aniline as a starting material.¹⁴ Aniline is produced industrially from the hydrogenation of nitrobenzene, which in turn is derived directly from benzene via treatment with nitric acid and sulfuric acid. En route to hydroquinone, aniline is first oxidized to *p*-quinone with stoichiometric amounts of MnO₂ or CrO₃ in combination with H₂SO₄. Quinone is subsequently reduced to hydroquinone with iron metal. The major draw back of this process is the generation of large amounts of manganese, chromium, and iron salts and ammonium sulfate. Several methods have been developed to recycle the manganese but none have reached industrial scale. Because of the environmental concerns raised with waste disposal, China remains the only country using this process.

A second route to hydroquinone is the acid catalyzed hydroxylation of phenol (Figure 66).¹⁵ Phenol, the second largest volume chemical derived from benzene, is converted to hydroquinone using a variety of homogeneous and heterogeneous catalysts in combination with hydrogen peroxide. One of the oldest reactions, known as the Fenton reaction, uses cobalt, copper, or iron salts in an aqueous solution (pH 2-3). Besides generating metal salts, the yield of this reaction is generally low (< 60% based on H₂O₂). More recently, strong proton catalysts, such as perchloric and trifluoromethanesulfonic acid, have also be used. Heterogeneous catalysis for the hydroxylation of phenol comes in the form of zeolites. Development of titanium silicate (TS-1) in the 1980's allowed for high yielding conversions based on both phenol and H₂O₂. All of these reactions employ phenol, which is toxic and corrosive, and H₂O₂ which can present an explosion hazard. Byproduct formation is another drawback of phenol

hydrox

produc

from r

first

benz

to y

hyd

wit

dih

ren

co

hy

hydroxylation reactions resulting in the poor product ratios. Catechol is the major side product with ratios as high as 1.5 : 1. Small amounts of resorcinol can also be formed from radical side reactions and is difficult to separate from hydroquinone.

The third major route to hydroquinone is the Hock process (Figure 66).¹⁶ The first step in this process is the Friedel/Crafts alkylation of benzene to yield diisopropyl benzene. Subsequent air oxidation produces the dihydroperoxide which is acid cleaved to yield hydroquinone. Incomplete oxidation of diisopropyl benzene forms hydroxyhydro-peroxide and dicarbinol. Prior to acid cleavage, this mixture is treated with H_2O_2 in a biphasic water-toluene system to complete the conversion to dihydroperoxide. Acetone, the byproduct of the cleavage reaction, can combine with the remaining peroxides and form acetone peroxides, which are sensitive, explosive compounds. Despite this risk, the Hock process provides 7.7×10^6 kg/year of hydroquinone.¹⁷

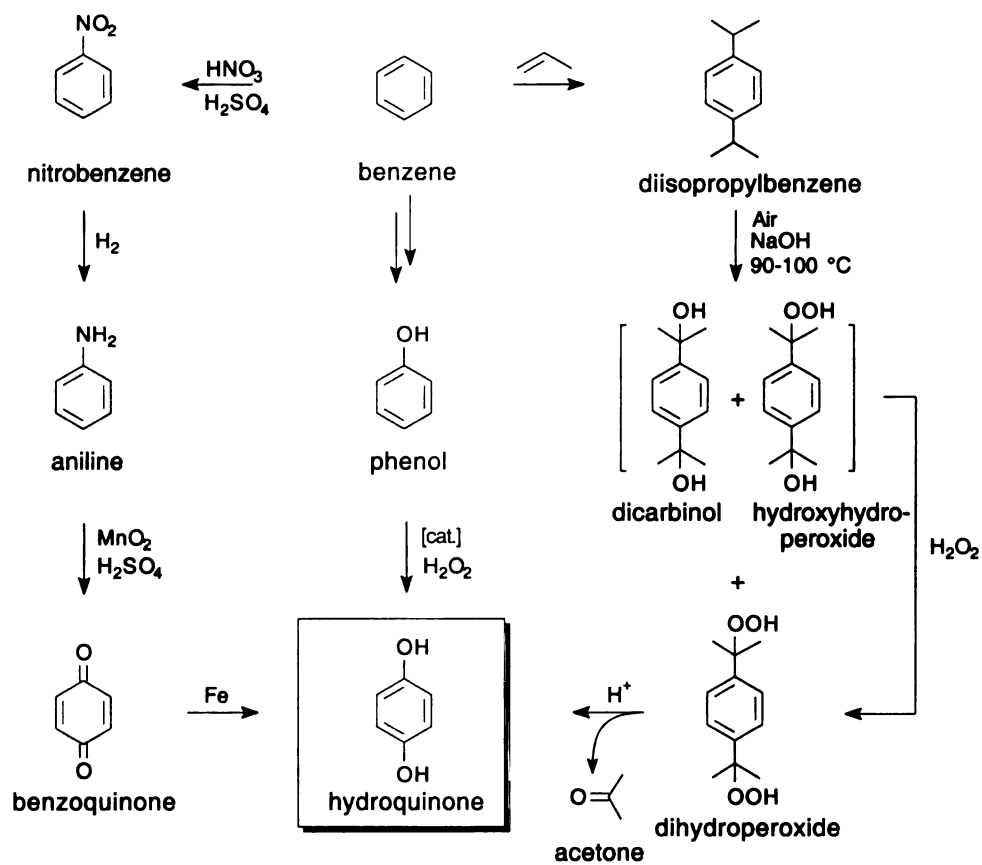


Figure 66. Commercial Routes to Hydroquinone.

In the next two sections, alternative routes to hydroquinone will be elaborated (Figure 67). As shown in chapter two, PHB can be synthesized from glucose using an *E. coli* biocatalyst. PHB can then be transformed to hydroquinone by either *Phanerochaete chrysosporium* or *Candida parapsilosis*. Both of these routes constitute an environmentally friendly procedure for the production of hydroquinone as they start from renewable, non-toxic glucose and avoids hazardous reagents and intermediates.

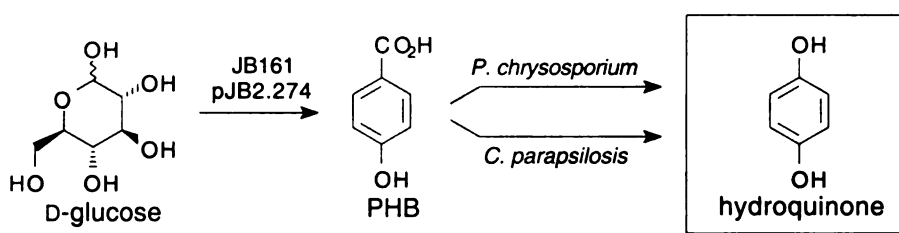


Figure 67. Environmentally Benign Synthesis of Hydroquinone from Glucose.

B. Synthesis of Hydroquinone using *Phanerochaete chrysosporium*

i) Background

Phanerochaete chrysosporium

The fungus *Phanerochaete chrysosporium* is classed as a white-rot basidiomycete.¹⁸ Scientific interest in this fungus stems from its ability to degrade lignin (Figure 68).¹⁹ Lignin is an amorphous, water-insoluble, aromatic polymer that give higher plants their strength and serves as a barrier against microbial attack and as a water impermeable seal.²⁰ As the most abundant aromatic polymer on earth, lignin constitutes 20-30% of wood and other vascular tissues.²¹

Lignin degradation is essential to the earth's carbon cycle as it is second only to cellulose in abundance.²² Lignin however is only degraded by three types of fungi (soft-rot, brown-rot, and white-rot) and a few kinds of bacteria (belonging to the genus actinomycetes and eubacteria).²³ The polymer, composed of phenylpropanoid monomers linked via carbon-carbon and aryl ether bonds, is impervious to enzyme hydrolysis. Adding to its chemical inertness, lignin is found as lignocellulose, an intricate matrix of hemicellulose and lignin that surround cellulose microfibrils.²⁴

Although lignin cannot be used as a sole carbon source, white-rot fungi have developed complex enzymatic system for the degradation of lignocellulose. With the discovery of the first lignin-degrading enzyme in 1982, interest in these organisms has grown due to their commercial potential in the pulp and paper industry and in the bioremediation of toxic waste sites.²⁵ Positive results have been obtained with *P. chrysosporium* in the paper industry to help break down lignin and decolorize wood pulp. Studies have also shown that the lignin degrading pathway of *P. chrysosporium* can be used to degrade chlorinated and nitroaromatic compounds which are common components of toxic wastes.²⁶

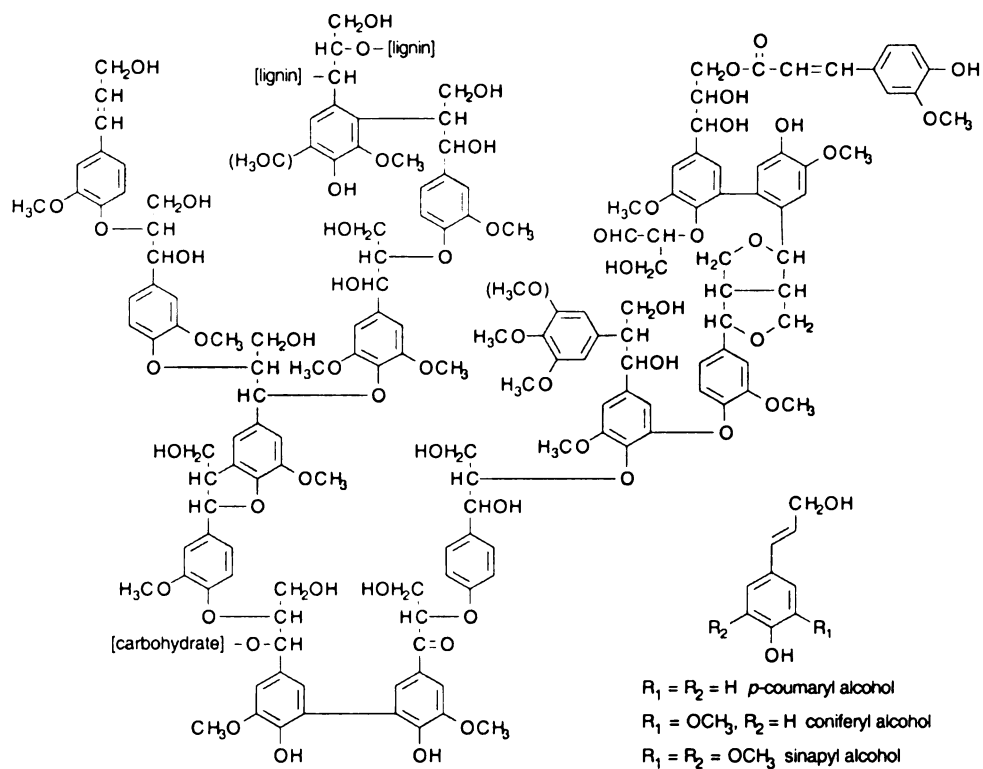


Figure 68. Schematic Structural Formula of Lignin, Adapted from Ander.²⁷
 One-electron oxidation followed by polymerization of the three precursor alcohols (shown lower right) produces lignin.

Vanillate Hydroxylase

Vanillic acid, 4-hydroxy-3-methoxybenzoic acid (Figure 69), was found to be one of the products formed from the oxidative degradation of lignin by *P. chrysosporium*.²⁸ This raised the question as to how vanillate was further metabolized by the organism. In bacteria and certain fungi metabolism of vanillate normally begins with demethylation to protocatechuic acid followed by ring cleavage (Figure 69).²⁹ It has also been found in specific strains of *Bacillus* and *Streptomyces* that vanillate was decarboxylated to guaiacol (2-methoxyphenol) (Figure 69).³⁰ A third pathway was found with the discovery of the metabolite 3-methoxyhydroquinone (MHQ) in cultures of *Sporotrichum pulverulentum* when grown in the presence of vanillate (Figure 69).³¹ *S. pulverulentum* was later determined to be a *P. chrysosporium* in the asexual phase.

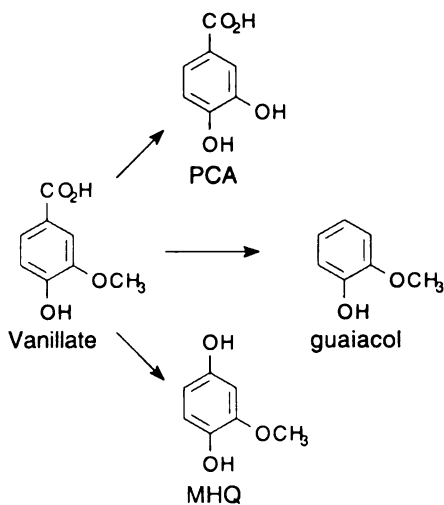


Figure 69. Degradation Pathways for Vanillate in Microorganisms.

The enzyme responsible for the oxidative decarboxylation of vanillate to MHQ was isolated by two independent groups in 1979 and named vanillate hydroxylase.³² Believed to be a mono-oxygenase, vanillate hydroxylase was found require oxygen and a nicotinamide co-factor (NADH or NADPH) to yield MHQ, CO₂, H₂O, and NAD(P) (Figure 70). Expression of vanillate hydroxylase activity is induced by the vanillate with maximum activity occurring 40-50 h after induction.³³ Studies with the crude enzyme extract found that vanillate hydroxylase has a relatively broad substrate range with the only structural requirement being a hydroxyl group situated *para* to the carboxylic acid on the aromatic ring. The enzyme activity of vanillate hydroxylase with PHB as substrate was found to be 98% relative to the activity measured with vanillate.³⁴ Based on these studies, *P. chrysosporium* was examined as a possible biocatalyst for the conversion of PHB to hydroquinone.

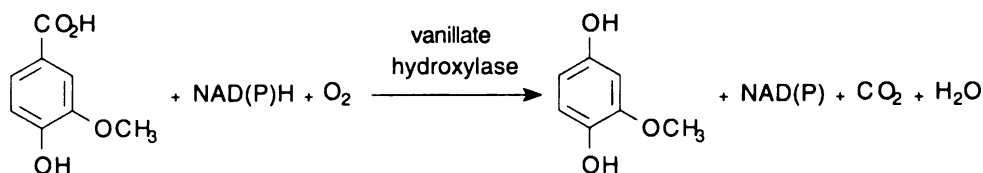


Figure 70. Reaction Stoichiometry for Vanillate Hydroxylase.

ii) Conditions for the Biotransformation of PHB using *P. Chrysosporium*

Initial Experiment

Since published reports only showed PHB could serve as a substrate for vanillate hydroxylase in vitro, the first experiment was to prove that PHB could be converted to hydroquinone with intact mycelia. Initial conditions for this biotransformation were based on the work of Buswell et al. who examined vanillate hydroxylase activity over

time. Buswell's work showed that when *P. chrysosporium* is grown in Norkran's medium at 30 °C, enzyme activity peaks at approximately 48 h. Therefore, if PHB were introduced into the medium at 48 h, rapid conversion to hydroquinone should take place.

P. chrysosporium (#32629) was originally obtained from the American Type Culture Collection (ATCC) and maintained as an aqueous suspension of spores stored at 4 °C. Cultures were inoculated by directly introducing 2.5×10^6 spores per liter of medium. For the initial experiment, referred to as reaction A, 1 L of Norkran's medium was prepared in a 4 L Erlenmeyer flask. Norkran's medium is a phosphate-buffered minimal-type medium supplemented with trace minerals, yeast extract (0.1 g/L) and glucose (2.5 g/L). Specific to these experiments, vanillate (0.5 g/L) is also added to the medium to induce the expression of vanillate hydroxylase. Once inoculated, the culture was maintained at 30 °C with shaking (250 rpm). After 48 h of growth, PHB was introduced as a 1 M stock solution to give a final concentration of 5 g/L and another 2.5 g of glucose was added to maintain growth. Aliquots were removed over the next 95 h to monitor the progress of the reaction by ¹H NMR. Analysis showed that 0.44 g/L of hydroquinone was produced along with 0.1 g/L of *p*-hydroxybenzaldehyde and 0.18 g/L *p*-hydroxybenzyl alcohol (PHBA) (Table 11). Respectively, yields were 9%, 2%, and 3% relative to the amount of PHB added to the culture medium (Table 11). Although conversion rates were low, this experiment showed that PHB could be taken into the cell and serve as the substrate for not only vanillate hydroxylase but for enzymes responsible for the reductive degradation of vanillate.

Table 11. Titters and yields from reaction A.

	hydroquinone	PHBA	<i>p</i> -hydroxy-benzaldehyde
g/L	0.44	0.18	0.10
yield	9%	3%	2%

Role of Glucose

Previous studies on the metabolism of vanillate by *P. chrysosporium* has implicated three possible routes depending on culture conditions. These three pathways initiate with either oxidative decarboxylation to MHQ, reduction to vanillin and vanillyl alcohol, or decarboxylation to *p*-methoxyquinone which is subsequently reduced to MHQ.³⁵ Once induced, conversion of vanillate to MHQ with vanillate hydroxylase is the dominant pathway but was found to be repressed by glucose. The reduction pathway is not utilized unless an easily metabolized carbon source, such as glucose or cellobiose (a dimer of glucose), is present to provide the energy necessary to supply reducing equivalents.³⁶ The third pathway, catalyzed by phenoxidase laccase and peroxidase, is not as well understood but appears to be expressed as part of the lignin degrading system of *P. chrysosporium*.³⁷

The biotransformation of PHB to hydroquinone therefore is greatly affected by the amount of glucose present in the medium. In reaction A, the glucose concentration upon addition of PHB was 5 g/L. This led not only to lower yields of hydroquinone but to formation of PHBA and *p*-hydroxybenzaldehyde. It is therefore desirable to reduce the quantity of glucose present in the medium. The catch however, is that neither vanillate or

PHB can be utilized as a sole carbon source and so limiting the quantity of glucose limits the mass of the biocatalyst that can be obtained.

Two methods were explored to increase the mycelial mass while still keeping glucose to a minimum. One way to increase the quantity of mycelia is to first grow the mycelia in rich medium followed by resuspension in glucose-free Norkran's medium. In reaction **B**, 4 L of 3% malt extract medium containing 0.5 g/L vanillate were inoculated with 2.5×10^6 spores/L and grown at 37 °C and 250 rpm. Cultures were incubated at a warmer temperature as it was previously found to increase the quantity of mycelia without adversely affecting vanillate hydroxylase activity. After 48 h of growth, the mycelia were harvested on a large Buchner funnel and resuspended in glucose-free Norkran's medium containing 5 g of PHB and 0.5 g/L vanillate. Analysis of the culture supernatant directly after resuspension showed the presence of 9.5 g/L glucose that was entrapped in the mycelia mat and carried over from the rich medium.

Monitoring reaction **B** by ^1H NMR for an additional 48 h showed PHBA to be the major product. Hydroquinone was produced at a titer of 0.02 g/L in a 0.5% yield while PHBA accumulated to 0.74 g/L in a 20% yield (Table 12). While this method did increase the mycelial mass roughly 4-fold (38.4 g wet wt.), it resulted in very poor yields of hydroquinone due perhaps not only the presence of glucose but because vanillate hydroxylase may not be correctly induced in rich medium.

A second method used to increase the amount of biocatalyst was to grow several liters of mycelia in minimal medium and to combine them into one flask prior to the introduction of PHB. In reaction **C**, 8 L of mycelia were grown separately in Norkran's medium containing 2.5 g/L glucose and 0.5 g/L vanillate for 48 h at 37 °C and 250 rpm.

Seven liters of mycelia were then collected by filtration and resuspended in the eighth. To reflect the concentration of PHB present in JB161/pJB2.274 fermentation broths the amount of PHB added to the flask was increased to 10 g. Progress of the biotransformation was monitored for an additional 48 h under the same incubation conditions. Analysis of reaction C showed hydroquinone titers reaching 1.3 g/L representing a 15% yield from PHB (Table 12). Although the 2.5 g/L of glucose carried over to the medium after resuspension was rapidly consumed in the first 12 h, a 2% conversion to PHBA was obtained at a concentration of 0.24 g/L.

Table 12. Titrers and Yields from Reactions B and C.

reaction	hydroquinone		PHBA	
	g/L	yield	g/L	yield
B	0.02	0.5%	0.74	20%
C	1.3	15%	0.24	2%

The mass balance for reaction C however does not equal 100%. With 71% of the PHB remaining in solution and 17% converted to products, that remains 12% of the PHB unaccounted for. This implies that some amount of PHB and/or hydroquinone was either further metabolized by *P. chrysosporium* or was chemically unstable under the reaction conditions. Both explanations are plausible as PHB, already shown to be a substrate for the reductive pathway, could share enough structural characteristics with vanillate to serve as a substrate for multiple enzymes. Possible chemical degradation of the aromatic

compounds is evidenced by the black color that develops over the course of the reaction suggesting oxidized byproducts are formed.

In a control for chemical stability, 1 L of Norkran's medium (without glucose) was doped with 1.7 g/L hydroquinone, 3.3 g/L PHB and 0.5 g/L vanillate. After 48 h at 37 °C and 250 rpm, ¹H NMR analysis showed a 3% loss in hydroquinone and PHB while vanillate concentrations were reduced by 8%. There was no indication of other products formed as only the three starting aromatics were visible in the spectrum. This result suggests that both chemical and biological degradation of PHB and hydroquinone are possible explanations for low mass recovery.

Conversion of Fermentation-Derived PHB to Hydroquinone

As shown in chapter two, PHB can be synthesized from glucose using the *E. coli* biocatalyst JB161/pJB2.274 in 13% yield. To complete the environmentally benign synthesis of hydroquinone, it must be shown that the biotransformation of fermentation-derived PHB behaves the same as commercially obtained PHB.

Initially, it was hoped that *P. chrysosporium* could convert PHB to hydroquinone directly in fermentation broth. To test this idea, 8 L of mycelia were grown in Norkran's medium and after 48 h, were harvested and resuspended in 1 L of cell-free fermentation broth (10.8 g/L PHB) to which 0.5 g/L vanillate was added. After 48 h, only 0.1 g/L of hydroquinone was formed in a 1% yield. Obviously, optimal biotransformation conditions were not provided by the crude fermentation broth thus necessitating the need for PHB purification.

A final optimized reaction was conducted in which PHB was first isolated from fermentation broth as outlined in the previous chapter. Mycelia were grown as described in reaction C with the exception that the eighth flask used to resuspend the remaining mycelia was equipped with baffles. This was done to promote better oxygen transfer to the fungal surface over the course of the reaction as published reports show that greater oxygen availability in shaking cultures favors the oxidative decarboxylation pathway.

After resuspension, 10 g of fermentation-derived PHB was added to the culture and grown for only 36 h as the hydroquinone concentration decreased between 30 and 36 hours. Final analysis showed that 18.8 g (wet wt.) of mycelia produced 1.2 g of hydroquinone representing a 15% conversion of substrate to product (Figure 71). Although 1.9 g/L of glucose was present upon resuspension, only a trace of PHBA was detectable by NMR.

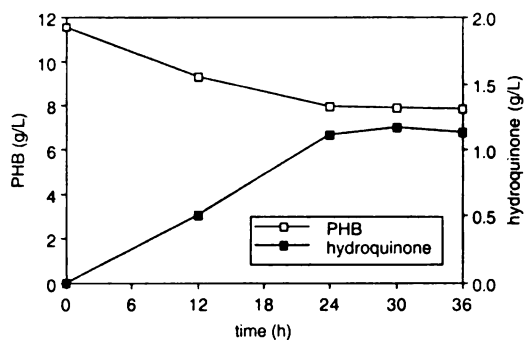


Figure 71. Biotransformation of Fermentation-Derived PHB to Hydroquinone using *P. chrysosporium*.

C. Synthesis of Hydroquinone using *Candida parapsilosis*

i) Background

Candida parapsilosis

Yeasts are unicellular fungi that are most commonly found on the surfaces of plants and are also a part of the microflora found in the gut of insects and animals.³⁸ Some species, such as *Candida albicans*, are pathogenic to warm-blooded animals usually through infection of the skin or mucus membranes.³⁹ *Candida parapsilosis* is a non-pathogenic, ascomycetous yeast that has the ability to utilize PHB as a sole source of carbon.⁴⁰ The ability of *C. parapsilosis* to grow on PHB is a characteristic it shares with soil bacteria such as *Pseudomonas*. The ability to metabolize compounds such as PHB and vanillate benefits microorganisms as aromatics are common soil components due to lignin degradation.⁴¹

Nature's predominate pathway for the metabolism of PHB begins with oxidation to protocatechuic acid followed by degradation through the 3-oxoadipate pathway (Figure 72).⁴² An alternate pathway was suggested for *C. parapsilosis* CBS604 as it showed the ability to grow on 2,4-dihydroxybenzoic acid.⁴³ Organisms possessing the enzyme 4-hydroxybenzoate 3-hydroxylase,⁴⁴ the activity necessary to convert PHB to PCA, could not utilize 2,4-dihydroxybenzoate as a carbon source as it cannot be directly be converted to PCA and further metabolized. It was found that *C. parapsilosis* could grow equally on PHB, PCA, and 2,4-dihydroxybenzoate, suggesting that all three aromatic compounds could be enzymatically converted to the common intermediate 1,2,4-trihydroxybenzene (hydroxyhydroquinone, Figure 72).⁴⁵

The enzymes required to convert PHB to hydroquinone and subsequent hydroxylation to hydroxyhydroquinone were isolated from *C. parapsilosis* and named 4-hydroxybenzoate 1-hydroxylase and 1,4-dihydroxybenzene monooxygenase (Figure 72).⁴⁶ A 1,2-dioxygenase catalyzes ring-cleavage en-route to 3-oxoadipate. Experiments with the purified enzyme showed that 4-hydroxybenzoate 1-hydroxylase could also catalyze the oxidative decarboxylation of PCA and 2,4-dihydroxybenzoate to hydroxyhydroquinone explaining their ability to support growth.

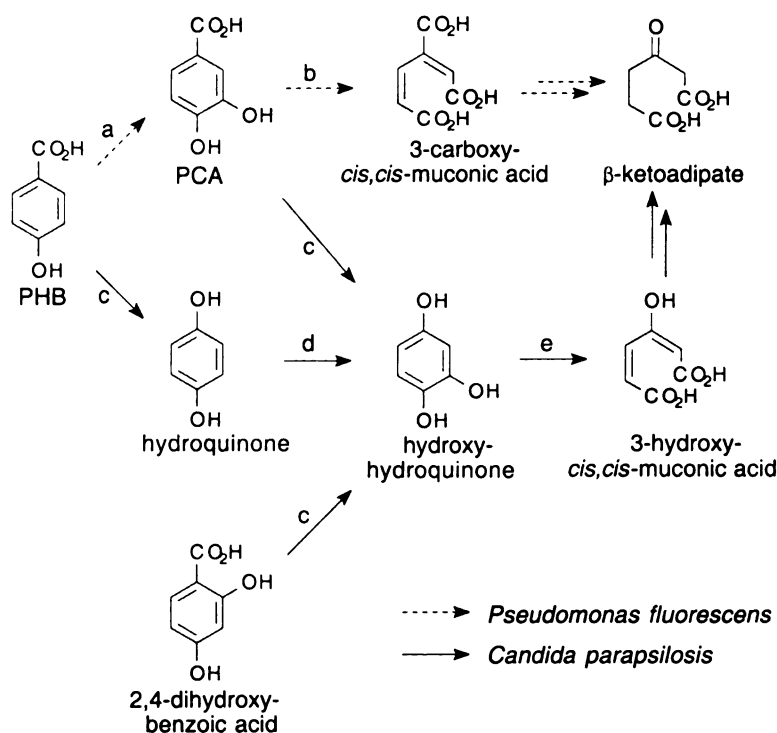


Figure 72. Degradation of Hydroxylated Aromatics in *Pseudomonas* and *Candida*. Enzymes are as follows: (a) 4-hydroxybenzoate 3-hydroxylase (b) protocatechuate-3,4-dioxygenase (c) 4-hydroxybenzoate 1-hydroxylase (d) phenol monooxygenase (e) trihydroxybenzene 1,2-dioxygenase

Expression of 4-hydroxybenzoate 1-hydroxylase is induced by growth on either PHB, PCA, or 1,2-dihydroxybenzoate.⁴⁷ Unlike vanillate hydroxylase purified from *P.*

chryso sporium, the protein isolated from *C. parapsilosis* was shown to be a monooxygenase requiring flavin adenine dinucleotide (FAD) as a co-factor (Figure 73).⁴⁸ This suggests that the enzyme may have a similar mechanism to other flavoprotein aromatic hydroxylases and proceeds through a flavin hydroperoxide intermediate. Similar to vanillate hydroxylase however, 4-hydroxybenzoate 1-hydroxylase was shown to consume stoichiometric amounts of NAD(P)H and oxygen (Figure 73). Thorough analysis of the reaction between PHB and 4-hydroxybenzoate 1-hydroxylase showed hydroquinone to be the only aromatic product. Based on the above evidence, it was proposed that *C. parapsilosis* CBS604 would make a good biocatalyst for the conversion of PHB to hydroquinone.

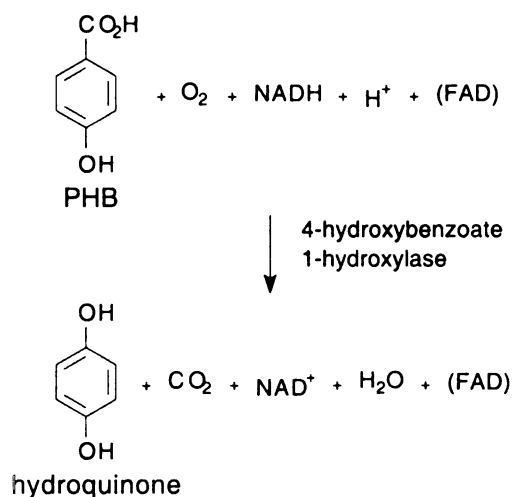


Figure 73. Reaction Stoichiometry for 4-Hydroxybenzoate 1-Hydroxylase.

ii) Conditions for the Biotransformation of PHB using *C. parapsilosis*

Selection of Culture Medium

Standard shake-flask protocols, designed to accumulate products with *E. coli* biocatalysts, were used as a model for the initial experiments with *C. parapsilosis*. Traditionally, cells are first grown in a rich medium to accumulate a large quantity of biomass and then isolated and resuspended in a minimal medium to promote product accumulation. For *C. parapsilosis*, YM broth was used for the rich medium and double-concentrated Reader's medium was used as the minimal solution. YM broth is a rich undefined medium consisting of yeast extract, malt extract, peptone, and glucose while (2X) Reader's medium is a potassium phosphate buffered salt solution containing $(\text{NH}_4)_2\text{SO}_4$ as a nitrogen source, glucose (5 g/L), and trace mineral and vitamin supplementations. Cells were routinely cultured in 4 L Erlenmeyer flasks at 250 rpm and 30 °C.

C. parapsilosis CBS604 was obtained from ATCC (#22019) and maintained on YM agar slants as recommended by the provider. Reaction A began with a starter culture prepared by sterile introduction of cells from the agar slant into 10 mL of YM medium. After 12 h of growth at 30 °C, the inoculum was transferred to 1 L of YM medium. Following an additional 12 h of growth, the cells were collected and resuspended in 1 L of (2X) Reader's medium containing 5 g of glucose and 1 g of PHB. An additional gram of PHB was added 5 h and 10 h after resuspension. The PHB was introduced to the culture medium by increments to help alleviate any toxicity the aromatic acid may have against the yeast. Monitoring the culture supernatant by ^1H NMR revealed the presence

of 0.35 g/L of hydroquinone 24 h after resuspension representing a 15% yield (Table 13). By 48 h however, all the PHB and hydroquinone had been consumed by the host.

Since both the starting material and product were metabolized by *C. parapsilosis* in reaction **A**, a second experiment was run with excess glucose to hopefully repress the consumption of aromatics in favor of the carbohydrate. In reaction **B**, 1 L of YM grown cells were resuspended in 1 L of (2X) Reader's medium containing 40 g of glucose and 3 g of PHB. Although the glucose was consumed within 48 h, the concentration of PHB remained constant and hydroquinone was not detected (Table 13). This suggests that glucose not only represses the consumption of PHB but prevents the induction of 4-hydroxybenzoate 1-hydroxylase as well.

Table 13. Results of reactions A, B, and C.

reaction	glucose ^a	PHB ^a	time ^b	hydroquinone ^c	yield ^d
A	5	3 x 1	24	0.35	15%
B	40	3	48	0	0%
C	5	10	48	2.7	33%

^aquantity (g) added upon resuspension. ^btime (h) after resuspension. ^creported in (g). ^dmol of hydroquinone/mol PHB.

Since the over-metabolism of the product could not be easily suppressed in reaction **B**, another way of obtaining higher hydroquinone titers was to increase the quantity of PHB. The belief being that with large quantities of substrate available, an excess of hydroquinone could build up within the cell and be readily exported to the culture supernatant. Therefore, for reaction **C**, 1 L of YM grown cells were resuspended

in 1 L of (2X) Reader's medium containing 5 g of glucose and 10 g of PHB. After 48 h of additional growth, 2.7 g/L of hydroquinone were produced in a 33% yield (Table 13).

As positive results were obtained with higher additions of PHB in reaction **C**, the next experiments were designed to find the optimum PHB starting concentration. Since high glucose concentrations hampered the biotransformation in reaction **B**, glucose was eliminated from the resuspension medium in the next series of reactions. Two PHB concentrations were examined. In reaction **D**, cells were resuspended in (2X) Reader's medium containing 10 g of PHB. As second 10 g aliquot was added ten hours later. In reaction **E**, a liter of cells was resuspended with 10 g of PHB followed by three more 10 g additions at 5 h, 9 h and 24 h.

After an additional 72 h, reaction **D**, with 20 g of PHB added, produced 4.9 g of hydroquinone in a 30% yield (Table 14). Cells that were cultured with 40 g of PHB in reaction **E** produced 6.5 g of hydroquinone in a 21% yield after 100 h (Table 14). These results show that although 40 g of PHB allowed for higher titers to be reached, the yield was lowered meaning there is not a linear correlation between PHB concentration and the quantity of hydroquinone produced. This effect does not appear to be a consequence of toxicity as the mass recovery was almost the same for both runs. In reaction **D**, 64% of the mass (PHB remaining + hydroquinone formed) could be accounted for after 72 h while 67% was recovered in reaction **E**. Comparison of the mass recovered in each reaction is a measure of the cell's ability to consume aromatic substrates. Since both sets of cells consumed ~35% of the mass, it would imply that their growth was not affected by the quantity of PHB.

Table 14. Results of Reactions D and E.

reaction	glucose ^a	PHB ^a	time ^b	hydroquinone ^c	yield ^d
D	0	2 x 10	72	4.9	30%
E	0	4 x 10	100	6.5	21%

^aquantity (g) added upon resuspension. ^btime (h) after resuspension. ^creported in (g). ^dmol of hydroquinone/mol PHB.

Increasing Biomass and Yield

In the experiments outlined above, the removal of glucose from the culture medium after resuspension did not appear to have a detrimental effect. Since YM broth contains both rich extracts and 10 g/L of glucose, it was decided to inoculate directly into (2X) Reader's medium for the next series of reactions. Two other variables were examined in this set of four experiments to improve titer and yield. One variable was the addition of PHB as a single aliquot versus addition as multiple aliquots over time and the second was increased cell mass. For these experiments, data collection ($t = 0$) began with the addition of PHB.

In reaction **F**, 1 L of (2X) Readers medium containing 5 g/L of glucose was inoculated with 10 mL of a 12 h YM culture. After 12 h of growth, 10 g of PHB was added followed by a second 10 g addition 9 h later. Reaction **G** was identical to **F** with the exception that 20 g of PHB was added as a single aliquot after 12 h of growth. For reactions **H** and **I**, two-1 L cultures were grown for each reaction in (2X) Reader's medium. After 12 h, cells from one of the flasks were collected and resuspended in the second followed by addition of 20 g of PHB. Reaction **I** differs from **H** in that at upon

resuspension, a 60 mL solution containing the same quantity of medium components normally found in 1 L of (2X) Reader's medium was added to the reaction creating a (4X) medium.

The results provided by Table 15 and Figure 74 show reaction **F** to have the highest quantity of hydroquinone after 78 h with 7.8 g formed in a 49% yield. A similar conversion was obtained with reaction **I** (7.5 g, 47% yield), but the rate of conversion was increased by doubling the cell and medium concentrations (Table 15, Figure 74). Comparison of reactions **F** and **G** show that the addition of PHB in one aliquot could be a shock to the cells as a decreased yield resulted (6.4 g, 40% yield, Table 15, Figure 74) although this is offset by increased conversion rate (note: in Figure 74, reactions **F** and **G** appear closer in yield due to differences in the final volume of broth). Another important variable obtained from this data relates to the health of the cell. Comparison of reaction **H** and **I** show the drastic difference in both conversion rate and yield when cells are provided with enough nutrients. With twice the amount of cells present relative to the medium components in reaction **H**, the ability of *C. parapsilosis* to convert PHB to hydroquinone was compromised and only 3.7 g of hydroquinone was produced in a 24% yield (Table 15, Figure 74).

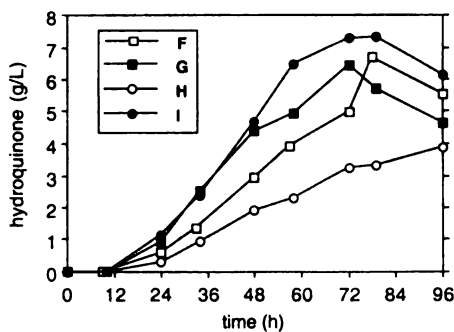


Figure 74. Comparison of Hydroquinone Production in Reactions F, G, H, and I.

Table 15. Results of reactions F, G, H, and I.

reaction	glucose ^a	PHB ^a	time ^b	hydroquinone ^c	yield ^d
F	5	2 x 10	78	7.8	49%
G	5	20	72	6.4	40%
H	5	20	96	3.7	24%
I	5	20	79	7.5	47%

^aquantity (g) added upon resuspension. ^btime (h) after resuspension. ^creported in (g). ^dmol of hydroquinone/mol PHB

D. Purification of Hydroquinone

Industrially, hydroquinone is purified via fractional distillation.⁴⁹ Here a bench-scale purification procedure was established using selective extraction. The biocatalyst was first separated from the culture supernatant by filtration through a Buchner funnel in the case of *P. chrysosporium* or centrifugation in the case of *C. parapsilosis*. It was found that by raising the pH of the resulting broth to 9.1 with NaOH, hydroquinone could be selectively extracted with *t*-butyl methyl ether. In biotransformations employing *C. parapsilosis*, only hydroquinone and PHB are present at the end of the reaction simplifying the purification. The organic layer could be stripped down directly to give a 98% recovery of hydroquinone. ¹H NMR shows the product to be 99.9% pure with just a trace of PHB present. The remaining aqueous layer contains PHB as the only aromatic product. Using *C. parapsilosis* as a biocatalyst, PHB can be converted to hydroquinone

in a 48% isolated yield. When coupled with the biocatalytic synthesis of PHB, hydroquinone can be made from glucose in a 4% overall yield.

Purification of the resulting broth from *P. chrysosporium* biotransformations is complicated by the presence of PHBA and vanillate. Extraction of the broth at pH 9.1 with *t*-butyl methyl ether followed by solvent removal afforded a black solid in 59% yield. Analysis revealed the presence of small quantities of PHB and PHBA (molar ratio of hydroquinone : PHB : PHBA was 37 : 1 : 4). Recrystallization from a solution of ethyl acetate and petroleum ether yielded a 49% recovery of hydroquinone however, there remained a trace amount of PHBA (molar ratio of hydroquinone to PHBA was 23 : 1). Using *P. chrysosporium*, hydroquinone can be synthesized from PHB in a 4% yield. If the PHB is fermentation-derived, hydroquinone can be obtained in a 0.3% yield from glucose.

Although the conversion yields are relatively low with both fungal biotransformations, the unreacted PHB can be recovered at the end of the reaction increasing the viability of these processes. After the extraction of hydroquinone, the pH of the remaining aqueous layer can be lowered to 4 with H₂SO₄ and extracted again with *t*-butyl methyl ether. Stripping the resulting organic layer to dryness afforded PHB in a 78% yield. A trace amount of hydroquinone was detectable in the recovered solid (molar ratio of PHB to hydroquinone was 39:1) but would be inconsequential if the PHB was recycled as starting material.

II. *p*-CRESOL

A. Background

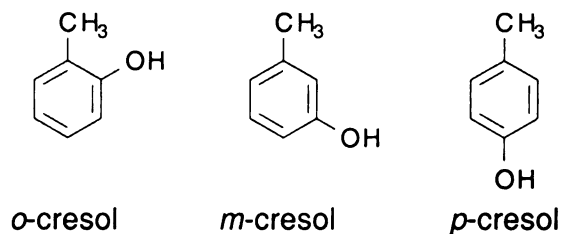


Figure 75. Structure of *o*-, *m*-, and *p*-Cresol.

Cresols (Figure 75), the monomethyl derivatives of phenol, have historically been classed together with phenol, dimethyl phenols (xylenols), and other alkylated phenols as cresylic acid, tar acids, or tricresol.⁵⁰ Originally derived from coal tar, a by-product of coke production, cresylic acid went unnoticed by the chemical industry until its antiseptic properties were discovered by Joseph Lister in 1869. In the 1920's, phenolic plastics became the major end-use of cresylic acid. Today, cresols are isolated from petroleum or coal tar as the pure *ortho* isomer and a mixture of *m*-cresol and *p*-cresol.⁵¹ The *meta* and *para* isomers cannot be separated directly by distillation due to the proximity of their boiling points (b.p. for *m*-cresol is 202.3 °C and the b.p. for *p*-cresol is 201.9 °C).⁵²

The mixture of *m*- and *p*-cresols is used for the manufacture of phenol-formaldehyde resins and tricresyl phosphates (Figure 76).⁵³ Reaction of the mixture with phosphorous oxychloride produces tricresyl phosphates, a plasticizer used mainly in PVC production and as an additive for gasoline and hydraulic fluids. The major use of purified *p*-cresol is as the starting material for butylated hydroxy toluene (BHT). BHT is used as an antioxidant in oils, rubber, and polyolefins and is one of the few phenolic antioxidants

approved as a direct food additive by the FDA. The *para* isomer also serves as the starting material for the synthesis of bisphenol antioxidants and perfumes.

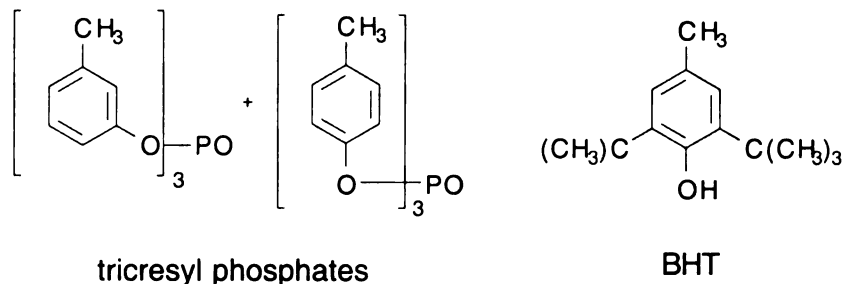


Figure 76. Derivatives of *p*-cresol.

Direct synthesis of *p*-cresol begins with the sulfonation of toluene to yield *p*-toluenesulfonic acid (Figure 77).⁵⁴ After neutralization with sodium sulfite, the sulfonate is converted to the sodium cresylate by fusion with NaOH at 330-360 °C. Acidification with H₂SO₄ yields a mixture that consists of 80% *p*-cresol with the *meta* and *ortho* isomers as impurities. Pure *p*-cresol is recovered by fractionation. The *m*-, *p*-cresol mixture is commercially synthesized (Figure 78) by the cleavage of cymenes (isopropylmethylbenzenes).⁵⁵ Similar to the production of hydroquinone, toluene is alkylated with propylene in the presence of AlCl₃ to give a mixture of cymenes comprising mainly of the *meta* and *para* isomers. This mixture is air oxidized in the presence of a catalyst to form hydroperoxycymenes. Subsequent acid cleavage yields *m*-cresol, *p*-cresol (3 : 2 molar ratio respectively) and acetone.

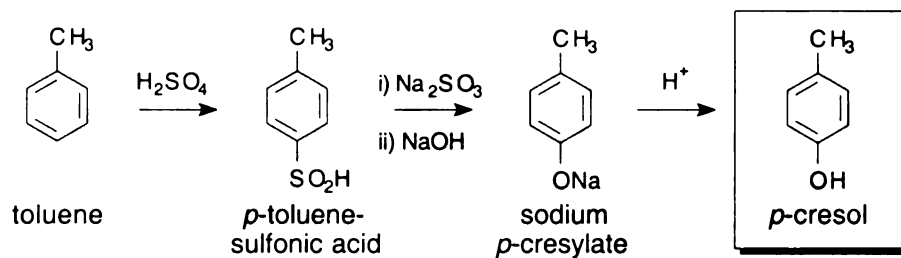


Figure 77. Commercial Synthesis of *p*-Cresol via *p*-Toluenesulfonic acid.

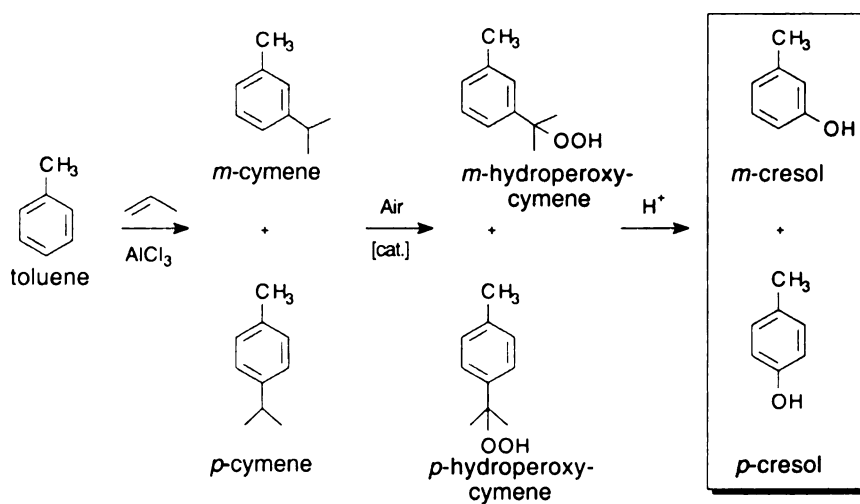


Figure 78. Commercial Synthesis of *m*-, *p*-Cresol via Cymenes.

In this section, an alternative synthesis of *p*-cresol will be elaborated. It is proposed that *p*-cresol can be synthesized from glucose via PHB intermediacy. Reduction of PHB with the fungus *P. chrysosporium* yields *p*-hydroxybenzyl alcohol which is easily hydrogenated to *p*-cresol in the presence of a Pd catalyst (Figure 79). The outlined synthesis would be environmentally superior to the present commercial routes as it originates with glucose, a renewable, nontoxic feedstock. It was shown in chapter two that glucose can biocatalytically converted to PHB. Biotransformation of PHB to *p*-hydroxybenzyl alcohol followed by hydrogenation is free of hazardous intermediates and employs moderate reaction conditions. This is opposed to the industrial production of *p*-cresol that originates with non-renewable petroleum or coal feedstocks and proceeds through harmful reagents in the form of toluene sulfonic acid and hydroperoxides. The proposed biocatalytic route to *p*-cresol has the added advantage in that only one isomer is produced simplifying its purification.

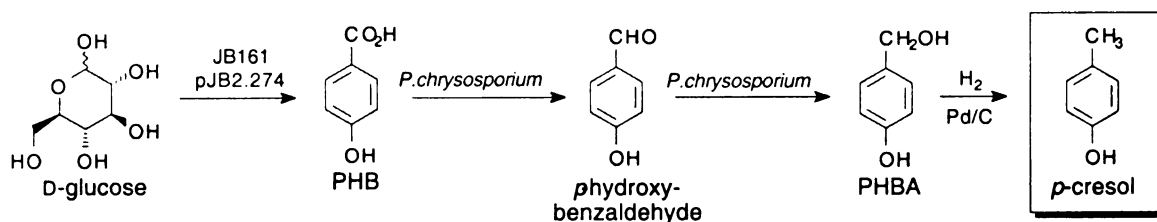
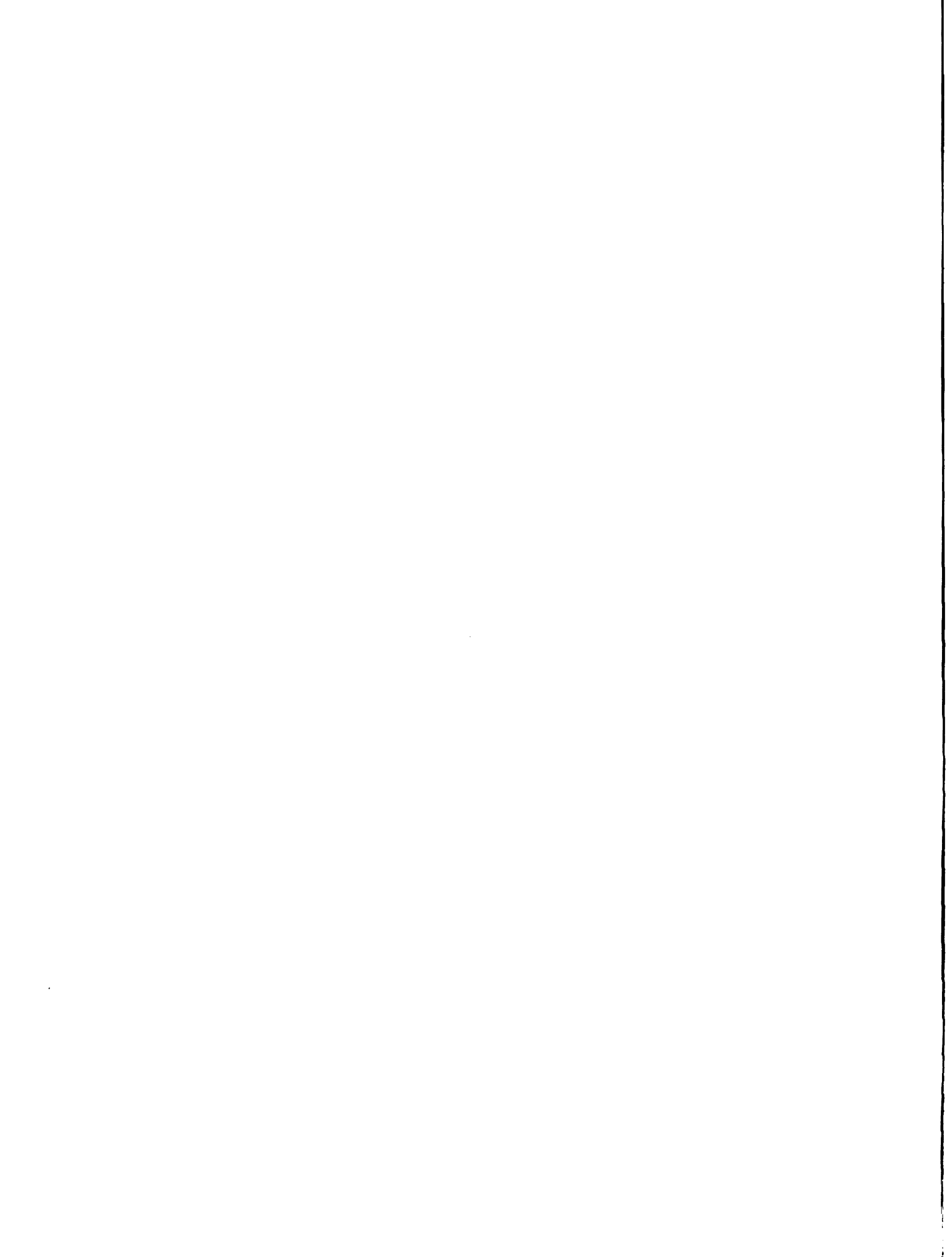


Figure 79. Benign Synthesis of *p*-Cresol.



B. Synthesis of *p*-Cresol from PHB.

Reduction of Aromatic Acids by White-Rot Fungi

Studies conducted by Ander et al. show that an easily metabolizable carbon source, such as glucose or cellobiose (a glucose dimer derived from the hydrolysis of cellulose), is the only requirement for the vanillate reductive pathway to be active in *P. chrysosporium*.⁵⁶ Unlike vanillate hydroxylase, the reductase enzymes appear not to require induction by vanillate. Muheim and co-workers purified an aryl-alcohol dehydrogenase from *P. chrysosporium* based on the enzyme's ability to reduce veratraldehyde (3,4-dimethoxybenzaldehyde) to veratryl alcohol (3,4-dimethoxybenzyl alcohol).⁵⁷ Expression of the dehydrogenase was linked to the appearance of ligninolytic activity, which is induced by nitrogen limitation. Vanillin and *p*-hydroxybenzaldehyde were shown to be reduced to the corresponding benzyl alcohols with the purified aryl-alcohol dehydrogenase but with only 30% and 11% (respectively) of the relative reduction rate compared to veratryl aldehyde as substrate (Figure 80). It is unclear however if this enzyme is solely responsible for the in vivo reduction of vanillin to vanillyl alcohol or if it is part of a family of aromatic reductase enzymes present in *P. chrysosporium*.

The aromatic reduction pathway in white-rot fungi have previously been exploited to catalyze the biotransformation of *p*-anisic acid (*p*-methoxybenzoic acid) and vanillate to their corresponding aldehydes.⁵⁸ Culturing the white-rot fungus *Bjerkandera* sp. strain BOS55 in the presence of *p*-anisic acid and glucose produced a mixture of the aldehyde

and alcohol with equilibrium favoring the formation of the aldehyde in 80% yield (Figure 81). A parallel experiment with *P. chrysosporium* (ATCC 24725) also reduced *p*-anisic acid but favored the formation of the alcohol in roughly 70% yield (Figure 81).

substrate	product	relative specific activity
<chem>COc1cc(C=O)cc(OC)c1</chem> veratraldehyde	<chem>COc1cc(CO)cc(OC)c1</chem> veratryl alcohol	100%
<chem>COc1cc(C=O)c(O)c1</chem> vanillin	<chem>COc1cc(CO)c(O)c1</chem> vanillyl alcohol	30%
<chem>Oc1ccc(C=O)cc1</chem> PHB	<chem>Oc1ccc(CO)cc1</chem> <i>p</i> -hydroxybenzyl alcohol	11%

Figure 80. Relative Specific Activity of Aryl-Alcohol Dehydrogenase.

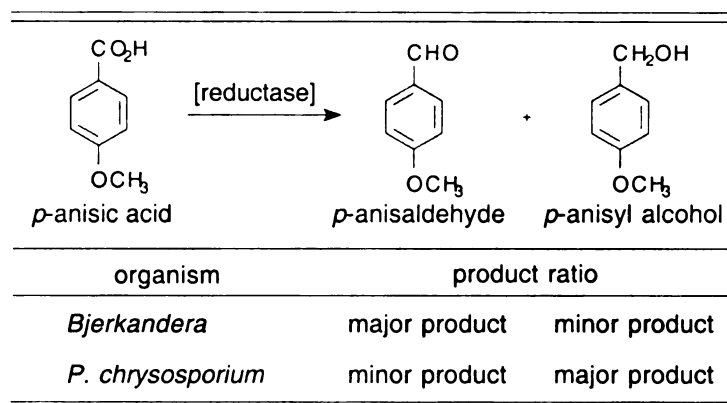


Figure 81. Reduction of *p*-Anisic Acid by White-Rot Fungi.

The white-rot fungus *Pycnoporus cinnabarinus* favored formation of the aldehyde when cultured in the presence of vanillate and cellobiose (Figure 82).⁵⁹ Optimal production of vanillin was found under the conditions of low dissolved oxygen concentration and gentle agitation with cellobiose supplementation. Under these culture conditions, vanillate (2.4 g/L) was converted to vanillin (1.3 g/L) in a 60% yield with methoxyhydroquinone (0.35 g/L) and vanillyl alcohol (0.088 g/L) as byproducts (Figure 82).

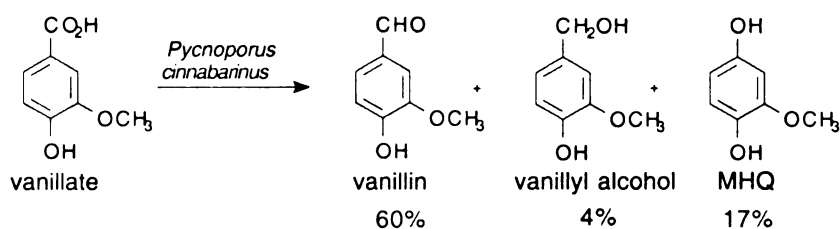


Figure 82. Reduction of Vanillate with *Pycnoporus cinnabarinus*.

Biotransformation of PHB to *p*-Hydroxybenzoic Alcohol

As discussed previously, *p*-hydroxybenzyl alcohol (PHBA) was observed as the major product when *P. chrysosporium* was initially grown in rich medium and resuspended in Norkran's medium containing PHB. In order to optimize this conversion, glucose was added to the medium upon resuspension as the literature showed this to be a necessary component for the reductive pathway. Glucose rich conditions were examined with two different concentrations of PHB and vanillate.

Three reactions were performed in parallel using 4 L of *P. chrysosporium* mycelia cultured initially in malt broth and resuspended in 1 L of Norkran's medium containing 40 g/L of glucose. In reaction **A**, the mycelia was resuspended in the presence of 0.5 g/L vanillate and 5 g of PHB. The quantity of PHB was lowered to 2.5 g for reaction **B** while maintaining a concentration of 0.5 g/L vanillate. To investigate if vanillate concentrations affected the reducing activity of the biocatalyst, reaction **C** contained 0.25 g/L vanillate and 5 g of PHB.

Four days after resuspension, ¹H NMR analysis of the culture supernatants showed the presence of 2.0 g of PHBA, 0.0 g of PHB, and 21 g of glucose in reaction **B** representing a 90% conversion and mass recovery (Table 16). Reactions **A** and **C** were cultured for an additional 3 days and were stopped when PHBA concentrations leveled off. Analysis of the resulting broth from reaction **A** revealed 3.1 g of PHBA, 1.4 g of PHB and 9.3 g of glucose. PHB was converted to PHBA in a 70% yield with 99% of the mass accounted for (Table 16). Reaction **C** contained 3.1 g of PHBA, 1.1 g of PHB, and 8.3 g of glucose after 7 d. PHBA was formed in a 68% yield with a 92% mass recovery (Table 16). Trace amounts of hydroquinone were visible in NMR spectra of all three

reactions while *p*-hydroxybenzaldehyde was not. The presence of hydroquinone suggests that PHB can induce vanillate hydroxylase activity to some extent or there is a low level of enzyme constitutively expressed. The absence of *p*-hydroxybenzaldehyde indicates that the equilibrium lies greatly in favor of the alcohol under these conditions. These results show that PHBA can be formed in good yields when adequate glucose is present in the medium. Variance in the PHB concentration shows that while higher titers are obtained with higher quantities of PHB, there is a corresponding drop in yield. This suggests that an optimal concentration of PHB for this quantity of mycelial biocatalyst lies between 2.5 and 5 g. The similarity of results between reactions A and C correlates with literature that claims vanillate concentrations do not affect the reduction pathway in *P. chrysosporium*.

Table 16. Reduction of PHB to PHBA using *P. chrysosporium*: reactions A, B, C, and D.

reaction	vanillate ^{a,c}	glucose ^{b,c}	PHB ^{b,c}	time ^d	PHBA ^b	yield ^e	mass recovery ^f
A	0.50	40	5	7	3.4	70%	99%
B	0.50	40	2.5	4	2.0	90%	90%
C	0.25	40	5	7	3.1	68%	92%
D	0	30	3	6	2.2	83%	87%

^ag/L. ^bg. added upon resuspension. ^dtime (d) after resuspension. ^emol PHBA produced / mol PHB added. ^f(mol PHBA produced + mol PHB remaining) / mol PHB added

Taking these observations into account, an optimized biotransformation was run using fermentation-derived PHB. In this experiment, 4 L of mycelia were grown in 3% malt broth for 48 h, collected by filtration, and resuspended in Norkran's medium

containing 30 g of glucose and 3 g of PHB. Vanillate was not added to any of the cultures. After an additional 6 days of culturing, 2.3 g of PHBA was produced in an 83% yield. Further analysis showed 0.12 g of PHB and 3.9 g of glucose remaining in the culture supernatant (Figure 83). Together the quantities of PHB and PHBA represent an 87% mass recovery.

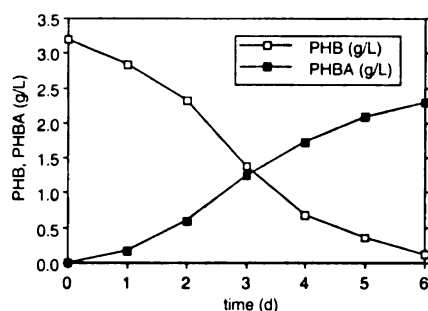
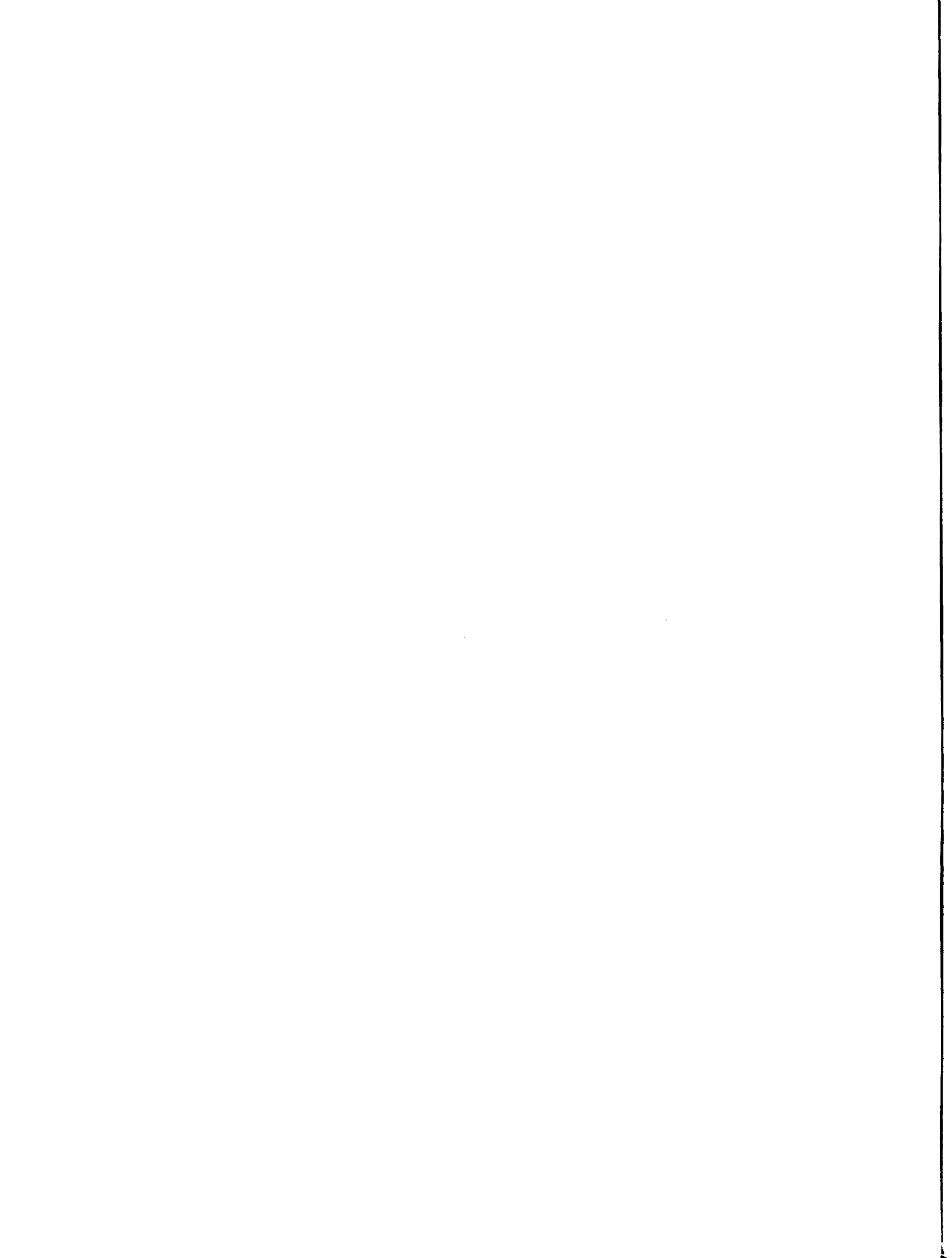


Figure 83. Biotransformation of Fermentation-Derived PHB to PHBA using *P. chrysosporium*

Hydrogenation of PHBA to *p*-Cresol

Purification of PHBA from the crude reaction broth began with filtration to remove the mycelial mass. The filtrate was placed in a continuous, liquid-liquid extractor with EtOAc for 3-9 h. To increase the extraction efficiency, the continuous extraction apparatus was modified by vigorous stirring of the organic and aqueous layers to create an emulsion. After the aqueous layer was checked by ^1H NMR to verify the complete extraction of PHBA, the apparatus was dismantled, and the organic layers were pooled and dried over MgSO_4 . The solvent volume was reduced to approximately 6 mL via rotary evaporation and allowed to stand. PHBA crystallized from this solution as a pale yellow solid. Concentration of the filtrates afforded two additional crops giving an



overall PHBA recovery of 67%. NMR analysis of the resulting crystals showed only trace quantities of HQ and PHB.

Standard hydrogenation conditions were employed for the reduction of purified PHBA to *p*-cresol (Figure 79). Typically, a 0.4 to 0.7 M solution of PHBA in MeOH was degassed with Ar. To this, 5 mol% of 10% Pd on C was added and the vessel was placed on a Parr hydrogenation apparatus at 50 psi of H₂. After 1.5-2 h, the catalyst was removed by filtration through Celite. The MeOH filtrate was stripped down to an oil using rotary evaporation. NMR analysis showed PHBA to have been completely converted to *p*-cresol. The product was isolated in an 85% yield. Overall, PHB can be converted to *p*-cresol in 46% yield via biocatalysis and hydrogenation. Coupling this result with biocatalytically-derived PHB allows *p*-cresol to be synthesized from glucose in 4% yield.

Possible Routes to *m*-Cresol and *o*-Cresol.

As the *meta* and *ortho* isomers of cresol are also commercially desirable molecules, the ability of *P. chrysosporium* to reduce *m*-hydroxybenzoic (MHB) acid and *o*-hydroxybenzoic acid (OHB) to their respective benzyl alcohols was examined. In this experiment, 12 L of malt broth were inoculated with spores and grown at 37 °C for 48 h. The mycelia was divided into three flasks where each flask contained 4 L of collected mycelia, 1 L of Norkran's medium, 30 g of glucose, and 3 g of either PHB, MHB, or OHB. The flasks were incubated for an additional 5 d and the culture supernatant was analyzed by ¹H NMR. Comparison of the percent yields for the synthesis of the benzyl alcohols relative to PHB (63%) shows that MHB (54%) was reduced fairly well by *P.*

chryso sporium while OHB (5%) was not. Therefore, reduction of MHB to the *m*-hydroxybenzyl alcohol followed by hydrogenation could be a possible route to *m*-cresol.

III. Discussion

Hydroquinone

This chapter outlined a synthetic route to hydroquinone that is environmentally superior to the current commercial route. All industrial manufacture of hydroquinone is derived from petroleum feedstocks via benzene. It is accepted as fact that one day these feedstocks will be gone. Although supplies are plentiful today, chemical companies as well as the average buyer of gasoline are at the mercy of foreign politics. In the alternative synthesis outlined here, hydroquinone can be derived from PHB which can be synthesized directly from glucose. Not only is glucose a renewable feedstock obtained from plants such as corn, it is a commodity produced on American soil. The synthesis of hydroquinone from glucose via PHB also has the advantage of avoiding harmful reagents, intermediates, and wastes. Commercial manufactures of hydroquinone must deal with carcinogenic benzene, toxic phenol, or explosive peroxides. As environmental and worker-safety laws tighten, compliance will become not only expensive but necessary to avoid social reproof.

The pilot study presented here utilizes two different organisms to catalyze the oxidative decarboxylation of PHB to hydroquinone. The use of the enzymes vanillate hydroxylase and 4-hydroxybenzoate 1-hydroxylase represents a novel alternative to traditional chemical reagents needed for the conversion of a carboxylic acid group to a

hydroxyl group. Employing traditional methodologies would entail an oxidizing agent, such as $\text{Pb}(\text{OAc})_4$ or $\text{Cu}(\text{OAc})_2$, to first form the acetoxy ester in conjunction with other radical products. Acid cleavage of the ester would complete the functional group transformation to the hydroxy group. Enzymatic whole-cell conversion has the advantage of a single reaction step that does not generate stoichiometric quantities of metal salts. Use of *C. parapsilosis* also guarantees the formation of a single product.

Evolution of this biotransformation would be directed at increasing titers, yields, selectivity, and mass recovery. One approach would be to clone either of the genes responsible for vanillate hydroxylase or 4-hydroxybenzoate 1-hydroxylase activity. Over expression of either of these proteins in a suitable host would help to increase the titer and yield obtainable for a given quantity of biomass. Selectivity and mass recovery would be dependent on the phenotype of the host. Ideally the host should not be able to metabolize the starting material or the product and have only one reaction pathway for the molecule to follow.

This ideal host could be created by mutagenesis of the *Candida* strain already discussed. Unlike other *Candida* strains, *C. parapsilosis* is not pathogenic to mammals and from the experience gained, it appears to be relatively resistant to any toxicity imparted by PHB or hydroquinone. Since *Candida* is a yeast, there are more protocols established for the culturing and genetic manipulation of this organism compared to filamentous fungi. As there is only one degradation pathway for PHB in this organism, all of the starting material would be channeled through 4-hydroxybenzoate 1-hydroxylase to produce the desired product. Overmetabolism of the product could be prevented by mutagenesis to knock out the subsequent 1,4-dihydroxybenzene monooxygenase activity.

To obtain this strain, established protocols for mutagenesis on yeasts could be employed followed by selection of a strain that failed to grow on PHB as a sole carbon source but retained the ability to utilize PCA. Overexpression of the gene encoding 4-hydroxybenzoate 1-hydroxylase in this mutagenized strain followed by optimization of fermentation conditions would create an efficient, scalable process for the conversion of PHB to hydroquinone. It should be noted that *E. coli* would be an unsuitable host for expression of the cloned gene as it was found that hydroquinone is highly toxic to the bacteria.

p-Cresol

Similar to hydroquinone, the environmentally benign synthesis of *p*-cresol presented here holds several advantages over the commercial sources of cresols. Most notably, *p*-cresol can be synthesized as a single isomer simplifying its purification. Industrially, the *meta* and *para* isomers must be derivitized in order to be isolated individually. As with hydroquinone, the alternative route to *p*-cresol employs glucose as a renewable starting material and proceeds through innocuous intermediate steps without generating noxious by-products.

Future development of this process would involve isolation of the genes responsible for the two reductase activities. Cloning of the genes would first entail the construction of a cDNA library. As *P. chrysosporium* is a eukaryote, there is a high possibility that its genes contain introns. A cDNA library is derived from messenger RNA, which has the introns already removed. Actually several organisms besides *P. chrysosporium* could also be used to generate this library as similar enzyme activities

have been found in *Neurospora crassa* and *Nocardia*.⁶⁰ This library could be cloned into commercially available vectors and expressed in *E. coli*.

The desired clone could be selected for in a variety of ways. One way would be to directly screen for the correct DNA using degenerate radio-labeled oligonucleotide probes that corresponded to a portion of the protein sequence. This method necessitates that the desired protein be purified to a degree that confident sequence information can be attained. A second method that could be used to isolate the desired clone is to directly select for the enzyme activity based on a colorimetric assay. For example, a compound, such as pararosaniline, that turns colored in the presence of aldehydes could be used to select for the first reductase enzyme. This method requires that the protein is expressed properly in the heterologous host.

If these genes were cloned and separately expressed, one would have the ability to selectively synthesize a variety of benzaldehydes and benzyl alcohols. In the case of PHB as substrate, an environmentally friendly route to *p*-hydroxybenzaldehyde could be elaborated. *p*-Hydroxybenzaldehyde is used as the starting material for the herbicides bromoxynil and inoxynil and the raspberry fragrance 4-(*p*-hydroxyphenyl)-butanone (Figure 84). Underivatized, *p*-hydroxybenzaldehyde is used as a brightening and leveling agent in zinc electroplating.⁶¹ Although there is no widespread commercial use of *p*-hydroxybenzyl alcohol it has been found to be one of the active components in the plant *Gastrodia elata Bl.* Known as Tianma in Chinese medicine, this plant is believed to improve circulation and cure such ailments as rheumatism, paralysis, headaches, and vertigo.⁶² The benzyl alcohol may also have a developing place in western medicine as a derivative known as TA-064 (Figure 84) is an inotropic cardiotonic agent.⁶³

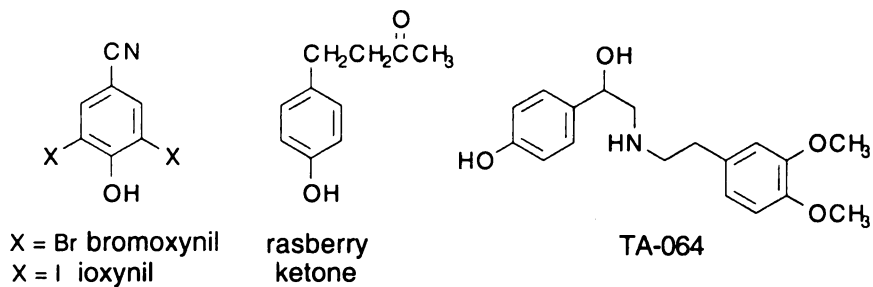


Figure 84. Derivatives of *p*-Hydroxybenzaldehyde and PHBA.

Individual expression of the genes encoding the reductase enzymes also holds great potential as a broad synthetic tool. The direct reduction of benzoic acids to their corresponding aldehydes currently requires a metal hydride reducing agent. The difficulty in this reaction is preventing reduction to the alcohol since the aldehyde is more actively reduced than the starting acid. A variety of borane and alane-based reagents have been developed to prevent over reduction to the alcohol, such as *t*-hexBHBBr·S(CH₃)₂ and diisobutylaluminum hydride (dibal-H). Drawbacks to these reagents include the necessity for dry reaction conditions, careful catalyst preparation, and the generation of salt waste streams. Comparatively, enzyme catalysts would not be air and water sensitive, yields a single product, and does not produce a large volume of metallic salts.

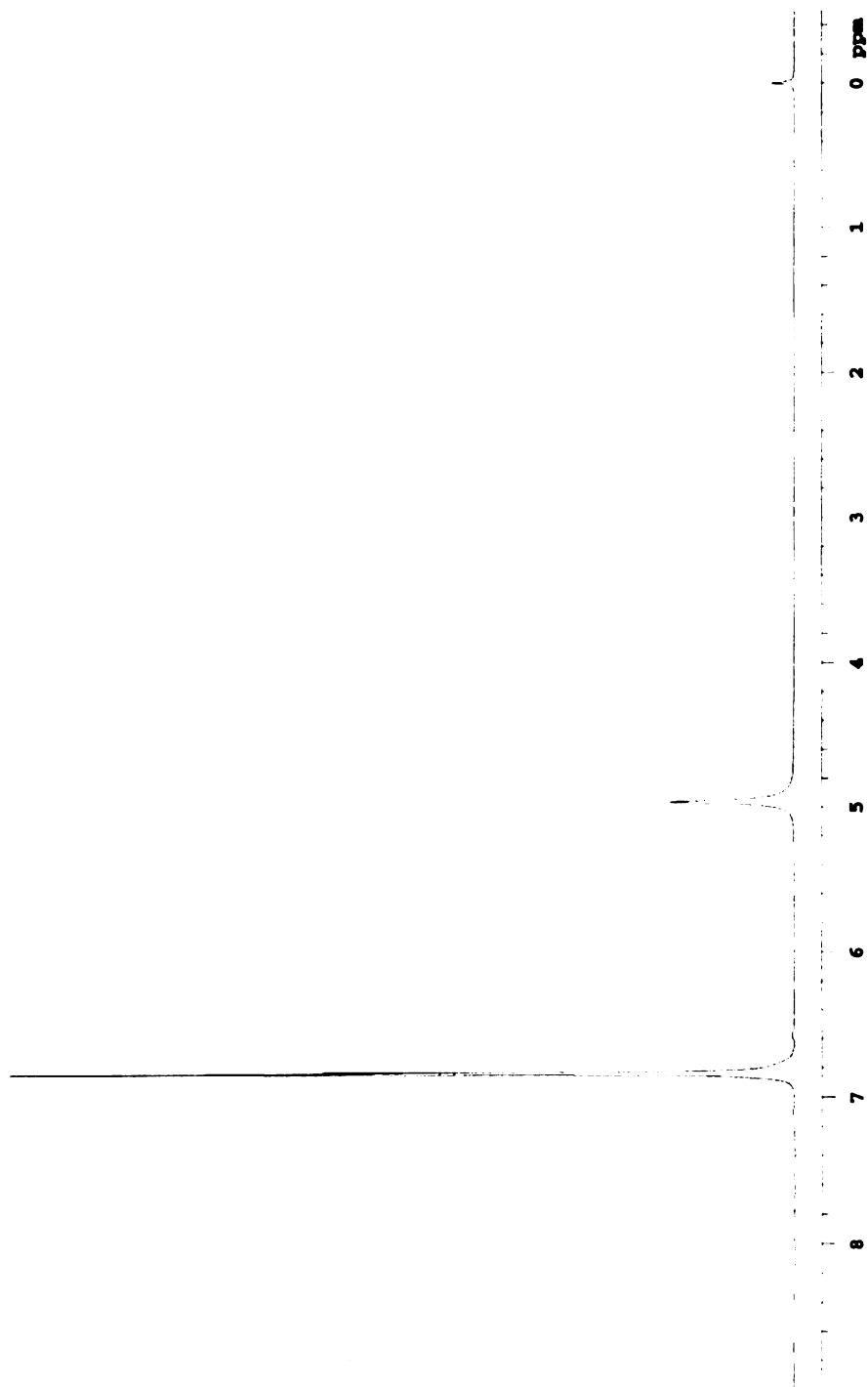


Figure 85. Control ^1H NMR of Hydroquinone. Resonances: δ 6.83 (s, 4H)

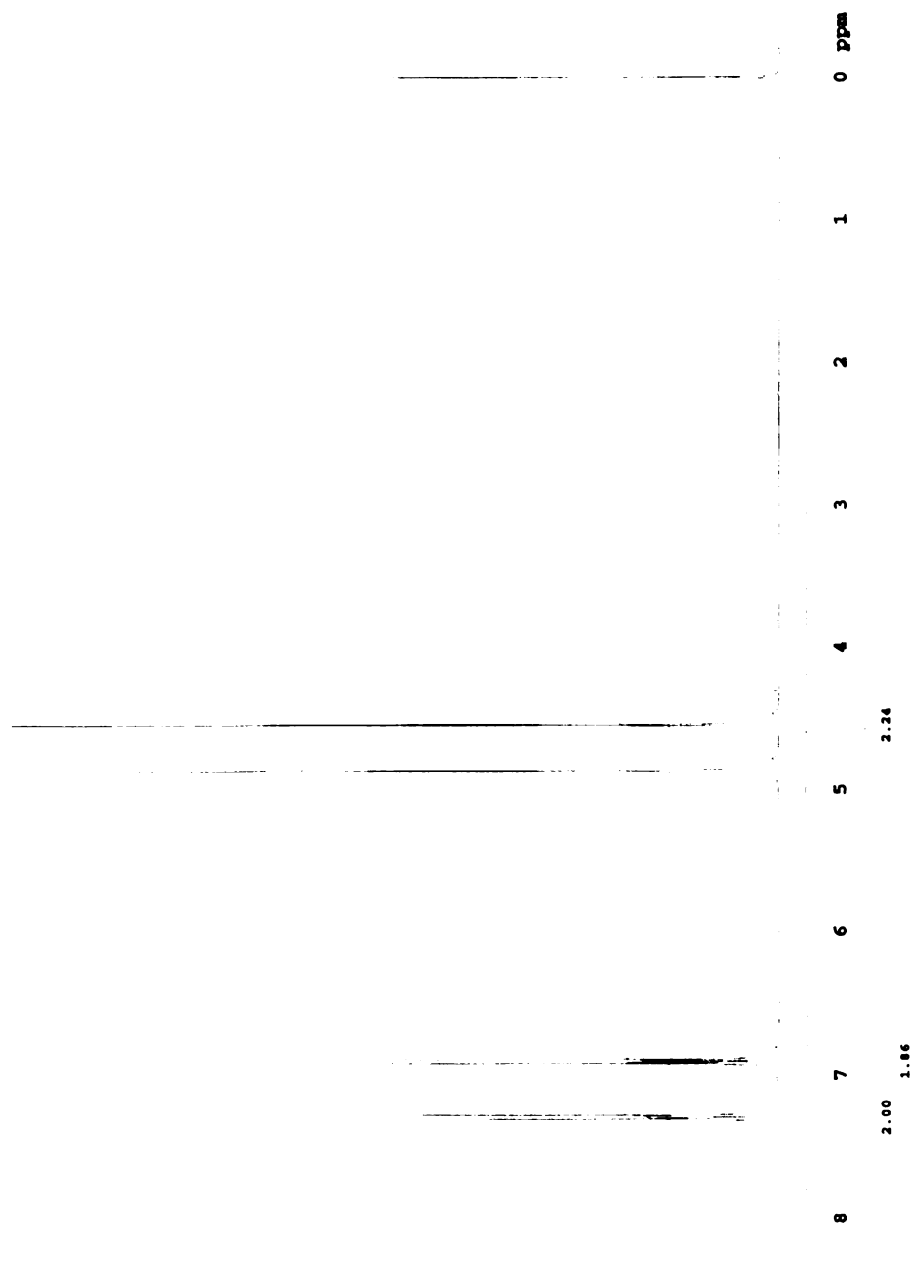


Figure 86. Control ¹H NMR of *p*-Hydroxybenzyl Alcohol. Resonances: δ 7.30 (d, 2 H), 6.91 (d, 2 H), 4.55 (s, 2 H).

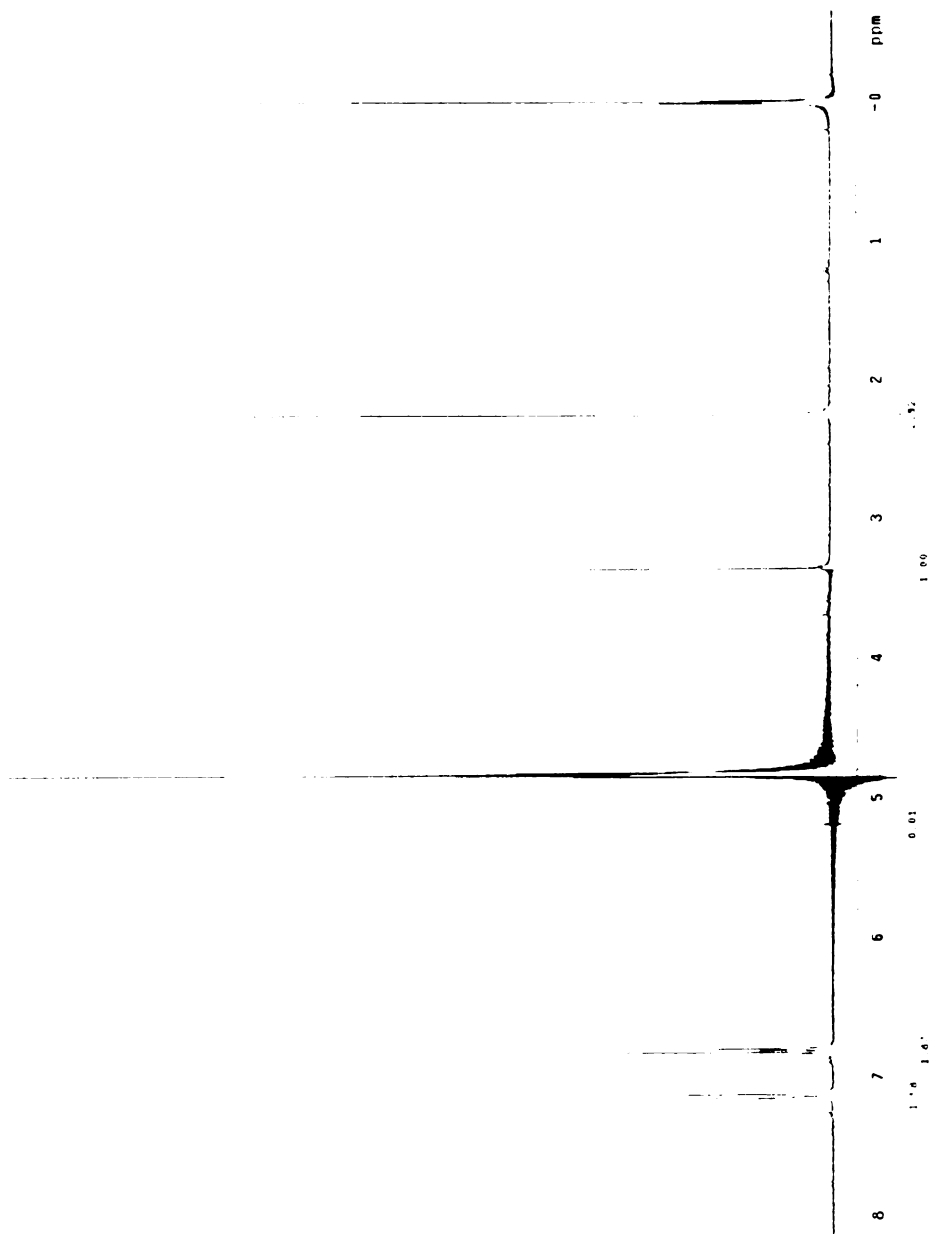


Figure 87. Control ¹H NMR of *p*-Cresol. Resonances: δ 7.15 (d, 2 H), 6.82 (d, 2 H), 2.25 (s, 3 H).

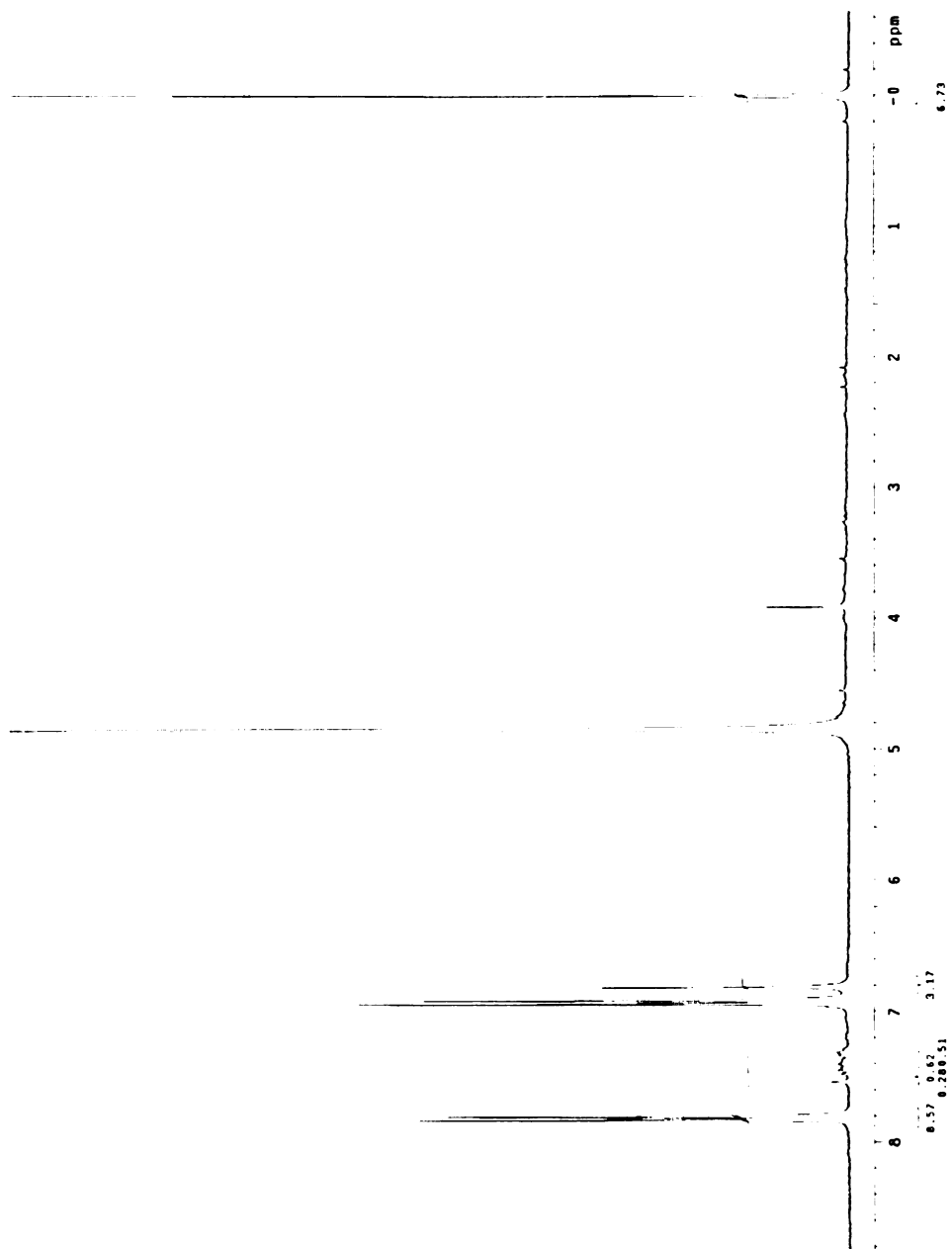


Figure 88. Typical ¹H NMR of Hydroquinone Formation with *P. chrysosporium*. Hydroquinone resonances: δ 6.83 (s, 4H).

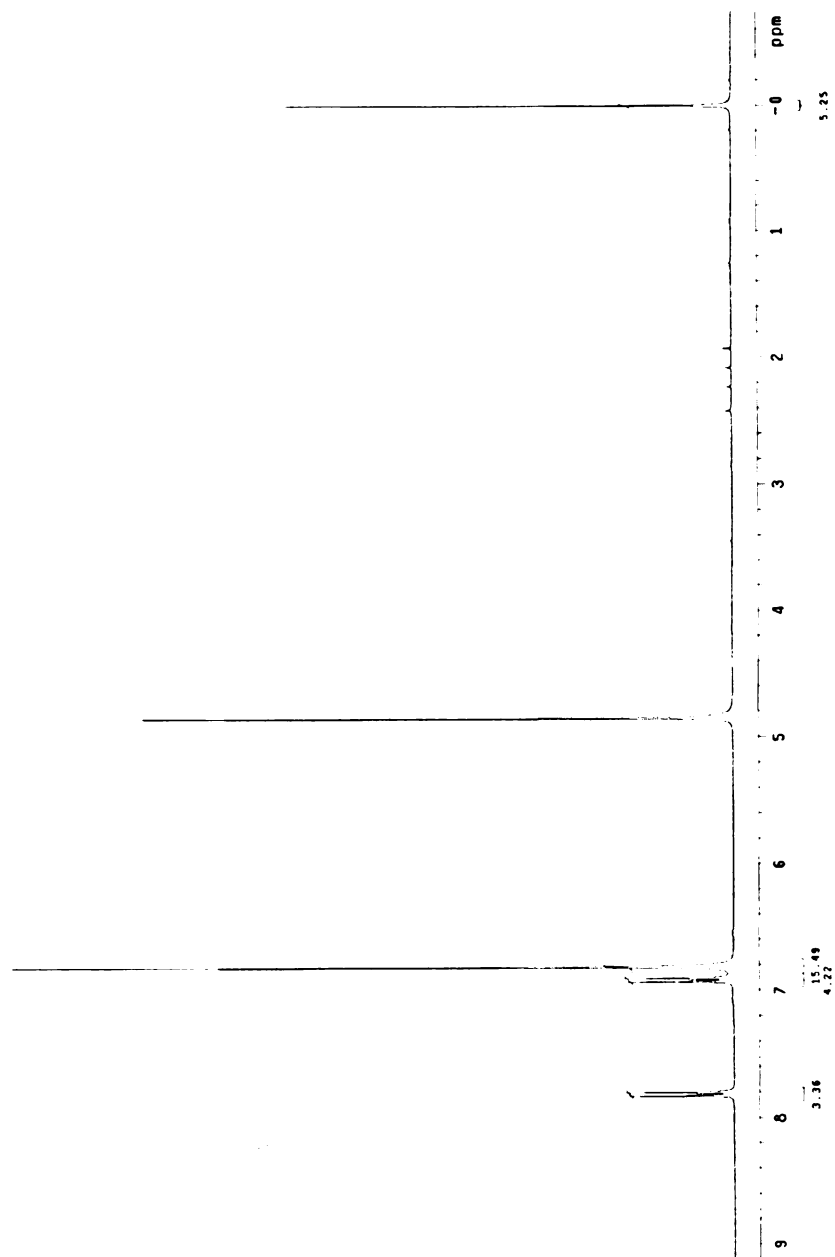


Figure 89. Typical ¹H NMR of Hydroquinone Formation with *Candida parapsilosis*. Hydroquinone resonances: δ 6.83 (s, 4H)

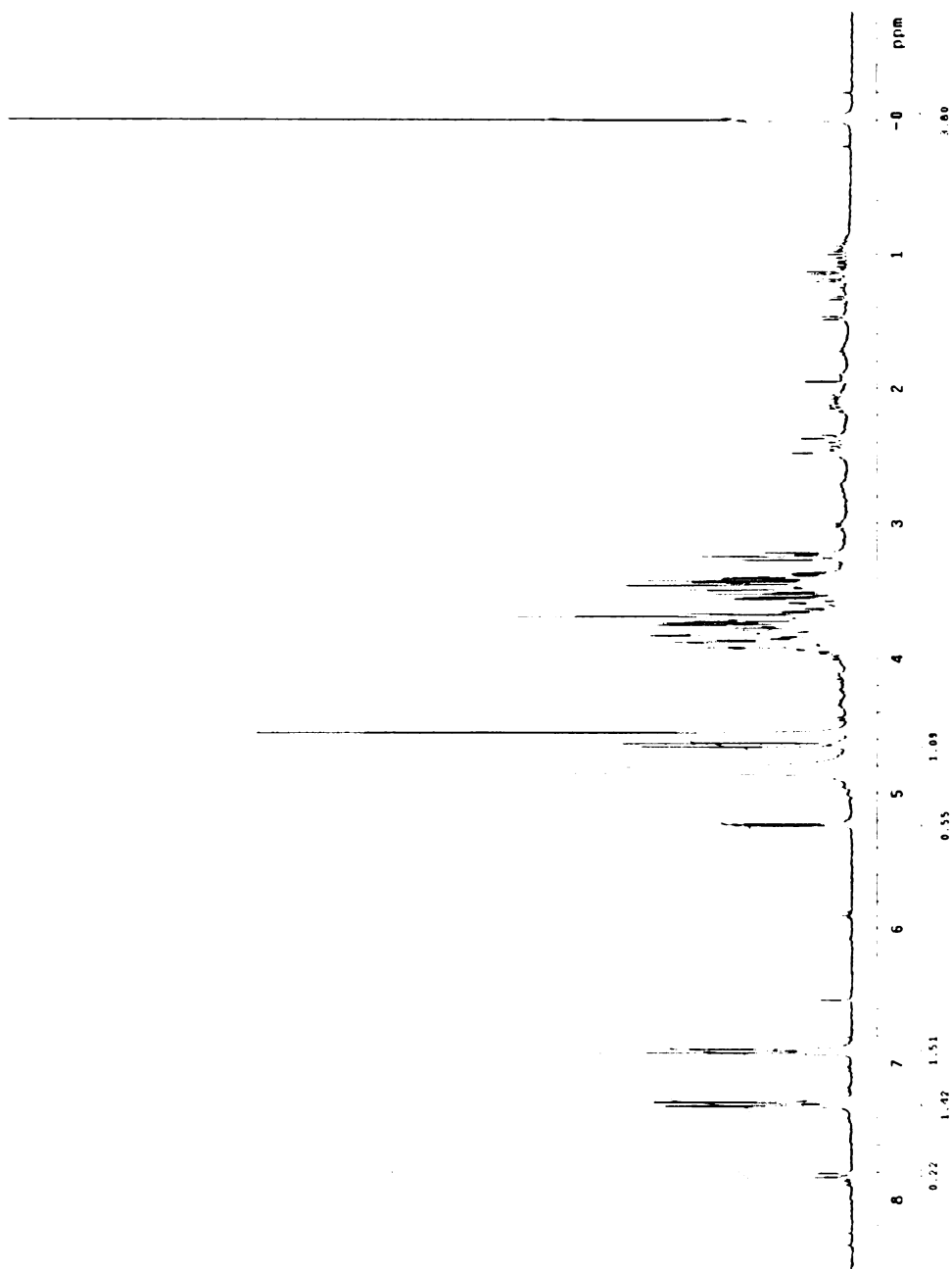


Figure 90. Typical ¹H NMR of *p*-Hydroxybenzyl Alcohol Formation with *P. chrysosporium*. PHBA resonances: δ 7.30 (d, 2 H), 6.91 (d, 2 H), 4.55 (s, 2 H).

References

-
- ¹ Kurtzman, C.P. In *Yeast: Biotechnology and Biocatalysis*, Verachtert, H.; DeMot, R., Eds.; Marcel Dekker: New York, 1990, p. 1.
- ² Roberts, S. M.; Turner, N. J.; Willetts, A. J.; Turner, M. K. In *Introduction to Biocatalysis using Enzymes and Micro-organisms*; Cambridge University Press: New York, 1995; p. 1-31.
- ³ Roberts, S. M.; Turner, N. J.; Willetts, A. J.; Turner, M. K. In *Introduction to Biocatalysis using Enzymes and Micro-organisms*; Cambridge University Press: New York, 1995; p. 1-31.
- ⁴ Csuk, R. *Chem. Rev.* **1991**, *91*, 49.
- ⁵ Stewart, J. D. *Current Opin. Biotech.* **2000**, *11*, 363.
- ⁶ (a) Ward, O.P.; Young, C. S. *Enzyme Microb. Technol.* **1990**, *12*, 482. (b) Csuk, R. *Chem. Rev.* **1991**, *91*, 49.
- ⁷ Ward, O.P.; Young, C. S. *Enzyme Microb. Technol.* **1990**, *12*, 482.
- ⁸ Krumenacker, L.; Constantini, M.; Pontal, P.; Sentenac, J. In *Kirk-Othmer Encyclopedia of Chemical Technology*, 4th ed. Kroschwitz, J. I.; Howe-Grant, M., Eds.; Wiley: New York, 1995; Vol. 13, p. 996.
- ⁹ Varagnat, J. In *Kirk-Othmer Encyclopedia of Chemical Technology*, 3rd ed.; Grayson, M., Ed.; Wiley: New Youk, 1981; Vol. 13, p. 39.
- ¹⁰ Casas, D. A.; Pitta-Alvarez, S. I.; Giulietti, A. M. *Appl. Biochem. Biotech.* **1998**, *69*, 127.
- ¹¹ (a) Krumenacker, L.; Constantini, M.; Pontal, P.; Sentenac, J. In *Kirk-Othmer Encyclopedia of Chemical Technology*, 4th ed. Kroschwitz, J. I.; Howe-Grant, M., Eds.; Wiley: New York, 1995; Vol. 13, p. 996. (b) Varagnat, J. In *Kirk-Othmer Encyclopedia of Chemical Technology*, 3rd ed.; Grayson, M., Ed.; Wiley: New Youk, 1981; Vol. 13, p. 39.
- ¹² (a) Krumenacker, L.; Constantini, M.; Pontal, P.; Sentenac, J. In *Kirk-Othmer Encyclopedia of Chemical Technology*, 4th ed.; Kroschwitz, J. I.; Howe-Grant, M., Eds.; Wiley: New York, 1995; Vol. 13, p. 996. (b) Varagnat, J. In *Kirk-Othmer Encyclopedia of Chemical Technology*, 3rd ed.; Grayson, M., Ed.; Wiley: New Youk, 1981; Vol. 13, p.

39. (c) Weissermel, K., Arpe, H.-J. In *Industrial Organic Chemistry*, 3rd ed.; VCH: New York, 1997; p 361.

13 (a) Krumenacker, L.; Constantini, M.; Pontal, P.; Sentenac, J. In *Kirk-Othmer Encyclopedia of Chemical Technology*, 4th ed.; Kroschwitz, J. I.; Howe-Grant, M., Eds.; Wiley: New York, 1995; Vol. 13, p. 996. (b) Varagnat, J. In *Kirk-Othmer Encyclopedia of Chemical Technology*, 3rd ed.; Grayson, M., Ed.; Wiley: New York, 1981; Vol. 13, p. 39. (c) Weissermel, K., Arpe, H.-J. In *Industrial Organic Chemistry*, 3rd ed.; VCH: New York, 1997; p 361.

14 Weissermel, K., Arpe, H.-J. In *Industrial Organic Chemistry*, 3rd ed.; VCH: New York, 1997; p 361.

15 (a) Krumenacker, L.; Constantini, M.; Pontal, P.; Sentenac, J. In *Kirk-Othmer Encyclopedia of Chemical Technology*, 4th ed.; Kroschwitz, J. I.; Howe-Grant, M., Eds.; Wiley: New York, 1995; Vol. 13, p. 996. (b) Varagnat, J. In *Kirk-Othmer Encyclopedia of Chemical Technology*, 3rd ed.; Grayson, M., Ed.; Wiley: New York, 1981; Vol. 13, p. 39.

16 (a) Krumenacker, L.; Constantini, M.; Pontal, P.; Sentenac, J. In *Kirk-Othmer Encyclopedia of Chemical Technology*, 4th ed.; Kroschwitz, J. I.; Howe-Grant, M., Eds.; Wiley: New York, 1995; Vol. 13, p. 996. (b) Varagnat, J. In *Kirk-Othmer Encyclopedia of Chemical Technology*, 3rd ed.; Grayson, M., Ed.; Wiley: New York, 1981; Vol. 13, p. 39. (c) Weissermel, K., Arpe, H.-J. In *Industrial Organic Chemistry*, 3rd ed.; VCH: New York, 1997; p 361.

17 Weissermel, K., Arpe, H.-J. In *Industrial Organic Chemistry*, 3rd ed.; VCH: New York, 1997; p 361.

18 Carlile, M. J.; Watkinson, S. C. *The Fungi*; Academic Press: San Diego, 1994; p 52.

19 (a) Broda, P.; Birch, P.; Brooks, P.; Copa-Patino, J. L.; Sinnott, M. L.; Tempelaars, C.; Wang, Q.; Wyatt, A.; Sims, P. *FEMS Microbiol. Rev.* **1994**, *13*, 189. Umezawa, T.; Nakatsubo, F.; Higuchi, T. *Arch. Microbiol.* **1982**, *131*, 124.

20 de Jong, E.; Field, J. A.; de Bont, J. A.; *FEMS Microbiol. Rev.* **1994**, *13*, 153.

21 (a) Kirk, T. K.; Farrell, R. L. *Ann. Rev. Microbiol.* **1987**, *41*, 465. (b) Vicuna, R. *Molecular Biotech.* **2000**, *14*, 173.

22 Kirk, T. K.; Farrell, R. L. *Ann. Rev. Microbiol.* **1987**, *41*, 465.

23 Buswell, J. *CRC Crit. Rev. Biotech.* **1987**, *6*, 1.

-
- 24 Broda, P.; Birch, P.; Brooks, P.; Sims, P. *Molecular. Microbiol.* **1996**, *19*, 923.
- 25 (a) Buswell, J. *CRC Crit. Rev. Biotech.* **1987**, *6*, 1. (b) Broda, P.; Birch, P.; Brooks, P.; Sims, P. *Molecular. Microbiol.* **1996**, *19*, 923.
- 26 Valli, K.; Gold, M. *J. Bacteriol.* **1991**, *173*, 1991. (b) Valli, K.; Brock, B.; Joshi, D.; Gold, M. *Appl. Environ. Micorbiol.* **1992**, *58*, 221.
- 27 Adler, E. *Wood Sci. Technol.* **1977**, *11*, 169.
- 28 Chen, C.-L.; Chua, M. G.S.; Evans, J. E., Chang, H.-m., Kirk, T. H. *Intern. Symp. Wood Pulping Chem.* **1981**, *3*, 75.
- 29 Ander, P.; Hatakka, A.; Eriksson, K.-E. *Arch. Microbiol.* **1980**, *125*, 189.
- 30 Buswell, J.; Ander, P.; Pettersson, B.; Eriksson, K.-E. *FEBS Lett.* **1979**, *103*, 98.
- 31 Ander, P.; Hatakka, A.; Eriksson, K.-E. *Arch. Microbiol.* **1980**, *125*, 189.
- 32 (a) Yajima, Y.; Enoki, A.; Mayfield, M.; Gold, M. *Arch. Microbiol.* **1979**, *123*, 319. (b) Buswell, J.; Ander, P.; Pettersson, B.; Eriksson, K.-E. *FEBS Lett.* **1979**, *103*, 98.
- 33 Buswell, J.; Ander, P.; Pettersson, B.; Eriksson, K.-E. *FEBS Lett.* **1979**, *103*, 98.
- 34 Buswell, J.; Eriksson, K.-E.; Pettersson, B. *J. of Chromatog.* **1981**, *215*, 99.
- 35 (a) Ander, P.; Hatakka, A.; Eriksson, K.-E. *Arch. Microbiol.* **1980**, *125*, 189. (b) Ander, P.; Eriksson, K.-E.; Yu, H.-s. *Arch. Microbiol.* **1983**, *136*, 1.
- 36 Ander, P.; Hatakka, A.; Eriksson, K.-E. *Arch. Microbiol.* **1980**, *125*, 189.
- 37 Krisnangkura, K.; Gold, M. *Phytochemistry* **1979**, *18*, 2019.
- 38 Griffin, D. H. *Fungal Physiology*; Wiley-Liss: New York, 1994; p. 4.
- 39 Griffin, D. H. *Fungal Physiology*; Wiley-Liss: New York, 1994; p. 151.
- 40 (a) Middelhoven, W. J. *Antonie van Leeuwenhoek*, **1993**, *63*, 125. (b) Karasevich, Y. N.; Ivoilov, V. S. *Microbiology* **1977**, *46*, 687. (c) Middelhoven, W. J.; Coenen, A.; Kraakman, B.; Gelpke, M. D. S. *Antonie van Leeuwenhoek* **1992**, *62*, 181.
- 41 Whitehead, D. C. *Nature* **1964**, *202*, 417.
- 42 Middelhoven, W. J. *Antonie van Leeuwenhoek*, **1993**, *63*, 125.

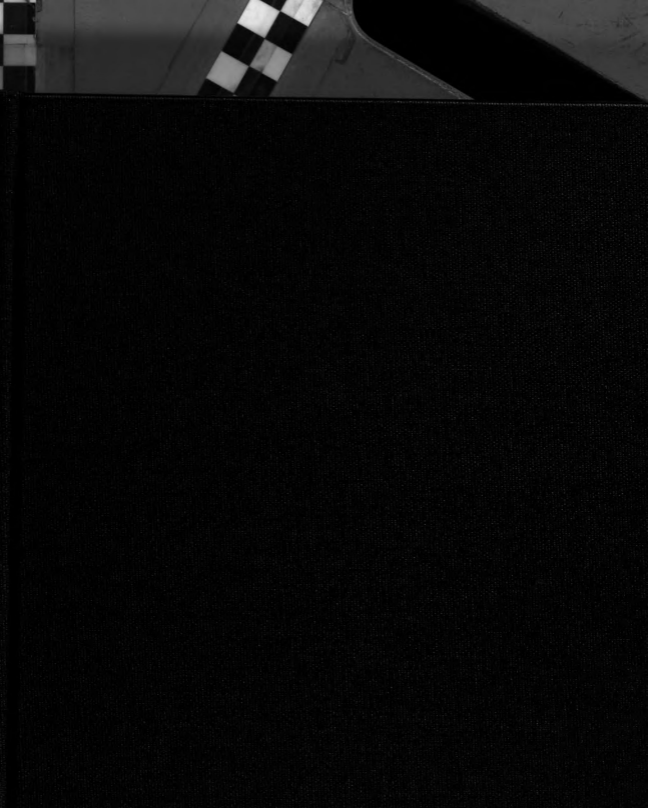
-
- 43 Eppink, M. H. M.; Boeren, S. A.; Vervoort, J.; van Berkel, W. J. H. *J. Bacteriol.* **1997**, *179*, 6680.
- 44 Seibold, B.; Matthes, M.; Eppink, M. H. M.; Lingens, F.; van Berkel, W. J. H.; Müller, R. *Eur. J. Biochem.* **1996**, *239*, 469.
- 45 Eppink, M. H. M.; Boeren, S. A.; Vervoort, J.; van Berkel, W. J. H. *J. Bacteriol.* **1997**, *179*, 6680.
- 46 (a) Eppink, M. H. M.; Boeren, S. A.; Vervoort, J.; van Berkel, W. J. H. *J. Bacteriol.* **1997**, *179*, 6680. (b) van Berkel, W. J. H.; Eppink, M. H. M.; Middelhoven, W. J.; Vervoort, J.; Rietjens, I. M. C. M. *FEMS Microbiol. Lett.* **1994**, *121*, 207.
- 47 van Berkel, W. J. H.; Eppink, M. H. M.; Middelhoven, W. J.; Vervoort, J.; Rietjens, I. M. C. M. *FEMS Microbiol. Lett.* **1994**, *121*, 207.
- 48 Eppink, M. H. M.; Boeren, S. A.; Vervoort, J.; van Berkel, W. J. H. *J. Bacteriol.* **1997**, *179*, 6680.
- 49 (a) Krumenacker, L.; Constantini, M.; Pontal, P.; Sentenac, J. In *Kirk-Othmer Encyclopedia of Chemical Technology*, 4th ed.; Kroschwitz, J. I.; Howe-Grant, M., Eds.; Wiley: New York, 1995; Vol. 13, p. 996. (b) Varagnat, J. In *Kirk-Othmer Encyclopedia of Chemical Technology*, 3rd ed.; Grayson, M., Ed.; Wiley: New York, 1981; Vol. 13, p. 39.
- 50 Weissermel, K., Arpe, H.-J. In *Industrial Organic Chemistry*, 3rd ed.; VCH: New York, 1997; p 361.
- 51 (a) Mcneil, D. In *Kirk-Othmer Encyclopedia of Chemical Technology*, 3rd ed.; Grayson, M., Ed.; Wiley: New York, 1981; Vol. 6, p. 434 (b). Weissermel, K., Arpe, H.-J. In *Industrial Organic Chemistry*, 3rd ed.; VCH: New York, 1997; p 361. (c) Lorenc, J. F.; Lambeth, G.; Scheffer, W. In *Kirk-Othmer Encyclopedia of Chemical Technology*, 4rd ed. Kroschwitz, J. I.; Howe-Grant, M., Eds.; Wiley: New York, 1995; Vol. 2, 113.
- 52 Mcneil, D. In *Kirk-Othmer Encyclopedia of Chemical Technology*, 3rd ed.; Grayson, M., Ed.; Wiley: New York, 1981; Vol. 6, p. 434
- 53 (a) Mcneil, D. In *Kirk-Othmer Encyclopedia of Chemical Technology*, 3rd ed.; Grayson, M., Ed.; Wiley: New York, 1981; Vol. 6, p. 434 (b). Weissermel, K., Arpe, H.-J. In *Industrial Organic Chemistry*, 3rd ed.; VCH: New York, 1997; p 361. (c) Lorenc, J. F.; Lambeth, G.; Scheffer, W. In *Kirk-Othmer Encyclopedia of Chemical Technology*, 4rd ed. Kroschwitz, J. I.; Howe-Grant, M., Eds.; Wiley: New York, 1995; Vol. 2, 113.

-
- ⁵⁴ (a) Mcneil, D. In *Kirk-Othmer Encyclopedia of Chemical Technology*, 3rd ed.; Grayson, M., Ed.; Wiley: New York, 1981; Vol. 6, p. 434. (b) Lorenc, J. F.; Lambeth, G.; Scheffer, W. In *Kirk-Othmer Encyclopedia of Chemical Technology*, 4rd ed. Kroschwitz, J. I.; Howe-Grant, M., Eds.; Wiley: New York, 1995; Vol. 2, 113.
- ⁵⁵ (a) Mcneil, D. In *Kirk-Othmer Encyclopedia of Chemical Technology*, 3rd ed.; Grayson, M., Ed.; Wiley: New York, 1981; Vol. 6, p. 434. (b) Lorenc, J. F.; Lambeth, G.; Scheffer, W. In *Kirk-Othmer Encyclopedia of Chemical Technology*, 4rd ed. Kroschwitz, J. I.; Howe-Grant, M., Eds.; Wiley: New York, 1995; Vol. 2, 113.
- ⁵⁶ Ander, P.; Hatakka, A.; Eriksson, K.-E. *Arch. Microbiol.* **1980**, *125*, 189.
- ⁵⁷ Muheim, A.; Waldner, R.; Sanglard, D.; Reiser, J.; Schoemaker, H. E., Leisola, M. S. *Eur. J. Biochem.* **1991**, *195*, 369.
- ⁵⁸ Hage, A.; Schoemaker, H. E.; Field, J. A. *Appl. Microbiol. Biotechnol.* **1999**, *52*, 834.
- ⁵⁹ Stentelaire, C.; Lesage-Meessen, L.; Oddou, J.; Bernard, O.; Bastin, G.; Ceccaldi, B. C.; Asther, M. *J. Biosci. Bioeng.* **2000**, *66*, 684.
- ⁶⁰ (a) Gross, G.; Bolkart, K.; Zenk, M. *Biochem. Biophys. Res. Comm.* **1968**, *32*, 173. (b) Li, T.; Rosazza, J. *Appl. Environ. Microbiol.* **2000**, *66*, 684.
- ⁶¹ Maliverney, C.; Mulhauser, M. In *Kirk-Othmer Encyclopedia of Chemical Technology*, 4rd ed. Kroschwitz, J. I.; Howe-Grant, M., Eds.; Wiley: New York, 1995; Vol. 13, 1030.
- ⁶² Zhao, Y.; Cao, Q.; Xiang, Y.; Hu, Z. *J. Chromatog. A* **1999**, *849*, 277.
- ⁶³ Suzuki, T.; Hashimura, Y.; Takeyama, S. *Drug Metabol. Disposit.* **1983**, *11*, 377.

MICHIGAN STATE LIBRARIES



3 1293 02316 3177



THESIS
4
2002

LIBRARY
Michigan State
University

**PLACE IN RETURN BOX to remove this checkout from your record.
TO AVOID FINES return on or before date due.
MAY BE RECALLED with earlier due date if requested.**

DATE DUE	DATE DUE	DATE DUE

ENVIRONMENTALLY BEGNIGN SYNTHESIS OF
AROMATIC COMPOUNDS FROM D-GLUCOSE

VOLUME II

By

Jessica L. Barker

A DISSERTATION

Submitted to
Michigan State University
in partial fulfillment of the requirements
for the degree of

DOCTOR OF PHILOSOPHY

Department of Chemistry

2001

CHAPTER FOUR

SYNTHESIS OF SHIKIMIC ACID AND PHENOL

Introduction

In this chapter, biocatalysis will be used in conjunction with environmentally benign chemistry to elaborate a synthetic route to phenol that originates from glucose. First, heterologous expression of a *Nicotiana tabacum* gene in a shikimate-synthesizing *E. coli* biocatalyst will be explored as a method to eliminate contaminating quinic acid formation. Second, the aromatization of shikimic acid under and subcritical water conditions will be examined as routes to phenol. The overall conversion of glucose to phenol via shikimic acid intermediacy (Figure 91) constitutes an alternative route to this commercially important chemical that not only is environmentally benign but is derived from a renewable, nontoxic feedstock.

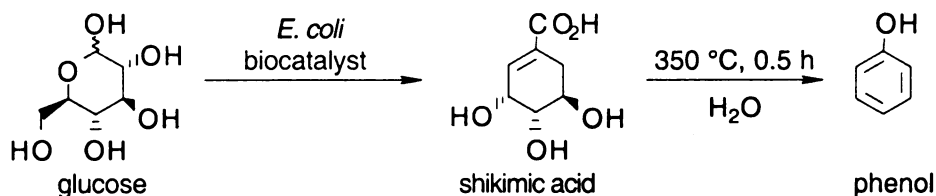


Figure 91. Environmentally Benign Synthesis of Phenol from Glucose

An illustration of a combined biocatalytic and benign chemical strategy is provided by the synthesis of 1,2,3,4-tetrahydroxybenzene from glucose (Figure 92).¹ Plasmid-based expression of the *Saccharomyces cerevisiae* *INO1* gene encoding for *myo*-inositol 1-phosphate synthase allowed for the conversion of D-glucose 6-phosphate to *myo*-inositol 1-phosphate. Following dephosphorylation by undefined phosphatase

activity, *E. coli* JWF1/pAD1.88A synthesized 21 g/L of *myo*-inositol when cultured under fed-batch fermentor conditions (Figure 92). Following isolation from the culture supernatant, *myo*-inositol was oxidized to *myo*-2-inosose by the intact bacteria *Gluconobacter oxydans* (Figure 92). *Myo*-2-inosose was then dehydrated to 1,2,3,4-tetrahydroxybenzene in refluxing aqueous H₂SO₄ (Figure 92). 1,2,3,4-Tetrahydroxybenzene has synthetic utility as the aromatic core of coenzyme Q_n, an antioxidant popular in cosmetics and vitamin supplements.

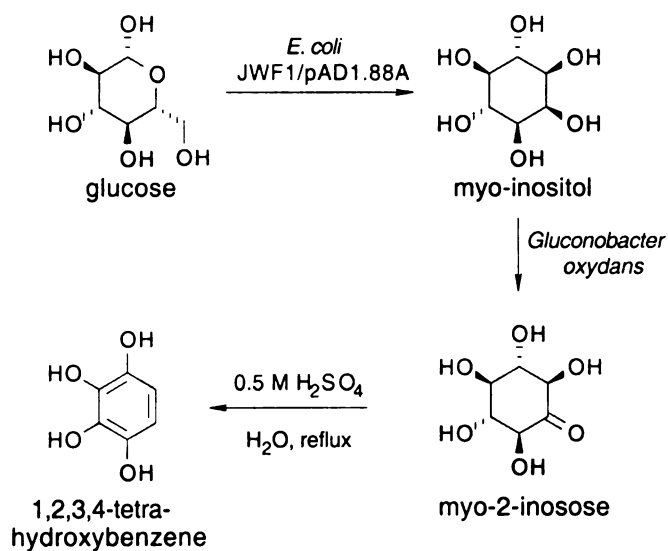


Figure 92. Environmentally Benign Synthesis of 1,2,3,4-Tetrahydroxybenzene from Glucose.

I. Shikimic Acid

A. Background

Shikimic acid is a prominent intermediate in the biosynthesis of aromatic amino acids and aromatic metabolites in plants and microorganisms. With its absolute stereochemistry confirmed by NMR studies in the 1960's, shikimic acid was the first established intermediate in the common pathway of aromatic amino acid biosynthesis, providing the alternative name of the shikimate pathway.² First isolated from the Japanese tree shikimi-no-ki (*Illicium religiosum*) by Eykmann in 1885,³ shikimic acid is still obtained from the fruit of *Illicium* plants today.⁴ With its three stereocenters, shikimic acid could be a valuable chiral synthon but its low availability has precluded its widespread use in industrial-scale syntheses.

Medicinally, shikimic acid has been found to have an analgesic effect and inhibit arterial and venous blood clots in rats.⁵ Recently, a new drug developed by Roche Pharmaceuticals and marketed under the name Tamaflu (Figure 93), gained FDA approval for treatment against influenza.⁶ Synthesis of the neuraminidase inhibitor begins with shikimic acid. A combinatorial library generated from shikimic acid is also currently being developed and screened for pharmacological activity.⁷ Therefore, the low availability and high marketability of shikimic acid has created a need for a facile synthesis capable of producing multi-ton quantities.

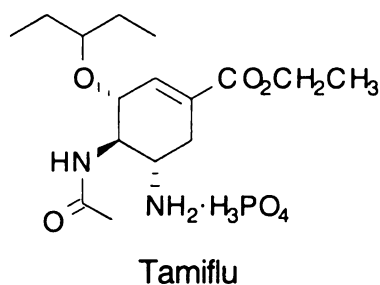


Figure 94. Structure of Tamiflu.

B. Biocatalytic Synthesis of Shikimic Acid.

Previous work by the Frost group has generated a shikimic acid-producing *E. coli* strain, SP1.1/pKD12.112 (Figure 94, Figure 95).⁸ Host strain SP1.1 was constructed from *E. coli* RB791 by insertion of *aroB* into the genomic *serA* locus and disruption of the *aroL* and *aroK* loci via P1 phage-mediated transductions of *aroL478::Tn10* and *aroK17::Cm^R*. Shikimic acid accumulates due to the absence of *aroL*- and *aroK*-encoded shikimate kinase while the second copy of *aroB* increases the catalytic activity of rate-limiting 3-dehydroquinate (DHQ) synthase. Disruption of the genomic *serA* locus provides the basis for plasmid maintenance, as described for PHB-producing JB161/pJB2.274. Plasmid pKD12.112 contains *aroF^{FBR}*-encoded DAHP synthase, *serA*-encoded phosphoglycerate dehydrogenase, and *aroE*-encoded shikimate dehydrogenase (Figure 95). Overexpression of *aroF^{FBR}* increases the flow of carbon into the common pathway while increased shikimate dehydrogenase activity compensates for this enzyme's feedback inhibition by shikimic acid.

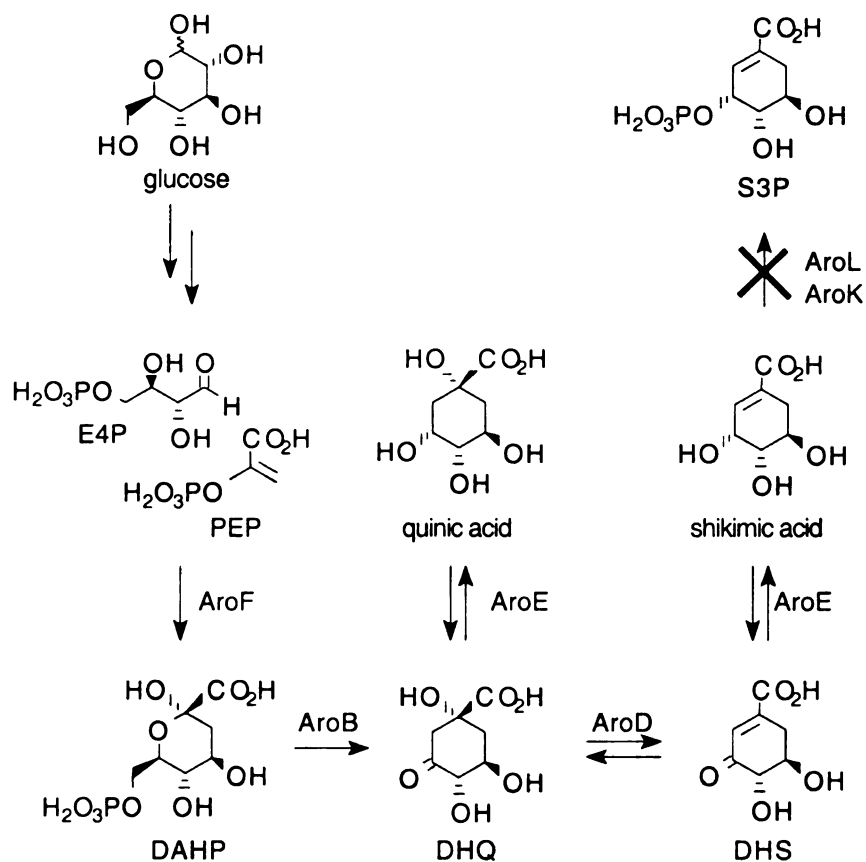


Figure 94. Biosynthesis of Shikimic Acid and Quinic Acid. Genetic loci are as follows: AroF, DAHP synthase; AroB, DHQ synthase; AroD, DHQ dehydratase; AroE, shikimate dehydrogenase; and AroL, AroK, shikimate kinase.

Surprisingly when SP1.1/pKD12.112 was cultured under fed-batch fermentation conditions, not only was 26 g/L of shikimic acid produced, but 8 g/L of quinic acid in a 3:2 molar ratio of shikimic acid and quinic acid (Table 17).⁹ It was found that *aroE*-encoded shikimate dehydrogenase, an enzyme necessary to convert 3-dehydroshikimate

(DHS) to shikimic acid, was also able to reduce (DHQ) to quinic acid (Figure 94). Further research by the Frost group has shown that as shikimic acid is synthesized by the cell and exported into the culture supernatant, the molecule is also being transported back into the cell and converted to DHQ due to the reversible nature of shikimate dehydrogenase and DHQ dehydratase.¹⁰ Reduction of DHQ by shikimate dehydrogenase followed by exportation of the resulting quinic acid into the culture supernatant leads to a rapid equilibration of the synthesized products. This equilibration not only leads to lower shikimic acid titers but complicates purification of shikimic acid from the fermentation broth.

Several strategies have been employed to prevent the equilibration of shikimic acid to quinic acid by preventing the transport of shikimic acid back into the cell. It was found that shikimic acid transport is catabolically repressed in the presence of glucose.¹¹ Increasing the proportional gain (K_C) on the fed-batch fermentor glucose feed pump control loop was used to increase the average glucose concentration during fermentations of SP1.1/pKD12.112. The molar ratio of synthesized shikimic acid to quinic acid increased from 3:1 to 12:1 resulting in 26 g/L of shikimic acid produced in 42 h (Table 17). This pulsed glucose-feeding regime was often difficult to control and lead to unregulated glucose addition necessitating the early termination of fermentation runs.

E. coli SP1.1 *serA::aroB aroL::Tn10 aroK::Cm^R*

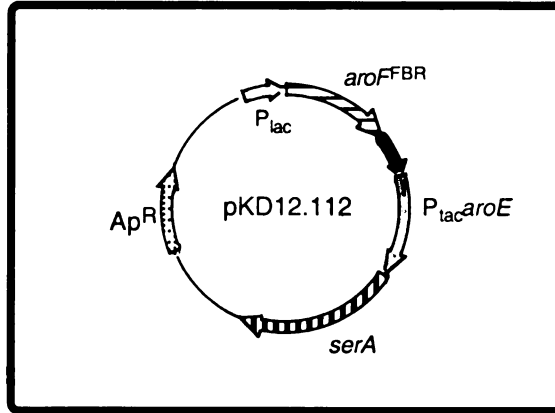


Figure 95. Shikimic Acid-Producing *E. coli* Construct SP1.1/pKD12.112. Genetic loci are as follows: *aroF^{FBR}*, feedback insensitive DAHP synthase; *aroE*, shikimate dehydrogenase; and *serA*, phosphoglycerate dehydrogenase.

E. coli SP1.1 *serA::aroB aroL::Tn10 aroK::Cm^R*

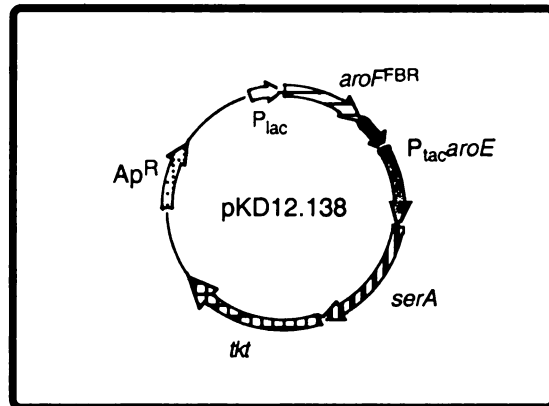


Figure 96. Shikimic Acid-Producing *E. coli* Construct SP1.1/pKD12.138. Genetic loci are as follows: *aroF^{FBR}*, feedback insensitive DAHP synthase; *aroE*, shikimate dehydrogenase; *serA*, phosphoglycerate dehydrogenase; *tkt*, transketolase

Table 17. Titrers and Yields of Shikimic Acid and Titrers of Accumulated Metabolites.

Construct	time ^b	SA ^{ac}	QA ^{ac}	DHS ^{ac}	% yield ^d	SA:QA ^e
SP1.1/pKD12.112	48	26	8.1	6.5	13	3:1
SP1.1/pKD12.112 w/ high average [glucose] ^f	42	14	1.2	4.6	10	12:1
SP1.1/pKD12.138	48	28	19	11	14	2:1
SP1.1/pKD12.138 w/ 1 mM MGP ^a	48	35	2.8	8.8	19	14:1
SP1.1shiA::Kan ^R /pKD12.138	48	23	22	9.6	13	1:1
JB4/pJB5.291at 33 °C	66	30	5.0	5.6	12	8:1
JB4/pJB5.291at 36 °C	66	34	1.3	6.6	15	30:1

^aAbbreviations: SA, shikimic acid; QA, quinic acid; DHS, 3-dehydroshikimic acid, and MGP, methyl- α -D-glucopyranoside. ^bh. ^cg/L. ^d mol SA/mol glucose. ^emol SA:mol QA. ^fhigh average glucose concentration due to high proportional gain on glucose feed pump.

An alternative to this method was to use a non-metabolizable, non-hydrolyzable analog of glucose to mimic the catabolic repression of shikimate transport. The inability of *E. coli* to catabolize methyl- α -D-glucopyranoside (MGP) and its structural similarity to glucose made it an ideal choice for use as a catabolic repressor. Addition of 1 mM MGP to fed-batch fermentations of SP1.1/pKD12.112 led to the synthesis of 27 g/L of shikimic acid and unquantifiable amounts of quinic acid (Table 17).¹² Inclusion of *tktA*-encoded transketolase on plasmid pKD12.138 (Figure 96) and transformation into SP1.1 yielded even higher titers of shikimic acid when cultured under fed-batch fermentation conditions. In the presence of 1 mM MGP, SP1.1/pKD12.138 synthesized 35 g/L of shikimic acid in a 14:1 molar ratio with quinic acid (Table 17).

Another method explored to prevent the equilibration of shikimic acid to quinic acid was to create a shikimate-producing strain that lacked the protein responsible for shikimic acid transport. This protein, encoded by the *shiA* gene, was recently identified and the gene was cloned by Pittard.¹³ P1 phage-mediated transduction of *shiA::kan^R* into *E. coli* SP1.1 created host strain SP1.1*shiA::Kan^R* which appeared to be deficient in shikimic acid transport using ¹⁴C-labeled shikimic acid uptake experiments.¹⁴ However, when SP1.1*shiA::Kan^R*/pKD12.138 was cultured under fed-batch fermentation conditions, 23 g/L of shikimic acid and 22 g/L of quinic acid were synthesized in a 1:1 molar ratio (Table 17).¹⁵ This experiment suggests that other proteins may mediate the import of extracellular shikimic acid.

C. *N. tabacum* DHQ dehydratase/Shikimate Dehydrogenase.

In this chapter, a different approach will be taken to prevent the equilibration of shikimic acid to quinic acid. While the previously discussed methods looked at only preventing the transport of shikimic acid, the strategy examined here looks to prevent the non-reversible conversion of DHQ to quinic acid by the heterologous expression of the *Nicotiana tabacum* shikimate dehydrogenase enzyme. In higher plants, such as tobacco and peas, the shikimate dehydrogenase domain is part of a single protein coupled with the DHQ dehydratase domain.¹⁶ It has been postulated that these two enzyme activities are part of a single protein to prevent the release of DHS into the intracellular environment where it could be converted to other aromatic metabolites, such as gallic acid, thus constituting a drain of carbon from the common pathway. The cDNA encoding the bifunctional AroD·AroE protein for *Nicotiana tabacum* was cloned and labeled SP3 by Bonner.¹⁷ It was hypothesized that by expressing the SP3 locus in a shikimate-producing strain deficient in native DHQ dehydratase and shikimate dehydrogenase activities, DHQ would be selectively channeled into shikimic acid formation by the bifunctional enzyme thereby preventing its reduction to quinic acid.

D. Preparation of *E. coli* JB4/pJB5.291.

Preparation of the *E. coli* JB4.

To create a shikimate-producing strain utilizing the tobacco SP3 locus, not only should shikimate kinase activity be absent, but the native DHQ dehydratase and

shikimate dehydrogenase activities should be eliminated to prevent competition between the monofunctional and bifunctional enzymes. Strain construction began with *E. coli* KL3 (Figure 97), a host previously used for the production of DHS.¹⁸ KL3 lacks shikimate dehydrogenase activity due to a mutation in the *aroE* locus and contains an additional genomic copy of *aroB* in the *serA* locus. Disruption of the genomic *serA* locus again provides a convenient method of plasmid maintenance by inclusion of *serA* on the desired plasmid while the additional AroB activity eliminates the rate-limitations caused by DHQ synthase thereby preventing accumulation of its substrate, 3-deoxy-D-arabino-heptulosonic acid 7-phosphate.

Conversion of KL3 from a DHS producing-strain to a shikimate-producing strain began with successive P1 phage-mediated transductions of *aroK17::Cm^R* and *aroL478::Tn10* to create *KL3aroK⁻aroL⁻*. (Figure 97). Elimination of DHQ dehydratase activity was accomplished by introduction of a *Tn10* mutation into the *aroD* locus via P1 phage-mediated transduction of *aroD25::Tn10*. However, selection for the desired *aroD* mutant is dependant on a colony that is *Tc^R* in a background of *Tc^S* colonies. The introduction of a *Tn10* mutation into the *aroL* locus imparts *Tc^R* to *KL3aroK⁻aroL⁻*. Therefore, *KL3aroK⁻aroL⁻* had to first be made sensitive to Tc while still leaving the *aroL*-encoded shikimate kinase activity disabled.

Spontaneous recombination events that result in excision of the *Tn10* insertion are known to disrupt the surrounding DNA leaving a non-functional gene.¹⁹ A standard technique that employs D-cycloserine was used to select for colonies that had lost the *Tn10* insertion from the *aroL* locus. Therefore, *KL3aroK⁻aroL⁻* was successively grown in LB medium without Tc, LB medium containing Tc, and LB medium containing Tc and

D-cycloserine. Growth in LB medium lacking Tc allows for the excision of *Tn10*. Tc is added to the medium to induce expression of the Tc^R protein and the addition of D-cycloserine enriches the culture in the desired strain as it is toxic only to cells expressing the Tc^R protein. After two cycles of growth in the presence of D-cycloserine, cells were plated on LB/Cm plates. Replicate plating of the resulting colonies showed approximately 10% to be Tc^S .

One of these colonies, named *KL3aroK⁻aroL-Tc^S* (Figure 97), was treated with P1 phage that had been generated from *E. coli* CL451²⁰, a strain containing the *aroD25::Tn10* allele. To ensure that shikimate kinase activity was still absent, the resulting colonies were screened on multiple plates to select for the correct phenotype. One candidate, *E. coli* JB4 (Figure 97), was isolated based on the following growth characteristics: no growth on M9 containing serine, no growth on M9 containing serine and shikimic acid, growth on M9 containing serine, aromatic amino acids, and aromatic vitamins, growth on LB containing Cm, growth on LB containing Cm and Tc.

Preparation of Plasmid pJB5.291.

The *aroD-aroE* cDNA clone, labeled SP3, was liberated from the pBluescript-based plasmid provided by Prof. Bonner by digestion with *EcoRI*. The 1.9-kb fragment was subsequently ligated to plasmid pKK223-3 that was previously digested with *EcoRI* to create the 6.5-kb plasmid pJB5.272A (Figure 98). The *aroD-aroE* gene is transcribed in the same orientation as the *tac* promoter in pKK223-3. Plasmid pJB3.141 was constructed by removing the *XbaI*-terminated *aroF^{FBR}* insert from pKL4.130B. Plasmid pKL4.130B, which contains two inserts of *aroF^{FBR}*, and single copies of *serA* and *tktA*,

was digested with *Xba*I and the 7.6-kb fragment corresponding to the linearized plasmid was isolated from an agarose gel. Re-ligation of the isolated DNA afforded the 7.6-kb plasmid pJB3.141 (Figure 99).

Plasmid pJB4.291 was obtained by ligating the 2.2 kb *P_{tac}*SP3 locus into pJB3.141. The *P_{tac}*SP3 fragment was liberated from plasmid pJB5.272A by digestion with treated with Klenow fragment. Plasmid pJB3.141 was digested with *Nco*I and treated with Klenow fragment. Subsequent ligation of the blunt fragments afforded the 8.9-kb plasmid pJB5.291 (Figure 100). The *P_{tac}*SP3 locus transcribed in the same direction as *aroF^{FBR}*, *serA*, and *tktA*.

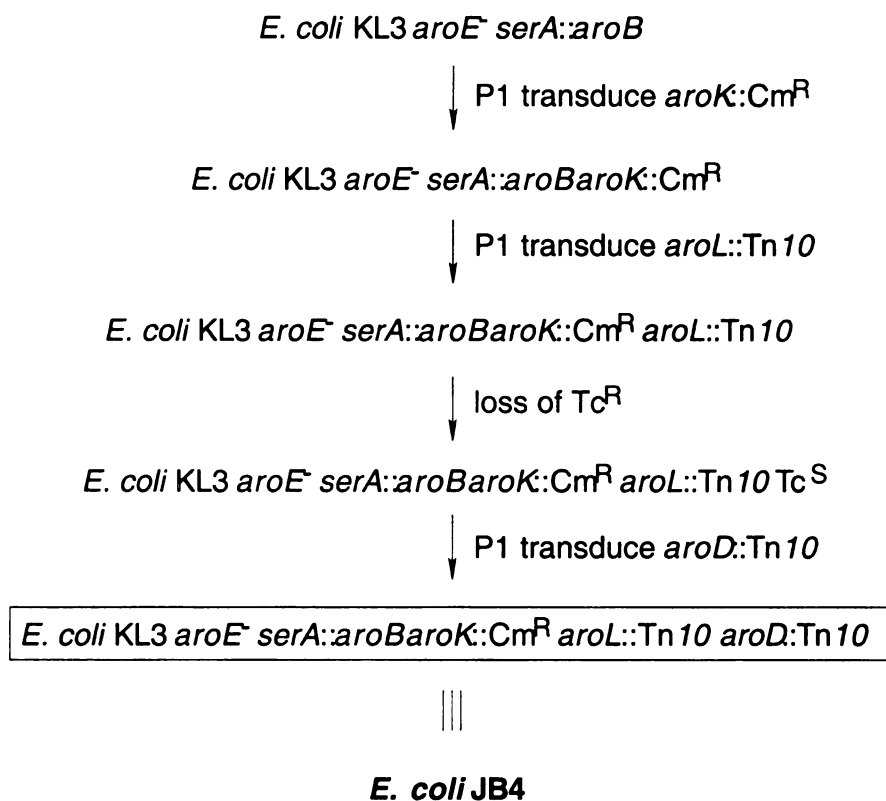


Figure 97. Preparation of JB4.

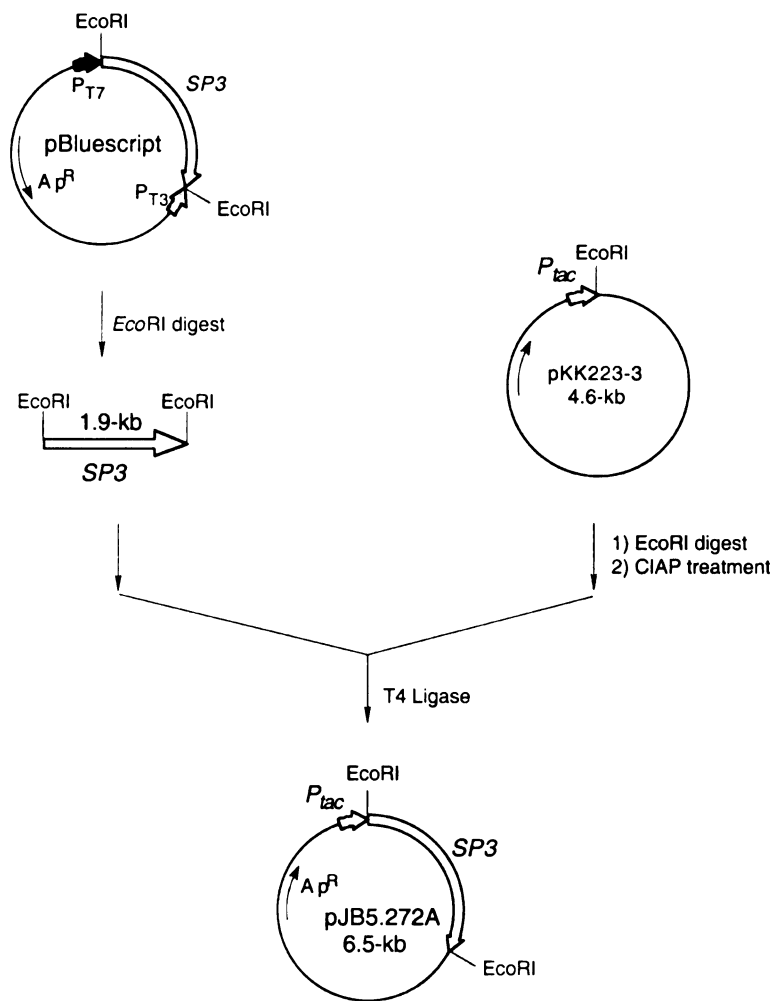


Figure 98. Preparation of Plasmid pJB5.272A.

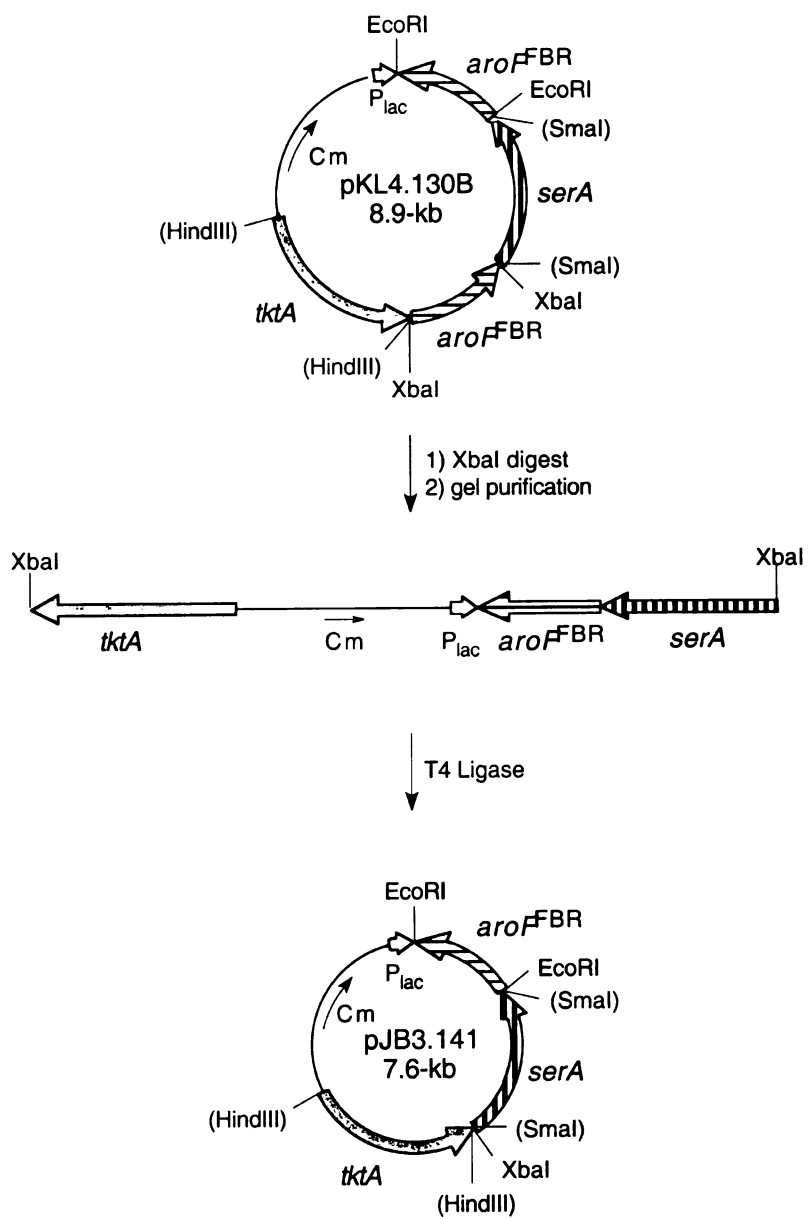


Figure 99. Preparation of Plasmid pJB3.141.

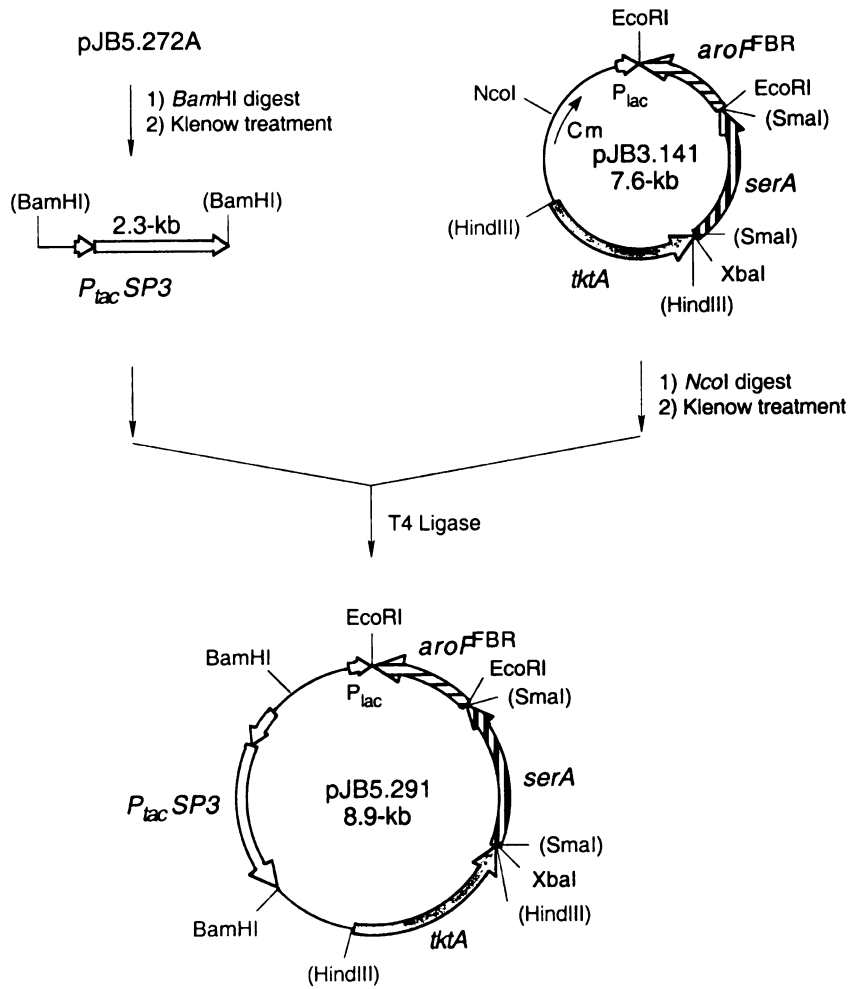


Figure 100. Preparation of Plasmid pJB5.291

E. Fed-Batch Fermentation of JB4/pJB5.291.

Metabolite Accumulation

Cultivation of JB4/pJB5.291, which was constructed to replace native DHQ dehydratase and shikimate dehydrogenase activities with the tobacco bifunctional enzyme, under similar fed-batch fermentation conditions as SP1.1/pKD12.138,²¹ notably 33 °C and 10% air saturation, synthesized 30 g/L of shikimic acid in 12% yield (mol/mol) from glucose (Figure 101, Table 17) after 66 h. Compared to SP1.1/pKD12.138 (Table 17), JB4/pJB5.291 not only synthesized more shikimic acid but less quinic acid, resulting in an increased molar ratio of shikimic acid to quinic acid of 8:1. Similar concentrations of DHS accumulated in the culture supernatants of both SP1.1/pKD12.138 and JB4/pJB5.291 (Table 17).

It was noticed however, that JB4/pJB5.291 grew slower relative to SP1.1/pKD12.138 at 33 °C. JB4/pJB5.291 was therefore cultured under fed-batch fermentation conditions at 36 °C for 66 h. At the higher temperature, JB4/pJB5.291 synthesized 34 g/L of shikimic acid in a 15% (mol/mol) yield from glucose (Figure 102, Table 17). Compared to 33 °C, JB4/pJB5.291 grown at 36 °C synthesized less quinic acid resulting in a molar ratio of shikimic acid to quinic acid of 30:1 (Table 17). Similar concentrations of DHS were synthesized whether JB4/pJB5.291 was grown at 33 °C or 36 °C (Table 17).

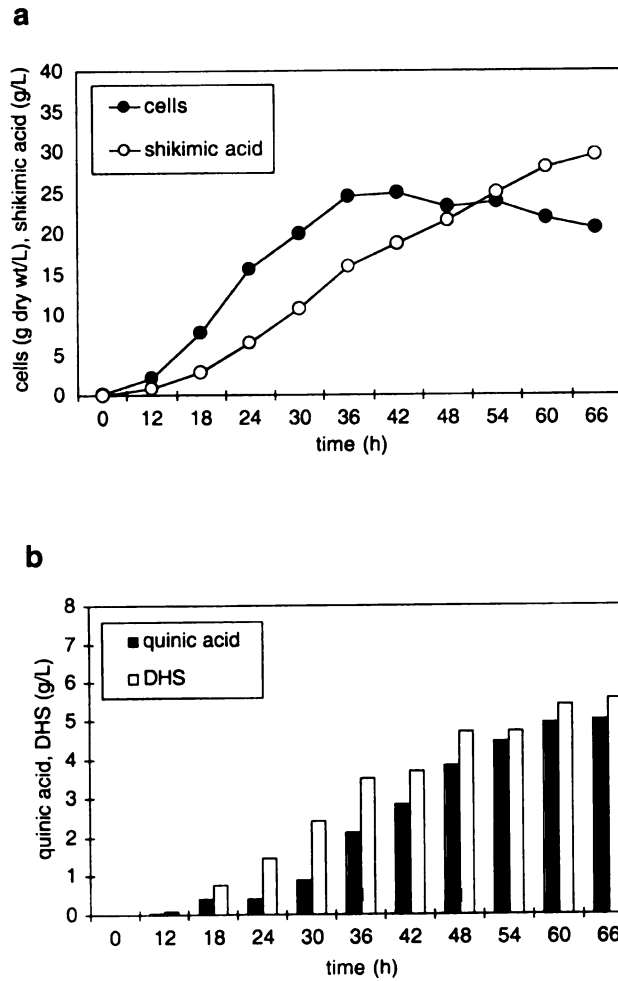
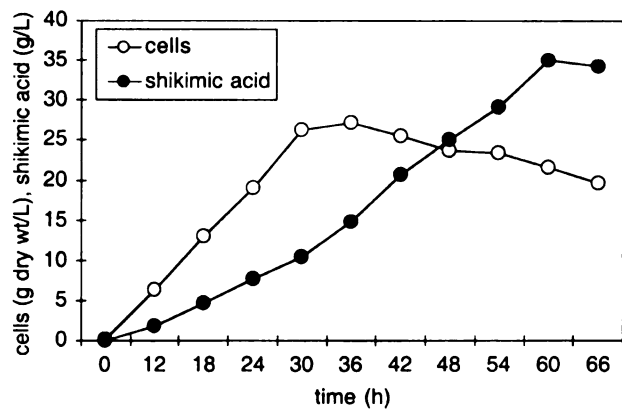


Figure 101. JB4/pJB5.291 at 33 °C. (a) cell growth, shikimic acid. (b) quinic acid, 3-dehydroshikimate.

a



b

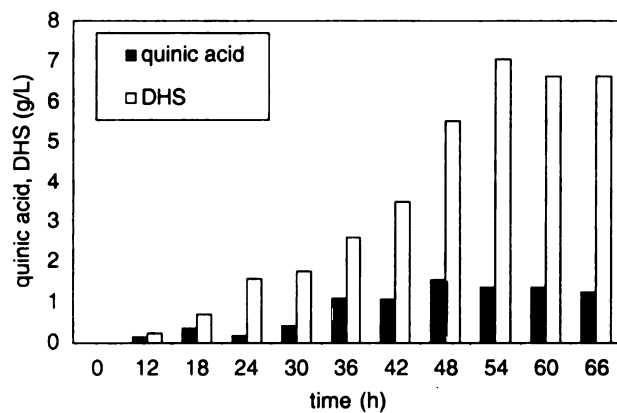


Figure 102. JB4/pJB5.291 at 36 °C. (a) cell growth, shikimic acid. (b) quinic acid, 3-dehydroshikimate.

DAHP Synthase and Shikimate Dehydrogenase Specific Activities

DAHP synthase activities were quantified over the course of the fermentations and the specific activities were determined using a standard literature technique.²² Shikimate dehydrogenase was also quantified over the course of the fermentations as a measure of the bifunctional enzyme's catalytic ability. Specific activities were measured by monitoring the formation of NADPH at 340 nm associated with the oxidation of shikimic acid to DHS catalyzed by the reversible shikimate dehydrogenase portion of the bifunctional tobacco enzyme. The DAHP synthase and shikimate dehydrogenase specific activities measured for JB4/pJB5.291 did not significantly vary when cells were cultured at 36 °C versus 33 °C although both the shikimic acid titer and ratio to quinic acid improved at the higher temperature (Table 18). Compared to SP1.1/pKD12.138,²³ the specific activities measured for shikimate dehydrogenase in JB4/pJB5.291 were slightly lower (Table 18). This lower activity did not appear to have any adverse effects as the concentration of DHS did not increase and DHQ, the initial substrate of the bifunctional enzyme, was absent from the culture supernatant of JB4/pJB5.291 (Table 17). DAHP synthase activities were 6-fold to 23-fold lower for JB4/pJB5.291 cultured at 36 °C than the activities measured for SP1.1/pKD12.138 (Table 18)²⁴. Despite the significant drop in DAHP synthase activities in JB4/pJB5.291, the quantity of shikimic acid and DHS remained comparable to quantities synthesized by SP1.1/pKD12/138 (Table 17)

Table 18. Enzyme Activities for Shikimic Acid Producing Constructs. (a) DAHP synthase Specific Activities. (b) Shikimate Dehydrogenase Specific Activities ($\mu\text{mol}/\text{min}/\text{mg}$).

a

time (h)	construct		
	SP1.1/ pKD12.138	JB4/ pJB5.291	JB4/ pJB5.291
	33 °C	33 °C	36 °C
12	0.44	—	—
18	—	0.12	0.078
24	1.2	—	—
30	—	—	0.052
36	0.55	0.061	—
48	0.67	0.051	0.041
66	—	0.049	0.056

b

time (h)	construct		
	SP1.1/ pKD12.138	JB4/ pJB5.291	JB4/ pJB5.291
	33 °C	33 °C	36 °C
12	1.2	—	—
18	—	1.6	0.81
24	2.2	—	—
30	—	—	1.1
36	2.4	1.4	—
48	2.8	1.2	1.1
66	—	1.2	1.2

F. Can the Tobacco DHQ Dehydratase/Shikimate Dehydrogenase
Catalyze Quinic Acid Formation?

Since the tobacco DHQ dehydratase/shikimate dehydrogenase enzyme appears to disfavor the formation of quinic acid when JB4/pJB5.291 was cultured at 36 °C under fed-batch fermentation conditions, an experiment was done to see if the bifunctional enzyme would catalyze the formation of quinic acid in vitro when given DHQ as substrate. A colony of *E. coli* KL3 $aroD^-$ /pJB5.272A was inoculated into 500 mL of LB containing Amp and grown at 37 °C and 250 rpm. Host strain KL3 $aroD^-$ was prepared by P1 phage-mediated transduction of the *aroD25::Tn10* into *E. coli* KL3, a strain auxotrophic in native shikimate dehydrogenase activity. Plasmid pJB5.272A contains the SP3 locus located behind a *tac* promoter. After 18 h of growth, the cells were harvested and resuspended in 100 mM K₂HPO₄ buffer, pH 7.5. Cell membranes were disrupted by passage through a French press and the clarified cellular lysate was obtained following centrifugation. A portion of the cellular lysate (1 mL) was combined with DHQ (25 mM) and NADPH (25 mM) in a final volume of 5 mL of 100 mM K₂HPO₄, pH 7.5, and incubated at 30 °C for 6 h with agitation.

To prepare the reaction mixture for ¹H NMR analysis, the protein was first precipitated by the addition of H₂SO₄. Following centrifugation to remove the precipitated protein, the reaction mixture was passed through a small column of Dowex 50 (H⁺ form) to remove NADP⁺. The column was washed with water and the combined eluents from the cation exchange column were combined with activated carbon to remove any remaining nicotinamide co-factor. After vigorous stirring, the activated carbon was

removed by filtration. The pH of the filtrate was raised to 6.5 with NaOH and evaporated to dryness using rotary evaporation. The residue was redissolved in D₂O, evaporated to dryness a second time, and redissolved in D₂O containing TSP. ¹H NMR (Figure 120) analysis of the sample showed the presence of unreacted DHQ and along with shikimic acid, DHS, and a trace of quinic acid. Shikimic acid was the major product formed as the shikimic acid:DHS:quinic acid ratio was 54:6:1 based on integrated areas of their corresponding resonances.

G. Feedback Inhibition of the Tobacco DHQ dehydratase/Shikimate Dehydrogenase.

Besides reducing the formation of quinic acid, it was hoped that replacement of the native *E.coli* DHQ dehydratase and shikimate dehydrogenase activities by the tobacco SP3 locus would reduce the concentration of DHS synthesized by JB4/pJB5.291 relative to the concentration synthesized by SP1.1/pKD12.138. JB4/pJB5.291 when cultured at 36 °C and SP1.1/pKD12.138 synthesized the almost the same amount, 6.6 g/L and 6.5 g/L respectively (Table 17). It is known that SP1.1/pKD12.138 accumulates DHS, despite significant over-expression of *aroE*, due to feedback inhibition of shikimate dehydrogenase by shikimic acid.²⁵ Alternatively, feedback inhibition of tobacco shikimate dehydrogenase by any of the common pathway intermediates has not been reported and so the accumulation of significant quantities of DHS in the culture supernatant of JB4/pJB5.291 was surprising. Therefore, the percent inhibition of the tobacco bifunctional enzyme was measured with increasing concentrations of shikimate given DHQ as the substrate.

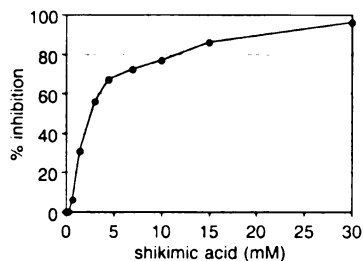


Figure 103. Percent Inhibition of Shikimate Dehydrogenase Specific Activity by Shikimic Acid.

Inhibition of the tobacco DHQ synthase/shikimate dehydrogenase, encoded by the SP3 locus, when given DHQ as substrate was found to increase with increasing levels of shikimate (Figure 103), eventually approaching 96% inhibition in the presence of 30 mM shikimic acid. Since the percent inhibition of the tobacco bifunctional enzyme was very similar to what had previously been measured for *E. coli* shikimate dehydrogenase, experiments were performed with crude cellular lysate from KL3*aroD*-/pJB5.272A to determine the type and extent of product inhibition. Kinetic studies performed at room temperature initially showed the shikimate dehydrogenase portion of the tobacco bifunctional enzyme to have a K_M of 83 μM and a V_{MAX} of 0.67 $\mu\text{mol}/\text{min}$ for DHS (Figure 104). The kinetics of the enzyme as a whole was measured with DHQ as the substrate to give a K_M of 144 μM and a V_{MAX} of 0.14 $\mu\text{mol}/\text{min}$ (Figure 107). Inhibition kinetics were measured on the shikimate dehydrogenase portion of the enzyme using NADPH concentrations equivalent to 2.4 times the K_M and DHS concentrations ranging from 0.9 to 6 times the K_M . Shikimic acid was found to be a product inhibitor exhibiting

competitive inhibition (Figure 106) and a K_i of 1 mM (Figure 105). This is the first reported K_i for the tobacco DHQ dehydratase/shikimate dehydrogenase enzyme.

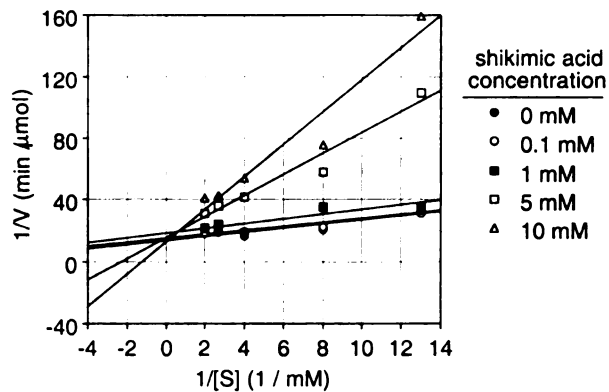


Figure 104. Lineweaver-Burk Plot of SP3 Inhibition by Product Shikimate with DHS Substrate.

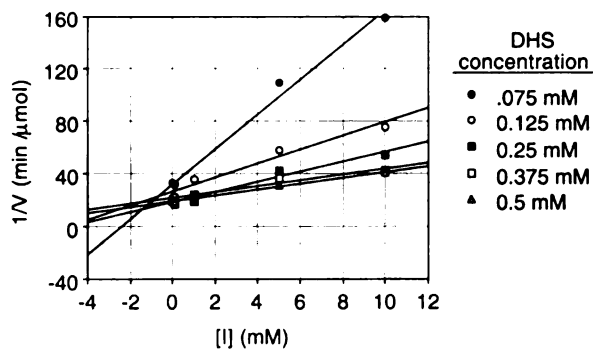


Figure 105. Dixon Plot of SP3 Inhibition by Product Shikimate with DHS Substrate.

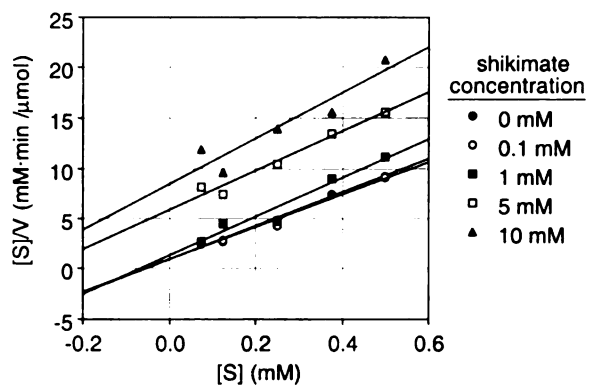


Figure 106. Hanes-Woolf Plot of SP3 Inhibition by Product Shikimate with DHS

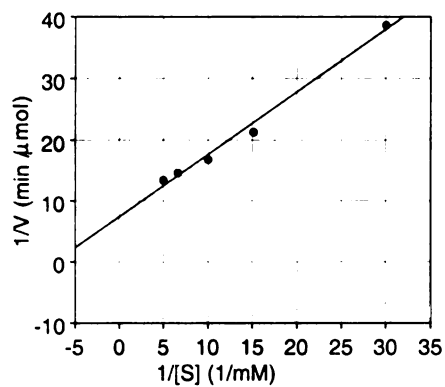


Figure 107. Determination of K_M and V_{MAX} for SP3 with DHQ as Substrate.

II. Conversion of Shikimic Acid to Phenol.

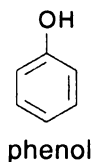


Figure 108. Structure of Phenol.

Introduction.

Phenol (Figure 108) was first recovered from distillation of coal tar in 1834. Known then as carbolic acid, phenol had limited application as a wood preservative and disinfectant.²⁶ It wasn't until the introduction of phenolic resins such as Bakelite, a condensation polymer of phenol and formaldehyde, around the turn of the century that a strong market demand developed. It wasn't until World War I that a synthetic route to phenol displaced its isolation from coal tar. However, processes such as the hydrolysis of benzene sulfonic acid and chlorobenzene were uneconomical due to the high cost of starting materials and the generation of salt wastes. In the 1950's the Hock process of cumene oxidation made phenol production economical because for every kilogram of phenol produced 0.62 kg of acetone is also synthesized.²⁷ Today, over 90% of the 5×10^9 kg of phenol produced annually is synthesized via the Hock process, making phenol the second largest volume chemical derived from benzene.²⁸

In the Hock process (Figure 109),²⁹ benzene is first converted to cumene via Friedel/Crafts alkylation with propene and a catalyst such as H_2SO_4 or AlCl_3 . Cumene oxidation with air affords cumene hydroperoxide. Following concentration, cumene hydroperoxide is cleaved with H_2SO_4 to yield phenol and acetone. Due to byproduct

formation, such as acetophenone and dimethylphenyl carbinol, the oxidation to cumene hydroperoxide is discontinued when the reaction is only 35-40% complete. Side reactions can also occur during the cleavage reaction resulting in the generation of byproducts such as α -methylstyrene, and α -cumylphenol. Reminiscent to the commercial production of PHB, hydroquinone and *p*-cresol, phenol is derived from non-renewable benzene and its synthesis proceeds through harmful intermediates in the form of organic peroxides. Because of the large volume of phenol synthesized annually, an alternative route that was both economical and environmentally sound would benefit not only the phenol manufacturers but perhaps society's view of the chemical industry as a whole.

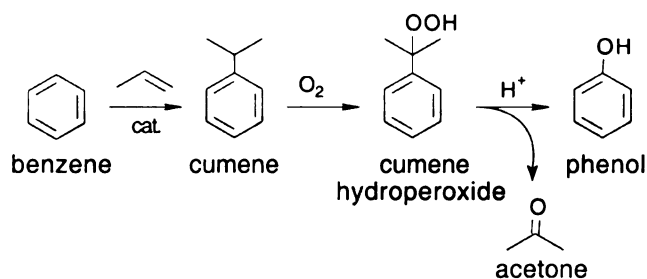


Figure 109. Hock Process for the Manufacture of Phenol.

Today, the major use of phenol is still in the production of phenolic resins (Figure 110), the polycondensation products of phenol and formaldehyde, comprising 34% of the market.³⁰ Phenolic resins are used in the manufacture of paints, adhesives, molding materials, and foam plastics. Synthesis of bisphenol A, the condensation product of acetone and phenol, constitutes the next largest consumption of phenol. Bisphenol A (Figure 110) is widely used in the manufacture of thermoplastics and synthetic resins, such as polycarbonates and epoxy resins. A large portion of synthesized phenol is also channeled into the production of ϵ -caprolactam (Figure 110), the precursor of nylon 6

(Perlon). Other derivatives of phenol include aniline (Figure 110), chlorophenols, plasticizers, and antioxidants.

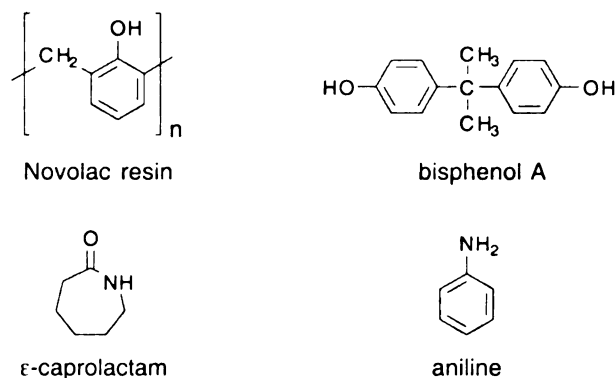


Figure 110. Major Products Derived from Phenol.

In the next section of this dissertation an alternative route for the synthesis of phenol will be outlined. This environmentally friendly route will begin with the conversion of renewable, non-toxic glucose to shikimic acid using *E. coli* biocatalysts such as those described in the previous section. It will then be shown that shikimic acid can be dehydrated and subsequently decarboxylated to phenol when heated in water to subcritical temperatures (350 °C) (Figure 91). The use of subcritical water avoids the use of hazardous reagents and intermediates as found with the Hock process.

A. Dehydration of Shikimic Acid.

After isolating shikimic acid from *Illicium religiosum* in the late 19th century, Eykmann found that shikimic acid can undergo two successive dehydrations in the presence of refluxing 12 M HCl to form a mixture of *m*- and *p*-hydroxybenzoic acids (MHB and PHB respectively).³¹ Repetition of Eykmann's experiments by the Frost

group³² showed that PHB could be formed in a 40% yield from shikimate with an accompanying 13% yield for MHB. Various dehydrating reagents were evaluated and it was found that 1 M H₂SO₄ in refluxing acetic acid increased both the yield and selectivity to PHB (Figure 111). The replacement of water for an organic acid had the effect of reducing the leveling effect caused by water and allowed for a higher reflux temperature of 130 °C.

Subsequent improvements in the titers reached by the shikimic acid-producing strains, such as SP1.1/pKD12.138 (Figure 96) with MGP addition (Table 17), led to the re-examination of these dehydration conditions with fermentation-derived shikimic acid as an alternative route to PHB. In this two-step combined biocatalytic and chemical route, the toxicity of PHB on the microbe would be avoided and could result in a higher overall yield of glucose to PHB.

Shikimic acid was purified from the culture supernatant of SP1.1/pKD12.138 with added MGP (0.5 mM) grown under fed-batch fermentation conditions. Shikimic acid was synthesized at a concentration of 38 g/L in a 17% (mol/mol) yield from glucose. Purification, based on the previously published procedure by Draths,³³ started by refluxing the cell-free broth as a way to convert DHS to PCA. Following adjustment to pH 2.5, the precipitated protein was removed by centrifugation and the solution was decolorized with two activated charcoal treatments. Following passage through successive anion and cation exchange columns and elution with 15% HOAc, the acidic solution was concentrated and dried under vacuum to remove water.

The resulting mixture of shikimic acid (43.4 g) and acetic acid was combined with 1 M H₂SO₄ in glacial acetic acid. After refluxing for 43 h at 130 °C, the reaction mixture

was filtered to remove the solid by-products and the filtrate extracted with ethyl acetate. Removal of the organic solvent affords a solid that is a 1:6 ratio of the *meta* to *para* isomer of hydroxybenzoic acid. After reprecipitation via pH adjustment in water, PHB can be obtained in 98% purity and a 45% isolated yield from shikimic acid. The black solid byproduct although easily removed by filtration, accounts for most of the yield loss. Its occurrence is believed to be due to decomposition of shikimate under the reaction conditions.

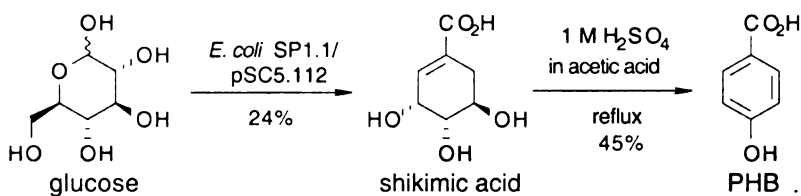


Figure 111. Conversion of Shikimic Acid to PHB via Acid Catalyzed Dehydration.

Overall, the two-step methodology outlined above represents an 11% yield (mol/mol) from glucose to PHB (Figure 111). Although it is comparable to the one-step microbial conversion in which PHB can be isolated in an 9% yield from glucose, it allows higher product titers per fermentation. In large-scale commercial operations, where fermentation time and space are premium, titer can become the crucial factor. Use of the two-step method also illustrates a way to alleviate end-product toxicity. Since it was shown that high concentrations of PHB are inhibitory to the biocatalyst, it is preferable to expose the microbe to shikimate which has negligible toxicity. The major disadvantage of the combined synthetic methodologies is the loss of control over

isomeric purity. Although the formation of the *meta* isomer did not account for a large drop in yield, it was difficult to separate from PHB and remains a 2% impurity in the final product. Conversely direct fermentation of glucose to PHB inherently provides isomerically pure product.

B. Subcritical Water.

Interest in fluids near or above their critical point has grown substantially in the last decade as the demand for environmentally benign processes are sought as alternatives to traditional chemical practices.³⁴ The critical point of a substance is the temperature and pressure above which it exists as a single phase.³⁵ Common supercritical fluids being studied are carbon dioxide and water. With a critical point of 31 °C and 72.8 bar,³⁶ carbon dioxide has become a favorable solvent for extraction of organics. Once the desired products or undesired contaminants are solvated in the supercritical CO₂ phase, the mixture can be cooled, the solutes easily recovered from the gaseous CO₂ layer, and the CO₂ can be readily recycled.³⁷

Table 19. Comparison of Water’s Properties at Different Temperatures.

	ambient	sub-critical	super-critical
temperature (°C)	25	275	400
pressure (bar)	1	60	230
density	1	0.7	0.1
dielectric constant	80	20	2
relative ionization constant	1	1000	<0.01

Supercritical and subcritical water have also found applications in areas traditionally performed by organic solvents. Near its critical point of 374 °C and 218 bar,³⁸ water can solvate organic molecules that are insoluble in water at ambient temperatures and pressures. As the temperature of water approaches 374 °C, hydrogen bonding decreases resulting in a lower density and a decreased dielectric constant thus causing subcritical water to behave like an organic solvent (Table 19).³⁹ As water nears subcritical temperatures, the dissociation constant (K_w) increases by about three orders of magnitude increasing the concentration of H^+ and OH^- ions (Table 19). Therefore, not only can water at or near its critical point act as an organic solvent, but it can promote acid and base catalyzed reactions. Because of these unique properties, a variety of organic reactions, such as reductions, oxidations, eliminations, and Friedel/Crafts acylations, have been performed with subcritical and or supercritical water as both the solvent and catalyst.⁴⁰

The environmental benefits of such processes are clearly in line with the long term goals of “greening” the chemical industry. Volatile organic compounds (VOC’s), which are subject to workplace and environmental air quality standards, can be replaced with water, a recyclable, nontoxic substance. In reactions such as Friedel-Crafts acylations,⁴¹ the Lewis acid catalyst can be avoided thus lowering the amount of salt wastes generated. Costly organic separations can also be avoided if the organic product, insoluble in ambient water, simply precipitates out of solution as the reaction mixture cools.

C. Reaction of Shikimic Acid in Subcritical Water.

Reaction at Various Temperatures

Because of the favorable environmental aspects of subcritical water and its ability to promote acid-catalyzed dehydrations, conversion of shikimic acid to PHB in subcritical water was examined. Shikimic acid was combined with degassed water in a stainless steel high temperature reaction vessel (Parr), sealed under Ar and heated for 0.5 h at temperatures ranging from 250 °C to 374 °C. After the reaction was complete and the vessel cooled to room temperature, the contents were extracted with ether to isolate the organic products. A portion of this organic material was silylated and analyzed using gas chromatography against an internal standard of dodecane. Any products remaining in the aqueous layer were analyzed by ¹H NMR.

Unreacted shikimic acid remained up to 310 °C in combination with its isomer 3-*epi*-shikimic acid (Figure 112, Table 20). Analysis of the organic products not only revealed the presence of PHB and MHB but phenol was formed as the major product (Figure 112, Table 20). Between 330 °C and 374 °C, phenol is formed in a 53% (mol/mol) yield, MHB in a 18% (mol/mol) yield, and PHB in a 1% (mol/mol) yield (Table 20). Based on these results, 350 °C was chosen as the optimal temperature for shikimic acid's conversion to phenol. However, as the temperature increases the mass recovery for the reaction decreases to approximately 72% (Table 20). This is reminiscent of the mineral acid dehydration of shikimic acid with its 30% loss to an undefined black, solid by-product. What appears to be the same material resulting from the pyrolysis of shikimic acid is also formed under subcritical water conditions decreasing the overall

yield. It does not interfere with analysis or purification of the products as it is easily filtered away.

Table 20. Conversion of Shikimic Acid to Phenol at Various Temperatures.

temperature (°C)	% yield ^b				SA ^{a,c}	% mass recovery ^d
	phenol	MHB ^a	PHB ^a	3- <i>epi</i> -SA ^a		
374	54	18	1	0	0	73
350	53	18	1	0	0	72
330	53	20	1	0	0	74
310	49	19	6	1	2	77
290	21	11	5	17	29	83
270	34	16	5	7	12	74
250	8	4	0	34	56	102

^aAbbreviations: MHB, *m*-hydroxybenzoic acid; PHB, *p*-hydroxybenzoic acid; 3-*epi*-SA, 3-*epi*-shikimic acid; and SA, shikimic acid. ^bmol/mol with respect to SA. ^cpercent remaining in solution. ^d(mol phenol + mol MHB + mol PHB + mol 3-*epi*-SA + mol SA)/ mol SA initial

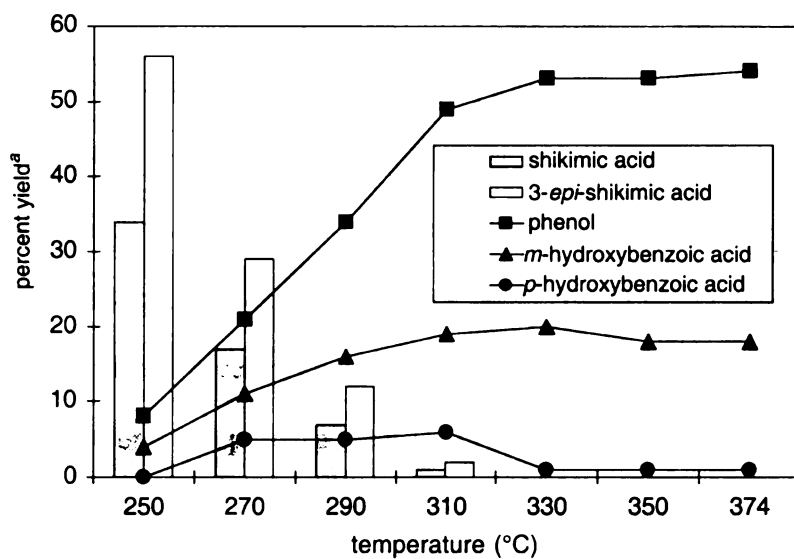


Figure 112. Conversion of Shikimic Acid to Phenol at Various Temperatures. ^amol/mol with respect to initial shikimic acid.

Mechanism

As shikimic acid is heated above 250 °C, the epimerization of the allylic alcohol to the more thermodynamically stable isomer appears to be the dominant reaction (Figure 113). The structure of 3-*epi*-shikimic acid was confirmed by comparison to the ¹H NMR of a mixture of shikimic acid and 3-*epi*-shikimic acid obtained from the NaBH₃CN reduction of 3-dehydroshikimic acid (DHS, Figure 122).⁴² As the temperature is increased, dehydration of the allylic alcohol of shikimic acid and 3-*epi*-shikimic acid yields two possible diene intermediates (Figure 113). Aromatization of the two cyclic dienes leads to the formation of PHB and MHB (Figure 113). It is known that aromatic acids can be decarboxylated when heated in the presence of a strong acid via an arenium ion mechanism which is accelerated by electron-donating groups in the *ortho* and *para* positions.⁴³ Therefore, one possible mechanism for phenol production is that shikimic acid and 3-*epi*-shikimic acid undergo two successive dehydrations to yield a 3:1 mixture of PHB and MHB. The PHB is then rapidly decarboxylated to phenol, thus accounting for its low concentration in the reaction mixtures from all temperatures (Table 20).

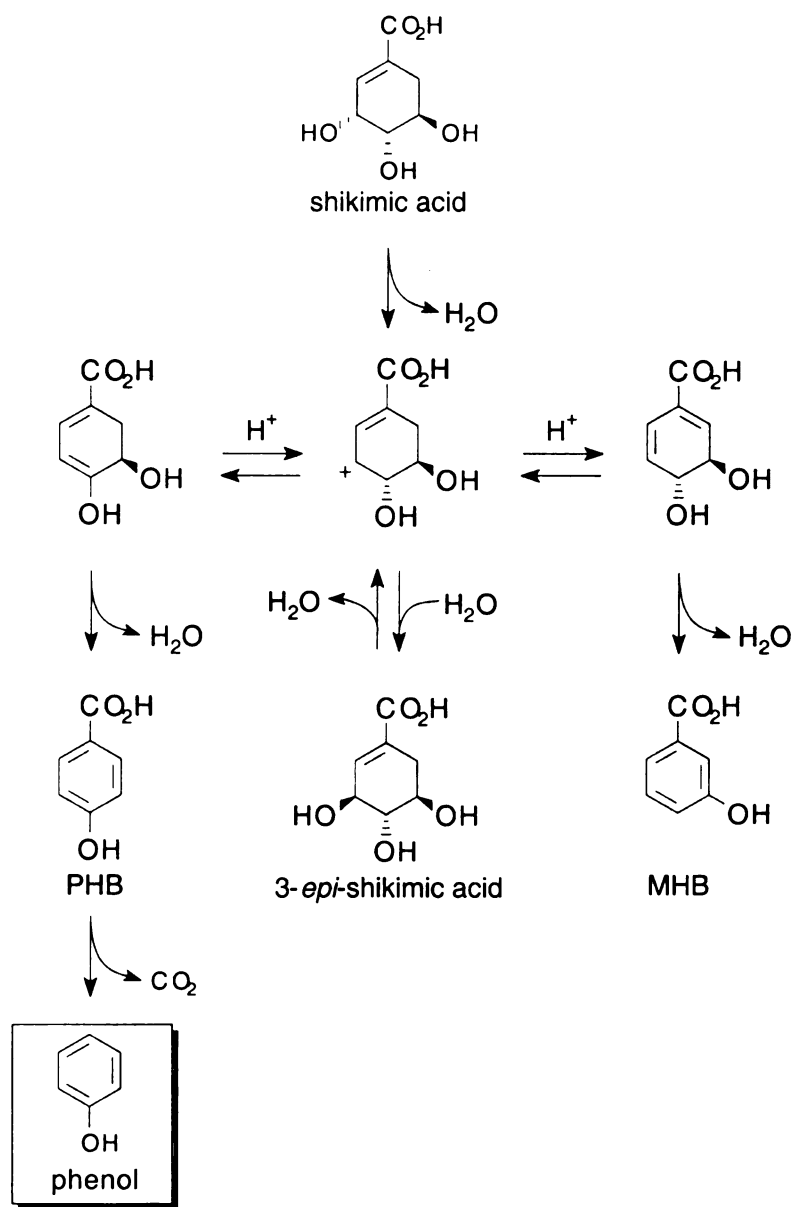


Figure 113. Proposed Mechanism for the Conversion of Shikimic Acid to Phenol.

D. Copper Assisted Decarboxylation of MHB

One way to increase the yield of phenol is to find conditions that allow for the decarboxylation of MHB. The standard reaction employed for the decarboxylation of aromatic acids has been the copper-quinoline method. Despite its widespread synthetic use, the exact mechanism is still uncertain.⁴⁴ It has been proposed that the actual catalytic species is the copper (I) ion as rates tend to increase when copper (I) oxide is used in place of copper powder under an oxygen-free atmosphere. Assuming that enough OH⁻ ions are present in subcritical water at 350 °C to serve as a Lewis base in place of quinoline, the decarboxylation of MHB was studied in the presence of copper powder and copper (I) acetate.

MHB in the absence of copper catalysts yields only 20% phenol when reacted in water at 350 °C for 5 h. In the presence of one equivalent of copper powder, MHB was decarboxylated to phenol in a 96% (mol/mol) yield in 3 h at 350 °C (Table 21). With only 0.1 equivalents of copper powder, the yield of phenol dropped to 60% (mol/mol) in 3 h and was not significantly improved by extending to longer reaction times (Table 21). One equivalent of CuOAc behaved similarly to one equivalent of copper powder resulting in a 92% yield of phenol in 3 h (Table 21). Reducing the equivalent of CuOAc to 0.1 necessitated extension of the reaction time to 4 h to obtain a maximum yield of 74% (mol/mol) phenol (Table 21). These results suggest that Cu(0) is either being oxidized to Cu(I) in situ or a mechanism dissimilar from the copper-quinoline reaction is in play. Generally the mass recovery for the copper catalyzed decarboxylation of MHB

were good suggesting that the starting material and product are not subject to decomposition in the presence of either catalyst.

Table 21. Decarboxylation of *m*-Hydroxybenzoic Acid in the Presence of Copper Catalysts.

catalyst		time (h)				
		1	2	3	4	5
none	%MHB ^a	67	60	50	69	79
	%pheno ^b	5	3	5	31	20
Cu (0), 1equiv. ^c	%MHB ^a	20	11	5	53	1
	%pheno ^b	79	88	96	79	97
Cu (0), 0.1equiv. ^c	%MHB ^a	54	49	33	30	36
	%pheno ^b	38	39	60	40	66
CuOAc, 1equiv. ^c	%MHB ^a	32	2	3	0	0
	%pheno ^b	59	66	92	87	83
CuOAc, 0.1equiv. ^c	%MHB ^a	58	29	24	25	30
	%pheno ^b	30	65	52	74	70

^amol MHB remaining/mol MHB initial. ^bmol phenol/mol MHB initial. ^cequivalents based on mol MHB initial.

E. Two-Step Conversion of Shikimic Acid to Phenol.

To obtain an optimized, isolated yield of phenol from shikimic acid, the following reaction was done. Shikimic acid was combined with degassed water and sealed in the Parr reaction vessel. The vessel was heated slowly (approximately 1.5 °C/min) in a sand bath to allow thermal equilibration between the sand and vessel. Once a temperature of 350 °C was reached, it was maintained for 0.5 h and then the vessel was removed from the sand bath and cooled to room temperature. The vessel was unsealed and the contents were extracted with ether. After drying over Na₂SO₄, the organic layers were

concentrated to a brown residue. Kugelrohr distillation of this residue afforded phenol in a 45% isolated yield (Figure 114).

The solid material containing MHB that remained after distillation was dissolved in boiling water, and filtered to remove insoluble impurities. The aqueous MHB solution was concentrated to an appropriate volume and returned to the reaction vessel with one equivalent of copper powder. After 3 h at 350 °C, the vessel was cooled to room temperature, unsealed, and the contents extracted with ether. Kugelrohr distillation of the dried, concentrated organic layers afforded an additional portion of phenol corresponding to a 6% yield (mol/mol) based the starting quantity of shikimic acid. Overall, shikimic acid was converted to phenol in a 51% isolated yield (Figure 114).

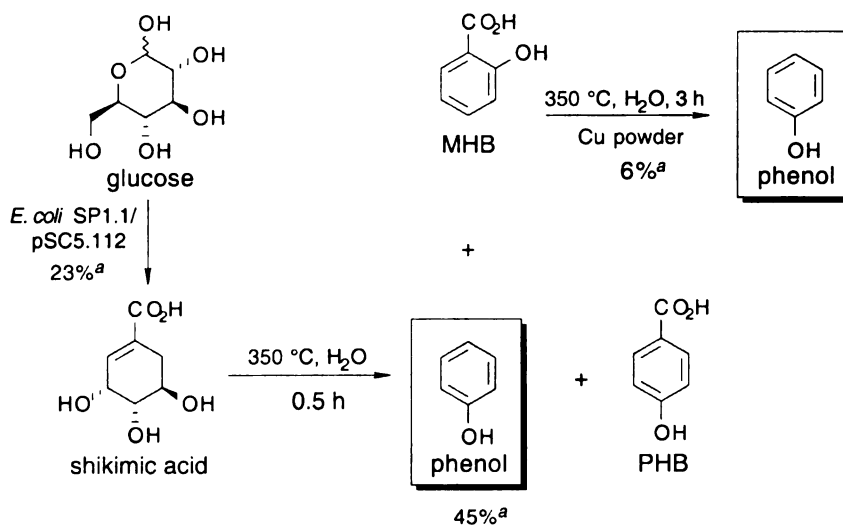


Figure 114. Overall Conversion of Glucose to Phenol.
^aisolated yields.

F. Conversion of Fermentation Broth to Phenol.

Purification of Fermentation Broth.

To streamline the isolation of microbe-synthesized shikimic acid to its chemical conversion to phenol and, the purification of shikimic acid from fermentation broth was re-examined. The goal was to see which steps, if any, could be eliminated from the published purification scheme in hopes of reducing the number of unit operations necessary to go from glucose to phenol. Therefore, six samples of fermentation broth were prepared as follows that differed by their level of purification (Figure 116).

E. coli SP1.1 *serA::aroB aroL::Tn10 aroK::Cm^R*

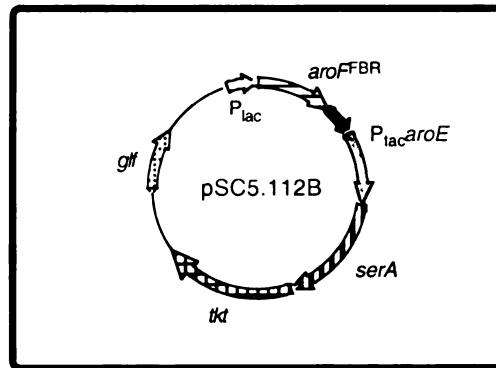


Figure 115. Shikimic Acid Producing Construct SP1.1/pSC5.112. Genetic loci are as follows: *aroF^{FBR}*, feedback insensitive DAHP synthase; *aroE*, shikimate dehydrogenase; *serA*, phosphoglycerate dehydrogenase; *tkt*, transketolase; *glf*, glucose facilitator.

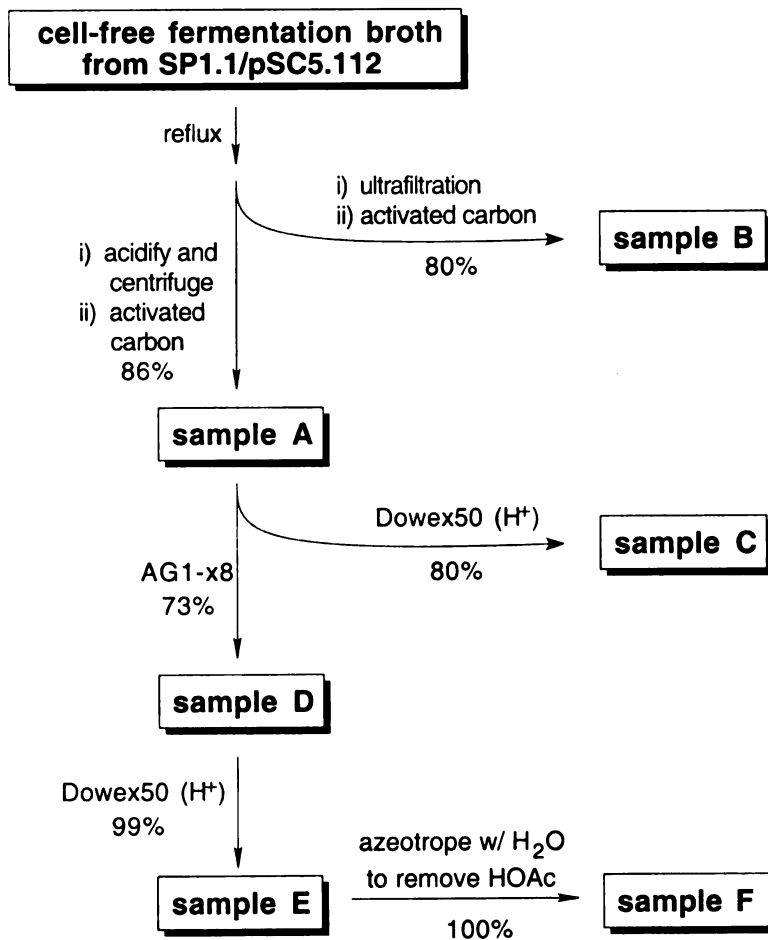


Figure 116. Preparation of Samples A-F.

Cell-free fermentation broth from *E. coli* SP1.1/pSC5.112B (Figure 115), a strain producing 70 g/L of shikimic acid in a 24% yield (mol/mol) from glucose,⁴⁵ was initially refluxed for 4 h, to break down the extracellular protein and convert the DHS to PCA. A portion was set aside and the pH of the remaining solution was adjusted to 2.5 by addition of concentrated H₂SO₄ to precipitate the protein. After centrifugation, the precipitated protein was discarded and the resulting a clear yellow solution was combined with Darco KB-B activated carbon, stirred on a magnetic stirrer for 1 h and then filtered through Whatman 5 filter paper to remove the generated PCA and decolorize the solution. The filtrate was treated in the same way with a second batch of activated carbon (86% recovery, Figure 116). A portion of the resulting acidic, protein-free solution, designated as sample A, was evaporated to a concentration of 2 M shikimic acid and stored at 4 °C.

The portion of broth reserved after reflux was passed through an ultrafiltration membrane to remove the protein. The resulting black solution was combined with Darco KB-B activated carbon, stirred on a magnetic stirrer for 1 h and then filtered through Whatman 5 filter paper. The filtrate was treated in the same way with a second batch of activated carbon (80% recovery, Figure 116). This protein-free, neutral solution, designated as sample B, was evaporated to a concentration of 2 M shikimic acid and stored at 4 °C.

The solution remaining after acidification and decolorization was divided into two portions. One portion was eluted through a column of Dowex 50 (H⁺ form) at 4 °C which was then washed with water. The eluents off the cation exchange column were combined

and concentrated to 2 M shikimic acid. The resulting K^+ , Na^+ , and NH_4^+ -free solution (69% recovery, Figure 116), designated as sample C, was stored at 4 °C.

The second portion of acidified, decolorized solution was diluted and passed through a column of AG1-x8 (acetate form) at 4 °C. Following elution of the column with 15% aqueous acetic acid, the combined eluents were concentrated by boiling. A portion of this PO_4^- , SO_4^- -free solution (63% recovery, Figure 116) was concentrated to 2 M shikimic acid, designated as sample D, and stored at 4 °C. A second portion of the eluents remaining after anion exchange chromatography was eluted through a column of Dowex 50 (H^+ form) at 4 °C which was then washed with water. The eluents off the cation exchange column were combined and concentrated to by boiling (62% recovery, Figure 116). A portion of this solution free of inorganic salts was concentrated to 2 M shikimic acid, designated as sample E, and stored at 4 °C.

The eluent remaining after cation exchange was concentrated to dryness by rotary evaporation. The resulting solid was resuspended in water and concentrated to dryness a second time. Cycles of resuspension and concentration were repeated until acetic acid was removed from solution by azeotropic distillation. The resulting solid (62% recovery, Figure 116) was resuspended in water to afford a 2 M solution of shikimic acid. This acetate-free solution void of inorganic salts was designated as sample F and stored a 4 °C.

Conversion of Fermentation Broth to Phenol.

Each of the six samples (6 mL, 2 M shikimic acid) was reacted at 350 °C for 0.5 h. Analysis of the resulting products showed that the presence of ions found in the

fermentation broth, namely K^+ , Na^+ , NH_4^+ , PO_4^- , SO_4^- , and OAc^- , severely decrease the yield of phenol. Only the sample of broth that had undergone cation and anion exchange and removal of acetic acid produced the same yield of phenol (55%) as was obtained with purified shikimic acid (Table 22). With only acetate present, modest yields of 37% phenol were obtained. The next highest yield of phenol was obtained with sample A, the protein-free solution that had been adjusted to pH 2.5 with H_2SO_4 (Table 22). Since no shikimic acid remained in the three remaining samples B, C, and D, phenol may have been synthesized but could have subsequently decomposed (Table 22)

Sample A at Lower Temperatures.

Since a 24% yield of phenol was obtained from fermentation broth that had been acidified with H_2SO_4 , it was thought that perhaps the added sulfate ions could be catalyzing the decomposition of phenol. Therefore, perhaps reaction of this sample at lower temperatures could lead to higher phenol yields. Temperatures of 150 °C to 500 °C were evaluated (Table 23). Unreacted shikimic acid was the major product at 150 °C and 200 °C. Increasing the temperature did reduce the amount of unreacted shikimic acid but it did not correlate to higher phenol yields (Table 23).

Table 22. Conversion of Fermentation Broth at Different Levels of Purity (Samples A-F) to Phenol

sample	% yield ^b				SA ^{a,c}	% mass recovery ^d
	phenol	MHB ^a	PHB ^a	3- <i>epi</i> -SA ^a		
A	24	18	0	0	0	42
B	2.7	10	1.9	0.77	0	16
C	6.7	4.3	0	0	0	11
D	3.2	24	5	2.1	0	34
E	37	9.3	1.3	0	0	48
F	55	13	1.7	0	0	70

^aAbbreviations: MHB, *m*-hydroxybenzoic acid; PHB, *p*-hydroxybenzoic acid; 3-*epi*-SA, 3-*epi*-shikimic acid; and SA, shikimic acid. ^bmol/mol with respect to SA. ^cpercent remaining in solution. ^d(mol phenol + mol MHB + mol PHB + mol 3-*epi*-SA + mol SA)/ mol SA initial

Table 23. Conversion of Sample A at Various Temperatures.

temperature (°C)	% yield ^b				SA ^{a,c}	% mass recovery ^d
	phenol	MHB ^a	PHB ^a	3- <i>epi</i> -SA ^a		
350	26	17	0	0	0	43
300	27	25	0	0	0	52
250	17	11	1	20	9	58
200	0	0	0	0	100	100
150	0	0	0	0	77	77

^aAbbreviations: MHB, *m*-hydroxybenzoic acid; PHB, *p*-hydroxybenzoic acid; 3-*epi*-SA, 3-*epi*-shikimic acid; and SA, shikimic acid. ^bmol/mol with respect to SA. ^cpercent remaining in solution. ^d(mol phenol + mol MHB + mol PHB + mol 3-*epi*-SA + mol SA)/ mol SA initial

G. Extraction of Shikimic Acid from Fermentation Broth.

The previous results show that inorganic salts and acetate to need to be removed from shikimic acid-containing fermentation broth in order to achieve the maximum conversion to phenol, thus necessitating a lengthy, multi-step process in which shikimic acid is isolated in modest yields (Figure 116). To make this process more commercially appealing and further integrate the biotic and abiotic steps of phenol synthesis, an alternative method for shikimic acid isolation was investigated. It was found that shikimic acid could be extracted in high yields from protein-free, decolorized fermentation broth with ethyl acetate when 12 equivalents of ethanol (per equivalent of shikimic acid) was added to the aqueous solution prior to extraction.

In this experiment, culture supernatant from a fermentation of SP1.1/pSC5.112B was refluxed, acidified, and decolorized as was described in the previous section. A portion of this solution (50 mL) was mixed well with ethanol (11 mL) and loaded in a modified continuous extraction apparatus with ethyl acetate (250 mL). The extraction apparatus was modified to allow vigorous stirring of the organic and aqueous layers in order to create a colloidal suspension. After 24 h, the ethyl acetate was separated, dried, and concentrated to 40% of the volume and shikimic acid was allowed to precipitate. A significant portion of pure shikimic acid (86%) was recovered in this first step (Figure 117). The remaining aqueous layer was combined with an additional portion of ethanol and returned to the continuous extraction apparatus with fresh ethyl acetate. After 24 h, the separated ethyl acetate layer yielded an additional 11% shikimic acid. Using this method, shikimic acid could be recovered in a combined 97% yield from fermentation

broth (Figure 117). Coupling this result with the fermentation of SP1.1/pSC5.112B (24%), the highest yielding shikimic acid-producing microbe, and the reaction previously described for the conversion of phenol, it is conceivable that phenol could be synthesized from glucose in a 12 % (mol/mol) yield.

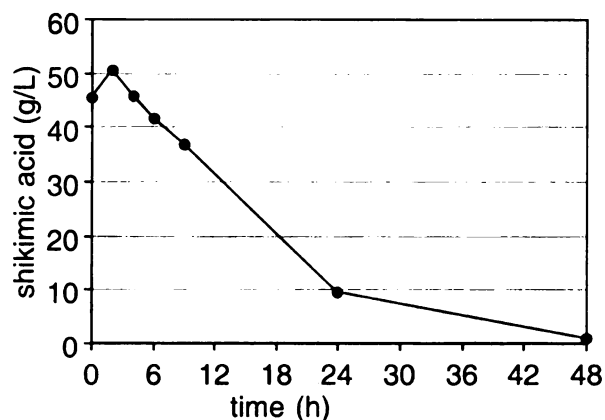


Figure 117. Concentration of Shikimic Acid Remaining in the Aqueous Layer over Time.

III. Discussion

Shikimic Acid Equilibration to Quinic Acid.

Replacement of the native *E. coli* DHQ dehydratase and shikimate dehydrogenase activities with the tobacco bifunctional DHQ dehydratase/shikimate dehydrogenase had the affect of greatly reducing the concentration of quinic acid synthesized by a shikimic acid-producing construct from a 2:1 ratio of shikimic acid to quinic acid in SP1.1/pKD12.138 to a 30:1 ratio in JB4/pJB5.291. Neither the yield nor titer was

affected by the heterologous expression of the tobacco enzyme providing comparable results with SPI.1/pKD12.138 cultured under quinic acid suppressing conditions.

The use of the tobacco *aroD*-*aroE* locus to circumvent quinic acid formation differs from other methods aimed at preventing shikimic acid transport in that it removes the microbe's inherent ability to catalyze quinic acid formation. This could be the result of competition between the AroD and AroE active sites on the bifunctional protein for substrate DHQ. If the AroD active site is encountered, DHQ is converted to DHS and channeled forward to shikimic acid. If the AroE active site is encountered, DHQ is reduced to quinic acid. Since only minor amounts of quinic acid are formed both in vivo and in vitro, the tobacco AroE active site could be poorly accessible or does not readily accept DHQ as a substrate relative to the AroD active site.

A surprising result was the feedback inhibition of the shikimate dehydrogenase portion of the tobacco enzyme resulting in DHS accumulation during JB4/pJB5.291 fermentations. It was originally hoped that DHS formation could be avoided by channeling it forward to shikimic acid using the bifunctional enzyme. Analysis of the shikimate dehydrogenase portion of the tobacco protein with *E. coli* shikimate dehydrogenase show a high degree of homology suggesting it is evolutionary closer to the prokaryotic homologues than to homologues of lower eukaryotes such as yeast and fungi.⁴⁶ This could imply that feedback inhibition of shikimate dehydrogenase by shikimic acid is a ubiquitous mechanism for regulation of the common pathway in plants and microbes.

Synthesis of Phenol

The conversion of glucose-derived shikimic acid to phenol using subcritical water represents an environmentally benign synthesis of this commercially important aromatic chemical that not only avoids hazardous reaction conditions and intermediates but originates with a renewable, non-petroleum feedstock. It should be noted this process has large energy demands in order to attain the temperatures required for subcritical water. However, high temperature water is already being generated by many electric power plants as part of their cooling system and could be a potential source of subcritical water. A completely fossil fuel-free process could also be envisioned as advances in solar and nuclear energy sources are made in the future.

In optimizing the conversions of shikimic acid to phenol, it was found that temperatures close to the critical point of water (330-374 °C) are needed to completely dehydrate shikimic acid and its epimer. It was also found that the ions present in fermentation broth, namely phosphate, sulfate, and ammonium ions, lead to severely decreased yields, perhaps by promoting further phenol degradation. Another drop in yield is due to the poor ability of MHB to decarboxylate. Although pure MHB was shown to decarboxylate in the presence of Cu catalysts, this reaction is hindered by contaminating byproducts carried over from the initial reaction with shikimate. The largest yield loss however still comes from the unpreventable pyrolysis of shikimic acid.

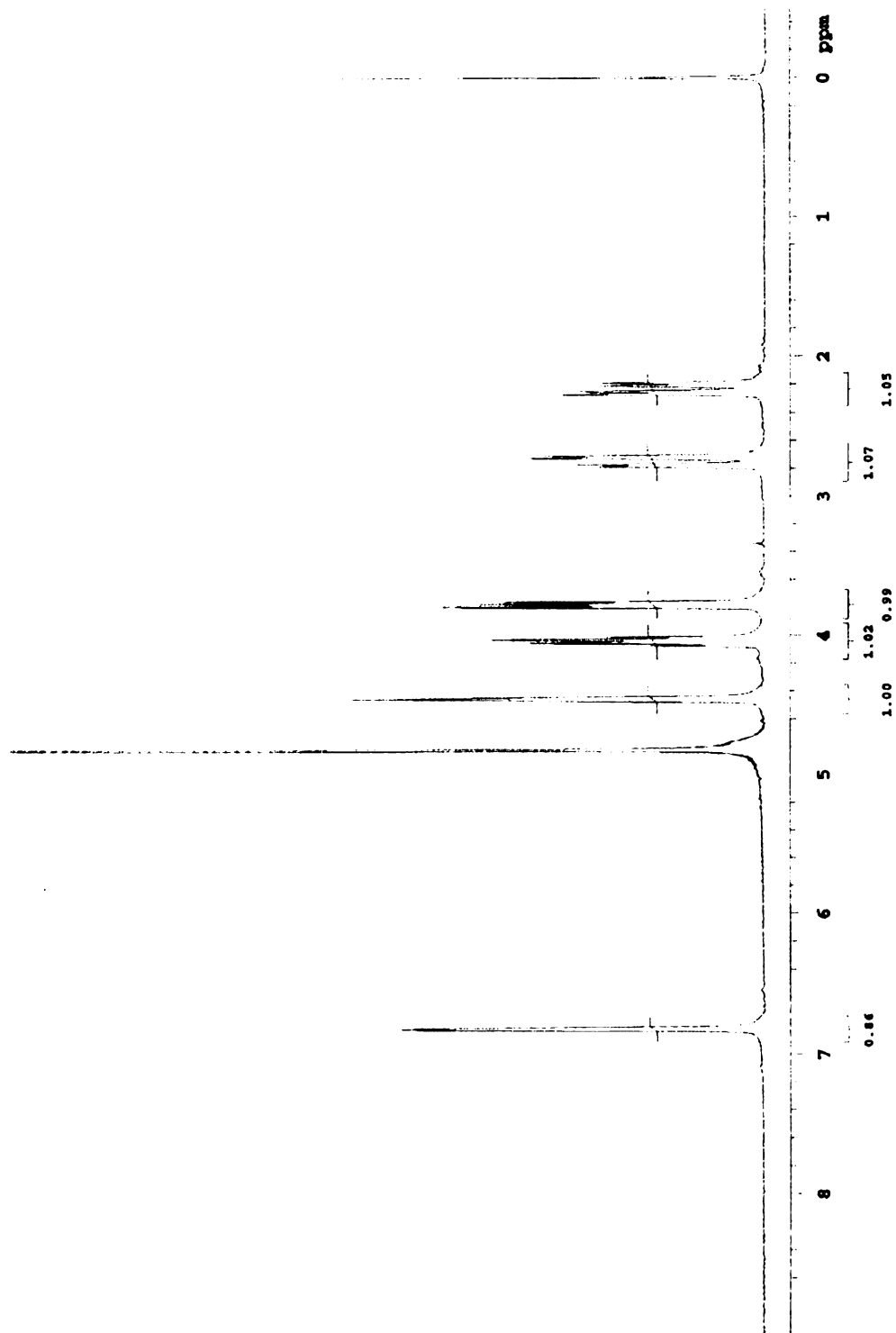


Figure 118. Control ¹H NMR of Shikimic Acid. Resonances: δ 6.84 (s, 1 H), 4.57 (s, 1 H), 4.05 (m, 1 H), 3.78 (dd, 1 H), 2.75 (dd, 1 H), 2.23 (dd, 1 H).

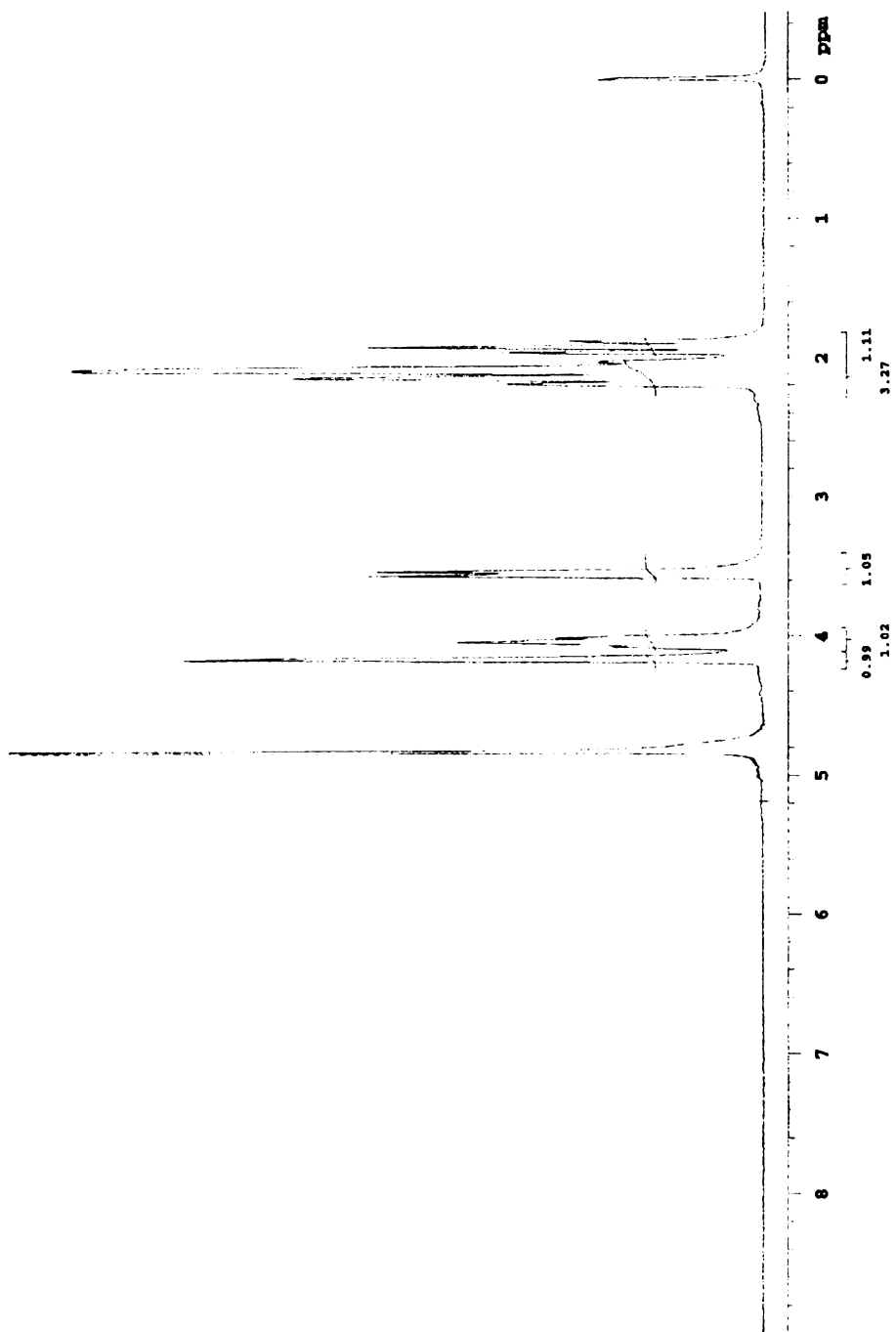


Figure 119. Control ¹H NMR of Quinic Acid. Resonances: δ 4.16 (s, 1 H), 4.04 (m, 1 H), 3.55 (t, 1 H), 2.11 (m, 3 H), 1.92 (t, 1 H).

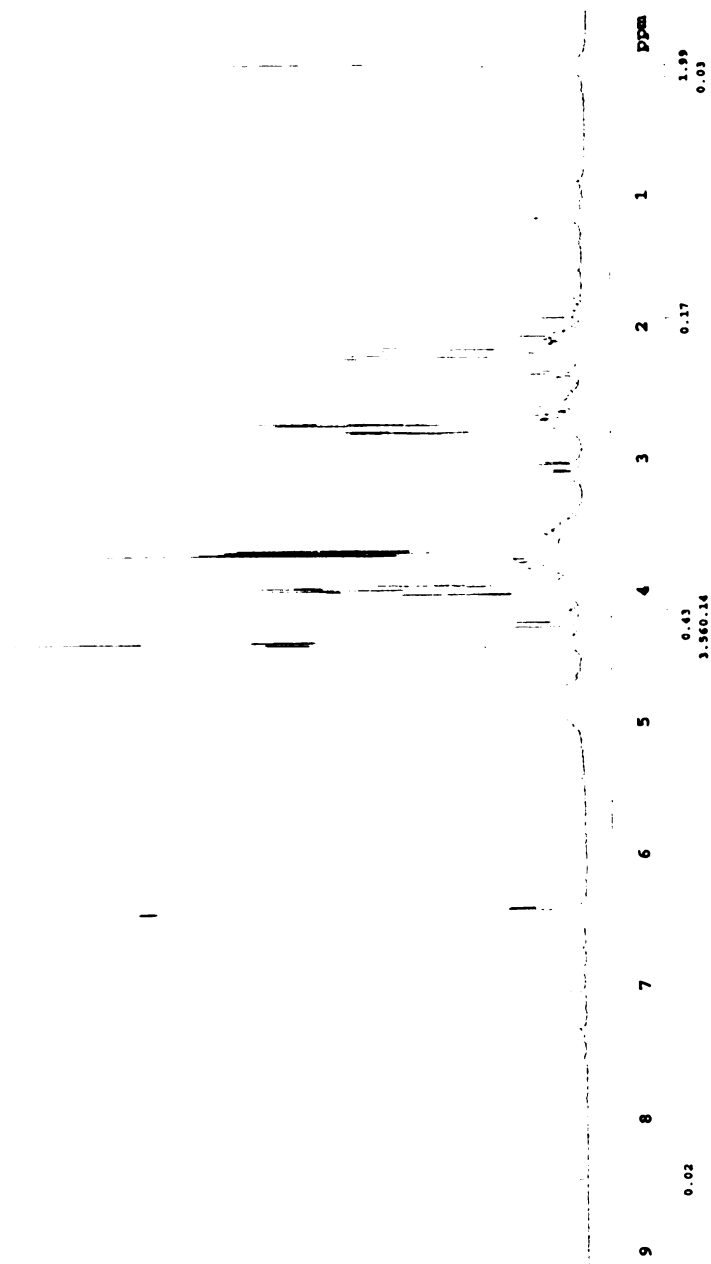


Figure 120. Typical 1H NMR of JB4/pJB5.291 (36 °C) Fermentation Broth. Shikimic acid resonances: δ 6.84 (s, 1 H), 4.57 (s, 1 H), 4.05 (m, 1 H), 3.78 (dd, 1 H), 2.75 (dd, 1 H), 2.23 (dd, 1 H). Quinic acid resonances: δ 4.16 (s, 1 H), 4.04 (m, 1 H), 3.55 (t, 1 H), 2.11 (m, 3 H), 1.92 (t, 1 H).

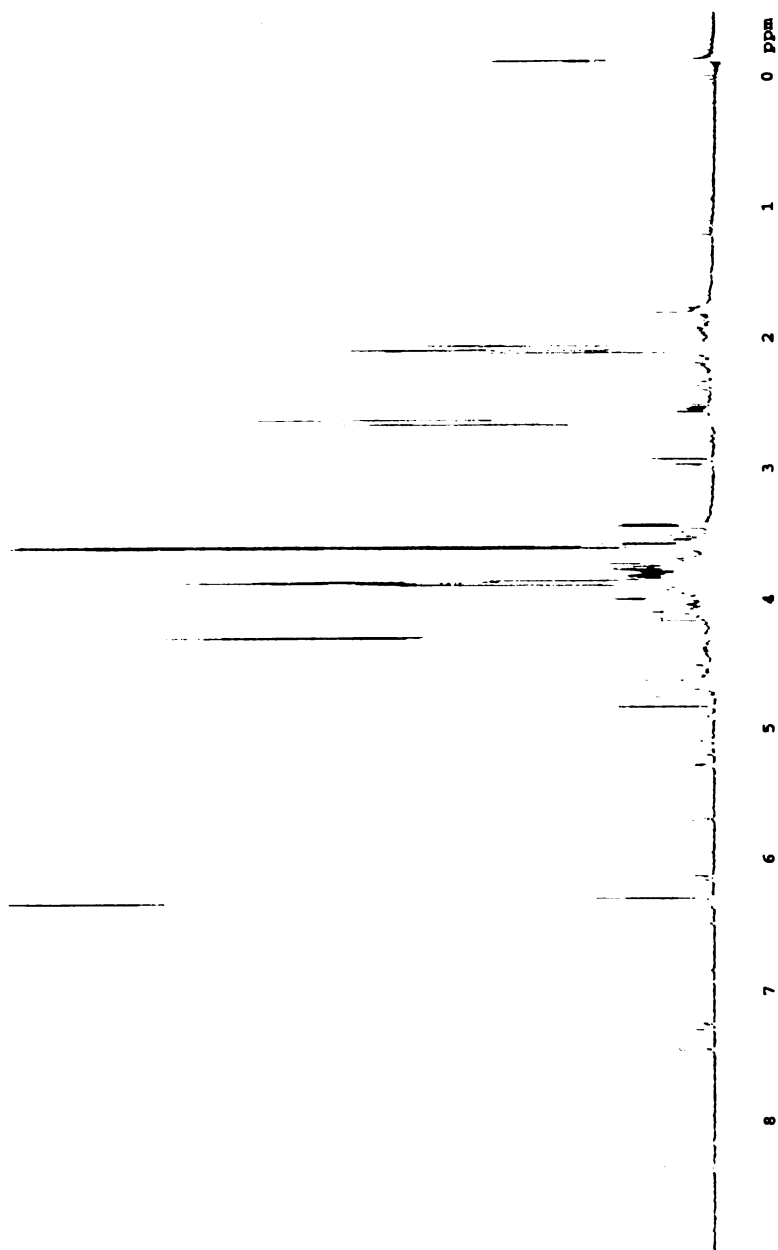


Figure 121. In vitro Accumulation of Quinic Acid with *KL3aroD*⁻/*pJB5.272A* lysate. Shikimic acid resonances: δ 6.84 (s, 1 H), 4.57 (s, 1 H), 4.05 (m, 1 H), 3.78 (dd, 1 H), 2.75 (dd, 1 H), 2.23 (dd, 1 H). Quinic acid resonances: δ 4.16 (s, 1 H), 4.04 (m, 1 H), 3.55 (t, 1 H), 2.11 (m, 3 H), 1.92 (t, 1 H). DHS resonances: δ 6.42 (d, 1 H), 4.28 (d, 1 H), 4.00 (ddd, 1 H), 3.07 (dd, 1 H), 2.66 (ddd, 1 H)

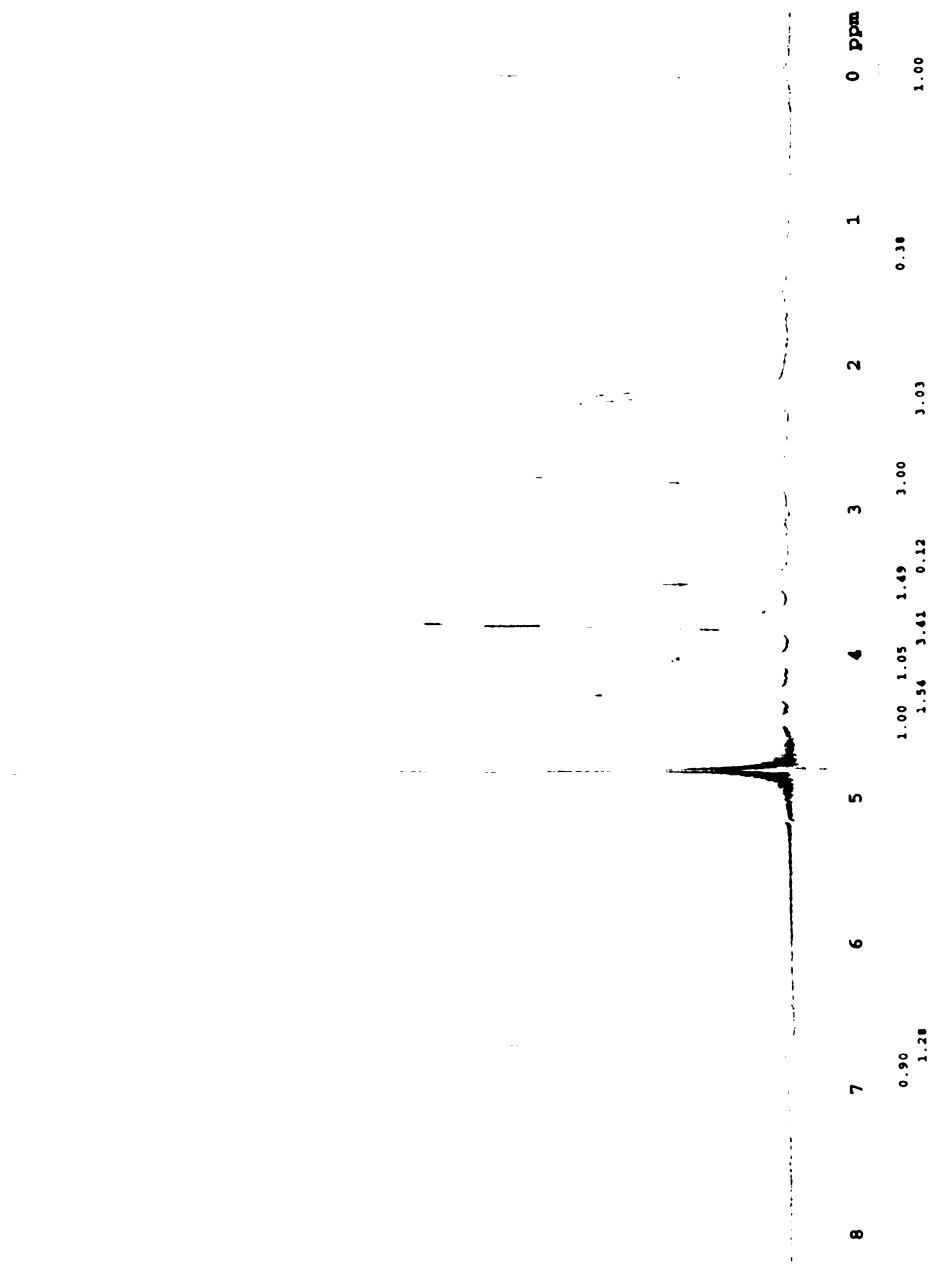


Figure 122. ^1H NMR of Shikimic Acid and 3-*epi*-Shikimic Acid Generated by the Reduction of DHS. Shikimic acid resonances: δ 6.84 (s, 1 H), 4.57 (s, 1 H), 4.05 (m, 1 H), 3.78 (dd, 1 H), 2.75 (dd, 1 H), 2.23 (dd, 1 H). 3-*epi*-Shikimic acid resonances: δ 6.69 (s, 1 H), 4.27 (s, 1 H), 3.79 (m, 1 H), 3.49 (t, 1 H), 2.77 (dd, 1 H), 2.22 (dd, 1 H).

References

-
- ¹ Hansen, C. A.; Dean, A. B.; Draths, K. M.; Frost, J. W. *J. Am. Chem. Soc.* **2000**
- ² Haslam, E. *Shikimic Acid: Metabolism and Metabolites*; Wiley: New York, 1993; p. 1.
- ³ Herrmann, K. M. In *Amino Acids: Biosynthesis and Genetic Regulation*; Addison-Wesley: Reading, 1983; p. 313.
- ⁴ Haslam, E. *Shikimic Acid: Metabolism and Metabolites*; Wiley: New York, 1993; p. 1.
- ⁵ Ma, Y.; Xu, Q.-P.; Sun, J.-N.; Bai, L.-M.; Guo, Y.-J.; Niu, J.-Z. *Acta Pharmacol. Sin.* **1999**, *20*, 701.
- ⁶ Barco, A.; Benetti, S.; De Risi, C.; Marchetti, P.; Pollini, G. P.; Zanirato, V. *Tetrahedron Asymmetry*, **1997**, *8*, 3515.
- ⁷ Tan, D. S.; Goley, M. A.; Shair, M. D.; Schreiber, S. L. *J. Am. Chem. Soc.* **1998**, *120*, 8565.
- ⁸ Draths, K. M.; Knop, D. R.; Frost, J. W. *J. Am. Chem. Soc.* **1999**, *121*, 1603.
- ⁹ Draths, K. M.; Knop, D. R.; Frost, J. W. *J. Am. Chem. Soc.* **1999**, *121*, 1603.
- ¹⁰ Chrandran, S. S. Ph.D. Dissertation, Michigan State University, 2001.
- ¹¹ Draths, K. M.; Knop, D. R.; Frost, J. W. *J. Am. Chem. Soc.* **1999**, *121*, 1603.
- ¹² Knop, D. R.; Frost, J. W. Unpublished Results.
- ¹³ Whipp, M. J.; Camakaris, H.; Pittard, A. J. *Gene* **1998**, *209*, 185.
- ¹⁴ Chrandran, S. S. Ph.D. Dissertation, Michigan State University, 2001.
- ¹⁵ Chrandran, S. S. Ph.D. Dissertation, Michigan State University, 2001.
- ¹⁶ (a) Schmid, J.; Amrhein, N. *Phytochemistry* **1995**, *39*, 737. (b) Herrmann, K. M. *The Plant Cell* **1995**, *7*, 907.
- ¹⁷ Bonner, C. A.; Jensen, R. A. *Biochem. J.* **1994**, *302*, 11.
- ¹⁸ Li, K.; Mikola, M.; Draths, K. M.; Worden, R. M.; Frost, J. W. *Biotechnol. Bioeng.* **1999**, *64*, 61.

-
- ¹⁹ Cobos, A.; Fernandez, M. F.; Hernandez, P. E.; Sanz, B. *Curr. Microbiol.* **1990**, *20*, 13.
- ²⁰ Berson, A.E.; Hudson, D.V.; Waleh, N.S. *Molec. Microbiol.* **1991**, *5*, 2261.
- ²¹ Draths, K. M.; Knop, D. R.; Frost, J. W. *J. Am. Chem. Soc.* **1999**, *121*, 1603.
- ²² Schoner, R.; Herrmann, K. M. *J. Biol. Chem.* **1976**, *251*, 5440.
- ²³ Knop, D. R.; Frost, J. W. Unpublished Results.
- ²⁴ Knop, D. R.; Frost, J. W. Unpublished Results.
- ²⁵ Dell, K. A.; Frost, J.W. *J. Am. Chem. Soc.* **1993**, *115*, 11581.
- ²⁶ Wallace, J. In *Kirk-Othmer Encyclopedia of Chemical Technology*, 4th ed.; Droschwitz, J. I.; Howe-Grant, M., Eds.; Wiley: New York, 1997, 19,p. 592.
- ²⁷ Weissermel, K.; Arpe, H.-J. In *Industrial Organic Chemistry*; VCH: New York, 1997; p. 347.
- ²⁸ Weissermel, K.; Arpe, H.-J. In *Industrial Organic Chemistry*; VCH: New York, 1997; p. 347.
- ²⁹ Wallace, J. In *Kirk-Othmer Encyclopedia of Chemical Technology*, 4th ed.; Droschwitz, J. I.; Howe-Grant, M., Eds.; Wiley: New York, 1997, 19,p. 592.
- ³⁰ Wallace, J. In *Kirk-Othmer Encyclopedia of Chemical Technology*, 4th ed.; Droschwitz, J. I.; Howe-Grant, M., Eds.; Wiley: New York, 1997, 19,p. 592.
- ³¹ Eykman, J. F. *Ber. Dtch. Chem. Ges.* 1891, *24*, 1278.
- ³² Harrup, M.; Frost, J. W. Unpublished Results.
- ³³ Draths, K. M.; Knop, D. R.; Frost, J. W. *J. Am. Chem. Soc.* **1999**, *121*, 1603.
- ³⁴ Savage, P. E. *Chem. Rev.* 1999, *99*, 603.
- ³⁵ Atkins, P. In *Physical Chemistry*, 4th ed.; Oxford University Press: New York, 1994; Chapter 6.
- ³⁶ Atkins, P. In *Physical Chemistry*, 4th ed.; Oxford University Press: New York, 1994; Chapter 6.

-
- ³⁷ Cann, M. C.; Connelly, M. E. *Real World Cases in Green Chemistry*; American Chemical Society: Washington D. C., 2000; Chapter 2.
- ³⁸ Atkins, In *Physical Chemistry*, 4th ed.; Oxford University Press: New York, 1994; Chapter 6.
- ³⁹ Savage, P. E. *Chem. Rev.* 1999, 99, 603.
- ⁴⁰ (a) Savage, P. E. *Chem. Rev.* 1999, 99, 603. (b) Zurer, P. *Chem. Eng. News*, **2000**, 78, 26. (c) Bryson, T. A.; Jennings, J. M.; Gibson, J. M. *Tet. Lett.* **2000**, 41, 3523.
- ⁴¹ Zurer, P. *Chem. Eng. News*, **2000**, 78, 26.
- ⁴² Klessig, D. *Polish J. Chem.* 1993, 67, 1251.
- ⁴³ March, J. *Advanced Organic Chemistry*, 4th ed.; Wiley: New York, 1992; p. 564.
- ⁴⁴ Aalten, H. L.; van Koten, G.; Tromp, J.; Stam, C. H.; Goubitz, K.; Mak, A. N. S. *Recl. Trav. Chim. Pays-Bas.* 1989, 108, 295.
- ⁴⁵ Chandran, S. S.; Frost, J. W. Unpublished Results.
- ⁴⁶ Bonner, C. A.; Jensen, R. A. *Biochem. J.* **1994**, 302, 11.

Appendix

Introduction

Vanillin, 3-methoxy-4-hydroxybenzoic acid, is the major flavor and aroma component of vanilla extract. Isolation of vanillin from vanilla beans is a tedious process that can only supply 0.2% of the demand for vanillin flavoring.¹ Although 12,000 tons/yr² of synthetic vanillin can be produced either from waste sulfite lye obtained from wood pulping operations or from petrochemical-derived guaiacol and glyoxylic acid¹, there is a strong market demand for natural vanillin. The limited availability of vanilla beans and the marketability that comes with the label of “natural flavoring” has spawned extensive research into the use of microbial transformations to convert natural substances into vanillin.^{2,3}

One such route, developed by the Frost group, synthesized 5 g/L of vanillic acid from glucose using a recombinant *Escherichia coli* biocatalyst under fed-batch fermentor conditions (Figure 123).^{3a} Subsequent reduction of vanillic acid to vanillin was catalyzed by aryl-aldehyde dehydrogenase, partially purified from *Neurospora crassa*. This synthesis qualifies both as a route to natural vanillin and as a first step towards large-scale environmentally benign manufacture of vanillin using biocatalysis.

In order to make this process more amenable to large-scale synthesis it would be desirable to directly convert glucose to vanillin in a single microbe, thus eliminating the need for enzyme purification and co-factor recycling. The first step towards this goal is to isolate the gene encoding aryl aldehyde dehydrogenase. Subsequent expression of this gene in a vanillate-synthesizing *E. coli* biocatalyst would provide a convenient one-step

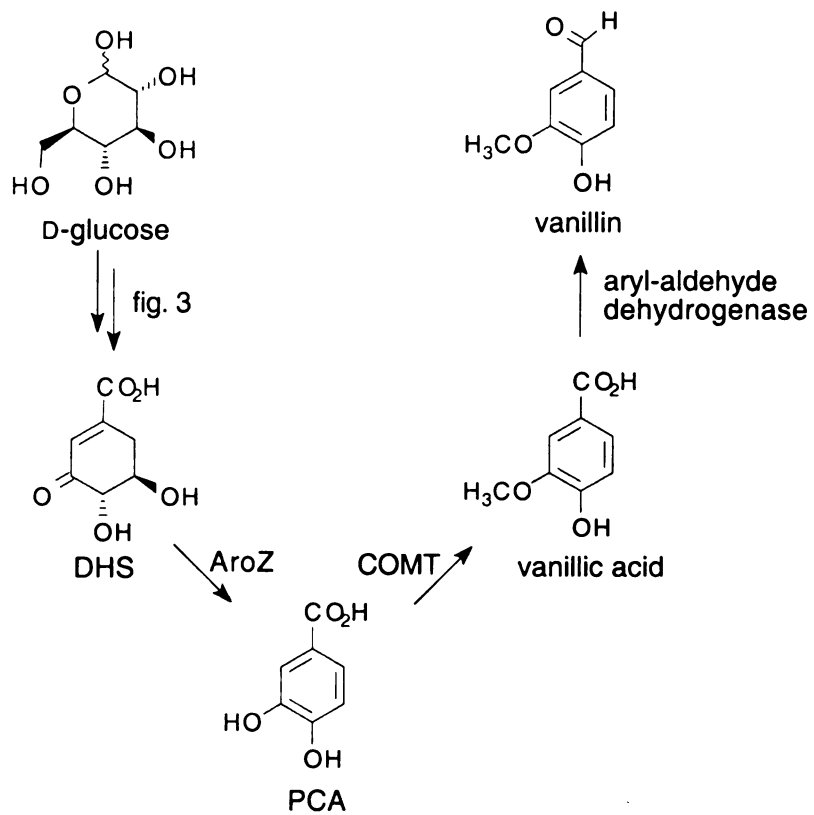


Figure 123. Synthetic Route to Natural Vanillin. Genetic loci are as follows: AroZ, DHS dehydratase and COMT, catechol-*O*-methyl transferase.

synthesis of natural vanillin. To obtain a clone of the gene encoding aryl aldehyde dehydrogenase, a cDNA library would be constructed from *N. crassa* mRNA. Since aryl aldehyde dehydrogenase is only expressed in the presence of salicylic acid, a subtractive cDNA library could be constructed. Using standard techniques, a library would be made that was enriched in cDNAs specific to growth in the presence of salicylic acid. Once a cDNA library is constructed, it must be screened to find the desired clone. A traditional method employs the use of synthetic, radio-labeled, oligonucleotide probes designed from the amino acid sequence of aryl-aldehyde dehydrogenase. The goal of the research described here was to determine the protein sequence of the amino-terminus of aryl-aldehyde dehydrogenase en route to the development of oligonucleotide probes capable of screening a cDNA library for the gene encoding aryl aldehyde dehydrogenase.

Purification of Aryl Aldehyde Dehydrogenase

Previous work has tentatively estimated the molecular weight of *N. crassa* aryl aldehyde dehydrogenase to be 120,000 Da.⁴ In order to determine the sequence of the amino-terminus of aryl aldehyde dehydrogenase, there must be a distinguishable band corresponding to this molecular weight in the SDS-PAGE gel. To perform the enzymatic reduction of vanillic acid to vanillin describe previously, aryl aldehyde dehydrogenase was partially purified by passing the mycelial lysate through DEAE cellulose and Red A columns.^{3a} SDS-PAGE analysis of the resulting protein only revealed several faint bands at the desired molecular weight necessitating additional purification of the enzyme.

Growth of *N. crassa* SY 74 was based on the method of Li and Frost.^{3a} *N. crassa* was grown on solid growth medium at 24 °C for 7 days and a mixture of mycelia and

spores were obtained. After suspension in sterilized water and filtration of the mixture through sterilized glass wool, a spore suspension was obtained. Spores (5×10^6) were used to inoculate liquid culture medium (2 L) supplemented with 10 g/L of sucrose and 1.6 g/L of sodium salicylate. After an initial lag phase, corresponding to the consumption of sucrose by the fungus, salicylic acid is reduced to salicylic alcohol, indicating aryl aldehyde dehydrogenase activity is present in the fungus. Generally, ^1H NMR analysis of the culture supernatant showed formation of salicylic alcohol to begin after 65 h. The mycelium were subsequently harvested by filtration and stored at $-20\text{ }^\circ\text{C}$.

Previous attempts to purify aryl aldehyde dehydrogenase show that a reasonable amount of purification can be obtained by passage of the mycelial lysate through a DEAE column. Therefore, this method was used as the first level of purification.^{3a,4} Generally, an 8-fold to an 11-fold purification could be obtained from the crude mycelial lysate resulting in specific activities of 0.0034 to 0.025 units/mg for aryl aldehyde dehydrogenase.

Several types of columns were examined as a second level of purification. After passage through a DEAE column, lysate was divided and passed through the following columns: Resource Q, Dye Matrex Green A, and hydroxylapatite. All three columns provided a sufficient level of purification such that three bands became distinct in the SDS-PAGE gel that corresponded to an approximate molecular weight of 120,000. In hopes of purifying away the contaminating high molecular weight proteins, crude lysate was passed sequentially through DEAE, hydroxylapatite, and Resource Q columns. SDS-PAGE analysis still showed the presence of three high molecular weight proteins (Figure 124). Therefore, all three of these proteins were submitted for sequencing.

Unfortunately, sequencing information could not be obtained on any of the proteins as blocking groups were situated on all three of the amino-termini.

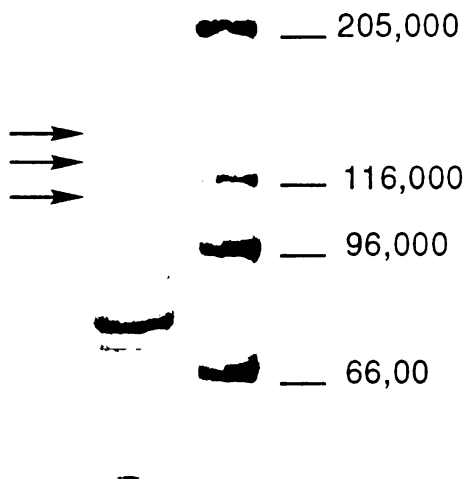


Figure 124. SDS-PAGE gel of Proteins Submitted for Sequencing.
Designated proteins were sequenced at their amino-terminus.

Molecular Weight Determination

To confirm that one of the three proteins submitted for sequencing was aryl aldehyde dehydrogenase, the molecular weight of the protein was verified using a calibrated Superdex 200 HR column. Mycelial lysate was passed through DEAE and hydroxylapatite columns and the resulting protein was injected onto the sizing column under nondenaturing conditions. The eluted protein was collected as seven fractions (Figure 125a). The fraction containing the highest specific activity was re-injected multiple times to give an average retention time of 41.03 min (Figure 125b). Based on a standard curve prepared by injecting a mixture of egg albumin (45,000), bovine albumin (66,000), yeast alcohol dehydrogenase (150,000), and β -amalyase (200,000), the native molecular weight was estimated to be 157,000 Da. The aryl aldehyde dehydrogenase-containing fraction was also co-injected with the mixture of standard proteins and appeared to co-elute with yeast alcohol dehydrogenase (Figure 125c). SDS-PAGE analysis of the aryl aldehyde dehydrogenase-containing fraction showed a significant number of bands correlating to proteins less than 156,000. This suggests that as the level of purification increases, aryl-aldehyde dehydrogenase is subject to increased protease degradation, thus hampering the purification process. Since the three high molecular weight proteins in the range of 120,000-150,000 that remained after three rounds of purification were submitted for sequencing and found to be blocked, it appears that aryl aldehyde dehydrogenase is one of the proteins blocked at its amino terminus.

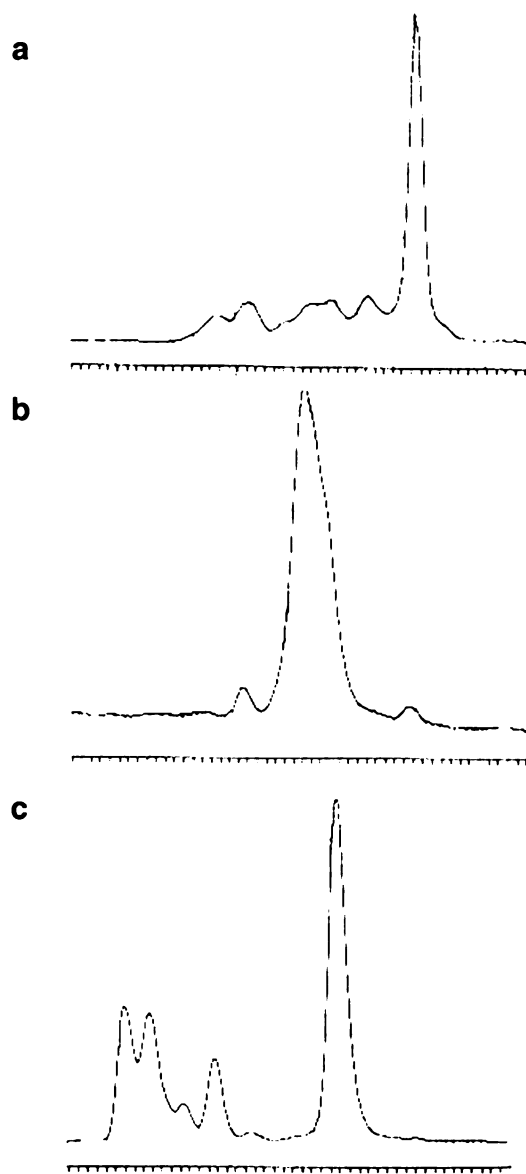


Figure 125. HPLC Trace of Eluted Protein from the Superdex Column. (a) Division of eluted protein into seven fractions. (b) Re-injection of the fraction containing aryl aldehyde dehydrogenase activity. (c) Co-injection of the fraction containing aryl aldehyde dehydrogenase activity with the standard proteins.

Colorimetric Detection of Aryl Aldehyde Dehydrogenase Activity

Because of the difficulties in obtaining sequence information from aryl aldehyde dehydrogenase, an alternative method for screening the cDNA library was examined. An expression library could be made in which the desired clone is selected based on its enzyme activity. To find the cDNA encoding aryl aldehyde dehydrogenase, the cDNA library would be cloned into an appropriate vector and transformed into a protocatechuic acid-producing *E. coli* strain. Only the desired clone would export the corresponding aldehyde of protocatechuic acid (PCA) due to aryl aldehyde dehydrogenase reduction of PCA into protocatechualdehyde. The aldehyde producing clone would be detected using a colorimetric indicator for aldehydes. One such molecule, known as pararosaniline or parafuschin (Figure 126), turns dark pink in the presence of aldehydes and is benign to microorganisms.⁵

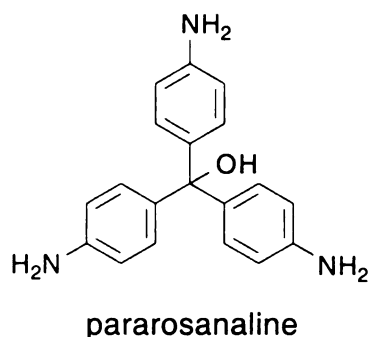


Figure 126. Structure of Pararosaniline.

In order to be a reliable screening method, pararosaniline should not turn color in the presence of colonies exporting PCA but should produce a distinguishable color in the presence of exported protocatechualdehyde. To verify that the background color

formation was minor, *E. coli* KL7/pJB1.141 was plated on Luria plates containing pararosaniline. The KL7 host strain lacks shikimate dehydrogenase activity and contains a genomic copy of *aroZ*-encoded DHS dehydratase and an additional genomic copy of *aroB*-encoded DHQ synthase.^{3a} Plasmid pJB3.141 carries inserts of *aroF*^{FBR}-encoded DAHP synthase, *serA*-encoded 3-phosphoglycerate dehydrogenase and *tktA*-encoded transketolase. When PCA-synthesizing KL3/pJB3.141 is grown in the presence of pararosaniline, pale pink colonies were observed. This color was the same as the surrounding medium due to Schiff-base formation with nonspecific aldehydes in the culture medium. To verify that a clone exporting protocatechualdehyde due to expression of aryl aldehyde dehydrogenase would be distinguishable against the background color formation, a plate was dotted with an acetone solution of protocatechualdehyde (approx. 50 mM). The resulting dark pink/orange color was rapid to develop and was persistent for several days. Based on these preliminary results, a selection scheme based on pararosaniline detection of an aldehyde-producing strain could be used to isolate the gene encoding aryl aldehyde dehydrogenase.

References

-
- ¹ (a) Esposito, L.; Formanek, K; Kientz, G.; Mauger, F.; Maureaux, V.; Robert, G.; Truchet, F. In *Kirk-Othmer Encyclopedia of Chemical Technology*; Fourth Ed., Kroschwitz, J. I.; Howe-Grant, M., Ed.; Wiley: New York, 1997; Vol 24, p 812. (b) Ranadive, A.S. In *Spices, Herbs, and Edible Fungi*; Charalambous, G., Ed.; Elsevier: Amsterdam, 1994; p 517. (c) Clark, G. S. *Perfum. Flavor.* **1990**, *15*, 45.
- ² Stentelaire, C.; Lesage-Meessen, L.; Oddou, J.; Bernard, O.; Bastin, G.; Ceccaldi, B. C.; Asther, M. *J. Biosci. Bioeng.* **2000**, *89*, 223.
- ³ (a) Li, K.; Frost J. W. *J. Am. Chem. Soc.* **1998**, *120*, 10545. (b) Li, T.; Rosazza, J. *Appl. Environ. Microbiol.* **2000**, *66*, 684.
- ⁴ Gross, G.; Bolkart, K.; Zenk, M. *Biochem. Biophys. Res. Comm.* **1968**, *32*, 173.
- ⁵ Conway, T.; Ingram, L. O. *J. Bacteriol.* **1987**, *169*, 2591.

CHAPTER FIVE

EXPERIMENTAL

I. General Methods

A. Chromatography

HPLC analysis was performed on a Rainin HPLC equipped with a Rainin C-18 Microsorb-MV column and Dynamax acquisition software. For analysis of aromatic molecules, the elution was isocratic at one mL/min using a H₂O:acetonitrile:acetic acid (85:10:5) solvent system. Solvents were routinely filtered through 0.45- μ m membranes (Gelman Science) and degassed under reduced pressure for 30 min prior to use. Analytes were detected at 250 nm.

Gas chromatography was performed on a Hewlett Packard 890GC fitted with a J & W Scientific DB-5 capillary column using He as the carrier gas. Temperature programming began with an initial temperature of 100 °C maintained for 3 min. The temperature was then ramped up to 300 °C at a rate of 15 °C/min and held at the final temperature for 1 min. The split injector was maintained at a temperature of 300 °C and the FID detector was maintained at 350 °C. An injection volume of 2 μ L was typically employed.

AG1-x8 (acetate and chloride form), diethylaminoethyl cellulose (DEAE), and hydroxylapatite Bio-Gel HTP gel were purchased from Biorad. Phosphate from used AG 1-x8 (acetate) was removed by passing 4 to 6 column volumes of 2 N NaOH through the column until effluent was free of inorganic phosphate. Dye Matrix Green A gel was

obtained from Amicon. Resource RPC (1 mL and 6 mL) Resource Q and Superdex 200 HR 10130 columns were purchased from Amersham Pharmacia Biotech. Hydroxylapatite was slurried in degassed H₂O before column packing. After elution with three column volumes of H₂O, the column was equilibrated with 3 column volumes of degassed buffer H. Dowex 50 (200-400, H⁺) was obtained from Sigma. Previously used Dowex 50 was cleaned using the following procedure: The pH of an aqueous suspension of resin was adjusted to pH 14 by addition of solid KOH. Bromine was added to the solution until the suspension turned a golden yellow color. Additional bromine was added (1-2 mL) to obtain a saturated solution. The mixture was left to stand at room temperature overnight and the Dowex 50 resin was collected by filtration and washed exhaustively with water and 6 N HCl. Dowex 50 (H⁺) was stored at 4 °C.

B. Spectroscopic Measurements.

Routine ¹H NMR spectra were recorded on a Varian VXR-300 FT-NMR spectrometer (300 MHz). Additional ¹H NMR spectra were recorded on a VXR-500 FT-NMR (500 MHz). Chemical shifts were reported in parts per million (ppm) downfield from internal sodium 3-(trimethylsilyl)propionate-2,2,3,3-*d*₄ (TSP, δ = 0.00) with D₂O as the solvent. TSP was purchased from Lancaster Synthesis Inc. UV and visible measurements were recorded on a Perkin-Elmer Lambda 3b UV-Vis spectrophotometer or on a Hewlett Packard 8452A Diode Array Spectrophotometer equipped with HP 89532A UV-Visible Operating Software.

C. Bacterial Strains and Plasmids.

E. coli DH5 α [*F'* *endA1 hsdR17(r_Km⁺_K) supE44 thi-1 recA1 gyrA relA1 ϕ 80lacZ Δ M15 Δ (*lacZYA-argF*)_{U169}]* and RB791 (W3110 *lacL8I^o*) were obtained previously by this laboratory. *E. coli* KL3 [AB2834 *aroE3353 malA352 (λ) serA::aroB*] was previously generated in this laboratory. *E. coli* CL451 [*aroD25::Tn10*] was obtained from Professor Bruce Stocker. *Klebsiella pneumoniae* KP62-1 was obtained from the American Type Culture Collection (ATCC 25306). Plasmid pNE130 was obtained from the laboratory of Professor David Ballou. The pBluescript plasmid containing the SP3 cDNA was obtained from Professor Carol Bonner.

D. Storage of Bacterial Strains and Plasmids.

All bacterial strains were stored at -78 °C in glycerol. Plasmids were transformed into DH5 α for long-term storage. Glycerol samples were prepared by adding 0.75 mL of an overnight culture to a sterile vial containing 0.25 mL of 80% (v/v) glycerol. The solution was mixed, left at room temperature for 2 h, and then stored at -78 °C.

E. Culture Medium

All solutions were prepared in distilled, deionized water. LB medium contained (1 L) Bacto tryptone (10 g), Bacto yeast extract (5 g), and NaCl (10 g). L-Broth (1 L) contained Bacto tryptone (10 g), Bacto yeast extract (5 g), NaCl (5 g), glucose (1 g), and L-cysteine (0.03 g). M9 salts (1 L) contained Na₂HPO₄ (6 g), KH₂PO₄ (3 g), NH₄Cl (1 g), and NaCl (0.5 g). M9 minimal medium contained D-glucose (10 g), MgSO₄ (0.12 g), and thiamine hydrochloride (0.001 g) in 1 L of M9 salts. M9 medium (1 L) was

supplemented where appropriate with L-phenylalanine, L-tyrosine, L-tryptophan, and L-serine to a final concentration of 40 $\mu\text{g/mL}$ and with *p*-hydroxybenzoic acid, potassium *p*-aminobenzoate, and 2,3-dihydroxybenzoic acid to a final concentration of 10 $\mu\text{g/mL}$. Antibiotics were added where required to the following final concentrations: chloramphenicol (Cm), 20 $\mu\text{g/mL}$; ampicillin (Ap), 50 $\mu\text{g/mL}$; spectinomycin (Spec), 50 $\mu\text{g/mL}$; tetracycline (Tc), 12.5 $\mu\text{g/mL}$; and kanamycin (Kan), 50 $\mu\text{g/mL}$. Isopropyl β -D-thiogalactopyranoside (IPTG) was added to the culture medium of strains containing inducible *tac* or *T7* promoters. Inorganic salts, D-glucose, and MgSO_4 solutions were autoclaved separately while thiamine hydrochloride, amino acids, aromatic vitamins, antibiotic stock solutions, and IPTG were sterilized through 0.22- μm membranes. Solid LB and M9 medium were prepared by the addition to 1.5% (w/v) Difco agar to the liquid medium. L-Broth plates were prepared by the addition of 1% (w/v) Difco agar and CaCl_2 (2.5 mM) to the liquid medium. A 0.5 M stock solution of CaCl_2 was prepared and autoclaved separately. Soft agar contained (per L) Bacto tryptone (10 g), Bacto yeast extract (5 g), and Difco agar (5.5 g).

Fermentation medium (1 L) contained K_2HPO_4 (7.5 g), citric acid monohydrate (2.1 g), ammonium iron (III) citrate (0.3 g), and concentrated H_2SO_4 (1.2 mL). Culturing of JB161, JB161(DE3), KL3, 98042-42, and JB4 required addition of L-phenylalanine (0.71 g), L-tyrosine (0.71 g), and L-tryptophan (0.35 g) to the fermentation medium (1 L). The fermentation medium was adjusted to pH 7.0 with concentrated NH_4OH prior to autoclaving. Before inoculation, the following supplements were added to the fermentation medium (1 L): D-glucose, MgSO_4 (0.24 g), and trace minerals including $(\text{NH}_4)_6(\text{Mo}_7\text{O}_{24}) \cdot 4\text{H}_2\text{O}$ (0.0037 g), $\text{ZnSO}_4 \cdot 7\text{H}_2\text{O}$ (0.0029 g), H_3BO_3 (0.0247 g), $\text{CuSO}_4 \cdot$

5H₂O (0.0025 g), and MnCl₂ · 4H₂O (0.0158 g). Culturing of KL3 and JB4 also required the addition of aromatic vitamins *p*-hydroxybenzoic acid (0.01 g), potassium *p*-aminobenzoate (0.01 g), and 2,3-dihydroxybenzoic acid (0.01 g) to the fermentation medium (1 L). Solutions of D-glucose and MgSO₄ were autoclaved separately while the trace minerals and aromatic vitamins were filtered through sterile 0.22-μm membranes.

F. General Fed-Batch Fermentation Conditions.

Fermentations were conducted in a B. Braun M2 culture vessel with a 2 L working capacity. The vessel was modified using a stainless steel baffle cage containing four 1/4" x 4" baffles for all fermentations except those using KL3/pKL4.130B and JB4/pJB5.291. Environmental conditions were supplied by a B. Braun Biostat MD controlled by a DCU-1. Data was acquired on a Dell Optiplex Gs+ 5166M personal computer utilizing B. Braun MFCS/Win software. PID control loops were used to control temperature, pH, and glucose addition. The temperature was maintained at 33 °C or 36 °C, and the pH was maintained at 7.0 by addition of NH₄OH or 2 N H₂SO₄. Glucose was added as a 65% (w/v) solution for KL3/pKL4.130B and JB4/pJB5.291 and as a 40% (w/v) solution for all other strains. Dissolved oxygen (D.O.) was monitored using a Mettler-Toledo 12 mm sterilizable O₂ sensor fitted with an Ingold A-type O₂ permeable membrane. D.O. was maintained at 10% air saturation throughout the course of JB4/pJB5.291 the fermentations and 20% for all other fermentations. Antifoam (Sigma 204) was manually pumped into the vessel as needed.

Inoculants were initiated by introduction of a single colony into 5 mL of M9 medium and grown at 37 °C with agitation for 12-36 h until the culture was turbid. After

this time, the starter cultures were transferred to 100 mL of M9 medium and grown for an additional 12 to 24 h at 37 °C and 250 rpm. For JB161/pJB2.274, 98042-42, and JB161(DE3)/pJB3.144B, M9 medium was supplemented with aromatic amino acids. For KL3/pKL4.130B and JB4/pJB5.291, M9 medium was supplemented with aromatic amino acids and aromatic vitamins. After an appropriate OD_{600} was reached (1.0-3.0), the inoculant was transferred to the fermentation vessel. The initial glucose concentration in the fermentation medium was 15 g/L for JB161/pJB2.274, JB161(DE3)/pJB3.144B, and 98042-42, 17 g/L for RB38/pJB2.274 and RB38(DE3)/pJB3.144B, 23 g/L for KL3/pKL4.130B, and 30 g/L for JB4/pJB5.291.

Three staged methods were used to maintain D.O. levels at 10% (shikimic acid-producing strains) or 20% (PHB and DHS-producing strains) air saturation during the course of the run. With the airflow at an initial setting of 0.06 L/L/min, D.O. concentration was maintained by increasing the impeller speed from its initial set point of 50 rpm to its preset maximum of 500 rpm. The preset maximum impeller speed for fermentations using KL3/pKL4.130B and JB4/pJB5.291 was 940 rpm. When the impeller reached its preset maximum, the mass flow controller then maintained D.O. levels by increasing the airflow rate from 0.06 L/L/min to a preset maximum of 1.0 L/L/min. At constant impeller speed and constant airflow rate, D.O. levels were finally maintained at 10% or 20% air saturation for the remainder of the fermentation by oxygen sensor-controlled glucose feeding. PID control parameters were set to 0.0 (off) for the derivative control (τ_D), and 999.9 s (minimum control action) for integral control (τ_I). X_p was set to 950.0% to achieve a K_c of 0.1. All strains were cultured in the fermentation vessel for a total of 72 h except KL3/pKL4.130B, which was cultured for 54 h. Isopropyl

β -D-thiogalactopyranoside (IPTG, 10 mg) was added every six hours beginning at the third phase of growth for fermentations using JB161(DE3)/pJB3.144B and RB38(DE3)/pJB3.144B. IPTG (10 mg/mL) was sterilized through 0.22- μ m membranes prior to addition. *p*-Hydroxybenzoic acid was added to a fermentor run of KL3/pKL4.130B to a final concentration of 10 g/L. *p*-Hydroxybenzoic acid was divided into two 5 g portions that were added at the beginning of the third stage of growth and 2 h later. *p*-Hydroxybenzoic acid (5 g) was dissolved in 50 mL of H₂O, neutralized to pH 7.0 with NaOH, and filtered through a sterile 0.22- μ m membrane.

G. Analysis of Culture Supernatant.

For strains being evaluated in shake flasks, samples (3-5 mL) of the culture were taken at timed intervals and the cells were removed by centrifugation using a Beckman microcentrifuge. Samples (5 mL) of fermentation broth were taken at indicated intervals. Cell densities were determined by dilution of fermentation broth with water (1:100) followed by measurement of absorption at 600 nm (OD₆₀₀). Dry cell weight for *E. coli* (g/L) was obtained using a conversion coefficient of 0.43 g/L/OD₆₀₀. The remaining fermentation broth was centrifuged using a Beckman microcentrifuge to obtain cell-free broth.

Solute concentrations in the cell-free culture supernatant were determined by ¹H NMR. For ¹H NMR quantitation of solute concentrations, solutions were concentrated to dryness under reduced pressure, concentrated to dryness on additional time from D₂O, and then redissolved in D₂O containing a known concentration of the sodium salt of 3-(trimethylsilyl)propionic-2,2,3,3-*d*₄ acid (TSP). Concentrations were determined by

comparison of the integrals corresponding to each compound with the integral corresponding to TSP ($\delta=0.00$ ppm) in the ^1H NMR. Compounds were quantitated using the following resonances: *p*-hydroxybenzoic acid (7.88 ppm, d, 2 H), prephenic acid (6.00 ppm, m, 4 H), L-phenylalanine (7.38 ppm, m, 5 H), L-tyrosine (7.20 ppm, d, 2 H), 3-dehydroshikimic acid (4.28 ppm, d, 1 H), 3-deoxy-D-*arabino*-heptulosonic acid (1.80 ppm, t, 1 H), acetate (1.92 ppm, s, 3 H), shikimic acid (4.57 ppm, d, 1 H), quinic acid (4.16 ppm, m, 1 H), and 3-*epi*-shikimic acid (3.49 ppm, t, 1 H).

II. Genetic Manipulations.

A. General Procedures

Standard protocols were used for construction, purification, and analysis of plasmid DNA.¹ *E. coli* DH5 α was used as the host strain for plasmid manipulations. T4 DNA ligase, Large Fragment of DNA polymerase I (Klenow fragment) and agarose (electrophoresis grade) were purchased from either Gibco BRL Products. Restriction enzymes were purchased from Gibco BRL Products or New England Biolabs. Calf intestinal alkaline phosphatase was purchased from Roche Molecular Biochemicals. The λ DE3 lysogenization kit was purchased from Novagen. PCR amplifications were performed as described by Sambrook.¹ Each reaction (0.1 mL) contained 10 mM KCl, 20 mM Tris-HCl (pH 8.8), 10 mM $(\text{NH}_4)_2\text{SO}_4$, 2 mM MgSO_4 , 0.1% Triton X-100, dATP (0.2 mM), dCTP (0.2 mM), dGTP (0.2 mM), dTTP (0.2 mM), template DNA (0.02 μg or 1 μg), 0.5 μM of each primer, and 2 units of Vent polymerase. Primers were synthesized by the Macromolecular Structure Facility at Michigan State University.

Phenol was prepared by addition of 0.1% (w/v) 8-hydroxyquinoline to distilled, liquefied phenol. Two extractions with an equal volume of 1 M Tris-HCl (pH 8.0) was followed by extraction with 0.1 M Tris-HCl (pH 8.0) until the pH of the aqueous layer was greater than 7.6. Phenol was stored at 4 °C under an equal volume of 0.1 M Tris-HCl (pH 8.0). SEVAG was a mixture of chloroform and isoamyl alcohol (24:1 v/v). TE buffer contained 10 mM Tris-HCl (pH 8.0) and 1 mM disodium EDTA (pH 8.0). Endostop solution (10X concentration) contained 50% glycerol (v/v), 0.1 M disodium EDTA, pH 7.5, 1% sodium dodecyl sulfate (SDS) (w/v), 0.1% bromophenol blue (w/v), and 0.1% xylene cyanole FF (w/v) and was stored at 4 °C. Prior to use, 0.12 mL of DNAase-free RNAase was added to 1 mL of 10X Endostop solution. DNAase-free RNAase (10 mg/mL) was prepared by dissolving RNAase in 10 mM Tris-Cl (pH 7.5) and 15 mM NaCl. DNAase activity was inactivated by heating the solution at 100 °C for 15 min. Aliquots were stored at -20 °C.

B. Large Scale Purification of Plasmid DNA.

Plasmid DNA was purified on a large scale using a modified lysis method described by Sambrook et al. In a 2 L Erlenmeyer flask, 500 mL of LB medium containing the appropriate antibiotic was inoculated from a single colony, and the culture was incubated at 37 °C or 30 °C for approximately 15 h with agitation at 250 rpm. Cells were harvested by centrifugation (4000g, 5 min, 4 °C) and then resuspended in 10 mL of cold solution 1 (50 mM glucose, 20 M Tris-HCl, pH 8.0, 10 mM EDTA, pH 8.0) into which lysozyme (5 mg/mL) had been added immediately before use. The suspension was

stored at room temperature for 5 min. Addition of 20 mL of solution 2 (1% SDS (w/v) in 0.2 N NaOH) was followed by gentle mixing and storage on ice for 15 min. Fifteen milliliters of ice cold solution 3 (3 M KOAc, prepared by combining 60 mL of 5 M potassium acetate, 11.5 mL of glacial acetic acid, and 28.5 mL of H₂O) was added. Vigorous shaking resulted in formation of a white precipitate. After the suspension was stored on ice for 10 min, the cellular debris was removed by centrifugation (48000g, 20 min, 4 °C). The supernatant was transferred to two clean centrifuge bottles and isopropanol (0.6 volumes) was added to precipitate the DNA. After the samples were left at room temperature for 15 min, the DNA was recovered by centrifugation (20000g, 20 min, 4 °C). The DNA pellet was then rinsed with 70% ethanol and dried.

The isolated DNA was dissolved in TE (3 mL) and transferred to a Corex tube. Cold 5 M LiCl (3 mL) was added and the solution was gently mixed. The sample was then centrifuged (12000g, 10 min, 4 °C) to remove high molecular weight RNA. The clear supernatant was transferred to a clean Corex tube and isopropanol (6 mL) was added followed by gentle mixing. The precipitated DNA was collected by centrifugation (12000g, 10 min, 4°C). The DNA was then rinsed with 70% ethanol and dried. After redissolving the DNA in 0.5 mL of TE containing 20 µg/mL of RNAase, the solution was transferred to a 1.5 mL microcentrifuge tube and stored at rt for 30 min. DNA was precipitated from solution upon addition of 500 µL of 1.6 M NaCl containing 13% polyethylene glycol (PEG-8000) (w/v) (Sigma). The solution was mixed and centrifuged (microcentrifuge, 10 min, 4 °C) to recover the precipitated DNA. The supernatant was removed and the DNA was then redissolved in 400 µL of TE. The sample was extracted sequentially with phenol (400 µL), phenol and SEVAG (400 µL each), and finally

SEVAG (400 μ L). Ammonium acetate (10 M, 100 μ L) was added to the aqueous DNA solution. After thorough mixing, 95% ethanol (1 mL) was added to precipitate the DNA. The sample was left at room temperature for 5 min and then centrifuged (microcentrifuge, 5 min, 4 $^{\circ}$ C). The DNA was rinsed with 70% ethanol, dried, and then redissolved in 250-500 μ L of TE.

The concentration of DNA in the sample was determined as follows: an aliquot (10 μ L) of the DNA solution was diluted to 1 mL in TE and the absorbance at 260 nm was measured relative to the absorbance of TE. The DNA concentration was calculated based on the fact that the absorbance at 260 nm of 50 μ g/mL of double stranded DNA is 1.0.

C. Small Scale Purification of Plasmid DNA.

An overnight culture (5 mL) of the plasmid-containing strain was grown in LB medium containing the appropriate antibiotics. Cells from 3 mL of the culture were collected in a 1.5 mL microcentrifuge tube by centrifugation. The harvested cells were resuspended in 0.1 mL of cold solution 1 into which lysozyme (5 mg/mL) had been added immediately before use and the solution was stored on ice for 10 min. Addition of solution 2 (0.2 mL) was followed by gentle mixing and storage on ice for 5-10 min. Solution 3 (0.15 mL) was added to the sample and shaken vigorously. The sample was stored on ice for 5 min and the cellular debris was removed by centrifugation (microcentrifuge, 15 min, 4 $^{\circ}$ C). The supernatant was transferred to another microcentrifuge tube and extracted with equal volumes of phenol and SEVAG (0.2 mL each). The aqueous phase (approximately 0.5 mL) was transferred to a fresh microfuge

tube and the DNA was precipitated by the addition of 95% ethanol (1 mL). The sample was left at room temperature for 5 min before centrifugation (15 min, rt) to isolate the DNA. The DNA pellet was rinsed with 70% ethanol, dried, and redissolved in 50-100 μ L TE. DNA isolated from this method was used for restriction enzyme analysis and the concentration was not determined by spectroscopic methods.

D. Restriction Enzyme Digestion of DNA.

Restriction enzyme digests were performed using buffer solutions supplied by Gibco BRL or New England Biolabs. A typical digest (20 μ L) contained approximately 0.8 μ L of DNA (0.1 μ g/ μ L in TE), 2 μ L of restriction enzyme buffer (10X concentration), 1 μ L of restriction enzyme, 1 μ L of Bovine Serum Albumin (BSA) (2 mg/mL), and 8 μ L of TE. Reactions were incubated at 37 °C for 1 h. Digests were terminated by addition of 2 μ L of Endostop solution (10X concentration) and subsequently analyzed by agarose gel electrophoresis. When DNA was required for subsequent cloning, restriction digests were terminated by addition of 1 μ L of 0.5 M EDTA (pH 8.0) followed by extraction of the DNA with equal volumes of phenol and SEVAG and precipitation of the DNA. DNA was precipitated by addition of 0.1 volume of 3 M NaOAc (pH 5.2) followed by thorough mixing and the addition of 3 volumes of 95% ethanol. Samples were stored for at least one h at -78 °C. Precipitated DNA was recovered by centrifugation (15 min, 4 °C). DNA was dried with 70% ethanol and redissolved in TE.

E. Agarose Gel Electrophoresis.

Agarose gels were run in TAE buffer containing 40 mM Tris-acetate and 2 mM EDTA (pH 8.0). Gels typically contained 0.7% agarose (w/v) in TAE buffer. Lower concentrations of agarose (0.3%) were used to resolve genomic DNA (note: electrophoresis was done at 4 °C). Ethidium bromide (0.5 µg/ml) was added to the agarose to allow visualization of DNA fragments under an UV lamp. The size of the DNA fragments were determined by using two sets of DNA standards: λ DNA digested with *Hind*III (23.1-kb, 9.4-kb, 6.6-kb, 4.4-kb, 2.3-kb, 2.0-kb, and 0.6-kb) and λ DNA digested with *Eco*RI and *Hind*III (21.2-kb, 5.1-kb, 5.0-kb, 4.3-kb, 3.5-kb, 2.0-kb, 1.9-kb, 1.6-kb, 1.4-kb, 0.9-kb, 0.8-kb, and 0.6-kb).

F. Isolation of DNA from Agarose

The band of agarose containing the DNA of interest was excised from the gel and chopped thoroughly with a razor in a plastic weighing tray. The agarose was then transferred to a spin column consisting of a 500 µL microfuge tube packed tightly with glass wool and a tiny hole in its bottom. The spin column was then placed in a 1.5 mL microfuge tube and centrifuged for 5 min using a Beckman microfuge to separate the DNA solution from the agarose. The collected DNA was precipitated with 3 M NaOAc and 95% ethanol as previously described and redissolved in TE.

G. Treatment of Vector DNA with Calf Intestinal Alkaline Phosphatase.

Following restriction enzyme digestion, plasmid vectors were dephosphorylated to prevent self-ligation. Digested vector DNA was dissolved in TE (88 µL). To this

sample was added 10 mL of dephosphorylation buffer (10X concentration) and 2 μ L of calf intestinal alkaline phosphatase (2 units). The reaction was incubated at 37 °C for 1 h. The phosphatase was inactivated by the addition of 1 μ L of 0.5 M EDTA (pH 8.0) followed by heat treatment (65 °C, 20 min). The sample was extracted with phenol and SEVAG (100 μ L each) to remove the protein, and the DNA was precipitated as previously described and redissolved in TE.

H. Treatment of DNA with Klenow Fragment.

DNA fragments with recessed 3' termini were modified to DNA fragments with blunt ends by treatment with the Klenow fragment of *E. coli* DNA polymerase I. After restriction digestion (20 μ L) of the DNA (0.8-2 μ g) was complete, a solution (1 μ L) containing each of the four dNTP's was added to a final concentration of 1 mM. Addition of 1-2 units of Klenow fragment was followed by incubation at rt for 30 min. Since the Klenow fragment works well in the common restriction enzyme buffers, there was no need to purify the DNA after restriction digestion and prior to filling recessed 3' termini. Klenow reactions were quenched by extraction with equal volumes of phenol and SEVAG. DNA was recovered by precipitation as described previously and redissolved in TE.

I. Ligation of DNA.

DNA ligations were designed so that the molar ratio of insert DNA to vector DNA was 3 to 1. A typical ligation reaction contained 0.03 to 0.1 μ g of vector DNA and 0.05 to 0.2 μ g of insert DNA in a combined volume of 7 μ L. To this sample, 2 μ L of

ligation buffer (5X concentration) and 1 μ L of T4 DNA ligase (2 units) was added. The reaction was incubated at 16 °C for at least 4 h and then was used to transform competent cells.

J. Preparation and Transformation of Competent Cells.

Competent cells were prepared using a procedure modified from Sambrook et al.² An aliquot (1 mL) from an overnight culture (5 mL) was used to inoculate 100 mL of LB containing the appropriate antibiotics. The cells were cultured at 37 °C with shaking at 250 rpm until the OD₆₀₀ was between 0.4 and 0.6. The culture was transferred to a centrifuge bottle that had been sterilized with bleach and rinsed exhaustively with sterile water. The cells were harvested by centrifugation (4000g, 5 min, 4 °C) and the culture medium was discarded. All manipulations were carried out on ice during the remainder of the procedure. The harvested cells were resuspended in ice cold 0.9% NaCl (100 mL) and the cells were reisolated by centrifugation (4000g, 5 min, 4 °C). The cells were resuspended in ice cold 100 mM CaCl₂ (50 mL) and stored on ice for 30 min. After centrifugation (4000g, 5 min, 4 °C), the cells were resuspended in 4 mL of ice cold 100 mM CaCl₂ containing 15% glycerol (v/v). Aliquots (0.25 mL) of competent cells in 1.5 mL microfuge tubes were frozen in liquid nitrogen and stored at -78 °C.

Frozen competent cells were thawed on ice for 5 min before transformation. A small aliquot (1 to 10 μ L) of plasmid DNA or a ligation reaction was added to the thawed competent cells (0.1 mL). The solution was gently mixed and stored on ice for 30 min. The cells were then heat shocked at 42 °C for 2 min and placed on ice briefly (1.5 min). LB (0.5 mL, no antibiotics) was added to the cells, and the sample was incubated at 37

°C (no agitation) for at least 1 h. Cells were collected by centrifugation in a Beckman microcentrifuge. If the transformation was to be plated onto LB plates, 0.5 mL of the culture supernatant was removed and the cells resuspended in the remaining 0.1 mL of LB, and spread onto plates containing the appropriate antibiotics. If the transformation was to be plated onto minimal medium plates, the cells were washed once with a solution of M9 inorganic salts. After resuspension in fresh solution of M9 inorganic salts (0.1 mL), the cells were spread onto the plates. A sample of competent cells with no DNA added was also carried through the transformation procedure as a control. These cells were used to check the viability of the competent cells and to verify the absence of growth on selective medium.

K. Purification of Genomic DNA.

An aliquot (1 mL) from an overnight culture (5 mL) was used to inoculate 100 mL of LB containing the appropriate antibiotics. The cells were cultured at 30 °C with shaking at 250 rpm for approximately 12 h. The cells were harvested by centrifugation (4000g, 5 min, 4 °C) and the culture medium was discarded. The harvested cells were resuspended in 9.5 mL of TE and transferred to a small (45 mL) centrifuge bottle and 0.5 mL of 10 % SDS and 0.05 mL of freshly prepared proteinase K (20 mg/mL) was added. The mixture was incubated for 1 h at 37 °C followed by the addition of 1.8 mL of 5 M NaCl. The sample was mixed thoroughly and 1.5 mL of CTAB/NaCl solution (aqueous solution containing 0.041 g/mL of NaCl and 0.1 g/ mL of hexadecyltrimethylammonium bromide) was added. After mixing thoroughly, the sample was incubated at 65 °C for 20 min. The sample was transferred to two Corex tubes and extracted with an equal volume

of SEVAG. After centrifugation (6000g, 10 min, 4 °C), the clear, aqueous portion was transferred to fresh Corex tubes and the DNA was precipitated by the addition of 0.6 volumes of isopropanol to each Corex tube. All transfers of aqueous layers were carried out using large bore pipette tips to minimize shearing of the genomic DNA. After storage for 2 h at room temperature, threads of DNA were spooled onto a flame-sealed Pasteur pipette and transferred to a single Corex tube containing 70 % ethanol. The ethanol was removed, the DNA was dried, and resuspended in 1 mL of TE. To this solution, 10 µL of RNAase (10 mg/ml) was added and the solution was stored at rt for 4 h. After a combined extraction with phenol (1 mL) and SEVAG (1 mL), 0.1 mL of 3 M NaOAc (pH 5.2) was added to the aqueous layer and mixed thoroughly. DNA was precipitated by the addition of 3 mL of 95% ethanol. After storage at rt for 1.5 h the DNA threads were spooled onto a flame-sealed Pasteur pipette and dipped into 1 mL of 70% ethanol. The spooled DNA was transferred to a 1.5 mL microfuge tube, dried, and redissolved in 0.5 mL of TE. DNA was quantified as described for the large scale preparation of plasmid DNA.

L. Generation of P1 lysate.

A single colony was introduced into 5 mL of LB medium containing the appropriate antibiotic and grown overnight at 37 °C with agitation. A portion of the culture (0.1 mL) was transferred into a series of sterile 13 x 100 mm tubes containing serial dilutions of P1-RB791 in LB medium. To each tube, 4 mL of soft agar (45 °C) was added and the tube was quickly vortexed and poured onto a pre-warmed L-broth plate.

The plates were incubated at 37 °C for 10 to 12 h. A plate was selected that contained confluent lysis (a plate that has an even distribution of lysed cells), 4 mL of L-broth was placed on top of the plate, and it was stored at 4 °C overnight. The following day, the L-broth was removed from the top of the agar and transferred to a centrifuge tube. Chloroform (4 mL) was added and the mixture was vortexed. The aqueous layer was aliquoted (1 mL) into 1.5 mL microfuge tubes containing 0.2 mL of CHCl₃ and stored at 4 °C.

M. P1 Transduction

A single colony was introduced into 5 mL of LB medium containing the appropriate antibiotics and grown overnight at 37 °C with agitation. The cells were harvested by centrifugation and resuspended in 2.5 mL of a sterile solution containing 100 mM MgSO₄ and 5 mM CaCl₂. Cells were then incubated at 37 °C for 20 min with agitation. A portion of the culture (0.1 mL) was transferred into a series of sterile microfuge tubes containing serial dilutions of the desired P1 phage in LB medium. Samples were incubated at 37 °C for 20 min without agitation. To each tube, 0.2 mL of 1 M sodium citrate (pH 7.0) was added to quench absorption of the phage. The samples were centrifuged and the cells resuspended in 0.2 mL of LB medium containing sodium citrate (29.4 g/L, pH 7) and incubated at 37 °C for 1 h without agitation. Cells were plated on LB medium containing the appropriate antibiotic. A sample of cells without added phage and one with phage only were carried through the procedure as a control. These controls should not be able to grow on the selective medium.

N. λ DE3 Lysogeny.

The λ DE3 lysogeny was performed according to the protocol provided by Novagen. The λ DE3 lysate (2.5×10^{10} pfu/mL), Helper phage lysate (3.6×10^{10} pfu/mL), and Selection phage lysate (5.6×10^{10} pfu/mL) were stored at -78 °C and thawed on ice immediately before use. A colony of the desired strain was inoculated into 5 mL of LB containing the appropriate antibiotics, 0.2% maltose and 10 mM MgSO_4 . The maltose stock solution was sterilized by passage through 0.22- μm membranes and the MgSO_4 solution was separately autoclaved. The culture was grown at 37 °C with agitation until the OD_{600} reached 0.5. Various amounts (1, 3, 5, 7, 10 μL) of the culture were transferred to individual microfuge tubes. λ DE3 lysate (4 μL), Helper phage lysate (2.78 μL), and Selection phage lysate (1.79 μL) were added to each tube and mixed gently. The host/phage mixture was incubated at 37 °C for 20 min. The mixture was plated onto LB plates with appropriate antibiotics and incubated overnight at 37 °C. Several of the resulting colonies were selected, transformed with a plasmid containing an assayable gene under a *T7* promoter, and the specific activity of the enzyme expressed from the *T7* promoter was measured. The host strain providing the highest specific activity was chosen and named as the (DE3) strain.

III. Enzyme Assays.

A. General.

After collection and resuspension in the proper buffer, the harvested cells were disrupted by two passages through a French pressure cell (SLM Aminco) at 16000 psi.

Cellular debris was removed from the lysate by centrifugation (30000g, 30 min, 4 °C). Protein concentrations were determined using the Bradford dye-binding procedure.³ Protein assay solution was purchased from Bio-Rad. Protein concentrations were determined by comparison to a standard curve prepared using bovine serum albumin.

B. DAHP Synthase.

DAHP synthase was assayed according to the procedure described by Schoner.⁴ A portion (20 mL) of the fermentation broth was removed from the vessel at the indicated intervals and centrifuged at 3000g for 5 min at 4 °C. The harvested cells were resuspended in 5 mL of DAHP synthase lysate buffer (50 mM potassium phosphate, pH 6.5, 10 mM PEP, and 0.05 mM CoCl₂) and stored at -80 °C. Samples were analyzed for enzyme activities when the fermentor run was complete. The cellular lysate was obtained as described above and diluted in potassium phosphate buffer (50 mM, pH 7.0) containing PEP (0.5 mM), and 1,3-propanediol (250 mM). A dilute solution of E4P was first concentrated to 12 mM by rotary evaporation and neutralized with 5 N KOH. Two different solutions were prepared and incubated separately at 37 °C for 5 min. The first solution (1 mL) contained E4P (6 mM), PEP (12 mM), ovalbumin (1 mg/mL), and potassium phosphate (25 mM, pH 7.0). The second solution (0.5 mL) consisted of the diluted lysate. After the two solutions were mixed (time = 0), aliquots (0.15 mL) were removed at timed intervals and quenched with 0.1 mL of 10% trichloroacetic acid (w/v). Precipitated protein was removed by centrifugation and the DAHP in each sample was quantified using thiobarbituric acid as described below.

An aliquot (0.1 mL) of the DAHP containing sample was reacted with 0.1 mL of 0.2 M NaIO₄ in 8.2 M H₃PO₄ at 37 °C for 5 min. The reaction was quenched by addition of 0.8 M NaAsO₂ in 0.5 M Na₂SO₄ and 0.1 M H₂SO₄ (0.5 mL) and vortexed until a dark brown color disappeared. Upon addition of 3 mL of 0.04 M thiobarbituric acid in 0.5 M Na₂SO₄ (pH 7), the sample was heated at 100 °C for 15 min. Samples were cooled (2 min), and the pink chromophore was then extracted into distilled cyclohexanone (4 mL). The aqueous and organic layers were separated by centrifugation (2000g, 15 min). The absorbance of the organic layer was recorded at 549 nm ($\epsilon = 68000 \text{ L/mol/cm}$). One unit of DAHP synthase activity was defined as the formation of 1 μmol of DAHP per min at 37 °C.

C. Chorismate Lyase.

Chorismate lyase activity of fermentor grown cells was measured in crude lysate prepared for the DAHP synthase assay. Lysate was diluted either 1:10 or 1:100 with chorismate lyase buffer A (50 mM Tris-HCl, pH 7.5, 10 mM β -mercaptoethanol). The reaction (1 mL) contained 0.15 mM NADPH, 5 μM FAD, 2.8 units of *p*-hydroxybenzoate hydroxylase, diluted cellular lysate (10-100 μL) and the corresponding volume of chorismate lyase buffer B (50 mM Tris-HCl pH 7.5, 5 mM EDTA, 10 mM β -mercaptoethanol) to obtain a final volume of 0.98 mL. The slope of this enzyme mixture was measured at 340 nm and recorded as background NADHP oxidation due to non-specific enzyme activity. Measurement of NADPH loss due to chorismate lyase activity was initiated with the addition of 0.020 mL of 6 mM chorismic acid. Chorismate lyase specific activity was calculated by subtracting the rate of NADPH loss due to non-

specific enzymes from the rate of NADPH loss obtained in the presence of chorismic acid. One unit of chorismate lyase activity is defined as one μmol of NADPH oxidized per minute per mg of protein.

D. *p*-Hydroxybenzoate Hydroxylase.

p-Hydroxybenzoate hydroxylase activity was assayed by measuring the PHB-dependant oxidation of NADPH at 340 nm in air saturated buffer at 25 °C. Harvested cells were resuspended in 100 mM Tris-base (pH 8.0), EDTA (0.8 mM) solution. Enzyme activity was calculated using a continuous assay of NADPH loss by measuring the absorbance at 340 nm. The assay was performed in a 1 mL solution by mixing the resuspension buffer (0.4 mL), H₂O (0.4 mL), diluted cellular lysate (0.1 mL), 30 mM PHB (0.05 mL, pH 8.0), 10 mM NADPH (0.025 mL), and 0.5 mM FAD (0.025 mL). The enzyme was diluted in the same buffer used for resuspension. One unit of enzyme activity was defined as 1 μmol of NADPH oxidized per minute per mg of protein.

E. *N. tabacum* DHQ Dehydratase/Shikimate Dehydrogenase

DHQ dehydratase/shikimate dehydrogenase activity of fermentor grown cells was measured in the reverse direction in the crude lysate prepared for the DAHP synthase assay. The reaction (1 mL) contained 780 μL of reverse assay buffer (100 mM Tris-base, pH 9), 100 μL of SA (40 mM in reverse assay buffer) and 20 μL of cellular lysate. The reaction was initiated by the addition of 100 μL of NADP⁺ (2 mM) and the formation of NADPH was monitored by following the increase in absorbance at 340 nm. One unit of

DHQ dehydratase/shikimate dehydrogenase activity is defined as 1 μmol of NADPH ($\epsilon = 6220 \text{ L/mol/cm}$) formed per min per mg of protein.

F. Aryl Aldehyde Dehydrogenase.

Aryl-aldehyde dehydrogenase assay solution (1 mL) contained Tris-HCl (100 mM), pH 8.0, MgCl_2 (10 mM), dithiothreitol (20 mM), NADPH (0.15 mM), ATP (20 mM), and benzoic acid (4 mM), and was pre-incubated at rt. After addition of solution containing aryl-aldehyde dehydrogenase, reduction of benzoic acid was monitored by following the loss of absorbance at 340 nm. One unit of aryl-aldehyde dehydrogenase activity is defined as the loss of 1 μmol of NADPH ($\epsilon = 6220 \text{ L/mol/cm}$) per min per mg of protein.

IV. Chapter Two.

A. Purification of PHB from Fermentation Broth

The fermentation broth (1100-1200 mL) was centrifuged at 14000g for 10 min at 24 ° C and the cells were discarded. The resulting dark brown solution was adjusted to pH 4.0 by addition of concentrated H_2SO_4 and centrifuged at 14000g for 10 min to clarify the broth. The clear solution was transferred to a 2 L separatory funnel and extracted with two portions (500 mL) of *t*-butyl methyl ether. The ether layers were combined and the volume reduced to approximately 6 mL by rotary evaporation under reduced pressure. Upon standing, *p*-hydroxybenzoic acid crystallized from solution and was obtained as a pale yellow solid. Second and third crops were obtained by concentration of the filtrates.

Total recovery was 65% based on *p*-hydroxybenzoic acid quantified in crude fermentation broth.

B. Preparation of JB161 and JB161(DE3)

E. coli JB161 was prepared from D2704⁵ by homologous recombination of a *P_{iac}aroAaroLaroCaroBkan^R* cassette into the genomic *serA* locus (*serA*::*P_{iac}aroAaroLaroCaroBkan^R*). Strain construction began with assembly of the genomic cassette. The previously synthesized *P_{iac}aroAaroCaroBkan^R* cassette, localized in plasmid pKAD77A, was prepared by Snell et al.⁶ This cassette was modified by ligating a *KpnI* terminated *aroL* locus to the *KpnI* site located between the *aroA* and *aroC* genes. The *aroL* insert was amplified from pJB2.8 using PCR with the following primers: 5'-GGGGTACCGGACCAGATAGCCTTT and 5'-GGGGTACCTCAATTGATCGTCTG. Ligation of the resulting 0.8-kb *aroL* PCR fragment to pKAD77A, which had previously been digested with *KpnI*, afforded the 10.6-kb plasmid pJB2.100. The *aroL* gene is transcribed in the same direction as *aroA*, *aroC*, *aroB*, and *kan^R*.

Plasmid pJB2.132 was constructed to prepare the cassette for site-specific recombination into the *serA* locus of D2704. Construction of pJB2.132 began with the vector pMAK705,⁷ which contains a temperature-sensitive pSC101 replicon. Since plasmids derived from pMAK705 replicate at 30 °C but are unstable at 44 °C, isolation of all pMAK705 derivatives required culturing of cells at 30 °C. Plasmid pMAK705 contains two *EcoRI* restriction sites: one located within the *Cm^R* marker and one contained within the multiple cloning site. To facilitate future cloning, the *EcoRI* site within the multiple cloning site was eliminated. Partial digestion of pMAK705 with

EcoRI followed by treatment with the Klenow fragment allowed for isolation of a 5.5-kb blunt end fragment from an agarose gel. Religation of the isolated DNA afforded plasmid pJB1.37. Elimination of the *EcoRI* site within the multiple cloning site was confirmed by growth of DH5 α /pJB1.37 on LB medium containing Cm.

Localization of the *serA* gene in pJB1.37 followed by insertion of the *P_{lac}aroAaroLaroCaroBkan^R* cassette into an *EcoRI* site internal to the *serA* gene directed recombination of the cassette into the *serA* locus of the D2704 genome. Digestion of pD2625 with *EcoRV* and *DraI* liberated a 1.9-kb *serA* fragment. Plasmid pJB1.37A was digested with *HincII* to produce blunt ends. Subsequent ligation of the *serA* fragment to pJB1.37A yielded the 7.4-kb plasmid pJB1.102B. The *serA* locus was oriented opposite the vector-localized *lacZ'*. The 6.3-kb *P_{lac}aroAaroLaroCaroBkan^R* cassette was liberated from pJB2.100 by digestion with *EcoRI*. Following *EcoRI* partial digestion of pJB1.102B, the DNA fragments were resolved on an agarose gel and the 7.4-kb fragment corresponding to the linearized plasmid was isolated. Ligation of linearized pJB1.102B to the 6.3-kb *EcoRI* fragment encoding the modified cassette afforded the 13.7-kb plasmid pJB2.132. The cassette is transcribed with all the genes in the same orientation as the *serA* promoter.

Conditions for homologous recombination were based on those previously described.⁸ Competent D2704 cells were freshly prepared and transformed with pJB2.132. Following heat-shock treatment, cells were incubated in LB at 37 °C for 2 h and subsequently plated onto LB containing Cm and Kan. Plates were incubated at 42 °C for approximately 24 h. The resulting colonies were inoculated into 5 mL of LB containing no antibiotics, and the cells were grown at 30 °C for 12 h to allow excision of

the plasmid from the genome. Cultures were diluted (1:20,000) in LB without antibiotics, and two more cycles of growth at 30 °C for 12 h were carried out to enrich cultures for more rapidly growing cells that had lost the temperature-sensitive replicon. Cultures were then diluted (1:20,000) in LB and grown at 44 °C for 12 h to promote plasmid loss from the cells. Serial dilutions of each culture were spread onto LB plates containing Kan and incubated at 30 °C overnight. The resulting colonies were screened on multiple plates to select for the correct phenotype. One candidate, *E. coli* JB161, was isolated based on the following growth characteristics: growth on M9 containing aromatic amino acids, aromatic vitamins, and serine; no growth on M9 containing aromatic amino acids and aromatic vitamins; growth on LB containing Kan; no growth on LB containing Cm; and growth on LB. JB161(DE3) was prepared using the λDE3 Lysogenization Kit according to the manufacturer's protocol.

C. Preparation of RB38 and RB38(DE3)

RB38 and RB38(DE3) were prepared from *E. coli* RB791 (ATCC 53622) using protocols described for preparation of JB161 and JB161(DE3).

D. Southern Hybridization to Confirm Phenotype of JB161.

Genomic DNA for Southern hybridization was prepared from strains JB161, D2704, and KAD11D. For hybridizations with the *serA* probe, the following genomic DNA digests were performed using approximately 1.5 µg of DNA: *KpnI* and *PvuII*; *KpnI*, *PvuII*, and *XbaI*; *KpnI*, *PvuII*, and *AscI*; and *KpnI*, *PvuII*, and *SalI*. Double and triple digests were performed simultaneously with the exception of the *KpnI*, *PvuII*, and *AscI*

digest. In this case, samples were first digested with *KpnI* and *PvuII*. Following extraction with phenol and SEVAG (100 μ L each), the DNA was precipitated using standard techniques, and then digested with *AscI*. DNA was resolved on an 0.7% agarose gel and visualized with ethidium bromide staining.

DNA from the agarose gel was blotted onto a Hybond-N⁺ membrane (Amersham Pharmacia Biotech, pore size 0.45 μ m) as follows. The agarose gel was denatured by soaking (15 min) in a solution containing 1.5 M NaCl and 0.5 N NaOH with periodic agitation. The buffer was removed and the denaturation process was repeated with fresh buffer. A Hybond-N⁺ membrane was cut to match the size of the gel, soaked in distilled water until thoroughly wet, and equilibrated (30 min) in 10X SSC buffer (20X SSC buffer (1 L) contains NaCl (175.3 g), and sodium citrate (88.2 g), pH 7.0). DNA was transferred from the gel onto the membrane using capillary transfer.

Following transfer of DNA, the Hybond-N⁺ membrane was soaked in 5X SSC buffer for approximately 15 min at room temperature. The membrane was exposed to UV (30 s) to covalently bind the DNA to the membrane and placed in a resealable bag (Ziploc) with prehybridization buffer (38 mL). The bag was sealed and incubated for 3 h at 42 °C. Prehybridization buffer (45 mL) contained 6X SSC, 10X Denhardt's reagent, 1.76% SDS (w/v), and 50 μ g/mL of fragmented denatured salmon testes DNA (Sigma). Denhardt's reagent (50X) contained ficoll (10 g), polyvinylpyrrolidone (10 g), and bovine serum albumin (BSA, 10 g) per L. Salmon testes DNA was denatured just prior to use by heating at 95 °C for 5 min.

A ³²P-labeled *serA* probe was prepared using a procedure described by Fienberg and Vogelstein.⁹ A DNA fragment containing *serA* was amplified from plasmid

pJB2.133 using the following primers terminated with *Xba*I recognition sequences: 5'-GCTCTAGATTAGTACAGCAGACGGGC and 5'-GCTCTAGATCCGGAATACCGTCAGGG. The 1.7-kb PCR fragment was digested with *Kpn*I and *Pvu*II and the 1.1-kb DNA fragment was isolated from an agarose gel. After precipitation, the DNA was resuspended in TE (10 ng/ μ L as estimated by inclusion on an agarose gel containing known concentrations of DNA).

Stock solutions for labeling of the *serA* probe were as follows: TM (250 mM Tris-HCl, pH 8, containing MgCl₂ (25 mM) and β -mercaptoethanol (50 mM)); DTM (100 mM of dATP, dGTP, and dTTP in TM); OL (1 mM Tris-HCl, pH 7.5, containing EDTA (1 mM)); and LS (25:25:7 solution of 1 M N-2-hydroxyethylpiperazine-N-2-ethane sulfonic acid (HEPES, pH 6.6), DTM, and OL). The following were added to a 1.5 μ L microfuge tube on ice: 11.4 μ L of LS, 1 μ L of BSA, 3.6 μ L of H₂O, and 2.5 μ L of a random hexanucleotides mixture (Roche Molecular Biochemicals). An aliquot of the *serA* fragment was denatured at 95 °C for 2 min, cooled to 4 °C, and 4.6 μ L (46 ng) was added to the microfuge tube. An aliquot (5 μ L) of deoxycytidine 5'-[α -³²P]-triphosphate (3000 Ci/mmol, Amersham Pharmacia Biotech) was added to the tube followed by 0.5 μ L of Klenow fragment (2.5 units). The sample was mixed and incubated at room temperature for 2 h. Water (75 μ L) was added to the reaction mixture and the sample was loaded on a disposable column containing 1 mL of G-10 sephadex. The column was placed in a test tube (13 x 100 mm) and centrifuged (2000g, 2 min). The eluent contained ³²P-labeled *serA* probe (2.34 x 10⁸ cpm/mL)

The prehybridization buffer was removed from the bag containing the membrane. Hybridization solution (15 mL) and ³²P-labeled *serA* probe (100 μ L, 2.34 x 10⁷ cpm) were

added and the bag was resealed. Hybridization buffer contained 6X SSC, 1.67% SDS (w/v), 50% formamide, and 50 µg/mL of fragmented denatured salmon sperm DNA. The probe was allowed to hybridize to the membrane for approximately 19 h at 42 °C.

Extensive washing of the membrane resulted in removal of non-hybridized radiolabeled probe. Washings were performed by removing the buffer from the bag, adding new buffer, and resealing the bag. The membrane was rinsed twice in 4X SSC, 0.5% SDS (55 mL, 15 min, room temperature), twice in 1X SSC, 1% SDS (55 mL, 15 min, 37 °C), and once in 0.1X SSC, 1% SDS (55 mL, 1 h, 45 °C). The membrane was removed from the bag wrapped in saran wrap, and exposed to film (hyperfilm MP from Amersham Pharmacia Biotech) for 8 h at room temperature.

For Southern hybridizations using an *aroL* probe, JB161 and KAD11D genomic DNA and plasmid DNA isolated from a large scale purification of pJB2.132 were digested with the following restriction enzymes: *KpnI*; *HincII*; and *PvuII* and *EcoRV*. The double digest with *PvuII* and *EcoRV* was performed simultaneously. Southern hybridization was performed as previously described. The resulting membrane was exposed to film for 7 h at room temperature. The DNA used to generate the *aroL* ³²P-labeled probe was amplified from plasmid pJB2.8 using the following primers: 5'-GGGGTACCGGACCAGATAGCCTTT and 5'-GGGGTACCTCAACAATTGATC-GTCTG. The 0.8-kb PCR fragment was isolated from an agarose gel and precipitated overnight. The resulting DNA was resuspended in TE (100 ng/µL as estimated by inclusion on an agarose gel containing DNA of known concentration).

E. Preparation of Plasmids

pJB1.137A

This 3.3-kb plasmid contained the *ubiC* locus located behind the *tac* promoter of pKAD49.¹⁰ The 0.8-kb *ubiC* fragment was excised from pKD10.049A¹¹ by *Xba*I digestion. Ligation to the *Xba*I site of pKAD49 afforded plasmid pJB1.137A. The *ubiC* locus is oriented in the same direction as *tac* promoter.

pJB1.273A

This 5.8-kb plasmid was constructed by ligating the open reading frame of *ubiC* into the *Eco*RI site of pJF118EH.¹² The *ubiC* fragment was amplified by PCR from pJB1.137A using the following primers containing *Eco*RI terminal recognition sequences: 5'-GGAATTCATGTCACACCCCGCGT and 5'-GGAATTCCTCTTAGTACAACGGT-GAC. The amplified 0.50-kb PCR fragment was ligated into the *Eco*RI site of pJF118EH to create plasmid pJB1.273 in which the *ubiC* gene is transcribed in the same orientation as the external *tac* promoter.

pJB2.8

This 5.4-kb *aroL* encoding plasmid was created by inserting *aroL* into pCL1920.¹³ The 0.8-kb *aroL* fragment was liberated from plasmid pKAD31¹⁴ by digestion with *Xba*I and *Kpn*I. Plasmid pCL1920 was digested with *Xba*I and *Kpn*I and ligated to the *aroL* fragment to provide the plasmid pJB2.8. The *aroL* gene is transcribed in the same orientation as *lacZ'*.

pJB2.125B

This 4.1-kb plasmid was constructed by inserting the $P_{lac}ubiC$ sequence of pJB1.273A into the $aroF^{FBR}$ containing plasmid pKL4.20B.¹⁵ The $P_{lac}ubiC$ fragment was amplified from pJB1.273A using the following PCR primers containing *KpnI* terminal recognition sequences: 5'-GGGGTACCGAGCTGTTGACAATTAA and 5'-GGGGTACCCCTC-TTAGTACAACGGTGAC. The 0.58-kb PCR product was ligated to the *KpnI* site of pKL4.20B to create plasmid pJB2.125B. The *ubiC* gene is transcribed in the opposite orientation as $aroF^{FBR}$.

pJB2.133

This 6.0-kb plasmid was created by ligation of a 1.9-kb fragment encoding *serA* into pJB2.125B. The *serA* locus was liberated from plasmid pJB1.102B by digestion with *XbaI* and *HindIII* and subsequently ligated to plasmid pJB2.125B that was previously digested with *XbaI* and *HindIII*. The *serA* gene is transcribed in the same orientation as *ubiC*.

pJB2.274

This 8.2-kb plasmid was constructed by ligation of the 2.2-kb *tktA* gene into pJB2.133. The *tktA* locus was isolated from pMF62A¹⁶ following *BamHI* digestion and treatment with Klenow fragment to provide a fragment with blunt ends. Plasmid pJB2.133 was digested with *HindIII*, and the overhanging ends were eliminated by treatment with Klenow fragment. Subsequent ligation of *tktA* to pJB2.133 afforded plasmid pJB2.274 in which *tktA* is transcribed in the same orientation as *ubiC*.

pJB3.111A

This 6.2-kb plasmid was created to express *ubiC* from the *T7* promoter. The *ubiC* open reading frame was liberated from pJB1.273 using an *EcoRI* digest and subsequently treated with Klenow fragment. This 0.5-kb fragment was ligated to plasmid pET-15b (Novagen) that had been prepared by digestion with *BamHI* and treatment with Klenow fragment. Ligation of the two fragments created plasmid pJB3.111A. Restriction analysis of pJB3.111A verified that *ubiC* was correctly oriented behind the *T7* promoter.

pJB3.127A

This 8.3-kb plasmid was created by inserting a single fragment encoding $P_{T7}ubiC$ and $lacI^Q$ into pKL4.33B.¹⁷ A 2.8-kb fragment encoding $P_{T7}ubiC$ and $lacI^Q$ was liberated from pJB3.111A by digestion with *EcoRI* and *NruI* and treated with Klenow fragment. Plasmid pKL4.33B was digested with *XbaI* and treated with Klenow fragment. Subsequent ligation of the blunt fragments yielded plasmid pJB3.127A. The $lacI^Q$ gene is transcribed in the same orientation as $aroF^{FBR}$ and *serA* while $P_{T7}ubiC$ is transcribed in the opposite orientation.

pJB3.144B

This 10.5-kb plasmid was created by ligation of *tktA* into pJB3.127A. The 2.2-kb *tktA* gene was isolated from plasmid pMF62A by digestion with *BamHI* and treated with Klenow fragment. Plasmid pJB3.127A was digested with *Sall* and treated with Klenow

fragment. Subsequent ligation of *tktA* to pJB3.127A afforded plasmid pJB3.144B. The *tktA* gene is transcribed in the opposite orientation as P_{T7ubiC} .

F. Purification of *p*-Hydroxybenzoate Hydroxylase.

Partial purification of *p*-hydroxybenzoate hydroxylase was based on the method of Entsch.¹⁸ All buffers were made in distilled, deionized water. Buffer components were of the highest grade commercially available. The buffers used were as follows: resuspension buffer, 50 mM K_2HPO_4 , pH 7.0, containing EDTA (0.5 mM) and *p*-hydroxybenzoic acid (0.5 mM); running buffer, 25 mM K_2HPO_4 , pH 7.0, containing EDTA (1 mM) and $(NH_4)_2SO_4$ (45% saturation); elution buffer, 25 mM K_2HPO_4 , pH 7.0, containing EDTA (1 mM) and $(NH_4)_2SO_4$ (32% saturation); affinity buffer, 10 mM Tris-maleate (Tris-base solution pH adjusted with a concentrated solution of maleic acid), pH 7.0, containing EDTA (0.3 mM); storage buffer, 50 mM K_2HPO_4 , pH 7.0, containing EDTA (0.5 mM).

A colony of JM105/pNE130 was inoculated into 100 mL of LB containing Amp (2X) and grown overnight. This culture was used to inoculate (10 mL) eight 4 L Erlenmeyer flasks with 1 L of LB medium containing Amp (2X) and the cells were grown at 37 °C and 250 rpm until the OD_{600} reached 0.12. IPTG (final concentration 250 μ M) was introduced into the medium and the cells were grown for an additional 10 h. IPTG stock solution (0.2 M) was sterilized by passage through a 22- μ m membrane. Cells (19 g) were harvested by centrifugation (4000g, 5 min, 4 °C) and frozen overnight at -20 °C. The next morning, the cells were thawed on ice for 1 h and resuspended in 35 mL of resuspension buffer. Cell membranes were disrupted by two passages through a French

press (16000 psi). Cellular debris was removed by centrifugation at 30000g for 30 min at 4 °C.

The lysate was diluted to a volume of 95 mL with resuspension buffer and the cellular protein was fractionated by the addition of $(\text{NH}_4)_2\text{SO}_4$ to 42% saturation at 4 °C. The pH was adjusted to 7.0 with NH_4OH and allowed to stir at rt until the temperature of the mixture reached 15 °C. The mixture was centrifuged (30000g, 20 min, 15 °C) to remove precipitated protein. The supernatant was applied to a column (75 mL) of DEAE cellulose equilibrated with running buffer at room temperature. The column was washed with 150 mL of running buffer and the enzyme was eluted with 250 mL of elution buffer. Fractions containing *p*-hydroxybenzoate hydroxylase activity were pooled and solid $(\text{NH}_4)_2\text{SO}_4$ was added to a final concentration of 75% saturation. The mixture was stirred for 10 min at room temperature and the precipitate was recovered by centrifugation at (20000g, 10 min, rt). The precipitated protein fraction was redissolved in 9 mL of ice cold affinity buffer. This material was dialyzed overnight against multiple changes of affinity buffer to remove $(\text{NH}_4)_2\text{SO}_4$. To store *p*-hydroxybenzoate hydroxylase, the affinity buffer was exchanged with storage buffer. The dialyzed protein was concentrated to 2.5 mL by ultrafiltration and then diluted with storage buffer (5 mL). After three more cycles of concentration and dilution, the resulting protein was divided into 500 μL aliquots, quick-frozen in liquid nitrogen, and stored at -78 °C.

G. Isolation of Chorismic Acid.

Chorismic acid was isolated from the culture supernatant of *Klebsiella pneumoniae* KP62-1 (ATCC 25306). Growth conditions for *K. pneumoniae* were based

on the method described by Gibson.¹⁹ Medium A (1 L) contained K_2HPO_4 (10 g), NH_4HPO_4 (2.2 g), citric acid monohydrate (2 g), and Bacto yeast extract (2 g). The following supplements were added to medium A (1 L) after autoclaving: casamino acids (2 g), glucose (1.6 g), $MgSO_4$ (0.1 g), and L-tryptophan (40 mg). Medium B (1 L) contained Na_2HPO_4 (12 g), NH_4Cl (2.7 g), KH_2PO_4 (1.4 g), and $MgCl_2 \cdot H_2O$ (0.002 g). The following supplements were added to medium B (1 L) after autoclaving: glucose (4 g) and L-tryptophan (0.095 g). Glucose and $MgSO_4$ solutions were autoclaved separately and solutions of casamino acids and L-tryptophan were sterilized by passage through 0.22- μ m membranes.

Two 1-L cultures of *K. pneumoniae* KP62-1 were prepared to yield 2 L of culture broth for chorismic acid isolation. Inoculants were initiated by introduction of a single colony of KP62-1 into 10 mL of LB and grown at 37 °C with agitation at 250 rpm for 12 h. Each inoculant was transferred to 1 L of medium A and cultured for 6 h at 30 °C with agitation at 250 rpm. Cells from each culture were harvested by centrifugation (4000g, 5 min, 4 °C), resuspended in 1 L of medium B, and grown for approximately 17 h at 30 °C and 250 rpm. The cultures were combined, centrifuged at 4000g for 5 min at 4 °C, and the cells were discarded. The resulting solution was divided into four 500 mL portions and stored at 4 °C.

A column of AG 1-x8 (chloride form, 2.5 cm x 16 cm) was prepared at 4 °C under positive N_2 pressure. The column was pretreated with 500 mL of 1 M NH_4Cl (pH 7.5) followed by 500 mL of water. A 500 mL portion of chorismate-containing culture supernatant was adjusted to pH 7.5 with 5 N NaOH and immediately applied to the column under N_2 pressure at 4 °C. The column was then washed under N_2 pressure with

H₂O (100 mL). Chorismic acid was eluted by gravity with 1 M NH₄Cl, pH 7.5. The absorbance at 275 nm of each fraction (10 mL) was measured to identify those containing chorismate. Chorismate-containing fractions were combined, adjusted to pH 1.7 by addition of 1 M HCl, and extracted with ether (6 x 50 mL). The organic layers were combined, washed with saturated NaCl, dried over MgSO₄, and the volume reduced to 10 mL using rotary evaporation. Chorismic acid crystallized from solution at 4 °C after addition of CH₂Cl₂ (10 mL). Chorismic acid (0.47 g) was isolated as white crystals which were dried under vacuum and stored at -20 °C.

H. Feedback inhibition of Chorismate Lyase.

An inoculant of JB161(DE3)/pJB3.144B was prepared by introduction of a single colony into 50 mL of LB containing Cm and cultured at 37 °C with agitation at 250 rpm for 12 h. Five milliliters of this culture was then added to LB (500 mL) containing Cm and the cells were grown at 37 °C and 250 rpm until the OD₆₀₀ reached 0.7. IPTG (final concentration 10 μM) was introduced into the medium and the cells were grown for an additional 3 h. IPTG stock solution (0.2 M) was sterilized by passage through a 22-μm membrane. Cells were harvested by centrifugation (4000g, 5 min, 4 °C) and resuspended in 6 mL of chorismate lyase buffer A. Cell membranes were disrupted by two passages through a French press (16,000 psi). Cellular debris was removed by centrifugation at 30000g for 30 min at 4 °C. The protein concentration was determined using the method of Bradford. Lysate was diluted (1:100) in chorismate lyase buffer A.

Chorismate lyase activity was measured in triplicate at 37 °C based on the method of Nichols et al. The reaction (4 mL) was performed in chorismate lyase buffer A

containing 60 μM chorismate, 0.044 mg of crude protein and 0, 15, 30, 60, 90, and 120 μM PHB. The reaction was initiated by the addition of chorismate to the pre-incubated solution. One, 3, 5, 7, 9, and 11 min after initiation of the reaction, 0.45 mL of solution was removed and immediately frozen in liquid nitrogen. Samples were stored at $-80\text{ }^{\circ}\text{C}$ until analyzed by HPLC. Prior to injection (100 μL) on the HPLC, samples were thawed on ice and 0.05 mL of vanillic acid (1 mM) was added as an internal standard. *p*-Hydroxybenzoic acid concentrations were determined by comparison of the area corresponding to *p*-hydroxybenzoic acid (16.5 min) with the area corresponding to vanillic acid (21.0 min). Chorismate lyase activity ($\mu\text{mol}/\text{min}/\text{mg}$) was determined from the slope of the line obtained by plotting *p*-hydroxybenzoate concentration verses time. Analysis was done on a Rainin HPLC equipped with a Rainin C-18 Microsorb-MV column and Dynamax acquisition software. Elution was isocratic at one mL/min using a H_2O :acetonitrile:acetic acid (85:10:5) solvent system. Analytes were detected at 250 nm.

I. Feedback inhibition of DHQ synthase.

Measurement of DHQ synthase activity was based the method of Tian et al.²⁰ The reaction (1 mL) was performed in 3-(*N*-morpholino)propanesulfonate (MOPS) buffer (100 mM MOPS, pH 7.5, 75 μM ZnSO_4) containing 500 μM DAHP, 10 μM NAD^+ , one unit of DHQ dehydratase, 0.024 units of DHQ synthase and 0, 60, 600, and 6,000 μM tyrosine. The reaction was initiated by addition of DHQ synthase and monitored for 60 s by following the formation of DHS at 234 nm. DHQ synthase was purified from *E. coli* RB791/pJB14 by according to the procedure of Frost et al.²¹ with the exception that CoCl_2 was replaced by 75 μM ZnSO_4 in all buffer solutions (enzymes purified by S.

Chandran, Frost group). DHQ dehydratase was purified from AB2848/pKL1.87A/pMF52A (Frost group collection) according to the procedure of Chaudhuri et al.²² DAHP was synthesized as described by Frost et al.²³

J. Isolation of *E. coli* 98042-42.

Cells were removed under sterile conditions from a fermentation of JB161/pJB2.274 at 42 h and streaked on M9 plates containing glucose and aromatic amino acids and M9 plates containing glucose, aromatic amino acids, and 50 mM PHB and grown for 48 h at 33 °C. Colonies were subsequently replicate plated on M9 plates containing glucose, aromatic amino acids, and 0, 50, 80, 90, 95, and 100 mM PHB and grown at 33 °C for 48 h. One of the colonies growing in the presence of 100 mM PHB was selected and named 98042-42. All media used to culture 98042-42 was supplemented with 50 mM PHB. A stock solution of PHB (1 M) was sterilized by passage through 0.22- μ m Steri-cup filter (Corning).

K. Synthesis of PHB *O*- β -D-Glucoside.

4-carbomethoxyphenyl 2,3,4,6-tetra-*O*-acetyl- β -D-glucopyranoside (3). A mixture of *p*-hydroxybenzoate methyl ester (**1**) (7.398g, 48.6 mmol), tetra-*O*-acetyl- α -D-glucopyranosyl bromide (**2**) (20 g, 48.6 mmol), and silver (II) oxide (11.21 g, 48.6 mmol) in freshly distilled, anhydrous pyridine (75 mL) was stirred vigorously at room temperature for 14 h. The reaction mixture was diluted with CHCl₃ (250 mL) and H₂O (75 mL) and filtered through Celite and Whatman 1 filter paper to remove suspended solids. The organic filtrate was washed with saturated aqueous CuSO₄ (4 x), H₂O (1 x),

and saturated aqueous NaHCO₃ (1 x). The aqueous filtrate was extracted with CHCl₃ (3 x 50 mL) and the resulting organic layers were washed with saturated aqueous CuSO₄ (1 x), H₂O (1 x), and saturated aqueous NaHCO₃ (1 x). Both portions of CHCl₃ were combined and dried over MgSO₄. The solvent was removed and the residue was recrystallized from MeOH. A second recrystallization from MeOH afforded **3** (8.4 g, 36 %) as a tan solid. ¹H NMR (CDCl₃): δ 8.00 (d, J = 6.7 Hz, 1 H), 7.01 (d, J = 6.7, 2 H), 5.33-5.30 (m, 2 H), 5.21-5.15 (m, 2 H), 4.29 (dd, J = 12, 5.5 Hz, 1 H), 4.17 (dd, J = 13, 2.2 Hz, 1 H), 3.90 (s, 3 H), 2.08-2.03 (m, 3 H). ¹³C (CDCl₃): δ (150.3, 122.5, 107.3, 91.3, 67.7, 67.1, 64.5, 61.0, 52.0, 8.4. HRMS (FAB) calcd for C₂₂O₁₂H₂₆ (M+H⁺): 505.1322. Found: 505.1330.

***p*-Hydroxybenzoate *O*-β-D-Glucoopyranoside (4).** The protected glucoside **4** (0.508g, 1.04 mmol) was added to a solution of MeOH (2.5 mL) and 4.2 M NaOH in MeOH (2.5 mL, 10 mmol) and stirred vigorously for 50 h at rt. The solution was adjusted to pH 6.0 with by the addition of Dowex 50 (H⁺ form) and filtered through Whatman 1. The filtrate was concentrated to dryness, and recrystallized from MeOH to afforded **4** (0.241g, 77%) as a white solid. ¹H NMR (D₂O): d 7.97 (d, J = 8.8 Hz, 2 H), 7.18 (d, J = 8.8 Hz, 2 H), 5.25 (d, J = 7.4 Hz, 1 H), 3.94 (d, J = 12 Hz, 1 H), 3.49-3.77 (m, 5 H). ¹³C NMR (D₂O): d 150.3, 122.5, 107.3, 91.3, 67.7, 67.1, 64.5, 61.0, 52.1. HRMS (FAB) calcd for C₁₃O₈H₁₆ (M+H⁺): 299.0767. Found: 299.0755.

L. Disk Diffusion Experiment with *p*-Hydroxybenzoate *O*- β -D-Glucopyranoside.

A colony of *E. coli* RB791 was inoculated into 5 mL of M9 medium supplemented with glucose and grown overnight at 37 °C with agitation. A sample of the culture was diluted (1:1000) with M9 salts and 150 μ L of the dilution was plated on each M9 plate. Paper discs (1/4" diameter, Aldrich) were submerged (25 μ L of solution absorbed) in a solution of the compound to be tested, blotted on a piece of Whatman 1 filter paper, and gently pressed onto the prepared M9 plate. Four discs were placed on each plate, the plates were incubated for 24 h at 37 °C, and the diameter of the zones around each disc that could not support cell growth were measured. A 1 M solution of PHB and PHB *O*- β -D-glucoside were prepared, adjusted to pH 7.0 with 10 N NaOH, and sterilized by passage through 0.22- μ m membranes. A quantity of 3.45 mg of PHB was deposited on each disk while 7.50 mg of PHB *O*- β -D-glucoside was deposited on each disk.

M. Cloning of *N. tabacum* TOGT1.

Culturing of *N. tabacum*.

Wild-type *Nicotiana tabacum* SRI seeds were obtained from the laboratory of Professor McIntosh at Michigan State University and stored at 4 °C. Seeds were sterilized by placing approximately 100 μ L of seeds in a 1.5 mL microfuge tube. Seeds were mixed gently by inversion with 70% ethanol (1 mL) for 15-30 s. The seeds were allowed to settle to the bottom of the microfuge tube and the ethanol was removed. Sterile water (1 mL) was added and the seeds were mixed gently by inversion and the seeds were allowed to settle. The water was removed and the seeds were rinsed two

additional times with sterile water. Seeds were next washed three times with a mixture of 15% aqueous bleach with added tween 20 (Aldrich). The bleach mixture, prepared just prior to use, consisted of 5 mL of 15% aqueous bleach with two drops (from a pipette) of tween 20. The seeds were rinsed three more times in sterile water and finally resuspended in 100 mL of sterile water. Seeds were spread on MS agar medium with a pipette tip.

Murashige and Skoog (MS) agar medium (1 L) contained one packet of MS salts (Gibco BRL), phytagar (8 g, Gibco BRL), sucrose (30 g), and vitamin B stock solution (10 mL). MS salts were prepared by combining one packet with 500 mL of water and adjusting the pH to 5.7 with KOH. Phytagar (8 g) was combined in 390 mL of water and sucrose (30 g) was combined with 100 mL of water. Vitamin B stock solution (100X) contained (1 L) nicotinic acid (100 mg), pyridioxine HCl (100 mg), thiamine HCl (1 g), and myo-inositol (10 g). Solutions of MS salts, Phytagar, and sucrose were autoclaved separately and combined. Vitamin B stock solution was sterilized by passage through 0.22- μ m membranes. MS agar plates were prepared in 20 mm x 100 mm petri dishes.

Seeds (approximately 20 per plate) were grown at room temperature with a 24 h photo period. Germination began after four days, and leaves were harvested after 13 days. (note: mold had appeared on some of the seedlings and so these were discarded). A total of 153 mg of leaf tissue were harvested, quick-frozen in liquid nitrogen, and stored at -80 °C.

Isolation of Genomic DNA from Tobacco Leaves

Genomic DNA was isolated from the frozen leaf tissue based on the method of Verwoerd et al.²⁴ The leaf tissue (153 mg) was placed in a tapered Glas-Co homogenizer (1 mL) and filled three-quarters of the way with liquid nitrogen. With the bottom of the homogenizer submerged in liquid nitrogen, the leaves were crushed a (5 min) to a fine powder using a tapered teflon pestel. Pre-warmed (80 °C) phenol/extraction buffer (500 µL, 1:1 pH neutralized phenol:extraction buffer) was added to the frozen leaf tissue and the mixture vortexed until the tissue was thawed (30-60 s). Extraction buffer contained Tris-HCl (100 mM), pH 8, LiCl (100 mM), EDTA (10 mM), and SDS (1% w/v). SEVAG was added (250 µL), the mixture was vortexed, transferred to a 1.5 mL centrifuge tube, and microcentrifuged for 5 min. The aqueous layer was transferred to a fresh 1.5 mL microfuge tube and the RNA was precipitated with an equal volume of cold 4 M LiCl. The solution was stored at -20 °C overnight and the precipitated RNA was removed by centrifugation (10 min, 4 °C). DNA was precipitated from the supernatant by the addition of two volumes of 95% ethanol. After storing at room temperature for 2 h, the DNA was collected by centrifugation (microcentrifuge, 30 min, 4 °C), rinsed with 70% ethanol, and resuspended in TE (200 µL). RNAase was added to a concentration of 20 µg/mL and the mixture was stored at rt for 30 min. The sample was extracted with phenol and SEVAG (200 µL each) and SEVAG (200 µL). Ammonium acetate (10 M, 20 µL) was added to the aqueous DNA solution. After thorough mixing, 95% ethanol (500 µL) was added to precipitate the DNA. The sample was left at room temperature for 30 min and then centrifuged (microcentrifuge, 5 min, 4 °C). The DNA (32 µg) was rinsed

with 70% ethanol, dried, and then redissolved in 100 μ L of TE. The concentration of DNA was determined as described previously for the large scale plasmid purification.

Preparation of Plasmids.

The open reading frame of *TOGT1* or *TOGT2* was amplified from *N. tabacum* genomic DNA using Taq DNA polymerase with the following primers, containing terminal *Bam*HI recognition sequences: 5'-CGGGATCCATGGGTCAGCTCCATAT and 5'-CGGGATCCTAACTTAATGACCAGTGG. Either gene could be amplified with the same primers due to their high sequence homology. The resulting 1.4-kb PCR fragment was shown to be *TOGT1* after *Sal*II digestion. Plasmid pSU18 was digested with *Bam*HI and ligated to the *TOGT1* PCR fragment, previously digested with *Bam*HI, to afford the 3.7-kb plasmid pJB5.203A with *TOGT1* transcribed in the same orientation as *lacZ*'. Plasmid pJB5.205A was created to express *TOGT1* from the *T7* promoter. The *TOGT1* open reading frame was liberated from pJB2.203A using a *Bam*HI digest. This 1.4-kb fragment was ligated to plasmid pET-15b that had been prepared by digestion with *Bam*HI. Ligation of the two fragments created the 7.1-kb plasmid pJB5.205A. Restriction analysis of pJB5.205A verified that *TOGT1* was correctly oriented behind the *T7* promoter

N. Microbial Synthesis of PHB *O*- β -D-Glucoside.

For analysis of product accumulation in shake flasks, bacterial strains were cultured as follows. Overnight cultures of JB161(DE3)/pJB2.274/pJB5.205A and JB161(DE3)/pJB2.274/pET-15b in LB containing Cm and Amp (2X) were used to

inoculate (10 mL) 2 L Erlenmeyer flasks of LB medium (500 mL) containing Cm and Amp (2X). The cells were grown for 10 h at 37 °C and 250 rpm and were then collected by centrifugation (4000g, 5 min). The harvested cells were directly resuspended in 500 mL of M9 medium (2 L Erlenmeyer flask) containing glucose (5 g), Cm, Amp (2X), Kan, IPTG (0.2 mM), and aromatic amino acids. Cultures were grown at 37 °C and 250 rpm for 72 h. The culture supernatants were neutralized (as measured with an ethanol-sterilized pH probe inserted into the culture flask) by manually adding 5 N NaOH after 2 h, 6 h, and 7.5 h. After 24 h, an additional 10 g of glucose was added to each culture. Product concentrations were measured by ¹H NMR as previously described.

V. Chapter Three.

A. Maintenance and Storage of Fungal Strains.

Phanerochaete chrysosporium (ATCC 32629), *Candida parapsilosis* CBS604 (ATCC 22019) and *Neurospora crassa* SY 74 (ATCC 24740) were obtained from the American Type Culture Collection. *P. chrysosporium* and *N. crassa* were stored as an aqueous suspension of spores at 4 °C. Spores were regenerated on a regular basis by growth on solid culture medium (see following section). *P. chrysosporium* spores were grown on solid Norkrans medium at 37 °C and *N. crassa* spores were grown on *N. crassa* solid growth medium at 24 °C. After a mixture of mycelium and spores was obtained (7-10 days), it was subsequently suspended in 20 mL of sterile water and filtered through glass wool that had been previously sterilized by autoclaving. The resulting spore

suspension can be stored at 4 °C for up to two weeks. The concentration of spores in the suspension was estimated by measuring the absorbance at 650 nm ($A_{650} 1.0 = 5.0 \times 10^6$ spores/mL²⁵). Long term storage of *C. parapsilosis* was performed as described for glycerol freeze storage of bacterial strains. For short-term storage, *C. parapsilosis* was maintained on agar YM slants.

B. Culture Media for Fungal Strains.

All solutions were prepared in distilled, deionized water. Malt medium contained 30 g of malt extract (Difco) per liter. YM medium (1 L) contained Bacto yeast extract (3 g), malt extract (3 g), peptone (5 g), and glucose (10 g) (note: complete medium was also purchased directly from Difco). Norkran's salts (1 L) pH 5.5, contained $(\text{NH}_4)\text{H}_2\text{PO}_4$ (2 g), KH_2PO_4 (0.6 g), K_2HPO_4 (0.4 g), Bacto yeast extract (0.1 g). Norkran's medium (1 L) contained glucose (quantity varied by experiment), thiamine (0.0001 g), MgSO_4 (0.50 g), CaCl_2 (0.056 g), ferric citrate (0.12 g, prepared just prior to use), vanillic acid (0.5 g), and 1 mL of a prepared trace mineral solution. Norkran's trace mineral solution contained (100 mL) ZnSO_4 (0.66 g), $\text{MnSO}_4 \cdot 4\text{H}_2\text{O}$ (0.5 g), and $\text{CoCl}_2 \cdot 6\text{H}_2\text{O}$. (2X) Reader's salts (1 L) contained $(\text{NH}_4)_2\text{SO}_4$ (3 g), NaCl (1 g), KH_2PO_4 (2 g), K_2HPO_4 (0.2 g). (2X) Reader's medium (1 L) contained MgSO_4 (0.69 g), CaCl_2 (0.3 g), FeCl_3 (0.1 g), 1 mL of a prepared trace mineral solution, 1 mL of a prepared vitamin solution, glucose, and PHB. The concentration of glucose and PHB varied by experiment. (2X) Reader's trace mineral solution (100 mL) contained H_3BO_3 (0.04 g), MnCl_2 (0.04 g), $\text{Na}_2\text{MoO}_4 \cdot 2\text{H}_2\text{O}$ (0.04 g), $\text{ZnSO}_4 \cdot 7\text{H}_2\text{O}$ (0.04 g), KI (0.02 g), CoCl_2 (0.02 g), and $\text{CuSO}_4 \cdot 5\text{H}_2\text{O}$ (0.008 g). (2X) Reader's vitamin solution (1 L) contained pantothenate

(0.04 g), nicotinic acid (0.04 g), pyridoxine (0.04 g), potassium *p*-aminobenzoate (0.04 g), inositol (0.08 g), biotin (0.25 mg), and thiamine (0.02 g). *N. crassa* solid growth medium (1 L) contained sucrose (20 g), sodium citrate dihydrate (2.5g), KH_2PO_4 (5.0 g), NH_4NO_3 (2.0 g), $\text{CaCl}_2 \cdot 2\text{H}_2\text{O}$ (0.1 g), MgSO_4 (0.1 g), biotin (5.0 μg), and trace elements including citric acid monohydrate (5.0 mg), $\text{ZnSO}_4 \cdot 7\text{H}_2\text{O}$ (5.0 mg), $\text{Fe}(\text{NH}_4)_2(\text{SO}_4)_2 \cdot 6\text{H}_2\text{O}$ (1.0 mg), $\text{CuSO}_4 \cdot 5\text{H}_2\text{O}$ (0.25 mg), $\text{MnSO}_4 \cdot \text{H}_2\text{O}$ (0.05mg), H_3BO_3 (0.05 mg), $\text{Na}_2\text{MoO}_4 \cdot 2\text{H}_2\text{O}$ (0.05 mg). Difco agar was added to a final concentration of 2% (w/v). The *N. crassa* liquid growth medium (1 L) differed from solid growth medium only in the addition of sucrose (10 g), Difco yeast extract (2.0 g), and sodium salicylate (1.6 g). Inorganic salts, glucose, salicylic acid, MgSO_4 , and CaCl_2 solutions were autoclaved separately while trace minerals, vitamins, PHB, and vanillic acid solutions were sterilized through 0.22- μm membranes. Solid Malt, Norkran's, and (2X) Reader's medium was prepared by the addition of 1.5% (w.v) Difco agar to the liquid medium.

C. Conditions for Shake-Flask Cultivation of *P. chrysosporium*.

i) Conversion of PHB to Hydroquinone

Reaction A.

For analysis of product accumulation in shake flasks, *P. chrysosporium* was cultured as follows. One liter of Norkran's medium (4 L Erlenmeyer flask) containing glucose (2.5 g) and vanillic acid (0.5 g) was inoculated with 2.5×10^6 spores and grown at 30 °C at 250 rpm for 48 h. PHB (5 g) and glucose (2.5 g) were introduced into the

medium and the mycelia were grown for an additional 95 h at 30 °C and 250 rpm. A 1 M stock solution of PHB was prepared, neutralized with 10 N NaOH, and sterilized by passage through a 0.22-mm membrane (Corning, Steri-cup filter). Aliquots (approximately 5 mL) were removed periodically, the mycelia were pelleted using a microcentrifuge (Beckman, 3 min, rt), and the supernatant was analyzed by ¹H NMR. Samples for ¹H NMR analysis were prepared as described previously for fermentation samples.

Reaction B.

Two liters of malt extract broth (4 L Erlenmeyer flask) supplemented with 3 mM vanillate was inoculated with 5×10^6 spores and grown at 37 °C and 250 rpm for 48 h. Mycelia were collected on a large Buchner funnel fitted with Whatman 1 filter paper. When collecting the mycelia by filtration, it is important to not over-dry the mat. Aspiration should be stopped at the moment free-standing liquid is no longer visible. The mycelia was resuspended in 1 L of Norkran's medium (4 L Erlenmeyer flask) supplemented with PHB (5 g) and vanillate (0.5 g), returned to the incubator, and cultured at 37 °C and 250 rpm for an additional 48 h. Product accumulation was monitored by ¹H NMR as described for reaction A.

Reaction C.

Eight liters of mycelia were grown as follows. Three 4 L Erlenmeyer flasks containing 2 L of Norkran's medium supplemented with glucose (5 g) and vanillate (1 g) were each inoculated with 5×10^6 spores. Two 4 L Erlenmeyer flasks containing 1 L of

Norkran's medium supplemented with glucose (2.5 g) and vanillate (1 g) were each inoculated with 2.5×10^6 spores. All flasks were grown at 37 °C and 250 rpm for 48 h. Seven liters of mycelia were collected by filtration as previously described and resuspended in one of the flasks containing 1 L of Norkran's medium. PHB (10 g) was added and the flask was returned to the incubator and cultured at 37 °C and 250 rpm for an additional 48 h. Product accumulation was monitored by ^1H NMR as described for reaction A.

Conversion of Fermentation Broth.

Four 4L Erlenmeyer flasks containing 2 L of Norkran's medium supplemented with glucose (5 g) and vanillate (1 g) were inoculated with 5×10^6 spores and grown at 37 °C and 250 rpm for 48 h. All the mycelia was collected by filtration as previously described and resuspended in 1 L of cell-free fermentation broth containing 10.8 g/L of PHB. Vanillate was added (0.5 g) and the concentrated mycelia were incubated for an additional 48 h at 37 °C and 250 rpm. Product accumulation was monitored by ^1H NMR as described for reaction A.

Chemical Stability of Hydroquinone in Norkran's Medium.

One liter of Norkran's medium (4 L Erlenmeyer flask) was supplemented with vanillate (0.5 g), PHB (3.3 g), and hydroquinone (1.7 g) and incubated at 37 °C and 250 rpm for 48 h. Vanillate and PHB were added from stock solutions (0.6 M and 1 M respectively) neutralized with NaOH while hydroquinone was added directly as a solid.

Analytes were monitored by ^1H NMR as described previously by directly removing 1 mL of solution at designated time points.

Conversion of Fermentation-Derived PHB.

Eight liters of mycelia were grown as follows. Three 4 L Erlenmeyer flasks containing 2 L of Norkran's medium supplemented with glucose (5 g) and vanillate (1 g) were each inoculated with 5×10^6 spores. One 4 L Erlenmeyer flask and one 4 L baffled Erlenmeyer flask containing 1 L of Norkran's medium supplemented with glucose (2.5 g) and vanillate (0.5 g) were each inoculated with 2.5×10^6 spores. All flasks were grown at 37 °C and 250 rpm for 48 h. Seven liters of mycelia were collected by filtration as previously described and resuspended in the baffled flask containing 1 L of Norkran's medium. PHB (10 g) purified as described previously from fermentation broth was added and the flask was returned to the incubator and cultured at 37 °C and 250 rpm for an additional 36 h. Product accumulation was monitored by ^1H NMR as described for reaction A.

ii) Conversion of PHB to *p*-Hydroxybenzyl Alcohol

Reactions A, B, and C.

Two 4 L Erlenmeyer flasks containing 2 L of malt broth were inoculated with 5×10^6 spores of *P. chrysosporium* and the mycelia was grown at 37 °C and 250 rpm for 48 h. The mycelia was collected by filtration as previously described and resuspended in 1 L of Norkran's medium (4 L Erlenmeyer) containing glucose (40 g). Reaction A was

supplemented with 5 g of PHB and 0.5 g of vanillate. Reaction **B** was supplemented with 2.5 g of PHB and 0.5 g of vanillate. Reaction **C** was supplemented with 5 g of PHB and 0.25 g of vanillate. Reactions **A** and **C** were cultured for an additional 7 d at 37 °C and 250 rpm while reaction **B** was cultured for an additional 4 d at 37 °C and 250 rpm. Product accumulation was monitored by ¹H NMR as previously described.

Conversion of Fermentation-Derived PHB to *p*-Hydroxybenzyl Alcohol.

Two 4 L Erlenmeyer flasks containing 2 L of malt broth were inoculated with 5 x 10⁶ spores of *P. chrysosporium* and the mycelia was grown at 37 °C and 250 rpm for 48 h. The mycelia was collected by filtration as previously described and resuspended in 1 L of Norkran's medium (4 L Erlenmeyer) supplemented with glucose (30 g) and PHB (3 g) isolated as previously described from fermentation broth. Mycelia were cultured for an additional 6 days at 37 °C and 250 rpm. Product accumulation was monitored by ¹H NMR as previously described.

Reduction of MHB and OHB

Six 4 L Erlenmeyer flasks containing 2 L of malt broth were each inoculated with 5 x 10⁶ spores of *P. chrysosporium* and the mycelia was grown at 37 °C and 250 rpm for 48 h. Four liters of mycelia was collected by filtration as previously described and resuspended in 1 L of Norkran's medium (4 L Erlenmeyer) supplemented with glucose (30 g) and either PHB (3 g), MHB (3 g), or OHB (3 g). Mycelia were cultured for an additional 5 days at 37 °C and 250 rpm. Product accumulation was monitored by ¹H NMR as previously described.

D. Conditions for Shake-Flask Cultivation of *C. Parapsilosis*.

Reactions A, B, and C.

Inoculants were prepared by introducing *C. Parapsilosis* cells from a YM agar slant into 50 mL of YM medium (250 mL Erlenmeyer flask). The cells were grown for 12 h at 30 °C and 250 rpm. A portion (10 mL) of this culture was used to inoculate 1 L of YM medium (4 L Erlenmeyer flask) and the cells were grown at 37 °C and 250 rpm for 12 h. The cells were collected by centrifugation in bleach-sterilized bottles (4000g, 5 min, 4 °C) and resuspended in 1 L of (2X) Reader's medium supplemented as follows: reaction **A** contained 5 g glucose and 1 g PHB, reaction **B** contained 40 g glucose and 3 g PHB, and reaction **C** contained 5 g glucose and 10 g PHB. To reaction **A**, 1 g PHB was also added 5 h and 10 h after resuspension. The resuspended cells were cultured at 30 °C and 250 rpm for 24 h in the case of reaction **A** and 48 h in the case of reactions **B** and **C**. A portion of culture medium (approximately 3 mL) was removed at designated time points and the cells were removed by centrifugation (microcentrifuge, 2 min, rt). The culture supernatant was analyzed by ¹H NMR as previously described.

Reactions D and E.

Inoculants were prepared by introducing cells from a YM agar slant into 50 mL of YM medium (250 mL Erlenmeyer flask). The cells were grown for 12 h at 30 °C and 250 rpm. A portion (10 mL) of this culture was used to inoculate 1 L of YM medium (4 L Erlenmeyer flask) and the cells were grown at 37 °C and 250 rpm for 12 h. The cells

were collected by centrifugation in bleach-sterilized bottles (4000g, 5 min, 4 °C) and resuspended in 1 L of (2X) Reader's medium supplemented with PHB (10 g). To reaction **D**, a second 10 g aliquot of PHB was added 10 h after resuspension. To reaction **E**, three additional 10 g aliquots of PHB were added 5 h, 9 h, and 24 h after resuspension. The cells were incubated at 30 °C and 250 rpm for 72 h in the case of reaction **D** and for 100 h in the case of reaction **E**. The culture supernatant was analyzed by ¹H NMR as previously described.

Reactions **F** and **G**.

Inoculants were prepared by introducing cells from a YM agar slant into 50 mL of YM medium (250 mL Erlenmeyer flask). The cells were grown for 12 h at 30 °C and 250 rpm. A portion (10 mL) of this culture was used to inoculate 1 L of (2X) Reader's medium (4 L Erlenmeyer flask) supplemented with glucose (5 g) and the cells were grown at 37 °C and 250 rpm for 12 h. PHB was added (10 g for reaction **F** and 20 g for reaction **G**) and the cells were cultured at 30 °C and 250 rpm for an additional 78 h in the case of reaction **F** and for 72 h in the case of reaction **G**. An additional 10 g aliquot of PHB was added to reaction **F** 9 h after the first addition. The culture supernatant was analyzed by ¹H NMR as previously described.

Reactions **H** and **I**.

Inoculants were prepared by introducing cells from a YM agar slant into 50 mL of YM medium (250 mL Erlenmeyer flask). The cells were grown for 12 h at 30 °C and

250 rpm. A portion (20 mL) of this culture was used to inoculate two 4 L Erlenmeyer flasks containing 1 L of (2X) Reader's medium supplemented with glucose (5 g) and the cells were grown at 37 °C and 250 rpm for 12 h. Cells from one of the flasks were collected by centrifugation (4000g, 5 min, 4 °C) and were resuspended in the second. PHB (20 g) was added and the cells were cultured at 30 °C and 250 rpm for an additional 96 h in the case of reaction **H** and for 79 h in the case of reaction **I**. Upon resuspension of the cells, a 60 mL solution containing (NH₄)₂SO₄ (3 g), NaCl (1 g), KH₂PO₄ (2 g), K₂HPO₄ (0.2 g), MgSO₄ (0.69 g), CaCl₂ (0.3 g), FeCl₃ (0.1 g), 1 mL of a prepared trace mineral solution, and 1 mL of a prepared vitamin solution was added to reaction **I**.

E. Purification of Hydroquinone from *P. chrysosporium* Culture Supernatant.

Mycelia were removed from the culture supernatant by filtration through a Buchner funnel fitted with Whatman 1 filter paper. The mycelia-free supernatant (500 mL, 1.5 g/L hydroquinone) was adjusted to pH 9.1 by the addition of 10 N KOH and extracted (2 x 100 mL) with *t*-butyl methyl ether. The ether layers were combined, washed with brine, and dried over MgSO₄. Removal of the solvent by rotary evaporation afforded a black solid. Recrystallization from ethyl acetate and petroleum ether afforded hydroquinone (220 mg, 29% recovery) as a gray solid. PHB could be recovered from the remaining aqueous layer by adjusting to pH 4.0 with H₂SO₄ and extracting (2 x 250 mL) with *t*-butyl methyl ether. The organic layers were pooled, washed with brine and dried over MgSO₄. Removal of the solvent by rotary evaporation afforded PHB (3.01g, 78% recovery) as a brown solid.

F. Purification of Hydroquinone from the Culture Supernatant of *C. parapsilosis*.

Following removal of the cells by centrifugation (4000g, 10 min, 4 °C), the culture supernatant (1055 mL, 4.6 g/L hydroquinone) was adjusted to pH 9.1 with 10 N NaOH and extracted (3 x 400 mL and 3 x 200 mL) with *t*-butyl methyl ether. The organic layers were combined and dried over MgSO₄. Removal of the solvent by rotary evaporation afforded hydroquinone (4.72 g, 98% recovery) as a black solid.

G. Purification of *p*-Hydroxybenzyl Alcohol from the
Culture Supernatant of *P. chrysosporium*.

Mycelia were removed from the culture supernatant by filtration through a Buchner funnel fitted with Whatman 1 filter paper. The filtrate (1136 mL, 1.4 g/L *p*-hydroxybenzyl alcohol) was adjusted to pH 8.6 with 10 N NaOH and loaded into a continuous liquid-liquid extraction apparatus with 750 mL of ethyl acetate. The extraction apparatus was modified to allow vigorous stirring of the organic and aqueous layers in order to create a colloidal suspension. After 5.5 h, the ethyl acetate was separated and replaced with a fresh portion (750 mL) of solvent. After an additional 4 h, the ethyl acetate was separated from the aqueous layer and the combined ethyl acetate layers were dried over MgSO₄. The organic layer was concentrated to a volume of approximately 5 mL and upon standing, *p*-hydroxybenzyl alcohol crystallized from solution (1.08 g, 67% recovery) as a tan solid.

H. Hydrogenation of *p*-Hydroxybenzyl Alcohol.

Purified *p*-hydroxybenzyl alcohol (0.5 g) was dissolved in MeOH (10 mL) and degassed with a sub-surface feed of Ar. The catalyst, 10% Pd on C (0.21 g), was added and the hydrogenation bottle was placed in the Parr apparatus. After 2 h at 50 psi, the reaction mixture was filtered through Celite to remove suspended solids and the filtrates were concentrated in vacuo. After drying overnight under reduced pressure, *p*-cresol was obtained (0.3 g, 69%) as a brown oil.

VI. Chapter Four.

A. Construction of Strains.

E. coli JB4.

E. coli JB4 was derived from *E. coli* KL3 *aroE353 serA::aroB*. Conversion of KL3 from a DHS producer to a shikimate producer was accomplished by successive P1 phage-mediated transductions of *aroK17::Cm^R* and *aroL478::Tn10* to create *KL3aroK⁻aroL⁻*.

KL3aroK⁻aroL⁻ was next made sensitive to tetracycline using D-cycloserine.²⁶ A single colony of *KL3aroK⁻aroL⁻* was introduced into 5 mL of LB and grown overnight with agitation at 37 °C. A dilution (1:500) was made of the overnight culture into 5 mL of fresh LB and grown with agitation at 37 °C for an additional 5 h. The cells were collected by centrifugation (microcentrifuge, rt) and resuspended in 5 mL of LB containing Tc and grown for 1 h at 37 °C with agitation. A freshly made aqueous solution of D-cycloserine was added to the culture supernatant to a final concentration of 6

mM. D-Cycloserine was sterilized by passage through 0.22- μ m membranes. After culturing with agitation for 3.5 h at 37 °C, 1 mL of culture was microcentrifuged. The harvested cells were washed with 1 mL of fresh LB, microcentrifuged, and resuspended in 1 mL of fresh LB. A portion of cells (10 μ L) were used to inoculate 5 mL of LB and the cells were grown overnight and the procedure was repeated. After the second treatment with D-cycloserine, the cell culture was diluted and plated on LB. Colonies were replicate plated on LB and LB/Tc to find candidates that were sensitive to tetracycline (approximately 10% were Tc^s). One of these colonies was selected and named KL3*aroK*⁻*aroL*⁻Tc^s.

Strain KL3*aroK*⁻*aroL*⁻Tc^s was made deficient in DHQ synthase activity by P1 phage-mediated transduction of *aroD25::Tn10*. To ensure that shikimate kinase activity was still absent, the resulting colonies were screened on multiple plates to select for the correct phenotype. One candidate, *E. coli* JB4, was isolated based on the following growth characteristics: no growth on M9 containing serine, no growth on M9 containing serine and shikimic acid, growth on M9 containing serine, aromatic amino acids, and aromatic vitamins, growth on LB containing Cm, growth on LB containing Cm and Tc.

E. coli KL3*aroD*⁻.

Strain KL3 was made deficient in DHQ synthase activity by P1 phage-mediated transduction of *aroD25::Tn10*. The resulting colonies were screened on multiple plates to select for the correct phenotype. One candidate, *E. coli* KL3*aroD*⁻, was isolated based on the following growth characteristics: no growth on M9 containing serine, growth on M9 containing serine and shikimic acid, growth on M9 containing serine, aromatic amino acids, and aromatic vitamins, and growth on LB containing Tc

B. Preparation of Plasmids

pJB5.272A.

This 6.5 kb plasmid was constructed by ligation of the 1.9 kb fragment encoding the *N. tabacum SP3* locus into the site of pKK223-3. The *SP3* locus was liberated from plasmid pBluescript by digestion with *EcoRI* and subsequently ligated to plasmid pKK223-3 that was previously digested with *EcoRI*. The *SP3* locus is transcribed in the same orientation as the *tac* promoter in pKK223-3.

pJB3.141

Plasmid pJB3.141 was constructed by removing the *XbaI*-terminated *aroF^{FBR}* insert from pKL4.130B.²⁷ Plasmid pKL4.130B was digested with *XbaI* and the 7.6-kb fragment corresponding to the linearized plasmid was isolated from an agarose gel. Re-ligation of the isolated DNA afforded the 7.6-kb plasmid pJB3.141.

pJB5.291

This 8.9 kb plasmid was obtained by ligating the 2.2 kb *P_{tac}SP3* fragment into pJB3.141. The *P_{tac}SP3* fragment was liberated from plasmid pJB5.272A by digestion with treated with Klenow fragment. Plasmid pJB3.141 was digested with *NcoI* and treated with Klenow fragment. Subsequent ligation of the blunt fragments afforded plasmid pJB5.291. The *P_{tac}SP3* locus transcribed in the same direction as *aroF^{FBR}*, *serA*, and *tktA*.

C. In Vitro Quinic Acid Accumulation.

A colony of *E. coli* KL3aroD⁻/pJB5.272A was inoculated into 500 mL of LB containing Amp and grown at 37 °C and 250 rpm. After 18 h of growth, the cells were harvested and resuspended in 5 mL of 100 mM K₂HPO₄ buffer, pH 7.5. Cell membranes were disrupted by passage through a French press and the clarified cellular lysate was obtained following centrifugation (30000g, 30 min, 4 °C). A portion of the cellular lysate (1 mL) was combined with DHQ (25.5 mg) and NADPH (100 mg) in a final volume of 5 mL of 100 mM K₂HPO₄, pH 7.5, and incubated at 30 °C for 6 h with agitation.

To prepare the reaction mixture for ¹H NMR analysis, the protein was first precipitated by the addition of H₂SO₄. Following centrifugation to remove the precipitated protein, the reaction mixture was passed through a column (20 mL) of Dowex 50 (H⁺ form) to remove NADP⁺. The column was washed with water (40 mL) and the combined eluents from the cation exchange column were combined with activated carbon (0.5 g) to remove any remaining nicotinamide co-factor. After vigorous stirring (15 min), the activated carbon was removed by filtration through Whatman 5 filter paper. The filtrate was raised to 6.5 with NaOH and evaporated to dryness using rotary evaporation. The residue was redissolved in D₂O, evaporated to dryness a second time, and redissolved in D₂O containing 10 mM TSP.

D. Enzyme Kinetics of the *N. tabacum* DHQ Dehydratase/Shikimate Dehydrogenase.

An inoculant of KL3aroD⁻/pJB5.272A was prepared by introduction of a single colony into 50 mL of LB containing Amp (2X) and cultured at 37 °C with agitation at 250 rpm for 10 h. Five milliliters of this culture was then added to LB (500 mL)

containing Amp (2X) and the cells were grown at 37 °C and 250 rpm for 14 h. Cells were harvested by centrifugation (4000g, 5 min, 4 °C) and resuspended in 5 mL of 100 mM K₂HPO₄, pH 7.5. Cell membranes were disrupted by two passages through a French press (16,000 psi). Cellular debris was removed by centrifugation at 30000g for 30 min at 4 °C.

For all DHQ synthase/shikimate dehydrogenase inhibition studies, the conversion of dehydroshikimate to shikimate with concomitant oxidation of NADPH was monitored at 340 nm at room temperature. One unit of DHQ synthase/shikimate dehydrogenase activity is defined as the loss of one mmol of NADPH ($\epsilon = 6220 \text{ L/mol/cm}$) per min. For determination of percent inhibition of SP3 with shikimate, assays contained (1 mL) 0.1 M KH₂PO₄ (pH 7.4), 0.2 mM NADPH, 33 mM DHQ, 4.2 mg of crude protein, and shikimate concentrations of 0, 0.1, 0.3, 0.7, 1.5, 3.0, 4.5, 7.0, 10, 15, and 30 mM. For determination of K_i, assays contained (1 mL) 0.1 M KH₂PO₄ (pH 7.5), 0.2 mM NADPH, 0.56 mg of crude protein, DHS concentrations of 0.075, 0.125, 0.250, 0.375, and 0.5 mM, and shikimate concentrations of 0.0, 0.1, 1.0, 5.0, and 10 mM. The class of inhibitor was identified from a Hanes-Woolf plot of kinetic data. The K_i for shikimate was obtained from a Dixon plot of kinetic data. The K_M and V_{max} for DHS was obtained from the control line of the Lineweaver-Burke plot generated in the absence of shikimate. The x intercept is equal to $-K_M^{-1}$. The V_{max} for DHS is equal to the reciprocal of the y intercept.

For determination of the K_M and V_{max} for dehydroquininate (DHQ), assays contained (1 mL) 0.1 M KH₂PO₄, pH 7.5, 0.2 mM NADPH, 5.6 mg of crude protein, and DHQ concentrations of 0.033, 0.066, 0.10, 0.15, and 0.20 mM. The x intercept of a plot of V⁻¹ versus [DHQ]⁻¹ is equal to $-K_M^{-1}$, where V is the velocity of the reaction

(mmol/min) and [DHQ] is the concentration of DHQ (mmol). The V_{\max} for DHQ is equal to the reciprocal of the y intercept.

E. Conversion of Shikimic Acid to *p*-Hydroxybenzoic Acid.

Purification of shikimate from the fermentation broth (650 mL) of SP1.1/pKD12.138 (with 0.5 mM MGP, obtained from K. M. Draths) paralleled that previously reported with the following modifications. Following centrifugation of acidified broth to remove denatured protein, the broth was kept at pH 2.5 for subsequent charcoal decolorization. The quantity of Darco KB-B was increased to approximately 20 g per liter of broth and was mechanically agitated by an overhead stirrer for 1-1.5 h. After removal of the activated carbon by filtration, the decolorization sequence was repeated a second time to give a pale yellow liquid. The shikimate obtained after concentration of the Dowex effluent was of satisfactory purity and did not require recrystallization.

Shikimic acid (10 g, 57 mmol) was added to a solution of 1 M H₂SO₄ in glacial acetic acid (269 mL) that had been degassed with N₂. While stirring under N₂, the reaction was refluxed for 29 h. After this time, the HOAc was removed *in vacuo*. After resuspending the resulting residue in H₂O (150 mL), a black solid was filtered through Whatman 5 paper by vacuum filtration. The brown filtrate was extracted with EtOAc (5 x 50 mL). The combined organics were washed with 0.1 M H₂SO₄ (4 x 70 mL), then decolorized by passing through a 2 mm bed of Darco KB-B activated carbon (3.7 g) supported on a Buchner funnel fitted with Whatman 5 filter paper. Drying and concentrating afforded a tan solid. The solids were resuspended in H₂O (20 mL) and the

pH raised to 5.9 with NaOH. The pH was then lowered to 5.3 with H₂SO₄ and stored at 4 °C for 2 h. The precipitated solids were recovered by filtration (1.4 g, 17%). More product was recovered by lowering the pH of the filtrate to 3.4, but it was contaminated with a small amount (3%) of *m*-hydroxybenzoic acid (2.2 g, 28%) ¹H NMR (D₂O) δ 7.88 (d, J=6 Hz, 2H), 6.92 (d, J=5 Hz, 2H). ¹³C NMR (D₂O) δ 176.4, 168.4, 131.7, 122.5, 117.7.

F. Purification of Shikimic Acid from Fermentation Broth.

The fermentation broth (1.5 L) was centrifuged at 14000g for 20 min and the cells were discarded. The resulting supernatant was refluxed for 4 h, cooled to room temperature, and the pH adjusted to 2.5 by addition of concentrated H₂SO₄. After centrifugation at 14000g for 20 min, a clear yellow solution was poured away from the cellular debris. The solution was combined with 30 g of Darco KB-B activated carbon, stirred on a magnetic stirrer for 1 h and then filtered through Whatman 5 filter paper. Filtered material was washed with an additional 200 mL of water. The combined filtrates were treated in the same way with a second batch of activated carbon (100% recovery).

Shikimic acid was extracted from the decolorized cell supernatant by continuous liquid-liquid extraction with ethyl acetate. The cell supernatant (50 mL, 31 mM shikimic acid) was initially combined with ethanol (11 mL) and the mixture was loaded into a continuous extraction apparatus with 250 mL of ethyl acetate. The extraction apparatus was modified to allow vigorous stirring of the organic and aqueous layers in order to create a colloidal suspension. After 24 h, the ethyl acetate was separated and replaced with a fresh portion (250 mL) of solvent while another portion of ethanol (11 mL) was

added to the aqueous layer. Extraction continued for an additional 24 h followed by separation of the aqueous and organic layers. The volume of ethyl acetate obtained from the first 24 h extraction was reduced to approx. 100 mL and chilled to -20 °C. The precipitated shikimic acid was recovered by filtration as an off-white solid (2.3 g, 86% recovery). The ethyl acetate layer from the second 24 h extraction was evaporated to dryness affording an additional quantity of shikimic acid (0.28 g, 11%). The total recovery was 97% based on shikimic acid quantified in crude fermentation broth.

G. Conversion of Shikimic Acid to Phenol.

Shikimic acid (2.0 g, 11 mmol) was combined with 6 mL of degassed water in a high-pressure, stainless steel reaction vessel (Parr 4120, 21 mL). Water was degassed by a 15 min sub-surface feed of Ar followed by a 15 min sub-surface feed of CO₂ just prior to use. After flushing the headspace with Ar, the vessel was sealed according to the manufacturer's specifications and submerged in a sand bath. The temperature of the sand was monitored by placing a mercury thermometer alongside the vessel. An average heating rate of 1.5 °C/min was maintained by manually adjusting the power supplied to the heating mantle. Once a temperature of 350 °C was reached, it was maintained (+/- 4 °C) for 30 min and then the vessel was removed from the sand bath and placed under a cooling fan.

Once the vessel cooled to room temperature, it was unsealed and the contents extracted with ether (5 x 20 mL). The vessel interior was thoroughly rinsed with ether (25 mL) and the organic layers were combined, dried and concentrated in vacuo to a

brown residue. Kugelrohr distillation of the residue under reduced pressure afforded phenol as white crystals (0.49 g) in a 45% yield from shikimic acid.

The residue remaining after distillation was dissolved in boiling water, gravity-filtered while hot, and evaporated to approximately 6 mL. This solution was returned to the vessel with Cu powder (0.22 g, mmol) and heated to 350 °C as previously described. After 3 h at 350 °C, the vessel was cooled to room temperature, unsealed, and the contents extracted with ether (5 x 20 mL). The vessel interior was thoroughly rinsed with ether (25 mL) and the organic layers were combined, dried and concentrated in vacuo to a brown residue. Kugelrohr distillation of the residue under reduced pressure afforded phenol as white crystals (0.067 g) in a 6% yield from shikimic acid. Overall, shikimic acid was converted to phenol in a 51% yield.

H. Conversion of Shikimic Acid to Phenol at Various Temperatures.

Shikimic acid (2.0 g, 11 mmol) was combined with 6 mL of degassed, carbonated water in the Parr reaction vessel. The vessel was sealed and heated as previously described to the following temperatures: 250 °C, 270 °C, 290 °C, 310 °C, 330 °C, 350 °C, and 374 °C. The desired temperature was maintained for 30 min and then the vessel was removed from the sand bath and placed under a cooling fan.

Once the vessel cooled to room temperature, it was unsealed and the contents extracted with ether (5 x 20 mL). The vessel interior was thoroughly rinsed with ether (25 mL) and the organic layers were combined. Dodecane (750 µL) was added to the pooled ether layers as an internal standard. A portion (approximately 1 mL) of this mixture was silylated by the addition of 1 mL of pyridine and 0.5 mL of BSTFA

containing 1% TMCS. The sample was allowed to stand at room temperature for at least 6 h and was then analyzed by gas chromatography. The aqueous layer remaining after extraction was diluted to known volume and the concentration of shikimic acid and 3-epi-shikimic acid were determined by ^1H NMR.

I. Decarboxylation of *m*-Hydroxybenzoic Acid.

m-Hydroxybenzoic acid (0.48 g, 3.4 mmol) was combined with water (6 mL) and various quantities of copper powder (0.22 g (3.4 mmol) or 0.022 g (0.34 mmol)) or copper (I) acetate (0.42 g (3.4 mmol) or 0.042g, (0.34 mmol)) in the Parr reaction vessel. The vessel was sealed and heated to 350 °C as previously described. The temperature was maintained at 350 °C for 1 h, 2 h, 3h, 4 h, or 5 h, and then the vessel was removed from the sand bath and placed under a cooling fan.

Once the vessel cooled to room temperature, it was unsealed and the contents extracted with ether (5 x 20 mL). The vessel interior was thoroughly rinsed with ether (25 mL) and the organic layers were combined and analyzed by gas chromatography as previously described.

J. Conversion of Fermentation Broth.

Six samples of fermentation broth were prepared that differed by their level of purification. Fermentation broth (0.8 L) was centrifuged at 14000g for 20 min and the cells were discarded. The resulting supernatant was refluxed for 4 h, cooled to room temperature. A portion (100 mL) was set aside and the pH of the remaining solution was adjusted to 2.5 by addition of concentrated H_2SO_4 . After centrifugation at 14000g for 20

min, a clear yellow solution was poured away from the cellular debris. The solution (700 mL) was combined with 14 g of Darco KB-B activated carbon, stirred on a magnetic stirrer for 1 h and then filtered through Whatman 5 filter paper. The filtrate was treated in the same way with a second batch of activated carbon (86% recovery). A portion (100 mL) of the resulting solution, designated as sample A, was evaporated to a concentration of 2 M shikimic acid and stored at 4 °C.

The portion of broth (100 mL) reserved after reflux was passed through an ultrafiltration membrane (Millipore, 10,000 MWCO) to remove the protein. The resulting black solution was combined with 2 g of Darco KB-B activated carbon, stirred on a magnetic stirrer for 1 h and then filtered through Whatman 5 filter paper. The filtrate was treated in the same way with a second batch of activated carbon (80% recovery). This protein-free, acidic solution, designated as sample B, was evaporated to a concentration of 2 M shikimic acid and stored at 4 °C.

The solution remaining after acidification and decolorization was divided into a 100 mL portion and a 500 mL portion. The 100 mL portion was eluted through a column of Dowex 50 (H⁺ form, 5 cm x 10 cm) at 4 °C which was then washed with 200 mL of water. The eluents off the cation exchange column were combined and concentrated to 2 M shikimic acid. The resulting solution (69% recovery), designated as sample C, was stored at 4 °C.

The 500 mL portion of acidified, decolorized solution was diluted to 1 L and eluted through a column of AG1-x8 (acetate form, 5 cm x 20 cm) at 4 °C. Following elution of the column with an additional 500 mL of 15% aqueous acetic acid, the combined eluents were concentrated to 500 mL by boiling. A portion of this solution

(100 mL) was concentrated to 2 M shikimic acid, designated as sample D, and stored at 4 °C. A second portion (200 mL) of the eluents remaining after anion exchange column was eluted through a column of Dowex 50 (H⁺ form, 5 cm x 20 cm) at 4 °C which was then washed with 200 mL of water. The eluents off the cation exchange column were combined and concentrated to 200 mL by boiling (62% recovery). A portion (100 mL) of this solution was concentrated to 2 M shikimic acid, designated as sample E, and stored at 4 °C.

The eluent remaining (100 mL) after cation exchange was concentrated to dryness by rotary evaporation. The resulting solid was resuspended in water (50 mL) and concentrated to dryness a second time. Cycles of resuspension and concentration were repeated until acetic acid was removed from solution. The resulting solid (5.3 g, 62% recovery) was resuspended in water to afford a 2 M solution of shikimic acid. This solution was designated as sample F and stored at 4 °C.

Each of the prepared samples was degassed by a 15 min sub-surface feed of Ar followed by a 15 min sub-surface feed of CO₂. Six milliliters of a prepared sample was placed in the Parr reaction vessel. The vessel was sealed and heated to 350 °C as previously described. The temperature was maintained for 30 min and then the vessel was removed from the sand bath and placed under a cooling fan.

Once the vessel cooled to room temperature, it was unsealed and the contents extracted with ether (5 x 20 mL). The vessel interior was thoroughly rinsed with ether (25 mL) and the organic layers were combined and analyzed by gas chromatography as previously described. The aqueous layer was diluted to a known volume and analyzed by ¹H NMR.

K. Sample A Reacted at Various Temperatures.

Fermentation broth was prepared as described for sample A. Six milliliters of the resulting 2 M solution of shikimic acid was degassed with Ar and CO₂ as previously described and placed in the reaction vessel. The vessel was sealed and heated as previously described to the following temperatures: 150 °C, 200 °C, 250 °C, and 300 °C. The desired temperature was maintained for 30 min and then the vessel was removed from the sand bath and placed under a cooling fan.

Once the vessel cooled to room temperature, it was unsealed and the contents extracted with ether (5 x 20 mL). The vessel interior was thoroughly rinsed with ether (25 mL) and the organic layers were combined and analyzed by gas chromatography as previously described. The aqueous layer was diluted to a known volume and analyzed by ¹H NMR.

L. Reduction of DHS to Shikimate and 3-*epi*-Shikimate.

3-Dehydroshikimate (0.4299 g, 2.5 mmol) was combined with MeOH (10 mL) and three drops of methyl orange indicator solution. A solution of 2 N HCl in MeOH was added dropwise until a red color developed. The NaBH₃CN (0.3142 g, 5 mmol) was added slowly with stirring while HCl/MeOH was continuously added dropwise to maintain a red color. After addition of NaBH₃CN was complete, HCl/MeOH was added dropwise until a persistent red color was obtained. The reaction mixture was filtered through Whatman 1 and the filtrate was evaporated to dryness in vacuo. The resulting solid was resuspended in boiling MeOH, the insoluble material was removed by filtration, and the filtrate was evaporated to dryness. A mixture of shikimate and 3-*epi*-shikimic acid (1:1.6) was obtained (0.42 g, 97% yield) as an off white solid.

VII. Appendix.

A. Cultivation of *N. crassa*.

Spores were inoculated into 2 L liquid growth medium in a 4 L Erlenmeyer flask to give a final concentration of 2.5×10^6 spores/L. After culturing at room temperature on a gyratory shaker at 200 rpm for approximately 65 h, the mycelium was harvested by filtration through Whatman filter paper on a Buchner funnel. The mycelium can be stored at $-20\text{ }^{\circ}\text{C}$ for at least 6 months with minimal loss of the aryl-aldehyde dehydrogenase activity.

B. Purification of Aryl Aldehyde Dehydrogenase.

Buffers Used in Aryl Aldehyde Dehydrogenase Purification.

All buffers were made up in distilled, deionized water. Buffer components were of the highest grade commercially available. Buffers used in HPLC purifications were filtered through 0.45- μm membranes and degassed prior to use. The buffers used were as follows: (A) 100 mM Tris-HCl, pH 7.6, containing L-cysteine (10 mM); (B) 50 mM Tris-HCl, pH 7.6, containing EDTA (50 mM), DTT (1 mM), and PMSF (0.4 mM); (C) 50 mM Tris-HCl, pH 7.6, containing EDTA (50 mM), DTT (1 mM), PMSF (0.4 mM), and KCl (400 mM); (D) 20 mM Tris-HCl, pH 8, containing EDTA (1 mM), DTT (1 mM), and PMSF (0.4 mM); (E) 20 mM Tris-HCl, pH 8, containing EDTA (1 mM), DTT (1 mM), PMSF (0.4 mM), and NaCl (500 mM); (F) 20 mM Tris-HCl, pH 7.5, containing DTT (1 mM), MgCl_2 (10 mM), and PMSF (0.15 mM); (G) 20 mM Tris-HCl, pH 7.5, containing DTT (1 mM), MgCl_2 (10 mM), PMSF (0.15 mM), EDTA (2 mM), and

NADP⁺ (5 mM); (H) 5 mM K₂HPO₄, pH 6.8, containing β-mercaptoethanol (1 mM); (I) 80 mM K₂HPO₄, pH 6.8, containing β-mercaptoethanol (1 mM); (J) 50 mM Na₂HPO₄, pH 7.0, containing DTT (1 mM), and NaCl (150 mM).

SDS-PAGE

Polyacrylamide gel electrophoresis in the presence of sodium dodecyl sulfate (SDS-PAGE) was performed according to Laemmli.²⁸ The stacking gel was buffered with Tris-HCl at pH 6.8, and the separating gel (6-10% acrylamide) was buffered with Tris-HCl at pH 8.8. Typically, 20-50 μg of protein were loaded per well. Gels were fixed with trichloroacetic acid solution and visualized with Coomassie Brilliant Blue. The standards (Sigma) used were rabbit muscle myosin (205,000), *E. coli* β-galactosidase (116,000), rabbit muscle phosphorylase b (97,400), bovine albumin (66,000), egg albumin (45,000), and bovine erythrocyte carbonic anhydrase (29,000). Gels were stored in a 20% solution of glycerol. For gels containing proteins to be sequenced, treatment with trichloroacetic acid and Coomassie Brilliant Blue were eliminated. Electroblothing and sequencing services were provided by the Macromolecular Structure Facility at Michigan State University.

General

All protein purification manipulations were carried out at 4 °C. Frozen mycelia (approximately 600-800 g wet weight) was thawed overnight at 4 °C. One-third of the mycelia was resuspended in buffer A (500-750 mL) and was disrupted in a Waring blender for 7.5 min at 4 °C. To prevent overheating of the lysate, the blending time was divided into five 1.5-min sessions with 10 min of cooling time between sessions. The

mycelial debris was removed by centrifugation at 18000g for 20 min at 4 °C. The lysate obtained after centrifugation was returned to the Waring blender and another third of the mycelia was added. After a second round of blending and centrifugation, the lysate was returned to the blender and the remaining mycelia were added. After a third round of blending and centrifugation, the lysate was passed through several layers of cheesecloth to remove remaining mycelial debris. The filtrate was centrifuged again at 18000g for 20 min at 4 °C to obtain a clear, yellow lysate. Concentration of all protein solutions utilized ultrafiltration membranes (10,000 M_r cutoff from Millipore). Prepared dialysis tubing (12,000-14,000 M_r cutoff from Spectrum) was stored at 4 °C and rinsed with H₂O prior to use. Proteins concentrations were determined by the method Bradford using a standard curve prepared with bovine serum albumin

Purification A.

Mycelia (616 g wet weight) was disrupted as described in the previous section using 900 mL of buffer A. After concentrating to a volume of 450 mL, the lysate was dialyzed overnight against multiple changes of buffer B. This material was applied to a column (400 mL) of DEAE cellulose equilibrated with buffer B. The column was washed with buffer B (400 mL), followed by elution with a linear gradient of buffer B (1.5 L) plus buffer C (1.5 L). The fractions containing aryl aldehyde dehydrogenase were concentrated to a volume of 110 mL. A portion of this material (37 mL) was dialyzed overnight against multiple changes of buffer D. The sample was concentrated to 9.5 mg/mL of protein and injected onto the Resource Q (6 mL) column equilibrated at 50% buffer D and 50% buffer E. Enzyme was eluted from the column by increasing the

concentration of buffer E to 100% over 15 min (flow rate = 1 mL/min). This was followed by 10 min of elution at 100% buffer E. The active fractions were pooled, concentrated and analyzed by SDS-PAGE (Table 24).

Table 24. Aryl Aldehyde Dehydrogenase Purification A.

	total units ^a	specific activity ^b	x-fold purification	yield
crude	2.1	8.5 x 10 ⁴	—	—
DEAE	2.37	0.0092	11	100%
Resource Q ^c	0.11	0.071	83	14%

^aone unit = 1 μmol NADH oxidized/min.
^bμmol/min/mg. ^cvalues correspond to 0.79 units of aryl aldehyde dehydrogenase applied to column.

Purification B

Mycelia (588 g wet weight) was disrupted as described in the previous section using 710 mL of buffer A. After concentrating to a volume of 650 mL, the lysate was dialyzed overnight against multiple changes of buffer B. This material was applied to a column (400 mL) of DEAE cellulose equilibrated with buffer B. The column was washed with buffer B (400 mL), followed by elution with a linear gradient of buffer B (1.5 L) plus buffer C (1.5 L). The fractions containing aryl aldehyde dehydrogenase were concentrated to a volume of 100 mL. A portion of this material (35 mL) was dialyzed overnight against multiple changes of buffer F. The enzyme was loaded on a column of

Dye Matrex Green A (20 mL) equilibrated with buffer F, which was then washed with buffer F (100 mL). Enzyme was eluted from the column with a linear gradient of buffer F (100 mL) plus buffer G (100 mL) followed by an additional 60 mL of buffer G. The active fractions were concentrated and analyzed using SDS-PAGE (Table 25).

A second portion (30 mL) of the material obtained after DEAE chromatography was dialyzed overnight against multiple changes of buffer H. This material was loaded onto a column (20 mL) of hydroxylapatite equilibrated with buffer H. The column was washed with buffer H (160 mL), followed by elution with a linear gradient of buffer H (160 mL) plus buffer I (160 mL). The active fractions were pooled, concentrated, and analyzed on SDS-PAGE (Table 25).

Table 25. Aryl Aldehyde Dehydrogenase Purification B

	total units ^a	specific activity ^b	x-fold purification	yield
crude	1.3	4.0 x 10 ⁴	—	—
DEAE	2.2	0.0034	8.4	100%
Green A ^c	0.10	0.023	57	14%
HA ^{d, e}	0.30	0.012	29	56%

^aone unit = 1 μmol NADH oxidized/min.
^bμmol/min/mg. ^cvalues correspond to 0.70 units of aryl aldehyde dehydrogenase applied to the column.
^dhydroxylapatite. ^evalues correspond to 0.54 units of aryl aldehyde dehydrogenase applied to the column.

Purification C

Mycelia (648 g wet weight) was disrupted as described in the previous section using 500 mL of buffer A. The lysate was dialyzed overnight against multiple changes of buffer B. This material was applied to column a (400 mL) of DEAE cellulose equilibrated with buffer B. The column was washed with buffer B (400 mL), followed by elution with a linear gradient of buffer B (1.5 L) plus buffer C (1.5 L). The fractions containing aryl aldehyde dehydrogenase were concentrated and then dialyzed overnight against multiple changes of buffer H. This material was applied to a column (10 mL) of hydroxylapatite equilibrated with buffer H. The column was then washed with buffer H (80 mL), and enzyme was eluted with a linear gradient of buffer H (80 mL) plus buffer I (80 mL). The active fractions were concentrated to 6 mL. A portion of this material (4 mL) was then dialyzed overnight against multiple changes of buffer D. The sample was concentrated to 1 mL and injected on the Resource Q (6 mL) equilibrated at 55% buffer D and 45% buffer E. Enzyme was eluted from the column by increasing the concentration of buffer E to 75% over 15 min, followed by increasing the concentration of buffer E to 100% over 10 min. The active fractions were pooled, concentrated and analyzed by SDS-PAGE (Table 26). An additional gel was prepared containing the purified protein and was submitted for sequencing.

Table 26. Aryl Aldehyde Dehydrogenase Purification C

	total units ^a	specific activity ^b	x-fold purification	yield
crude	5.6	0.0028	—	—
DEAE	2.7	0.0025	9	49%
HA ^c	0.66	0.053	19	24%
Resource Q ^d	0.026	0.041	15	6%

^aone unit = 1 μ mol NADH oxidized/min. ^b μ mol/min/mg.
^chydroxylapatite. ^dvalues correspond to 0.44 units of aryl
aldehyde dehydrogenase applied to column.

Purification D

Mycelia (802 g wet weight) was disrupted as described in the previous section using 750 mL of buffer A. After concentrating to a volume of 550 mL, the lysate was dialyzed overnight against multiple changes of buffer B. This material was applied to a column (400 mL) of DEAE cellulose equilibrated with buffer B. The column was washed with buffer B (400 mL), followed by elution with a linear gradient of buffer B (1.5 L) plus buffer C (1.5 L). The fractions containing aryl aldehyde dehydrogenase were concentrated and then dialyzed overnight against multiple changes of buffer H. This material was applied to a column (32 mL) of hydroxylapatite equilibrated with buffer H. The column was then washed with buffer H (250 mL) and the enzyme was eluted with a linear gradient of buffer H (250 mL) plus buffer I (250 mL). The active fractions were concentrated to 7 mL and DTT was added to a final concentration of 1 mM. The partially purified enzyme was quick-frozen in liquid nitrogen and stored at -20 °C for 6 weeks. This material was thawed on ice and the specific activity was checked. Only a 13% loss of specific activity had occurred while in storage. The enzyme sample was concentrated,

dialyzed overnight against multiple changes of buffer J, and injected onto the Superdex 200 column equilibrated at 100% buffer J (flow rate = 0.3 mL/min) (Table 27). The active fraction was re-injected three times to obtain an average retention time of 41.03 min. The column was calibrated using the following standards (from Sigma): egg albumin (45,000), bovine serum albumin (66,000), yeast alcohol dehydrogenase (150,000), and β -amylase (200,000).

Table 27. Aryl Aldehyde Dehydrogenase Purification D.

	total units ^a	specific activity ^b	x-fold purification	yield
crude	1.6	6.7×10^4	—	—
DEAE	2.0	0.0063	9	100%
HA ^c	0.43	0.016	24	22%
Superdex 200	0.22	0.098	146	11%

^aone unit = 1 μ mol NADH oxidized/min. ^b μ mol/min/mg. ^chydroxylapatite.

C. Colorimetric Detection of Aryl Aldehyde Dehydrogenase Activity.

Pararosaniline containing Luria plates (without carbohydrate supplementation) were prepared as follows. Luria broth (1 L) contained Bacto tryptone (10 g), Bacto yeast extract (5 g), and NaCl (0.5 g/L). Solid medium was prepared by the addition of 1.5 % Difco agar. After the Luria broth and agar solution were autoclaved, mixed and sufficiently cooled, 20 mL of pararosaniline solution was added per 1 L of medium. The pararosaniline solution was prepared just prior to use by dissolving 60 mg of pararosaniline in 20 mL of 95% ethanol. Sodium bisulfite (250 mg) was added directly

to the ethanol solution and mixed. Plates were covered with aluminum foil, cooled and used immediately to prevent high background color formation.

Host strain *KL7 aroE353 serA::aroBaroZ* was previously prepared by the Frost group. Colonies of *KL7/pJB3.141* were streaked onto freshly poured Luria plates containing pararosaniline and Cm and incubated overnight at 37 °C. To verify color formation with protocatechualdehyde, an acetone solution (approximately 50 mM) was spotted (3 µL) onto a freshly poured plate. A pink/orange color formed within minutes and was persistent over many days.

References.

-
- ¹ Sambrook, J.; Fritsch, E. F.; Maniatis, T. *Molecular Cloning: a Laboratory Manual*; Cold Spring Harbor, Plainview, 1990.
- ² Sambrook, J.; Fritsch, E. F.; Maniatis, T. *Molecular Cloning: a Laboratory Manual*; Cold Spring Harbor, Plainview, 1990.
- ³ Bradford, M. M. *Anal. Biochem.* **1976**, *72*, 248.
- ⁴ Schoner, R.; Herrmann, K. M. *J. Biol. Chem.* **1976**, *251*, 5440.
- ⁵ Mascarenhas, D.; Ashworth, D. J.; Chen, C. S. *Appl. Environ. Microbiol.* **1991**, *43*, 985.
- ⁶ Snell, K. A.; Draths, K. M.; Frost, J. F. *J. Am. Chem. Soc.* **1996**, *118*, 5605.
- ⁷ Hamilton, C. M.; Aldea, M.; Washburn, B. K.; Babitzke, P., Kushner, S. P. *J. Bacteriol.* **1989**, *171*, 4617.
- ⁸ (a) Hamilton, C. M.; Aldea, M.; Washburn, B. K.; Babitzke, P., Kushner, S. P. *J. Bacteriol.* **1989**, *171*, 4617. (b) Ohta, K.; Beall, D. S.; Mejia, J. P.; Shanmugam K. T., Ingram, L. O. *Appl. Environ. Microbiol.* **1991**, *57*, 893. (c) Li, K.; Mikola, M. R.; Draths, K. M.; Worden, R. M.; Frost, J. W. *Biotechnol. Bioeng.* **1999**, *64*, 61.
- ⁹ Feinberg, A. P.; Vogelstein, B. *Anal. Biochem.* **1983**, *132*, 6.
- ¹⁰ Snell, K. A.; Draths, K. M.; Frost, J. F. *J. Am. Chem. Soc.* **1996**, *118*, 5605.
- ¹¹ Draths, K. M.; Frost, J. W. Unpublished results.
- ¹² Fürste, J. P.; Pansegrau, W.; Frank, R.; Blöcker H.; Scholz, P.; Bagdasarian, M.; Lanka, E. *Gene* **1986**, *48*, 4470.
- ¹³ Lerner, C. G.; Inouye, M. *Nucleic Acids Res.* **1990**, *18*, 4631.
- ¹⁴ Dell, K. A.; Frost, J. W. *J. Am. Chem. Soc.* **1993**, *115*, 11581.
- ¹⁵ Li, K.; Mikola, M. R.; Draths, K. M.; Worden, R. M.; Frost, J. W. *Biotechnol. Bioeng.* **1999**, *64*, 61.
- ¹⁶ Farabaugh M. A., M.S. thesis, Michigan State University, 1996.
- ¹⁷ Li, K.; Mikola, M. R.; Draths, K. M.; Worden, R. M.; Frost, J. W. *Biotechnol. Bioeng.* **1999**, *64*, 61.

-
- ¹⁸ Entsch, B. *Methods Enzymol.* **1990**, *188*, 138.
- ¹⁹ Gibson, F. *Methods Enzymol.* **1970**, *17A*, 362.
- ²⁰ Tien F.; Montchamp, J.-L.; Frost, J. W. *J. Org. Chem.* **1996**, *61*, 7373.
- ²¹ Frost, J. W.; Knowles, J. R. *Biochemistry* *1984*, *23*, 4465.
- ²² Chaudhuri, S.; Duncan, K.; Coggins, J. R. *Methods Enzymol.* **1987**, *142*, 320.
- ²³ Frost, J. W.; Bender, J. L.; Kadonaga, J. T.; Knowles, J. R. *Biochemistry* **1984**, *23*, 4470.
- ²⁴ Verwoerd, T.; Dekker, B.; Hoekema, A. *Nucleic Acids Res.* **1989**, *17*, 2362.
- ²⁵ Kirk, T. K.; Schultz, E.; Connors, W. J.; Lorenz, L. F.; Zeikus, J. G. *Arch. Microbiol.* **1978**, *117*, 277.
- ²⁶ Cobos, A.; Fernandez, M. F.; Hernandez, P. E.; Sanz, B. *Curr. Microbiol.* **1990**, *20*, 13.
- ²⁷ Li, K.; Mikola, M. R.; Draths, K. M.; Worden, R. M.; Frost, J. W. *Biotechnol. Bioeng.* **1999**, *64*, 61.
- ²⁸ Laemmli, U. K. *Nature* **1970**, *227*, 680.

MICHIGAN STATE UNIV. LIBRARIES



31293023163177